INSTITUTO DE QUÍMICA
PROGRAMA DE PÓS-GRADUAÇÃO EM GEOCIÊNCIAS - GEOQUÍMICA

CLEUZA LEATRIZ TREVISAN

BIOGEOCHEMICAL PROCESSES IN A TROPICAL HYPERSALINE LAGOON:
TROPHIC CRISES, DIFFUSIVE FLUXES, AND PHYTOPLANKTON NUTRITION

NITERÓI
2023

CLEUZA LEATRIZ TREVISAN

BIOGEOCHEMICAL PROCESSES IN A TROPICAL HYPERSALINE LAGOON:

TROPHIC CRISES, DIFFUSIVE FLUXES, AND PHYTOPLANKTON NUTRITION

Thesis presented to the Graduate Program in Geosciences at Universidade Federal Fluminense, as a partial requirement for obtaining the Degree of Doctor. Concentration Area: Environmental Geochemistry.

Advisor:

Prof. Dr. Julio Cesar de Faria Alvim Wasserman

Coadvisor:

Dr. Teresa Cristina Soares de Mello Guimarães

NITERÓI

2023

Ficha catalográfica automática - SDC/BGQ
Gerada com informações fornecidas pelo autor

T814b Trevisan, Cleuza Leatriz
Biogeochemical processes in a tropical hypersaline lagoon : trophic crises, diffusive fluxes and phytoplankton nutrition / Cleuza Leatriz Trevisan. - 2023.
159 f.: il.

Orientador: Julio Cesar de Faria Alvim Wasserman.
Coorientador: Teresa Cristina Soares De Mello Guimarães.
Tese (doutorado)-Universidade Federal Fluminense, Instituto de Química, Niterói, 2023.

1. Laguna costeira. 2. Eutroficação. 3. Sedimento. 4. Meio Ambiente. 5. Produção intelectual. I. Faria Alvim Wasserman, Julio Cesar de, orientador. II. Soares De Mello Guimarães, Teresa Cristina, coorientador. III. Universidade Federal Fluminense. Instituto de Química. IV. Título.

CDD - XXX

Bibliotecário responsável: Debora do Nascimento - CRB7/6368

CLEUZA LEATRIZ TREVISAN

BIOGEOCHEMICAL PROCESSES IN A TROPICAL HYPERSALINE LAGOON: TROPHIC CRISES, DIFFUSIVE FLUXES, AND PHYTOPLANKTON NUTRITION

Tese de doutorado apresentada ao Curso de Pós - Graduação em Geociências da Universidade Federal Fluminense, como requisito parcial para a obtenção do **Grau de Doutor**. Área de Concentração**: Geoquímica Ambiental**.

Aprovada em novembro de 2023.

BANCA EXAMINADORA

Documento assinado digitalmente
gov.br JULIO CESAR DE FARIA ALVIM WASSERMAN
Data: 25/11/2023 10:42:24-0300
Verifique em https://validar.iti.gov.br

PROF. DR JULIO CESAR DE FARIA ALVIM WASSERMAN
ORIENTADOR / UFF

PROF. DRA. TERESA CRISTINA SOARES DE MELLO GUIMARÃES
CO-ORIENTADORA/UFF

PROFA. DRA. CRISTINA SCHULTZ
NU-EUA

Documento assinado digitalmente
gov.br HUMBERTO MAROTTA RIBEIRO
Data: 29/11/2023 21:49:01-0300
Verifique em https://validar.iti.gov.br

PROF. DR. HUMBERTO MAROTTA RIBEIRO
UFF

Documento assinado digitalmente
gov.br LETICIA COTRIM DA CUNHA
Data: 30/11/2023 13:20:08-0300
Verifique em https://validar.iti.gov.br

PROF. DRA. LETICIA COTRIM DA CUNHA
UERJ

Documento assinado digitalmente
gov.br WILSON THADEU VALLE MACHADO
Data: 30/11/2023 17:35:26-0300
Verifique em https://validar.iti.gov.br

PROF. DR. WILSON THADEU VALLE MACHADO
UFF

NITERÓI
2023

To Jonas,

Delair (*in memorian*), and João Ivo with love.

AKNOWLEDGEMENTS

To my parents, Delair *(in memorian*) and João Ivo, for all support. To my son, Jonas, who showed me an infinite love. To my beloved siblings, João and Cristiane.

To my very dear advisor and friend, Julio Wasserman. An admirable professional and scientist. Your support since our first conversation (and always) was decisive to my development.

To Teresa Guimarães, my special friend and coadvisor. Your patience and assistance in our long hours at the lab and field works were priceless.

This thesis was developed with financial support from different agencies. The author thanks Fundação Coordenação de Aperfeiçoamento de Pessoal de Nível Superior (CAPES, 2020–2021); and the special program for high performance doctorate students from Fundação Carlos Chagas Filho de Amparo à Pesquisa do Estado do Rio de Janeiro (FAPERJ Bolsa de Doutorado Nota 10 - Processo E-26/200.622/2021; 2021-2023). I also thank to thank ProLagos (the local water treatment plant) for sponsoring the field campaigns and Comitê da Bacia Hidrográfica Lagos–São João (the local watershed committee) to consent the use of the data from monthly monitoring reports.

I thank Institute of Chemistry and Institute of Geosciences for the infrastructure. I thank Department of Geochemistry, Emmanoel Vieira Silva Filho, Nicolás Strikis, and Gabriel Portela for all administrative support during these years. I especially thank all professors of the Geochemistry Department.

To Murilo Vicente, Angelo Carvalho, Maig Montel, and Bruno Rocha for all assistance, laughs, and beers! To my friends from Geochemistry. It was amazing to share this time with you.

I thank Ciça Filgueiras for supporting me with reagents and field equipment, and Manoel Moreira, Javier Salazar, and Alexandre Nisenbaum for the general assistance.

I thank professors Cristina Schultz, Leticia Cotrim, Humberto Marotta, and Wilson Machado for accepting to be part of this important step of my professional career.

I also thank Maria Helena Baeta Neves, Eduardo Santos (Dudu Barqueiro), the librarians of Geochemistry Library, Marcelo Lauretto (USP), Marlene Soares, Ana

Paula Fernandes, Ângela Esteves, and the cleaning staff of Institute of Geosciences for all support.

During the research period, the author was awarded two full grants to present oral works and posters at international conferences. Author thanks the scientific committees of the International Colloquium on Ocean Dynamics (Liège, Belgium, 2022) and Gordon Research Conference on Ocean and Coastal Dynamics (Rhode Island, USA, 2023) for the financial support and opportunity.

"*The mystery of human existence lies not in just staying alive, but in finding something to live for*."

— Fyodor Dostoyevsky, The Brothers Karamazov —

ABSTRACT

Coastal lagoons are among the most productive ecosystems in the world, but they have been severely impacted by cultural eutrophication, which affect both the ecosystem and the local community. Nutrients (nitrogen and phosphorus) that reach the lagoons can have different destinations. Part of nutrients is used by autotrophic organisms, another fraction remains in the water, or is deposited and accumulated in the sediment through diagenetic processes. At the sediment–water interface, chemical interactions can remobilize nutrients to the water column, alter existing chemical species, or form new compounds. Nutrient fluxes can favor an unbalanced increase in phytoplankton biomass and reduce water transparency by promoting the maintenance of primary productivity. The Laguna de Araruama (AL) is a coastal lagoon of great ecological and social relevance in the Região dos Lagos (Rio de Janeiro). However, anthropogenic changes since the 1970s have impacted this ecosystem, with the establishment of eutrophic conditions in 2005 and the occurrence of fish mortality and HAB since then. The present work was motivated by episodes of change in water transparency occurred between 2019 and 2022. The methodology comprised three different approaches, each one linked to a specific objective, forming the main axis of the thesis: 1) trophic crises and their causes; 2) quantification of nutrient fluxes; and 3) the nutritional requirements of local phytoplankton. Samples of water, sediment, and phytoplankton were collected in 9 campaigns between 2019 and 2022, and an equipment was developed to filtrate different sizes of phytoplankton. The Araruama Lagoon was compartmentalized into three sectors according to the salinity gradient from the sea connection to western portion: marine (32-35); central (50-67); and interior (35-50). The pore water presented very high nutrient contents, in some cases up to 100 times higher than the overlying water at the water–sediment interface. The direct indicators of trophic crises were phosphate, ammonium, and nitrite+nitrate and the N:P ratio favored by the diffusive fluxes of phosphorus and nitrogen. While the indirect descriptors were temperature, salinity, and turbidity. The turbid water (maximum Secchi =1.0 m) showed fluxes between 0.08–2.7 μmol L^{-1} (phosphate), 0.17–65 μmol L^{-1} (ammonium), and 15.6–70.3 μmol L^{-1} (nitrite+nitrate) and N:P ratio between 7–330. Non–turbid water (maximum Secchi =3.8 m) ranged from 0.08–1.3 μmol L^{-1} (phosphate), 0.17–9 μmol L^{-1} (ammonium), and 1.5–18 μmol L^{-1} (nitrite+nitrate). To complete, a mass balance determined the nutritional requirements of local phytoplankton (cyanobacteria, dinoflagellates, and diatoms) at 32.76 μg N g^{-1} and 26.66 μg P g^{-1}. The results indicated that sediments and sewage are the sources of nutrients for the maintenance of local phytoplankton, and that they can accentuate the critical state of the lagoon. Affirmative and effective environmental management actions are necessary to reduce future negative impacts on this unique environment.

Keywords: Eutrophication; hypersaline lagoons; nutrient fluxes; phytoplankton; coastal management.

RESUMO

Lagunas costeiras estão entre os ecossistemas mais produtivos do mundo, porém têm sido severamente impactadas pela eutrofização cultural, afetando tanto o ecossistema como a comunidade local. Os nutrientes (nitrogênio e fósforo) que chegam às lagunas podem ter diferentes destinos. Parte é utilizada pelos organismos autotróficos, outra fração permanece na água, ou é depositada e acumulada no sedimento através de processos diagenéticos. Na interface sedimento–água, as interações químicas podem remobilizar nutrientes para a coluna de água, alterar as espécies químicas existentes, ou ainda formar novos compostos. Os fluxos de nutrientes podem favorecer um aumento desequilibrado da biomassa fitoplanctônica e reduzir a transparência da água por promover a manutenção da produtividade primária. A Laguna de Araruama (AL) é uma laguna costeira de grande relevância ecológica e social da Região dos Lagos (Rio de Janeiro). No entanto, alterações antrópicas desde a década de 1970 impactaram este ecossistema, com o estabelecimento de condições eutróficas em 2005 e desde então mortalidade de peixes e HAB têm ocorrido. O presente trabalho foi motivado por episódios de mudança na transparência da água ocorridos entre 2019 e 2022. A metodologia compreendeu três abordagens diferentes, cada uma ligada a um objetivo específico, formando o eixo principal da tese: 1) crises tróficas e suas causas; 2) quantificação dos fluxos de nutrientes; e 3) as exigências nutricionais do fitoplâncton local. Amostras de coluna d'água, sedimento e fitoplâncton foram coletadas em 9 campanhas entre 2019 e 2022, e um equipamento de coleta foi desenvolvido para filtração de diferentes tamanhos de fitoplâncton. A laguna foi compartimentada em três setores, de acordo com o gradiente de salinidade a partir da conexão com o mar na direção oeste : marinho (32-35); central (50-67); e interior (35-50). A água intersticial apresentou teores de nutrientes muito elevados, alguns casos até 100 vezes maiores que a água sobrejacente à interface água–sedimento. Os indicadores diretos das crises tróficas foram: fosfato, amônio, nitrito e nitrato e a razão N:P, favorecidos pelos fluxos difusivos de fósforo e nitrogênio. Enquanto os indiretos foram temperatura, salinidade e turbidez. A água turva (Secchi máximo=1.0 m) apresentou fluxos entre 0.08–2.7 μmol L^{-1} (fosfato), 0.17–65 μmol L^{-1} (amônio), e 15.6–70.3 μmol L^{-1} (nitrito+nitrato) e razão N:P entre 7–330. A água não–turva (Secchi máximo=3.8 m) variou entre 0.08–1.3 μmol L^{-1} (fosfato), 0.17–9 μmol L^{-1} (amônio), e 1.5–18 μmol L^{-1} (nitrito+nitrato). Para completar, um balanço de massa determinou as necessidades nutricionais do fitoplâncton local (cianobactérias, dinoflagelados e diatomáceas) em 32.76 μg N g^{-1} e 26.66 μg P g^{-1}. Os resultados indicaram que sedimentos e esgoto são as fontes de nutrientes para manutenção do fitoplâncton local, e que podem acentuar o estado crítico da laguna. Ações afirmativas e eficazes de gerenciamento ambiental são necessárias para a redução dos impactos negativos futuros nesse ambiente tão singular.

Palavras–chave: Eutroficação; lagunas hipersalinas; fluxos de nutrientes; fitoplâncton; gerenciamento costeiro.

LIST OF FIGURES

LIST OF TABLES

LIST OF ACRONYMS

AL	Araruama Lagoon
BOD	Biochemical oxygen demand
C	Carbon
CARB	Carbonate content
CHLa	Chlorophyll–a
COD	Chemical oxygen demand
DIN	Dissolved inorganic nitrogen
DIP	Dissolved inorganic phosphorus
DO	Dissolved oxygen
DOC	Dissolved organic carbon
DOM	Dissolved organic matter
GRAN	Granulometry content
N	Nitrogen
Nox	Nitrite+nitrate
OM	Organic matter
P	Phosphorus
PAR	Photosynthetically active radiation
PHAEO	Phaeopigments
POC	Particulate organic carbon
PON	Particulate organic nitrogen
POP	Particulate organic phosphorus
S	Sulfur
SEC	Secchi's disk transparency
SWI	Sediment–water interface
TEMP	Temperature
TN	Total nitrogen
TPC	Total particulate carbon
TP	Total phosphorus
TSS	Total suspended solids
TURB	Turbidity

SUMMARY

1 INTRODUCTION

Coastal lagoons are ecosystems of the continent–ocean interface and widespread worldwide, comprising about 13% of coastal areas. The origin of coastal lagoons is related to the sea level variations during Holocene and their lifetime is noticeably short in geological time. They are usually shallow water bodies parallel to the coast, present one or more connections with the sea and variable salinities (Kjerfve, 1994). Due to their high productivity, they present many ecological functions (shelter and nursery for different species), and social importance (fisheries and tourism) (Anthony *et al.*, 2009). Also, coastal lagoons act as filters for the compounds that would reach the oceans, and be accumulated in their sediments (Schulz; Zabel, 2006). Despite their relevance, anthropic pressures like modification of land uses, pollution, and climate changes have led to changes in coastal zones (Cladas *et al.*, 2015; Tapia González; Herrera–Silveira; Aguirre–Macedo, 2008).

Nutrients are crucial for important biochemical processes (respiration and energy production) and their requirements are variable depending on the element. Macronutrients (carbon, nitrogen, and phosphorus) are the base blocks of life, while micronutrients (iron, sulfur, molybdenum, and others) are needed in smaller quantities. Their ubiquitous presence follows pathways from microorganisms to the large animals on Earth and back in cycles in aquatic, terrestrial and atmospheric systems. Unbalance in nutrient stoichiometry causes a cascade effect on ecosystems and negative impacts affect the entire trophic web. In the last decades, nutrient loads increased at critical levels due to anthropic activities and the quality of coastal environments has drastically reduced (Mosley *et al.*, 2023; Padedda *et al.*, 2019).

One concerning issue related to the excess of nutrients in aquatic systems is eutrophication, which is worsened in restricted water bodies, with low turnover time. Although it is a natural process, anthropic (or cultural) eutrophication is hastening it at rates that the environment cannot respond alone. The impacts on the environment include losses of biodiversity, increase of water turbidity, shifts of species, harmful algal blooms (HAB) and fish mortalities. But the effects are not restricted to the environment, and comprise impacts on tourism and economy, and human diseases caused by consumption of seafood contaminated with toxins from phytoplankton (Vilariño; Louzao, 2018). The question that arises is “whether these problems are caused by high nutrient loads, is it enough to reduce their inputs into coastal waters?”

And the answer is yes, but it is not that simple, because sediments are reservoirs that also play an important role in this scenario.

Nutrients reach coastal areas via runoff (soil leaching), groundwater, sewage direct disposal, or atmospheric inputs, and might remain in dissolved or particulate forms. Phosphorus and nitrogen are assimilated by aquatic biota or deposited into sediments, where they can reach high concentrations. Under certain circumstances, sediments release nutrients back to the water column and boost primary production (Lei *et al.*, 2021; Wu *et al.*, 2019). Porewaters entrap dissolved fractions of many compounds, which combine among themselves, changing their forms, precipitating, or burying deeper into sediments (Foster; Fulweiler, 2014; Isaji *et al.*, 2019; Rabouille *et al.*, 2007). Sediment–water interface is where various reactions happen at the same time and sediment physical–chemical properties have significant roles in nutrient cycling. In hypersaline environments, the amount of charged species (cations and anions) are higher and enhance, reduce, or favor some reactions.

Interactions among nutrient loads, sediments and primary production usually lead to dystrophic processes (Basset, *et al.*, 2013; Carpenter; Pace, 1997; Cladas *et al.*, 2015; Lenzi; Cianchi, 2022; Pérez-Ruzafa *et al.*, 2019), however the definition of dystrophy varies depending on the authors. For Valiela (1984) dystrophy is a reversible event in an aquatic ecosystem linked to white waters due to diffusion of sulfides from sediments. Carpenter (1997) described dystrophy, in the same sense of oligotrophy and eutrophy, as a trophic state distinguished by low productivity, high humic content and brown water. Lenzi and Cianchi (2022) used the term as the environmental responses to eutrophication and the changes from a eutrophic condition to one of nutrient absence. In the present work, the abrupt shifts of the water quality occurred in Araruama Lagoon, from high to low turbid conditions and vice-versa, will be referred as trophic crises.

Araruama Lagoon (AL), like other hypersaline systems, presents high urbanization and has undergone eutrophication processes over past 50 years (Souza; Azevedo, 2020). Diffuse sources of sewage and deficient infrastructure (sanitary sewer, water treatment plants) caused large nutrient inputs during decades. However, its alkaline waters acted as a buffer for the impacts of eutrophication until the lagoon reached its critical point and collapsed. In 2005, its clear waters abruptly shifted to a brownish color, resulting in posterior episodes of harmful algal blooms (Oliveira *et al.*, 2011) and fish mortality (Wasserman *et al.*, 2017). Shifts from phytobenthic to phytoplankton assemblages (Mello, 2007), and the presence of toxic species like *Dynophysis caudata*, *Oxytoxum scolopax*, *Amphora ostrearis* have been identified in the lagoon (Neves, 2019–2020, monitoring reports).

In 2019, episodes of fish mortality and high transparency in water column raised questions that are the subject of the present thesis: What are the descriptors for trophic crises in the lagoon? Are sediments involved in? Is phytoplankton supported by sediment fluxes? The present thesis focuses on identifying the processes responsible for the sudden breaks and recoveries in turbidity in the hypersaline Araruama Lagoon. The first chapter is a general introduction to the thesis, motivation, hypotheses, and objectives. The second is a literature review presenting important concepts on which the research is based on, especially regarding eutrophication. The third is a general description of the study area and an overview of the methodological approach. Chapters four, five and six form the main part of the thesis, comprising specific subjects of dystrophic processes, nutrient fluxes, and phytoplankton requirements, respectively. The seventh chapter is a general conclusion about the results produced by this thesis, gaps, and suggestions for further studies.

1.1 Motivation

Climate crisis is driving global changes on environments and bringing wealth insecurities for humans and wildlife. Biogeochemical cycles are part of the problem and are keys for the ecosystem maintenance. In AL, abrupt shifts from low to high, or high to low primary production led to changes in the trophic state of the lagoon. Trophic crises are interconnected with nutrient cycles, and both cause negative impacts on water and trophic state. The importance of this research lies in new approaches to access biogeochemical processes in coastal lagoons, which are vital for environmental actions and their management.

1.2 Hypotheses

The hypotheses of the research were:

- H1: The descriptors of turbid conditions will present distinctive range of values for turbid and non-turbid waters;

- H2: The trophic crises in Araruama Lagoon are the response to the positive diffusive nutrient fluxes;
- H3: Sediment in Araruama Lagoon is the main source of nutrients to water column and phytoplankton production.

1.3 Objectives

The general objective of the thesis is to identify the triggers and the role of sediments on the shifts of the water column turbidity occurred in 2019, 2020 and 2022 in AL.

The specific objectives of the research are:

- To investigate the descriptors that identify the different turbid conditions of water column in AL;
- To estimate phosphorus and nitrogen diffusive fluxes in sediment–water interface of AL during different water turbidities;
- To model a mass balance of the sources of nitrogen and phosphorus and the nutritional requirements of phytoplankton in AL.

2 LITERATURE REVIEW

2.1 A brief introduction about energy fluxes and coastal ecosystems

The theory of ecology comprises fundamental principles and includes environment, organisms, time, space, and evolution interacting one another (Scheiner; Willig, 2008). Since ecosystems are open, biotic and abiotic exchanges include energy flow, nutrient cycling, and limiting factors (Kareiva; Marvier, 2001) affecting the persistence of biotic assemblages (Covich, 2001). Different steady states in complex systems provide more potential connections among levels (Harris, 1986; Margalef, 1975). Regardless of the connections among environments, local combinations of physical properties and chemical reactions permit the existence of specific organic associations (Van der Ploeg, 1982). Light and nutrient availability are considered the most important limiting factors for phytoplankton growth, being essential for photosynthesis and nutrition of phytoplankton species (Lalli; Parsons, 1997).

As part of an ecosystem, energy transference comprises production, consumption, and decomposition by organisms, and it is important for trophic level maintenance and nutrient cycling (Covich, 2001; Van der Ploeg, 1982). In marine environments, particularly coastal lagoons, pelagic production (Carmouze; Knoppers; Vasconcelos, 1991) and benthic productivity (Alvarez–Borrego, 1994) are important factors for nutrient and energy transference. However, interactions among biotic and abiotic components are highly susceptible to changes and even small variations can lead to great disturbances in the environment. Fluxes of energy flow through the species, affect the persistence of ecosystems, and are dependent on land–use changes and geomorphologic factors (Covich, 2001).

Such fluxes are particularly important in marine environments because they provide important ecosystem services (Wolanski; Mclusky, 2011). Ecosystem functioning is important for biodiversity, and variation of species can be associated with dystrophy in coastal lagoons (Danovaro; Pusceddu, 2007). Unstable states allow community transitions by gradual steps, abrupt shifts or alternate states in response to environmental disturbances (Kennish; Paerl, 2010). Local water column geochemistry, for example, can drive shifts in producer community, depending on nutrient loads (Kennish; Paerl, 2010). In benthic ecosystems, prokaryote diversity allows varied pathways for ecosystem processes and benthic metabolism (Danovaro;

Pusceddu, 2007). Tropical coastal lagoons are also more sensitive to environmental modifications because climate changes can be more pronounced in regional scales in such systems (Grenz *et al.*, 2017).

Due to this intrinsic relationship of energy fluxes between biotic and abiotic systems, anthropic activities cause significant risks to equilibrium of coastal zones (Harris, 2008; Pérez–Ruzafa *et al.*, 2019; Webster; Harris, 2004). The intensification of disorders in aquatic ecosystems have the capacity to alter biota (micro and macro communities) and exacerbate biodiversity losses (Danovaro; Pusceddu, 2007). Natural and anthropogenic disturbances cause shifts in distribution patterns, including local extinctions or increasing species richness, which affect nutrient cycling, ecosystem functions and energy flows (Covich, 2001). The most common responses for these interferences are alterations in hydrological cycle (Mariani; Lessa; Marta–Almeida, 2022), introduction of marine pollutants (Hamdoun *et al.*, 2015; Palma; Ledo; Alvarenga, 2015), eutrophication (Cooley *et al.*, 2022) and toxic phytoplankton blooms (Al–Azri *et al.*, 2015; Sellner; Doucette; Kirkpatrick, 2003).

2.2 General characteristics of coastal lagoons

Coastal lagoons comprise 13% of coastal areas (Barnes, 2001), are geologically transient landscapes (Kjerfve, 1994), and vary in location, size, salinity, and connections with the sea (Bird, 1994; Harris, 2008; Kjerfve, 1986). They result from sea level changes during Late Quaternary (Barnes, 2001; Kjerfve, 1994) and their development is linked to sediment remobilization via waves (mainly), tides and currents (Bird, 1994; Nicholls *et al.*, 2007). Coastal lagoons are shallow water bodies isolated from the ocean by sand bars and connected to the sea by one or more channels (Barnes, 2001; Bird, 1994; Kjerfve, 1994; Nicholls *et al.*, 2007). Due to its location at land–ocean interface, coastal lagoons are strongly associated with marine and terrestrial ecosystems, establishing an ecological continuum (Padedda *et al.*, 2019).

Interactions among hydrological cycle, atmosphere, lithosphere and biosphere modify the water composition (Wolanski; Mclusky, 2011). In arid climates, coastal lagoons are usually hypersaline due to the high evaporation rates (Bird, 1994). Such hypersaline lagoons are extreme environments because normal cell physiologies cannot tolerate salinities higher than 35, and only specialized organisms are adapted (Esteban; Finlay, 2003; Ramos *et al.*, 2017; Rich; Maier, 2015). Salinity is also pointed as a control for zooplankton communities, and low salinities could favor large herbivores while higher salinities favor phytoplankton communities (Esteves *et al.*, 2008). Franco (2022) demonstrated that salinity was a key element for composition of trophic and habitat grouping of fish species.

2.3 An overview of water and sediment biogeochemistry in coastal lagoons

2.3.1 Water biogeochemistry

Physical properties of water, particularly salinity, temperature and turbidity, affect ecological systems and biological processes and vary in both space and time (Dodds; Whiles, 2010; Wolanski; Mclusky, 2011). Embayments, like coastal lagoons and estuaries, are exposed to different processes, such as sedimentation, biologic production and nutrient fluxes, which modify water characteristics (Wolanski; Mclusky, 2011). Moreover, water quality in coastal lagoons reflects a complex relation between compound concentration and water residence time which varies due to physical and geological processes (Miranda; Castro Filho; Kjerfve, 2002).

Oxidation–reduction reactions (redox) are crucial for all living organisms and affect the biological availability and mobility of various elements (Bleam, 2012; Dennis, 1987; Ibanez, 2007). In natural waters, composition and depth are relevant to establish the redox conditions depending on the dissolved oxygen (DO) content. Most oxidizing environments (high DO) are at the top layers while the reducing conditions (low DO) are at the bottom or lower layers (Ibanez, 2007). Further, acid–base reactions are responsible for processes such as dissolution and precipitation, ion exchange, and catalysis that occur at the interface between mineral surfaces and aqueous solutions (Moses, 2016).

Wind plays an important role in water mixing (Sethuraman, 1979), influences the seasonality and distribution (horizontal and vertical) of phytoplankton (Durham *et al.*, 2013; HARRIS, 1986), availability of light (Reynolds, 1998), nutrients (Arfi; Guiral; Bouvy, 1994; Chen *et al.*, 2023; Macintyre, 1998) and evolutionary adaptation (Moore–Maley; Allen, 2022; Wheeler *et al.*, 2019). Wind action mixes the water column, affecting heat distribution and dissolved oxygen concentration modifying local hydrodynamics, resuspending bottom sediments and its deposition and distribution (Arfi; Guiral; Bouvy, 1994).

2.3.2 Sediment biogeochemistry

In coastal lagoons, the supply of sediments occurs from erosion/deposition of surrounding shores, material washed or blown over the enclosing barriers, and accretion from river runoff (Bird, 1994). However, sediments are not solely compartments of ocean or lacustrine material (Stumm; Morgan, 1981), they are important reservoirs of nutrients and other pollutants resulting from different interaction processes (Burton, 2002; Wolanski; Mclusky, 2011). In certain circumstances, they are also the source of these compounds to the water column (Stumm; Morgan, 1996), and regeneration at the sediment–water interface influences nutrients in surface waters (Harris, 1986). Various processes occur in sediments are in Table 1, while processes concerning organic matter are in Figure 1.

Table 1 – Definition of processes in sediment

PROCESS	DEFINITION
Diagenesis[1]	the physical, chemical, and biological processes in sediments and sedimentary rocks just after deposition; it involves sediment, organic matter, and pore water at shallow areas under near surface temperatures (30^{o} C)
Sedimentation[2]	process in what organic or inorganic matter settles out of the suspension in water due to gravity effect
Diffusion[3]	transport responding to concentration and thermal gradients
Advection[3]	transport responding to a pressure gradient or body force
Mineralization[4]	decomposition of organic particles into inorganic forms by bacteria
Adsorption/ desorption[5]	it is a reversible process where molecules or ions are attached to or detached of a surface of a solid; it is important for ion exchanges and enzymatic reactions
Dissolution[6]	process of decomposition of plant material, bacteria and algae releasing dissolved compounds
Resuspension[3]	the movement of particles from sediments due to water movement
Bioturbation[3]	mechanical mixing of bottom sediments due to living organisms
Sediment zonation[7]	it is characterized by energy yields and electron acceptor variation, and it is linked to diagenetic processes
Benthic grazing[8]	heterotrophic organisms are important for storage and trophic cycling of nutrients, and are often related with abundance of primary producers
Degradation[9]	the disintegration of mainly photosynthetically produced organic matter by microorganisms

Source: [1]Montañez; Crossey (2018); [2]Gregory; Edzwald (2010); [3]Corey and Auvermann (2003); [4]Huettel *et al*. (1998); [5]Artioli, (2008); [6] USGS (2017); [7]Fenchel; King; Blackburn (2012); [8]Cebrián (2004); [9] Arndt and LaRowe (2018).

Figure 1 – Pathways of the general processes of organic matter

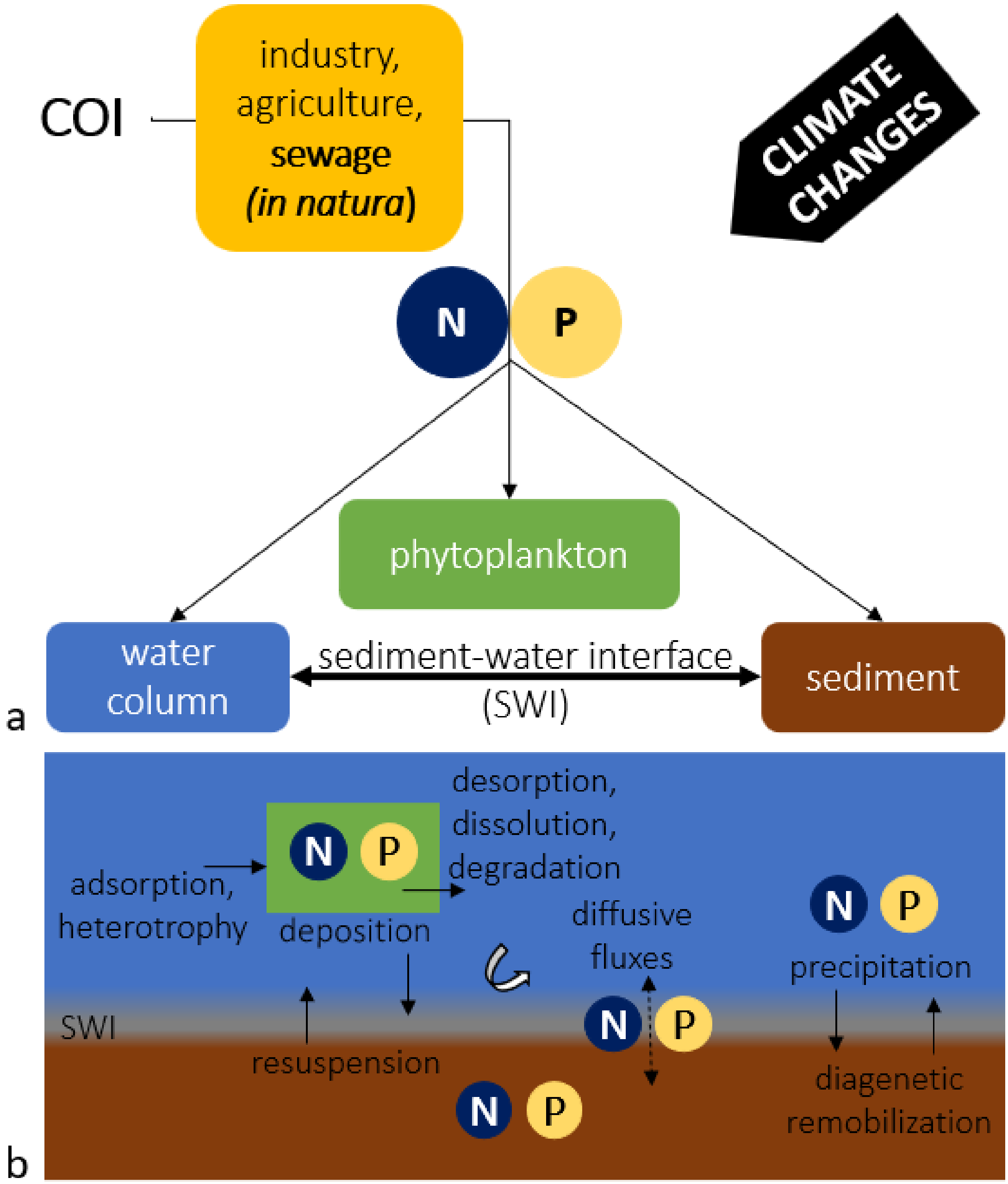

Source: modified and adapted from Turner and Millward (2002).
LEGEND: a) Generic N and P loads and faith at a COI (continent-ocean interface). In the specific case of Araruama Lagoon, the main contribution is from non-treated sewage (highlighted in bolded words). Colored boxes indicate the reservoirs of N and P - water column; sediment; phytoplankton. Climate changes impact each media in a different manner and boost the processes. b) Processes linking sediment, water column, suspended particles, and consumers according to Table 1. SWI=sediment-water interface. Diffusive fluxes can be in both directions - positive (from sediment to water column) or negative (from water column to sediment). advection turbulence (winds).

The early diagenesis occurs in the sediment pore water, where the reactions can be depicted from spatial–temporal distribution. The thickness of the oxic surface layers is variable depending on primary productivity, porosity and chemical composition of the bottom water (Schulz; Zabel, 2006). In the absence of bioturbation or any physical disturbance, the sediment (pore water) shows a characteristic chemical zonation (Froelich *et al.,* 1979) (Table 2) for the main aerobic and anaerobic mineralization processes (Kasten, 2011; Wolanski; Mclusky, 2011).

Table 2 – Sequence of the electron acceptance in early diagenetic processes

MINERALIZATION PROCESS	CHEMICAL REACTION	ΔG° (kJ mol C^{-1})
Aerobic Respiration (1)	$C_6H_{12}O_6 + 6O_2 \rightarrow 6CO_2 + 6H_2O$	−471
Denitrification (2)	$5C_6H_{12}O_6 + 24NO_3^- \rightarrow 12N_2 + 24HCO_3^- + 6CO_2 + 18H_2O$	–444
Manganese Reduction (2)	$C_6H_{12}O_6 + 18CO_2 + 6H_2O + 12\delta\text{–}MnO_2 \rightarrow 12Mn^{2+} + 24HCO_3^-$	−397
Iron Reduction (2)	$C_6H_{12}O_6 + 42CO_2 + 24Fe(OH)_3 \rightarrow 24Fe^{2+} + 48HCO_3^- + 18H_2O$	−131
Sulfate Reduction (3)	$2C_6H_{12}O_6 + 6SO_4^{2-} \rightarrow 6H_2S + 12HCO_3$	−76
Methanogenesis (3)	$2C_6H_{12}O_6 \rightarrow 6CH_4 + 6CO_2$	−49

Source: Froelich *et al.,* 1979.
LEGEND: Biochemical zones according to Froelich *et al*. (1979) – (1) oxic; (2) suboxic; (3) anoxic.

The main electron donors are organic matter, which are abundant in muddy and silty sediments. The hydrophobic texture of these particles associated with the restricted transport of acceptors, lead to the development of redox gradients. Under anaerobic conditions, the hydrophilic sediments promote low decomposition of organic matter. Such sediments allow advective transport of water, dissolved solutes, and fine suspended particles with low organic matter. Coarse grains are more available for suboxic chemical diagenesis, and the solute fluxes from sediment to water column are faster than from fine–grained sediments (Wolanski; Mclusky, 2011).

2.3.3 Diffusive fluxes at the sediment-water interface

Molecular diffusion is the microscopic random motion of compounds in a fluid or solid (Thibodeaux; Germano, 2012). At the sediment-water interface (SWI), diffusive fluxes are driven by temperature, pressure, and composition (Liang, 2018), and are affected by bioturbation (Barbanti *et al*., 1992), and winds (Rodellas *et al*., 2020). Diffusive fluxes are also affected by algal bloom decomposition, which act as a key nutrient reservoir of P, S and Fe to sediments. The increasing concentrations of labile forms of P, S and Fe occurred in both sediment and water column. Such a large decomposition changed the oxireduction conditions in SWI, favoring Fe oxyhydroxides reduction and dissolution and then P releasing (Han *et al*., 2015). In Thau Lagoon (France), seasonal changes in P concentration in pore water at the

SWI influenced diffusive fluxes and were responsible for P releasing to water column (Mesnage; Picot, 1995).

In two coastal lagoons in Macaé, state of Rio de Janeiro, the sediment oxygen consumption regulated the rate and extension of denitrification in the sediments by creating oxic-anoxic conditions (Enrich-Prast *et al*., 2016). The study also identified a pattern in which salinity was an important factor for nitrification in sediments with low benthic algae density. In AL, Silva (2019) quantified high amounts of nutrients in sediments, and Guimarães *et al*. (2021) observed diffusive fluxes of N and P in mesocosm experiments simulating *in situ* conditions.

2.4 Biogeochemistry of nutrients

Mineral nutrients are resources required to form living organic compounds and the quantities vary according to the specificities of each one (Begon; Townsend; Harper, 2006; Harris, 1986). Nutrients are found in the different compartments, forms and redox states, interact simultaneously according to geochemical conditions, and produce a variety of compounds (Gallardo–Rodríguez *et al.*, 2019). Such interactions occur in complex biogeochemical cycles that allow nutrients to pass from the abiotic to biotic environment and back (Odum, 2001). These cycles are interconnected, influence life on Earth in geological time (Ruttenberg, 2003), and vary depending on local conditions (Van der Ploeg, 1982).

Mineralization is the transformation of organic matter back to inorganic forms of elements, and it happens in both water column and pore water. Ecologically, the rate at which growth–limiting nutrients are recycled is the most important aspect of recycling in the sea. These rates vary in time from rapid (seasonally) to slow (geological time) depending on the site Scale (Lalli; Parsons, 1997; Wolanski; Mclusky, 2011). Besides, the behavior of primary production has a delayed response to nutrient inputs (Figure 2).

Figure 2 – Relation between nutrient input and response–time of primary production

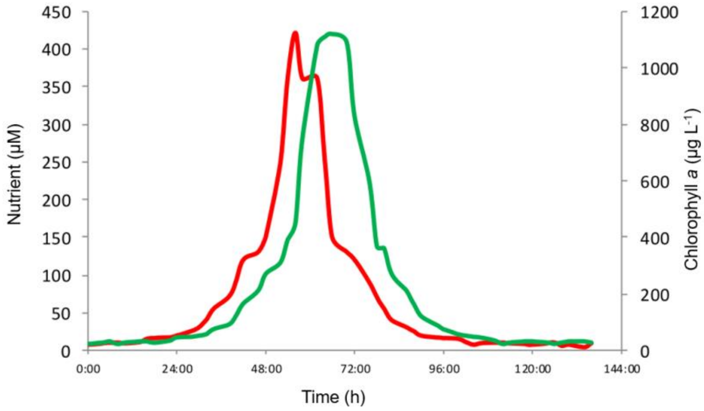

Source: Wasserman (2017). Authorized by the author.
LEGEND: —— nutrient concentration; —— primary production (chlorophyll *a*).

For the purposes of this thesis, only sulfur, carbon, nitrogen, and phosphorus will be described because they play a significant role on biogeochemistry of aquatic ecosystems.

2.4.1 Sulfur

Sulfur is abundant in seawater as sulfates (Van der Ploeg, 1982) and its importance relies on both organic and inorganic processes : i) it is used in many metabolic reactions for nutritional demands like production of proteins (Wetzel, 2001); ii) the widespread distribution of its different forms affects other nutrient and metal cycling (Dodds; Whiles, 2010). Organisms assimilate almost all sulfur as sulfate, however, during bacterial decomposition of organic matter, it is released as sulfide (specifically by sulfate reducing bacteria). The reduction of sulfate and oxidation of sulfide modify the conditions for mobilization of other nutrients. In anoxic sediments, the production of iron sulfide reduces the availability of sulfur in water column and allows phosphorus availability which could enhance primary production (Norici; Hell; Giordano, 2005).

The higher amount of sulfate in the seawater and the very reducing conditions of the sediments in Araruama Lagoon make sulfur an important element to the biogeochemical cycles. Studies indicated the importance of ORP (oxy–redox potential) on P concentration and the role of sulfide production in sinking or releasing phosphorus in coastal sediments (Li *et al.*, 2016). Ku *et al.* (1999) relate S coupling to carbonate dissolution in shallow low–Fe carbonate sediments. In such case, decomposition of organic matter by sulfate reduction/sulfide oxidation enhances carbonate content. (Gallagher *et al.*, 2012) demonstrated that sulfate–reduction bacteria change the local geochemistry and favor carbonate production depending on electron donor.

Blackburn and Blackburn (1993) noted the importance of sulfate and sulfide in the diffusion of nitrogen (nitrate and ammonium) in shallow sediments. Cotner *et al*. (2004) corroborates the connection between sulfur forms and N/P fluxes and the persistence of phytoplankton production. Han *et al.* (2015) reported degraded algal in surface sediments as a major source for fluxes of phosphorus and sulfur to the water column and sediment. The authors also verified that as algal decomposition progressed there was a development of favorable conditions for Fe–oxyhydroxides reduction promoting Fe–sulfide precipitation.

In spite of the thesis did not measure concentration of sulfur compounds, it was necessary to introduce the element due to its relevance to local process.

2.4.2 Carbon

Carbon (C) is the main construction block of life (Weathers; Strayer; Likens, 2021) due to: i) it is the major component of living forms; ii) biochemical reactions carried by carbon compounds are important for storage and transport of energy (Weathers; Strayer; Likens, 2021). Carbon is presented in environment in organic and inorganic forms. Organic compounds are: i) dissolved organic carbon (DOC) which refers to a mixture of simple and complex acids which are considered the major source of carbon for aerobic microbes; ii) particulate organic carbon (POC) which comprises material from plants, phytoplankton, microbes, any other organism and detritus (Vincent; Jennerjahn; Ramasamy, 2021). Inorganic forms are classified as dissolved inorganic carbon (DIC), present in water as carbon dioxide (CO_2), carbonate (CO_3^{2-}), and bicarbonate (HCO_3^-).

In water, the conversion between inorganic and organic carbon is via photosynthetic algae, which are later decomposed by heterotrophic organisms (Canuel; Hardison, 2018). In the ocean, the carbon pump is responsible for removing atmospheric carbon to deep ocean and sediments due to environmental or biological factors (Fakhraee; Planavsky; Reinhard, 2020). In shallow aquatic systems, carbon is present in two distinct paths according to oxygen levels. In oxic sediments, the labile organic carbon stimulates autochthonous consumption, and the sediment oxygenation enhances mineralization. While in anoxic sediments, microbes use this

DOC but the transference to higher trophic levels is not efficient, so this compartment acts as a pool for carbon in long term scales (Middelburg, 2018).

Carbon cycle varies from millions of years to days or thousands of years for geological and biological components respectively (Canuel; Hardison, 2018). The biological contribution to the carbon cycle depends on the balance of both carbon production/consumption and carbonate precipitation/dissolution (Abidi; Amor; Gueddari, 2018). This relation is responsible for the alkalinity of aquatic systems and leads to a buffering effect in natural waters (Gallardo–Rodríguez *et al.*, 2019). Coastal lagoons are important zones of filtration and modification of matter at land–sea interface and link the terrestrial and marine carbon cycle (Knoppers, 1994). Additionally, warmer tropical or subtropical oceanic regions, which includes hypersaline lagoons, are preferential places for carbonate precipitation (Grotzinger; Jordan, 2014). Particularly in these high–carbonate environments, the increasing diffusion of atmospheric CO_2 promotes dissolution of $CaCO_3$, while the opposite causes its precipitation (Krauskopf, 1995).

2.4.3 Nitrogen

Like other macronutrients, nitrogen is crucial for life and it is found in numerous biomolecules (Mancinelli, 1989) such as proteins, DNA, RNA (Van der Ploeg, 1982) and ATP (Dunn; Grider, 2023). In aquatic ecosystems, nitrogen is often considered a limiting nutrient for the primary producers (Begon; Townsend; Harper, 2006). However, nitrogen cycle has drastically changed due to industrial processes of nitrogen fixation for fertilizer production, altering nitrogen pools and affecting ecosystems (Palta; Hartnett, 2018). While assimilation by organisms originates particulate organic nitrogen (PON) and dissolved organic nitrogen (DON), decomposition of organic matter transforms nitrogen to inorganic compounds via remineralization (Begon; Townsend; Harper, 2006). In terrestrial and aquatic systems, the reduced and oxidized forms of nitrogen, which are sensitive to pH and dissolved oxygen, are largely cycled by organisms, and it is sensitive to pH and oxygen (Cartigny, 2018).

In oxic conditions, nitrification converts ammonia to nitrite and then to nitrate while in anoxic conditions, anammox occurs (Bernhard, 2010). The opposite pathway, denitrification, or nitrate reduction, delivers N_2 to the system again (Palta; Hartnett, 2018). In general, ammonium at photic zone of oxic waters is low due to its use by primary producers, while in anoxic zones ammonium is formed (ammonification). Nitrite is promptly oxidized and usually presents small concentrations, except in eutrophic lakes, where organic pollution is high. Nitrate often tends to have the opposite behavior of ammonium, and as oxidation occurs, more nitrate is formed (Wetzel, 2001). Howarth and Marino (2006) observed that nitrogen is a limiting factor for eutrophication, more than carbon or phosphorus. This deficiency is attributed to the long–term storage of fixed N and its pathway back to atmosphere as N_2 (Marcarelli; Fulweiler; Scott, 2022) while organisms present in an ecosystem alter concentration of N forms (Shen *et al.*, 2020; Zhou *et al.*, 2017).

2.4.4 Phosphorus

It is vital for biochemical reactions and it is important for DNA, RNA, ATP, and other organic structures, and essential to build photosynthetic organisms biomass (Van der Ploeg, 1982; Westheimer, 1987). Since phosphorus is highly required for the formation of biological compounds, it is often a limiting factor for primary production and can control carbon fixation (Li *et al.*, 2017; Mackey; Paytan, 2009). The main form in the environment is orthophosphate, or simply phosphate (PO_4^{3-}), the most oxidized state, however it can be found also as HPO_4^{2-}, $H_2PO_4^{-}$, H_3PO_4. Phosphorus cycle has been significantly altered by human activities (agriculture, mining, land–use changes, wastewater discharges), and aquatic ecosystems are more sensitive to phosphorus pollution (Smil, 2000).

Like other elements, phosphorus associations vary with time, space, and ocean depth and interactions will depend on local biogeochemistry (Defforey; Paytan, 2018). Microbially mediated processes also occur and promote release and removal of phosphate by cells under anoxic and oxic conditions, respectively (Mackey; Paytan, 2009). Contrasting to the other nutrient cycles that are governed by redox conditions, phosphorus is regulated by physical, biotic and chemical factors (Weathers; Strayer; Likens, 2021). However, the association with other elements is determined by the compound solubility characteristics, which can vary with ORP and determines P availability. Phosphorus solubility is also determined by pH and the presence of cation species which P is bound to (Koski–Vahala; Hartikainen, 2001).

Coastal environments with prominent upwelling and low terrigenous loadings are enriched in authigenic apatite ($Ca_5(PO_4)_3$). Microbial activity during diagenesis results in positive fluxes of dissolved phosphate from pore to overlaying waters (Ruttenberg, 2003). Experiments have shown that, in high Ca/P molar ratios, phosphate precipitation presents intermediate phases from the apatite–precursor to apatite formation. Also, results show that biogeochemical P cycling in natural environments is controlled by adsorption of $PO_{4(aq)}$ onto Ca–carbonates and in Fe, Mn, Al–mineral phases (Liang; Blake, 2007). During events of algal decomposition, sulfides mediate reduction of Fe–oxides and the connection of S–Fe cycle promotes substantial Fe–P mobilization in sediments (Zhang *et al.*, 2021).

2.5 Eutrophication

Eutrophication is the continuous increase of supply of organic matter in aquatic systems associated with nutrient loads (nitrogen and phosphorus) (Nixon, 1995). It is a natural process over the years, but it is intensified by anthropogenic activities and causes drastic changes in aquatic ecosystems (Carpenter *et al.*, 1998; Dodds; Whiles, 2010; Stumm; Morgan, 1981; Vollenweider, 1992). Often, in coastal zones, the most vulnerable areas for eutrophication are those which present limited interaction with the sea, for example fjords, estuaries, and lagoons (Vollenweider, 1992). The associated effects of eutrophication are deterioration of water quality, harmful algal blooms, shifts in phytoplankton community, changes in trophic linkages and reduction of biodiversity (Dorgham, 2014; Kennish; Jonge, 2011).

As advances on eutrophication knowledge increased, it arose the necessity to determine the eutrophication stages of a certain environment and a variety of trophic indexes were developed. Trophic state of aquatic environments indicates the extension of cultural eutrophication (=anthropic origin), and it is measured by a variety of parameters (Tugrul; Ozhan; Akcay, 2019). These indexes usually classify eutrophication in terms of ecosystem production: i) oligotrophic or low nutrition; ii) mesotrophic; iii) eutrophic or high nutrition; and iv) hypertrophic or very high nutrition (Dodds; Whiles, 2010). Despite of eutrophication and harmful algal blooms (HABs) can occur in natural and oligotrophic conditions, eutrophication is related to: i) an increasing of anthropogenic nutrient loading; ii) persistent and recurrent events; and iii) deleterious consequences on environments (losses of structure and function) (Lemley; Adams, 2019).

Oligotrophic environments do not sustain high primary production while eutrophicated environments are often extremely productive (Lalli; Parsons, 1997;

Marañón, 2019). The result of eutrophication is that only a few species are able to tolerate such conditions which favors the dominance of certain organisms (Dodds; Whiles, 2010). Unlike natural occurrences of high productivity areas, eutrophication is increased by anthropic nutrient loads, recurrent, deleterious to the environment. An example is the progressively reduction of diatom production by independent–Si algae and cyanobacteria in high eutrophicated environments due to removal of silica by sedimentation (Struyf *et al.*, 2009; Wetzel, 2001). Lürling *et al.* (2018) demonstrated that nutrient pulses promote larger blooms of cyanobacteria than climate changes alone.

Grain size is an important factor for pore water processes and contaminant retention (Wolanski; Mclusky, 2011). As it happens in water column, sediments reflect processes in aquatic environments (Coelho *et al.*, 2004; Han *et al.*, 2015), consequently they are important indicators of contamination by different pollutants. For the same reason, nutrients in sediment are important to diagnosis potential sources for primary production (Dell'anno *et al.*, 2002; Mesnage; PICOT, 1995). However, in tropical lakes, due to high temperatures (>20º C), the organic matter cycling is faster, and the concentrations may not reflect the production level (Chapman; Wang, 2001). Beyond that, biological disturbance and vertical alternation between production and consumption in pore waters are also important for nutrient fluxes in sediments (Matos *et al.*, 2016).

2.6 Phytoplankton

Despite controversies and uncertainties about the term (Harris, 1986), phytoplankton comprises bacteria, protists and plants that present some sort of movement in rivers, lakes, and oceans (Harris, 1986; Lalli; Parsons, 1997). They have crucial function in the aquatic food chain as the dominant autotroph organisms (Lalli; Parsons, 1997), particularly in estuarine areas, and affect nutrient cycling (Wolanski; Mclusky, 2011). Species vary in size and shape (Harris, 1986; Lalli; Parsons, 1997) due to seasonality (Harris, 1986; Seguro *et al.*, 2015), photosynthetic pigments (Begon; Townsend; Harper, 2006; Harris, 1986) nutrient limitation (Falkowski; Woodhead; Vivirito, 1992), among others. Moreover, phytoplankton species present different growth rates and adaptions to recognize environmental changes (Harris, 1986).

Algal bloom is the term used to indicate an occurrence of phytoplankton cell density above the average in a region or water body. They are indicated by ephemeral peaks of biomass and chlorophyll in the annual cycle of phytoplankton, when growth rates are higher than mortality (Assmy; Smetacek, 2009). The combination of physical and chemical elements favors algal blooms (Vollenweider, 1992) that reduces light availability at greater depths (Begon; Townsend; Harper, 2006) alter biotic communities in coastal waters, affecting benthic and demersal assemblages, cause water discoloration and increase anoxia (Kennish; de Jonge, 2011). Anthropogenic nutrient increment also results in HAB (high concentration of monospecific algae that produces toxic substances) raising ecological health risks (Glibert, 2017; Hwang, 2020). There are annual records of humans death due to consumption of seafood contaminated with toxins from HAB (Hallegraeff, 2004).

3 METHODOLOGY

Due to the chosen organization and subdivisions of this work, this chapter describes the general geomorphological characteristics of Araruama Lagoon in the section 3.1. The section 3.2 presents the methodological approach of the thesis and how it will lead to the attainment of the general objective. To avoid repetition of collection and analysis for water and sediment, these subjects are also presented in Section 3.2.

3.1 General characteristics of the study area

Araruama Lagoon (Figure 3) is a coastal choked lagoon (Kjerfve, 1994) presenting a watershed of 320 km^2, which includes the 210 km^2 of the waterbody itself. The geology (Figure 4) comprises Paleoproterozoic orthogneisses from Região dos Lagos Domain, and paragneisses from the supracrustal rocks of Búzios Complex. Plutonic alkaline rocks are associated with the event of the South Atlantic Ocean opening about 80 My BP. The Quaternary cover concord with the structural directions of the crystalline basement, whose embayment received sediments from the adjacent highlands. The transgressive events were not regular and continuous due to glacial activities and originated the lagoonal systems from Cabo Frio to Niterói (Turcq *et al.*, 1999; Souza; Schmitt; Stanton, 2017).

The lagoon system evolved from 123,000 years BP, the last Pleistocene interglacial stage, with the formation of the first sandy bars by waves (Silva, 2001; Turcq *et al.*, 1999). Biogenic carbonates indicate a sea level more than 100 m lower than the present, about 19,000 years BP in the Brazilian coast (Mahiques *et al.*, 2010; Veiga, 2005). Like other lagoon systems in Brazil, the lagoons of Região dos Lagos developed from 7,000 to 5,100 years BP, when inner and outer sandy barriers were formed (Martin; Landim Dominguez, 1994; Silva, 2001; Turcq *et al.*, 1999). The water covered the flat coastal areas while the sea level was 5 m higher and finally lowered to reach present level (Martin; Suguio *et al.*, 1996; Martin; Suguio; Flexor, 1993; Silva, 2001). Cuspate sand spit features delimit the lagoon in seven elliptical shapes developed later by the wave dynamic processes in the lagoon (Alves, 2006; Kjerfve *et al.*, 1996).

Figure 3 – Location of Araruama Lagoon

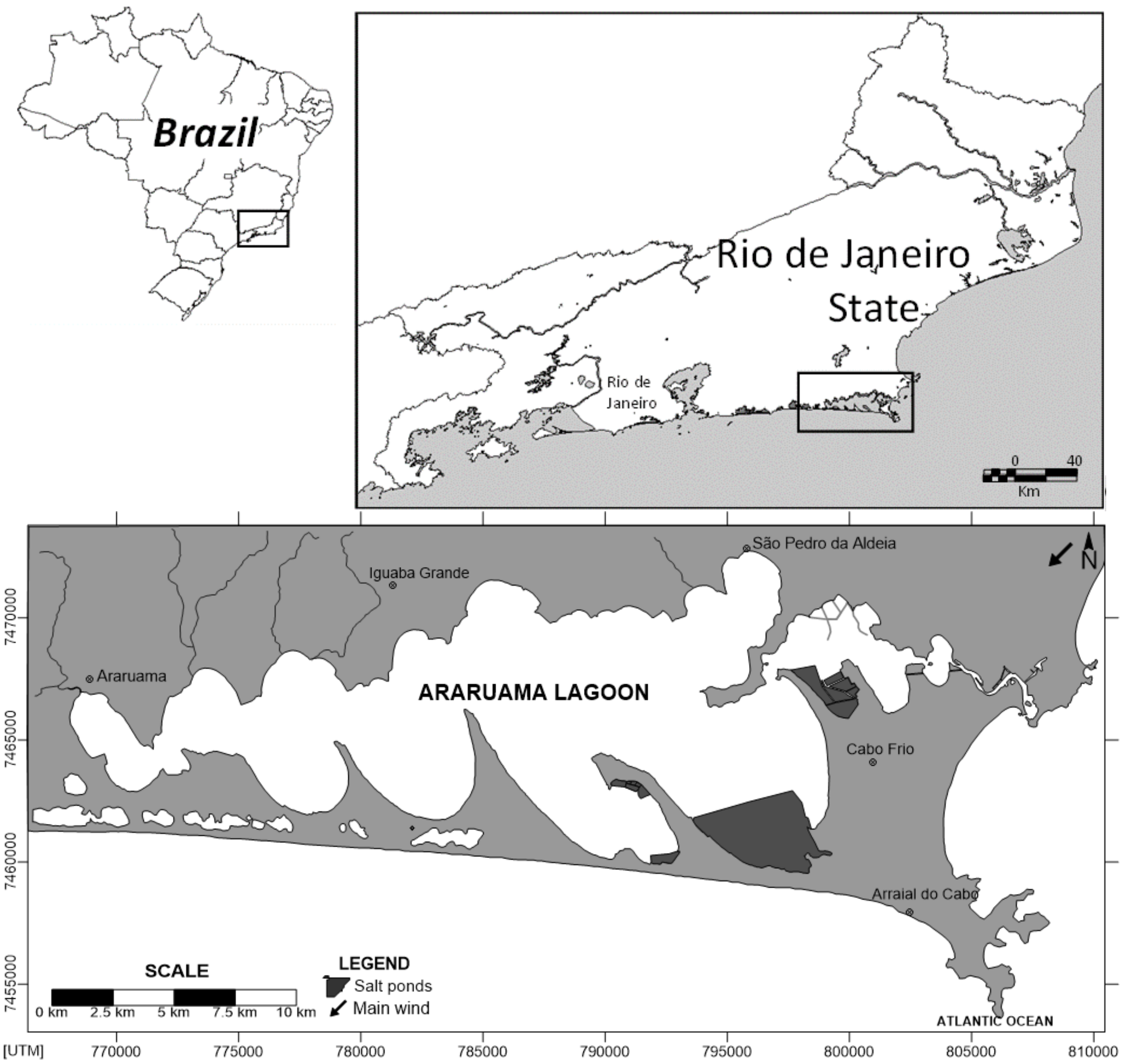

Source: Elaborated by the author, 2023.
LEGEND: Araruama Lagoon and the surrounding cities.

Figure 4 – Geology of Araruama Lagoon

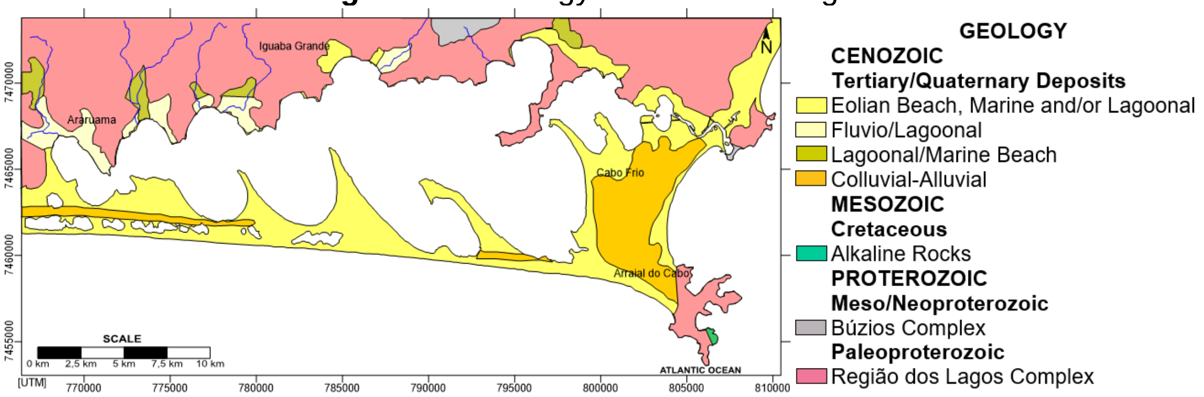

Source: Adapted from Kjerfve *et al.*, 1996; Silva, 2001.

Bathymetric studies revealed a shallow waterbody disposed along a longitudinal axis. The presence of paleo–channels near Sao Pedro da Aldeia embayment covered by muddy sediments suggests an ancient drainage erosion. Wind and erosion in the lagoon are associated with the cuspate features and dunes formation (Muehe, 2006). The local hydrodynamics is mainly determined by wind (up to 20 cm s^{-1}), and the tidal effect inside the lagoon is reduced by filtering of the Itajuru channel. Moreover, the wind circulation acts differently on each ellipsoidal cell in alternating cyclonic and anticyclonic circulation depending on the seasonal wind directions, NE or SW (Kjerfve; Oliveira, 2004). Also, these homogeneous internal cells (ellipsoids) control the nutrient distribution (Souza *et al.*, 2003; Vicente *et al.*, 2021). Trevisan *et al*. (2021) measured salinity and temperature using a CTD device and the profiles T-S confirmed the well mixing of water column (Appendix A).

Due to the filtering effect of Itajuru canal (connection with the ocean), the flushing half–life of the lagoon was calculated in 83.5 days, and it is considered long when compared with other local lagoons (Kjerfve; Knoppers, 1999). The water column is not stratified, including in the deepest areas, due to the strong wind that mixes well the lagoon (Kjerfve *et al.*, 1996; Trevisan *et al.*, 2021). The origin and maintenance of the hypersaline condition (salinity>35, according to Rich 2015) in Araruama Lagoon are due to: i) the semi-arid condition (Bsh - Köppen, according to Barbieri, 1975) with high evaporation rates and the proximity from the upwelling zone (Kjerfve *et al.*, 1996); ii) the small drainage basin and small freshwater inflows that are not sufficient to diminish the salinity (Kjerfve *et al.*, 1996); iii) the strangled and long Itajuru canal, a natural tidal filter and the only seawater entrance, does not favor the exchange within the lagoon (Knoppers; Kjerfve, 1999; Perrin, 1999).

Anthropic pressures in AL began after 1970, after the construction of Rio–Niterói Bridge, which reduced travel time by two hours. The lagoon was known for its beauty and recreational uses and, because of its hypersalinity, the lagoon has been considered a buffer for the eutrophication process (Kjerfve *et al.*, 1996). Lower salinity, higher amounts of nutrient loads, changes in soil use and population growth (Kjerfve; *et al.*, 1996; Souza *et al.*, 2003) resulted in environmental impacts, promoting a severe reduction in economic attractiveness. Changes in the salinity also affected primary production (Moreira–Turcq, 2000), zooplankton distribution (Rosa; Batista, 2020) and piscivore communities (Cruz; Santos; Santos, 2018). HABs were described by Oliveira *et al.* (2020) and were responsible for fish mortality episodes in the lagoon in 2005.

In 2009 and 2011, there were other two episodes of fish die-off and the Rio de Janeiro State Environmental Agency (INEA) collected and analyzed different parameters to identify the state of the water column in AL. The results were published by Vicente *et al.* (2021) and revealed that the quality of water was affected by sewage loadings. The authors observed that in an atypical precipitation period during summer 2010, there was a severe decrease in salinity, lasting for months and reflecting on the water quality. In 2019, 10 days after the first field campaign of the present work there was another fish mortality, indicating that the lagoon still faces serious environmental problems. Figure 5 shows some ecosystem services provided by Araruama Lagoon.

Figure 5 – Ecosystem services provided by Araruama Lagoon

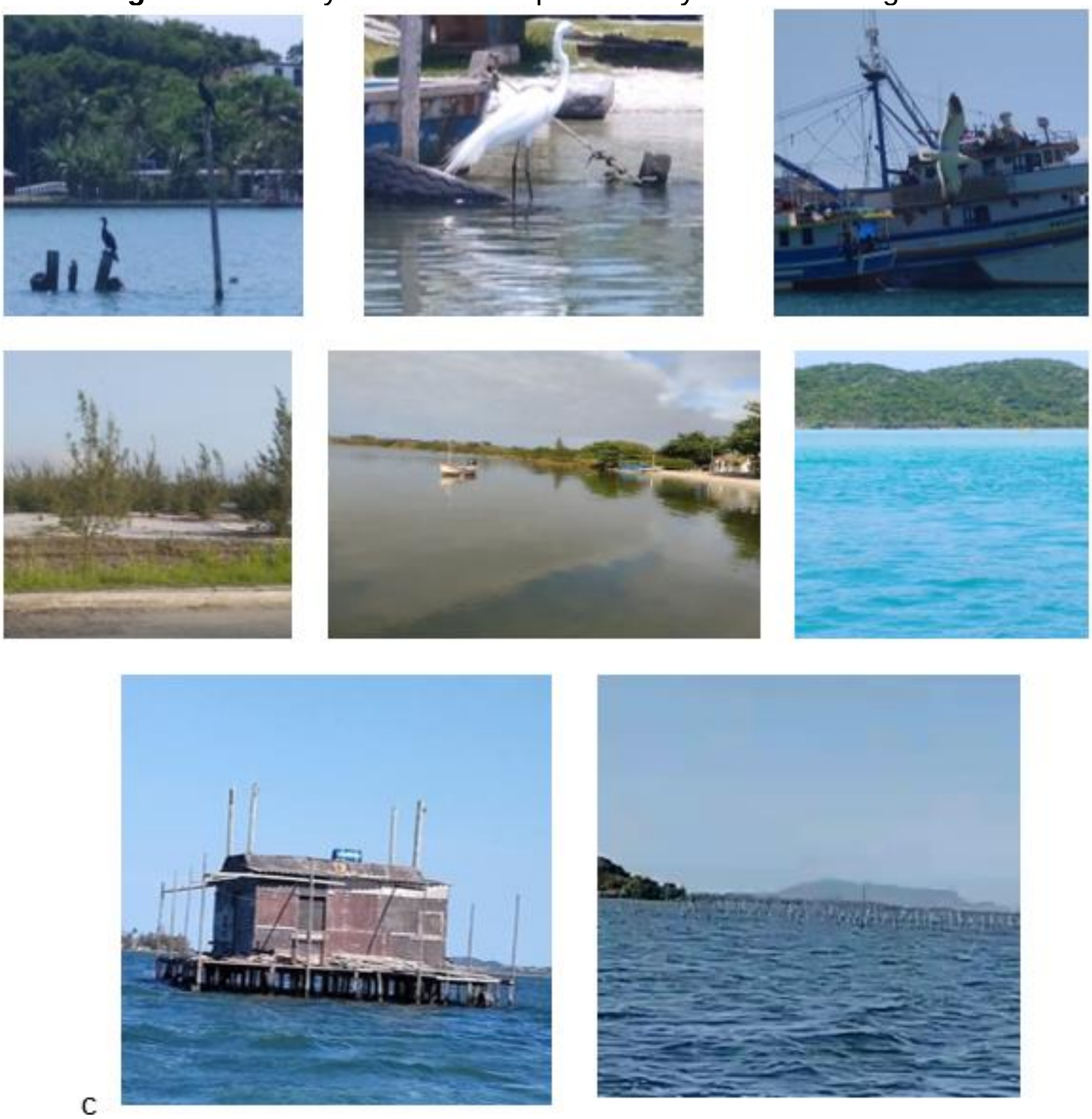

a

b

c

Source: Elaborated by the author, 2023.
LEGEND: Examples of ecosystem services provided by Araruama Lagoon. a) habitat for different marine birds; b) natural beauty; c) traditional fishing culture.

3.2 Methodological approach

An initial and important consideration about the methodological approach is that the research was developed in a joint effort among Universidade Federal Fluminense, the local watershed committee – Comitê da Bacia Hidrográfica Lagos/São João (CBHLSJ), and the local water treatment plant (ProLagos). The first campaign was part of a project to evaluate the trophic state in Araruama Lagoon to support calibration models for future environmental actions, led by Fundação Coordenação de Projetos, Pesquisas e Estudos Tecnológicos (COPPETEC). The subsequent campaigns were run under demands of the CBHLSJ, that reported any different water conditions. The thesis was the result of such commitment of different sectors of the society to understand the controlling factors of water quality in AL.

To cover the general objective of this thesis, the methodology included three different approaches (Figure 6), each one linked to an specific objective: i) trophic crises – descriptors of trophic crises that modified turbidity in the water column; ii) diffusive fluxes of nutrients at sediment–water interface – quantification of N and P forms present in the water column and the pore water in AL; and iii) phytoplankton requirements and main sources of nutrients – nutritional needs of primary producers and mass balance to identify the main supplying of nutrients in AL. Data used in each topic (Table 3) varied according to: i) trophic crises – water column from campaign 1 to campaign 9; ii) nutrient fluxes – sediment and water column from campaign 5 to campaign 9; and iii) phytoplankton from campaign 9.

Figure 6 – Methodological approach of the thesis

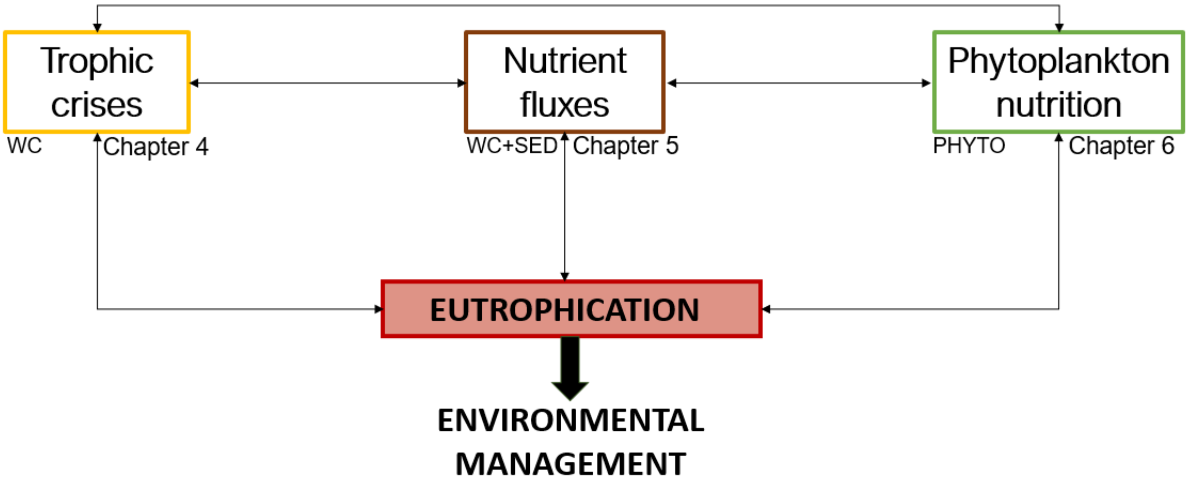

Source: Elaborated by the author, 2023.
LEGEND: Samples in each approach – WC= water column; SED= sediment; PHYTO=phytoplankton. The chapters 4, 5, and 6 indicate the respective specific objectives 1, 2 and 3.

Table 3 – Field campaigns

CAMPAIGN	DATE OF COLLECTION	SEASON
C1	Feb 12 and 13, 2019	Summer
C2	Jun 21, 2019	Winter
C3	Sep 24 ,2019	Spring
C4	Oct 10, 2019	Spring
C5	Mar 5 and 6, 2020	Summer
C6	Jun 17 and 18, 2020	Fall
C7	Jul 16 and 17, 2020	Winter
C8	Dec 11, 2020	Spring
C9	Sep 10, 17, and 18, 2022	Winter

Source: Elaborated by the author, 2023.
LEGEND: colored boxes follow the approach used in the thesis (Figure 6) . ▬ descriptors of trophic crises; ▬ nutrient fluxes; ▬ phytoplankton requirements and mass balance of the nutrients.

3.2.1 Water collection and analyses

We performed 9 field campaigns (C1 to C9; Chapters 4 and 5) in 2019, 2020 and 2022, and they covered different seasons and water column turbidity. Sampling collection and related material used in chapters 4, 5 and 6 varied according to Figure 6 and Table 3. As concluded by Vicente *et al.* (2021), the lagoon could be well characterized by 10 stations (Figure 7) and. Stations were distributed as follows: sea water control station outside the lagoon (P1, Praia do Forte) and 10 stations inside the lagoon (P2 to P11, one in each ellipsoidal unity). This sampling effort tried to cover spatial-temporal variations of the biogeochemical parameters of the lagoon and to improve the interpretation of its processes.

Water samples were collected in 9 field campaigns (C1–C9), Table 3, using a Van Dorn bottle for different depths. Samples were immediately filtered *in situ* by a Manifold filtration system, vacuum pump and Whatman™ GF/C glass microfiber filters (circa 0,7 µm aperture). Falcon tubes containing the filtered water were frozen for later analysis of dissolved nutrients. Filters were packed in petri slides and frozen until the analysis of the concentration of suspended particulate matter. In each station, pH and ORP (mV) were measured with a multi–probe Hanna®, DO with a multiparameter meter YSI, turbidity (NTU) with a Policontrol digital turbidimeter and the transparency of the water was obtained with a Secchi's disk. Salinity and temperature profiles were measured with a CastAway CTD (conductivity, temperature, and depth) from SonTek – YSI.

Figure 7 – Sampling stations

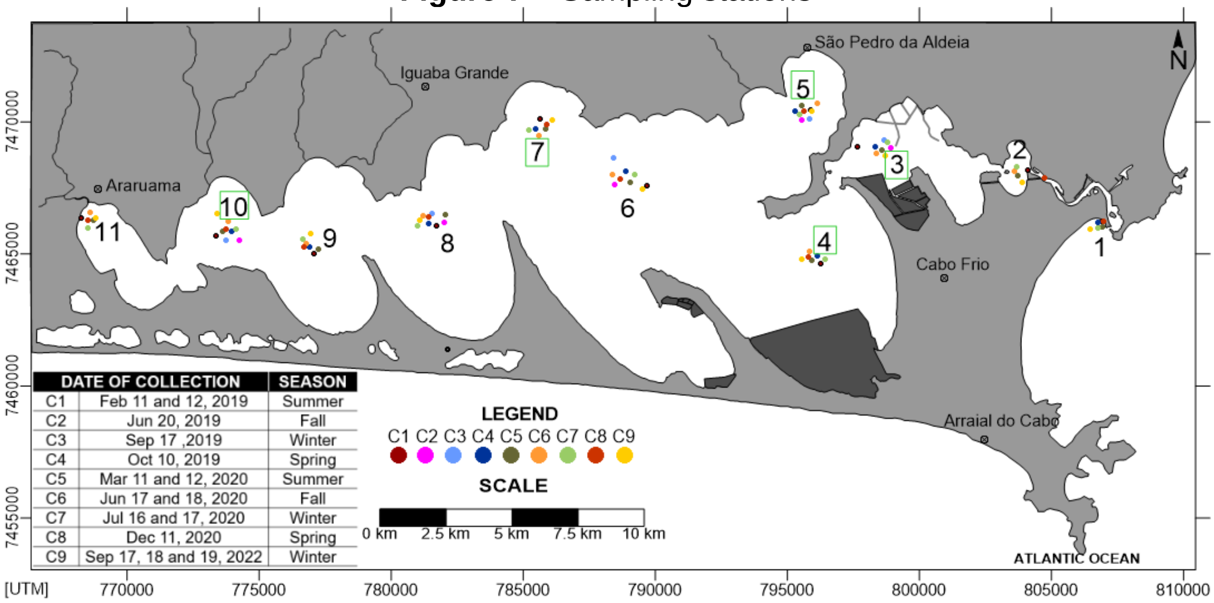

Source: Elaborated by the author, 2023.

LEGEND: Stations and date of the collection of the 9 campaigns. Green boxes indicate the stations where phytoplankton samples were collected (C9).

Dissolved fraction of both water column and pore water was analyzed for phosphate and ammonium (Grasshoff; Ehrhardt; Kremling, 1983), nitrite (Bendschneider; Robinson, 1952; Shinn, 1941), and nitrate (Zhang; Fischer, 2006). The analysis of suspended particulate matter included gravimetry, chlorophyll–a, phaeopigments and particulate organic carbon (Strickland *et al.*, 1972). Particulate nitrogen and phosphorus were also analyzed in the filters by oxidation with a persulfate solution. The resulting nitrate was analyzed according to Zhang and Fischer (2006) and the resulting phosphate was analyzed after Grasshoff; Ehrhardt and Kremling (1983). Detection limits of these procedures were presented in Table 4. Samples for BOD_5 were kept refrigerated at 20°C and in the dark and after 5–days incubation were analyzed according to Strickland *et al.* (1972).

Table 4 – Methods and detection limit (DL) of the analytical procedures

ANALYTE	DL	METHOD (REFERENCE)
Ammonium (µmol L^{-1})	0.17	Grasshoff; Ehrhardt; Kremling (1983)
Nitrite (µmol L^{-1})	0.04	Bend Schneider; Robinson (1952); Shinn (1941)
Nitrate (µmol L^{-1})	1.29	Zhang and Fischer (2006)
Phosphate (µmol L^{-1})	0.08	Grasshoff; Ehrhardt; Kremling (1983)
Particulate nitrogen (µmol L^{-1})	0.21	Zhang and Fischer (2006)
Particulate phosphorus (µmol L^{-1})	0.09	Grasshoff; Ehrhardt; Kremling (1983)
Chlorophyll a (mg L^{-1})	0.02	Strickland *et al.* (1972)
Phaeopigments (mg L^{-1})	0.04	

3.2.2 Sediment collection and analyses

From campaigns 5 to 9 (Chapter 5), measurements of temperature, pH, and ORP were made *in situ* using a multi–probe Hanna® electrodes previously calibrated (pH buffers 7 and 10; ORP – Hanna®). Dried sediment was used to determine granulometry (GRAN), carbonate (CARB) and organic matter contents (OM). Granulometry was analyzed using a digital particle analyzer CAMSIZER Rutsch® and class sizes were classified in a ternary diagram by Gradistat® software. Sizes were grouped in three main fractions (silt/clay, fine/medium sand, and coarse sand). Carbonate fraction in sediment was determined adding10 mL of HCl (1M) in glass beakers containing the samples, previously desalinated, dried, and weighted. The content is calculated by the difference between the dried weights before and after the HCl addition (Vieira–Campos; Costa; Yogui, 2017).

Total carbon (TC) from sediment samples were desalinated with deionized water and centrifuged, dried and then analyzed according to Strickland *et al.* (1972). Organic matter concentrations were determined adding H_2O_2 (1 M) to glass beaker containing the dried samples until the remaining material does not vary in mass. Phosphorus and nitrogen of sediment samples were determined after sediment was dried and weighted. Samples were oxidated using persulfate solution and total nitrogen and phosphorus were determined according to Zhang and Fischer (2006) and Grasshoff; Ehrhardt and Kremling (1983), respectively.

3.2.3 Phytoplankton collection and analyses

The method used to collect phytoplankton samples is described in the Chapter 6 because it is exclusive for the approach to phytoplankton requirements. However, analysis of particulate nitrogen and particulate phosphorus used to calculate the nutritional needs follow the same methodology used for water column characterization. Particulate nitrogen and phosphorus were analyzed by oxidation of the filters with a persulfate solution. The resulting nitrate was analyzed according to Zhang and Fischer (2006) and the resulting phosphate was analyzed after Grasshoff; Ehrhardt and Kremling (1983).

4 DESCRIPTORS OF WATER CONDITIONS DURING THE TROPHIC CRISES

Regarding the definitions of dystrophy presented in Chapter 1 (Wetzel, 1983; Valiela, 1984; Lenzi; Cianchi, 2022), and due to the lack of consensus about them, the term “trophic crises” is introduced in the present work. It refers to the abrupt shifts occurred in the water column in AL during this study, from high to low turbid conditions and vice-versa. As the trophic state is classified by different variables (Carlson, 1991), it is possible to identify changes in aquatic systems by quantification of such variables over time. Although trophic state is related to the nutritional conditions of the aquatic environment (Tugrul; Ozhan; Akcay, 2019), linking the phenomena (trophic crises) and the causes (responsible factors) is not as simple as it seems.

First, it is necessary to define clarity, because there are a variety of measurements for it. Turner; Fall and Friedrichs (2023) referred to clarity as the effect of light penetration and visible objects through water, measured by a variety of methods depending on the applications (Table 5). This work focused on Secchi depth, turbidity, chlorophyll *a* and total suspended solids because they were the methods available to measure the transparency of water. And despite water clarity is a property usually claimed to measure water quality, it is not the only one. Color, concentration of algae and inorganic turbidity are referred as displeasing by the public if they are associated with certain uses of the water bodies (Lee, Jones–Lee; Rast, 1995).

Table 5 – Methods for water clarity measurement

METRICS	METHODS (UNIT)	APPLICATIONS
General (apparent optical properties)	**Secchi disk depth** (m)	transparency/visibility
	light attenuation coefficients (K_d; m^{-1})	light penetration
	turbidity (NTU*[1])	light scattering
	beam attenuation (m^{-1})	proxy for POC
Component–basic (amount of components)	colored DOM (CDOM; m^{-1})	dissolved substances
	chlorophyll a (mg m^{-3})	primary production
	total suspended solids (mg L^{-1})	particle content

Source: Turner; Fall; Friedrichs, 2023.
LEGEND: *[1]Nephelometric Turbidity Units (USEPA, 1993). Bolded methods were measured in this work and will be described in the text.

Secchi depth is frequently related to the photic zone and is a function of reflection of light in the water and is affected by the amount of color, phytoplankton, and inorganic clastic materials (Wetzel, 1986)). Turbidity is the light scattering an is influenced by size and shape of suspended solids, the presence of phytoplankton, dissolved humic substances and dissolved mineral substances (Bilotta; Brazier, 2008; Branco; Kremer, 2005). Total suspended solids vary in size up to 0.45 µm and include both biogenic material and abiogenic particles (Turner; Millward, 2002). Chlorophyll *a* is commonly used as a proxy of primary production because it is the main pigment in phytoplankton and is easily measured by fluorescence (Turner; Fall; Friedrichs, 2023).

Fernández–Alías *et al.* (2022) and Webster and Harris (2004) pointed that when an assimilation limit is outpaced in an ecosystem, it triggers dystrophic crises. This abrupt changes lead to a system instability and causes shifts between top–down to bottom–up control due to nutrient overloads and change plant dominance from benthic to phytoplanktonic assemblages. Rapid P–cycling, refractory dissolved organic carbon or secondary production can trigger rapid changes in environments (Carpenter; Pace, 1997). Seasonal changes in phytoplankton reduce diversity and promote a fast grow of opportunistic species (sharp fluctuations) until a limit expressed by unfavorable conditions (Harris, 1986).

Other factor is the predator–prey interactions that are tied to size and growth rates and would improve the access of nutrient cycling through time (Behrenfeld; Boss; Halsey, 2021). Zooplankton, for example, exhibits different contents of C, N, and P if compared to phytoplankton assemblages (Kütter *et al.*, 2014). Pulses of bacteria usually happens during the senescent phase of a phytoplankton bloom in consequence of the increase of phytodetritus and releasing of dissolved compounds (Kennish; de Jonge, 2011; Lalli; Parsons, 1997).

Basset *et al.* (2013) determined important predictors for trophic crises in water (TP, CHL*a*, DO), sediment (NH_4^+, ORP, TN and TP), and phytoplankton (cell size and CHL*a*). Other descriptors are turbidity (Bilotta; Brazier, 2008; Lopez–Abbate *et al.*, 2019), wavelength dependance (Rose *et al.*, 2009; Danilov; Ekelund, 2001), DOC (Carpenter; Pace, 1997; Hessen; Tranvik, 1998), salinity and pH (Chandrasekara *et al.*, 2014), and fluctuations of dissolved oxygen and iron availability (Viaroli *et al.,* 2001). Metabolites found in sewage water (biotin, thiamin, vitamin B12) act as inhibitors or inducers of productivity and are modified by certain pollutants like detergents (Aubert, 1990).

4.1 Study area

Araruama Lagoon provide many ecosystem services (Esteves *et al.*, 2008) and it has been a touristic point for the last 5 decades. But lagoon underwent impacts by numerous anthropogenic activities as changes in land use, such as salt extraction and irregular urbanization (Costa; Seabra, 2021; Bertucci *et al.*, 2016; Carmouze; Barroso, 1989; Carvalho; Costa; Rosa, 2014; Costa *et al.*, 2022). In 2005, a sudden shift in water column color and transparency occurred and the original benthic primary producers were substituted by phytoplanktonic assemblages (Mello, 2007). After this event, negative consequences were recorded (Figure 8) and many works were conducted that identify these processes in water (Figure 9).

In 2019, a very turbid condition in water column in AL (Trevisan *et al*., 2021) was followed by an event of fish mortality 10 days later. Unexpectedly, in June (2019), an abrupt shift of water quality was observed, and an event of high transparency in the water column occurred. Shifts in water turbidity were registered for two years (this work) and it was possible to identify the main factors that affected the water transparency. Figure 10a shows the point where the pictures were taken to exemplify the two distinct turbidity conditions in AL: a turbid condition (Figure 10b) and a non-turbid condition (Figure 10c).

Figure 8 – Timeline of the impacts caused by changes in water conditions in AL

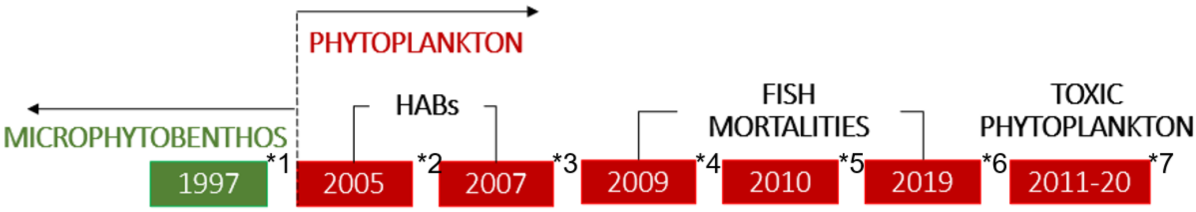

Source: *[1]SOUZA, 1997; *[2]MELLO, 2007; *[3]SOUZA, 1997; *[4]INEA; *[5]INEA; *[6]10 days after the first campaign of the present work; *[7]NEVES, 2011-2020.
LEGEND: After the shift from benthic microalgae to phytoplanktonic assemblages in 2005, the episodes of HABs, fish mortalities, and the presence of toxic phytoplankton were observed. The episode of fish mortality in 2019 occurred 10 days after the first campaign of this work.

Figure 9 – Timeline of some studies conducted in AL by different authors and their findings

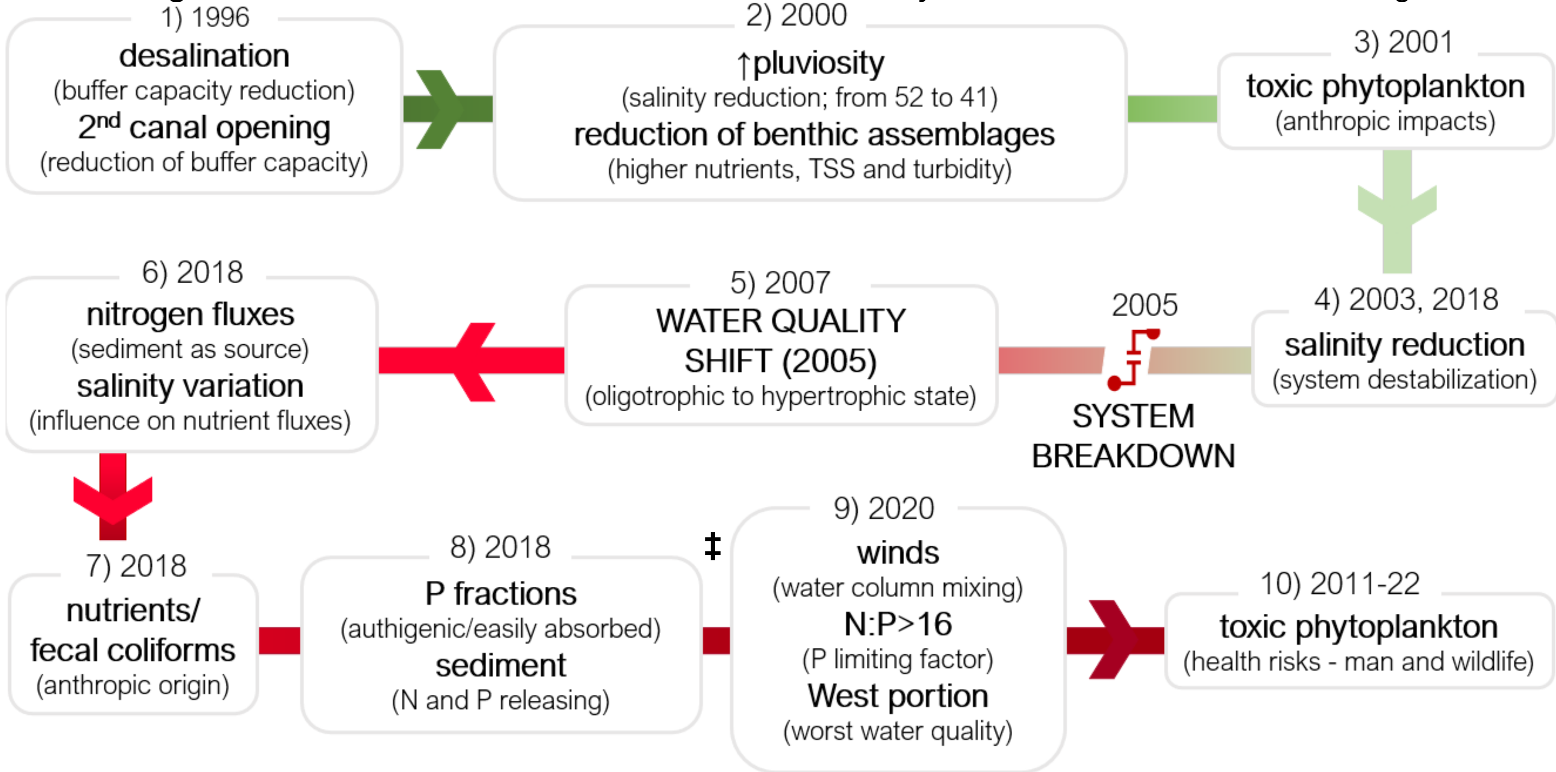

Source: Elaborated by the author, 2013.

LEGEND: Graphic emphasizing the studies and main conclusions of some studies in AL. Following the sequence of boxes, the studies reported: **1)** the desalination could diminish the buffer capacity of water column and the opening of a second channel at the west side would reduce the water quality (Kjerfve *et al*., 1996). **2)** A high pluviosity year reduced the water salinity and the decrease of benthic microalgae enhanced TSS and turbidity (Moreira-Turcq, 2000). **3)** the first observation of the presence of toxic phytoplankton related to the anthropic impacts (Sylvestre *et al*. 2001). **4)** the reduction of salinity would promote destabilization of the system (Carvalho, 2018; Cunha, 2003; Debeney *et al.* 2001). **5)** anthropic activities caused intense entry of organic matter in the AL system, triggering the shift of the trophic state (MELLO, 2007). **6)** Sediment would be the source of positive diffusive fluxes of nitrogen and salinity variation would influence the benthic fluxes (Guimarães, 2022). **7)** The origin of the nutrients and the fecal coliforms were identified as being from anthropic activities (Vicente *et al.* 2020). **8)** Identification of phosphorus fractions in sediments (mostly authigenic and easily absorbed) and the potential of sediments to release N and P (Silva, 2019; Silva *et al*. 2019). **9)** CTD data confirmed the good mixing and oxygenation of water column, dissolved nutrients data corroborated the P limiting of primary production, and the poor water quality in the west portion of the lagoon due to hydrodynamic and anthropic pressure (Trevisan *et al.* 2020). **10)** Monthly reports showed the presence of toxic phytoplankton species (Neves, 2011-2022). **‡** Fish die-off (10 days later the first campaign of this thesis).

Figure 10 – Pictures of the same point showing the two different water conditions

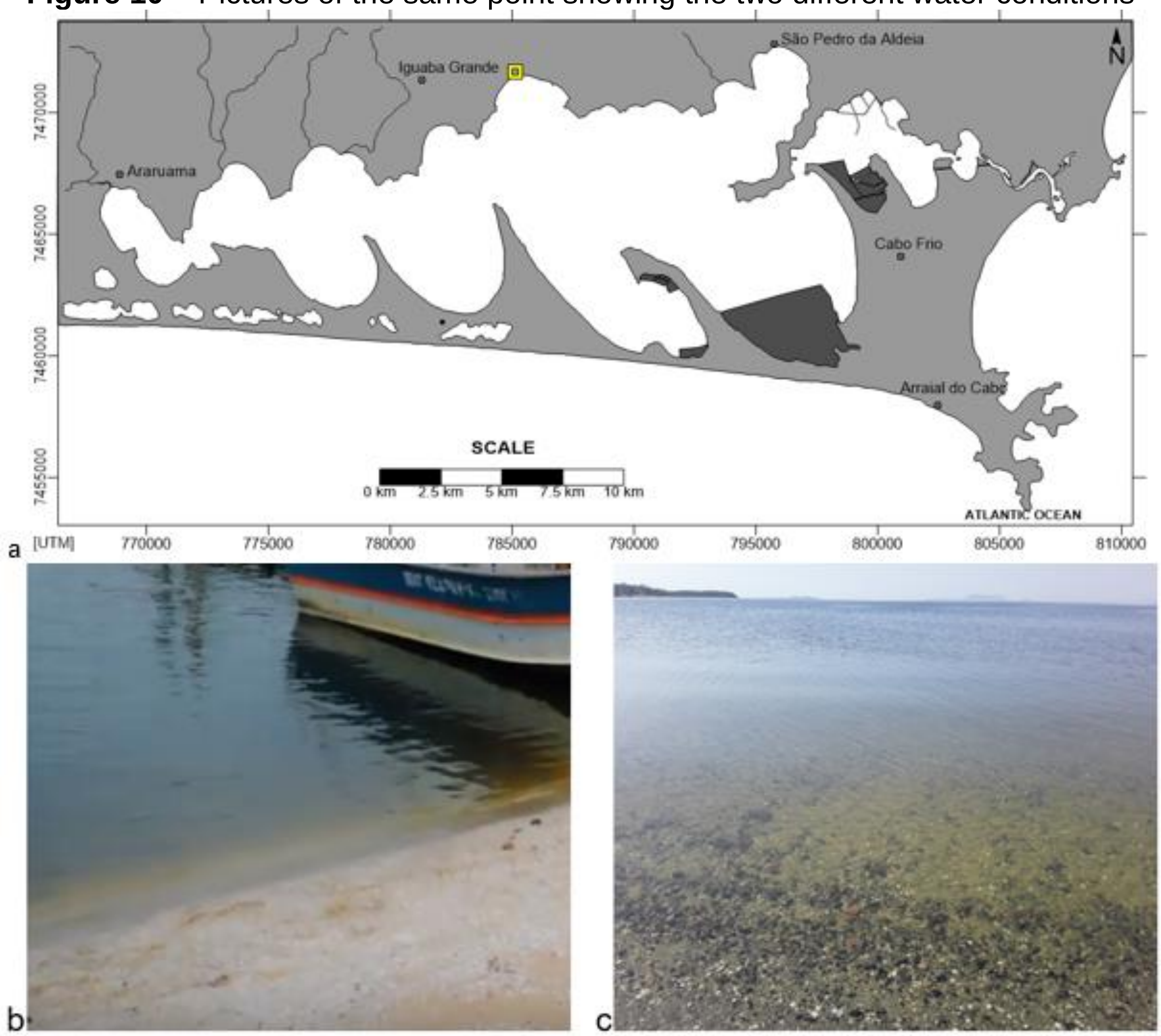

Source: Elaborated by the author, 2023. Pictures are from the author's file.
LEGEND: a) Map of AL showing the point where pictures of Figure 10b and 10c were taken (yellow square). b) C1 (turbid condition); c) C2 (non-turbid condition). In C1, the high turbidity does not allow to see the bottom at the shoreline, while in C2, the bottom can be seen for a larger distance from the shoreline due to non-turbid conditions.

4.2 Materials and methods

Because water transparency involves different measurement criteria (Table 6), a first statistical approach was to investigate some possible scenarios and their relationship with Secchi. In a satellite remoting study run by Braga; Vianna and Kjerfve (2003), points where SEC were equal to total depth were excluded to not underestimate water transparency. However, due to the approach of the thesis, all SEC were included in statistical analysis to characterize water conditions. The initial consideration was that parameters would present similar ranges of data depending on turbid/non–turbid conditions and specific minimum and maximum limits of Secchi depth. These ranges and limits would indicate the group of descriptors of each condition.

Table 6 – Suggested scenarios to analyze trophic crises in AL

SCENARIO	NOMINATION	TYPE OF DATA
1	total data	all parameters, campaigns, and depths
2	surface data	all parameters and campaigns, only surface depth
3	bottom data	all parameters and campaigns, only bottom depth
4	turbid (SEC≤1.0 m)	all parameters and depths of campaigns C1 and C5
5	non turbid (SEC≤1.0 m)	all parameters and depths of campaigns C2, C3, C4, C6, C7, C8, C9
6	mean data	mean values of all campaigns from surface and bottom, assuming the well mixed condition of AL
7	station data	all parameters, campaigns, and depths

Source: Elaborated by the author, 2023.

4.3 Results

4.3.1 Basic statistics

Basic statistics (Table 7) detail the variation of the values in all campaigns, according to Appendix A (Table A1.1 to A1.3). The highest variations are observed in ORP, TSS, POC and N:P ratios. Outliers are more frequent in non–turbid water for the same parameters. The suggested methodology did not identify properly the groups previously hypothesized, possibly due to some parameters were below of detection limit. Hence, Secchi was chosen as the guide parameter according to the scenarios 4 and 5 to investigate the descriptors for dystrophic processes. The choice was made regarding the mentioned methods to determine transparency, and due to SEC is easy to be visually detected and collected. To standardize the nomenclature, hereafter C1 and C5 are called turbid water condition and C2 to C4 and C6 to C9 are referred as non–turbid water condition.

Due to the number of studied parameters, results were separated in three groups and Secchi only composes the first group due to the criteria cited above. The second (physical–chemical) includes pH, ORP, DO, DBO_5, SAL, TEMP, TURB, and TSS; and the third (nutrients and primary production) comprises NH_4^+, NO_2^-, NO_3^-, PO_4^{3+}, DIN, N:P, PN, PP, CHL*a* and PHAEO. Stations 1–11 (X axis) were disposed in reverse order to respect the orientation of points in field campaigns and make the spatial visualization easier. As well as the sample depths are referred as S (surface), M (middle) and B (bottom), and a doble arrow indicates the W-E direction.

Table 7 – Basic statistics for water column (total data)

PARAMETERS	VALID n	MEAN	MINIMUM	MAXIMUM	STD. DEV.
DEPTH (m)	156	5.41	0.30	14.20	3.34
SEC (m)	156	1.33	0.30	3.80	0.80
pH	150	8.13	7.20	9.92	0.30
SAL	154	48.82	33.13	67.01	8.21
TEMP (°C)	151	26.23	19.80	30.76	2.78
ORP (mV)	154	54.45	–90.20	242.10	62.14
TURB (NTU)	138	8.58	0.39	57.70	8.63
TSS (mg L^{-1})	146	141.72	4.00	419.28	89.42
DO (mg L^{-1})	151	8.90	3.29	16.80	1.64
BOD_5 (mg L^{-1})	151	2.35	0.03	12.60	1.96
CHL *a* (mg L^{-1})	155	0.06	0.02	1.55	0.14
PHAEO (mg L^{-1})	155	0.05	0.04	0.28	0.03
POC (mg L^{-1})	145	27.00	0.07	435.00	51.50
PN (mg g^{-1})	155	41.35	0.03	1923.03	188.87
PP (mg g^{-1})	155	25.24	0.12	747.35	76.52
NH_4^+ (µmol L^{-1})	155	4.43	0.17	64.22	8.59
NO_2^- (µmol L^{-1})	155	1.97	0.03	8.22	1.98
NO_3^- (µmol L^{-1})	137	6.08	1.29	23.79	4.58
DIN (µmol L^{-1})	155	11.78	1.55	76.95	10.06
PO_4^{3-} (µmol L^{-1})	155	0.29	0.08	2.68	0.34
N:P	155	82.55	3.38	630.22	85.24

Source: Elaborated by the author. 2023.

4.3.2 Secchi transparency depth

Secchi depth (Figure 11) varied from 0.3 to 3.8 m, and in turbid water (C1 and C5) the values did not exceed 1m, except at the station 1 (control point outside the lagoon) where values always reached the total depth. The maximum Secchi depths in non–turbid water varied independently of the total depth. Turbid water presented the smallest values among campaigns maybe due to the seasonality and increase of population in summer. It is important to note that in 2020 (C5–C8) there was the lockdown due to COVID–19, however the pattern of SEC depths was the same. It means that SEC was smaller in summer and higher in the other seasons. The western portion of the lagoon generally presented smaller SEC values (≤1.0 m) than other portions, while transparency was higher at the central sector (SEC>1.0 m). It is possibly related with geomorphological characteristics and anthropic impacts in western sector as pointed by Vicente *et al*. (2021) and Trevisan *et al*. (2022).

Figure 11 – Secchi depth

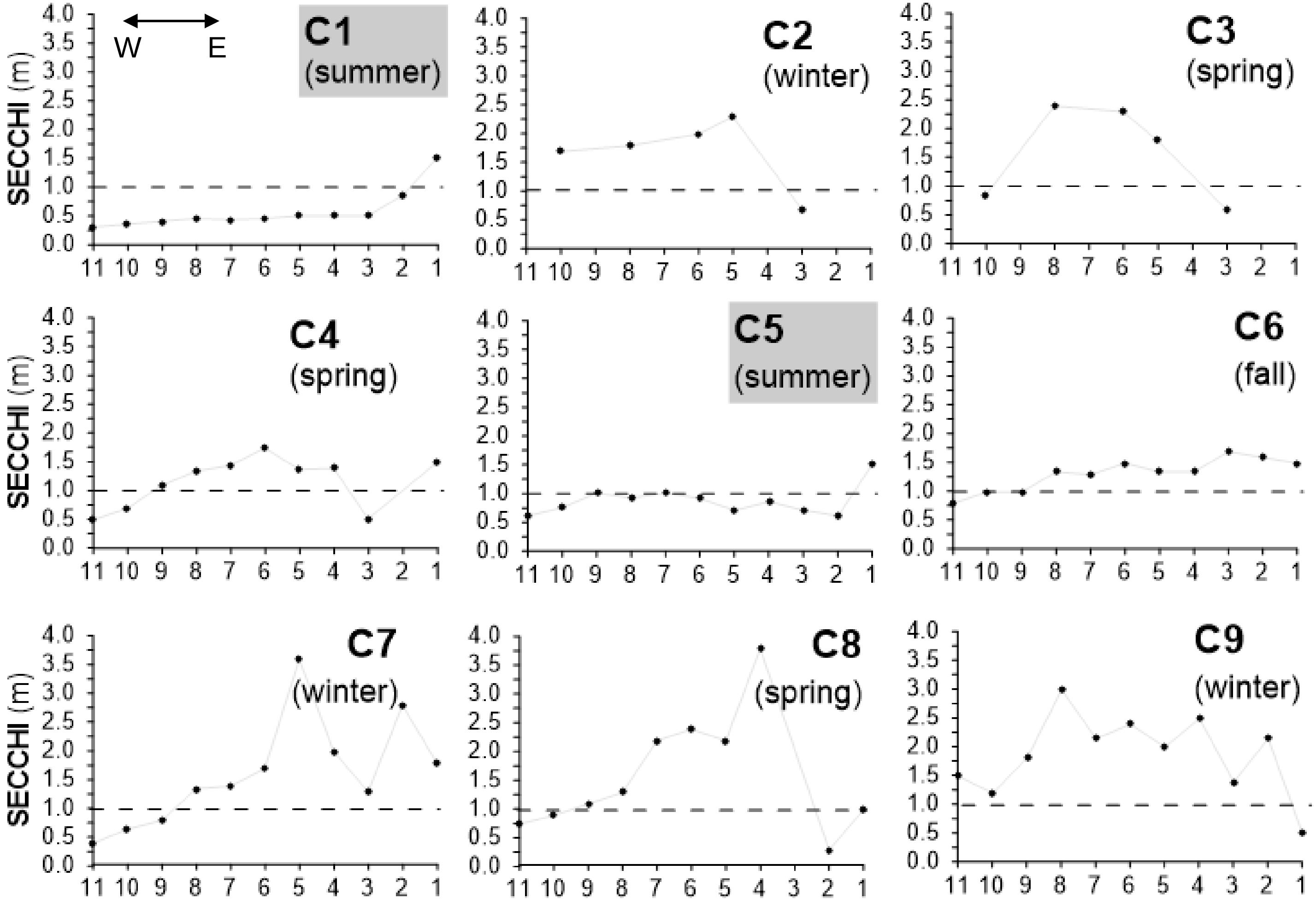

Source: Elaborated by the author, 2023.

LEGEND: Dashed line indicates the 1 m Secchi's disk. SEC≤1 m= turbid condition (C1 and C5, gray boxes); SEC>1 m=non-turbid condition. The highest value reached 3.8 m in C8, station 4 (non–turbid water). Higher variation was verified in the central portion of the lagoon where higher depths allowed to observe the greater differences among SEC measurements. There was a tendency to decrease SEC values in western portion of the lagoon, while the lower values in the eastern sector (stations 2 and 3) were due to the tides.

4.3.3 Physical–chemical parameters

Graphics of pH, ORP, DO, and BOD_5 are in Appendix B (Figure B2.1 to B2.4) and only description of these parameters are described in this section.

Values of pH (Appendix B, Figure B2.1) did not show significant differences and presented a slightly increase to west among campaigns. Most values varied between 8 and 9, and values of 7.3 (C7; P4) and 10 (C9; P10).

Despite ORP (Appendix B, Figure B2.2) was similar at surface and bottom, and most values were positive, there was great variability among campaigns and stations.

AL presented high values of DO (Appendix B, Figure B2.3) as it was expected due to the strong winds, and most samples were similar at surface and bottom.

DBO_5 (Appendix B, Figure B2.4) presented small values and variations which was expected because of strong winds. Western portion of AL usually presented a tendence to increase values and DBO_5 exhibited similar behavior of DO.

Salinity is an important parameter in AL, and due to the local conditions, the lagoon is permanently hypersaline (>35) (Kjerfve *et al*., 1996). In this study, salinity distribution (Figure 12) presented two remarkable features: a spatial salinity gradient related with the W–E axis, and a temporal decrease salinity among campaigns. According to the gradient, three sectors were observed; i) eastern sector (stations 1 to 3) – seawater values (32-35); ii) central sector (stations 4 to 8) – highest values in the lagoon (50-70); and iii) western sector (station 9 to 11) – intermediate values (35-50). An exception to this pattern was at station 11 (C1) which presented the highest value of all campaigns (67) and the smallest in C8 (33.1). Surface and bottom exhibited similar behavior and values decreased from C2 to C9.

Temperature (Figure 13) presented seasonal variation with higher values in turbid water (summer, 25–33 °C) and lower in non–turbid water (21–28 °C). In an unexpected warmer winter (C7), temperature was similar to summer. Despite the variability, in general, values were slightly higher in western portion of the lagoon.

Values for TURB (Figure 14) were similar between surface and bottom, despite the spatial–temporal variation, generally more turbid to the western sector. The smaller TURB values were coincident with higher SEC, indicating a non–turbid condition, and the opposite behavior was observed for turbid conditions.

Figure 12 – Salinity

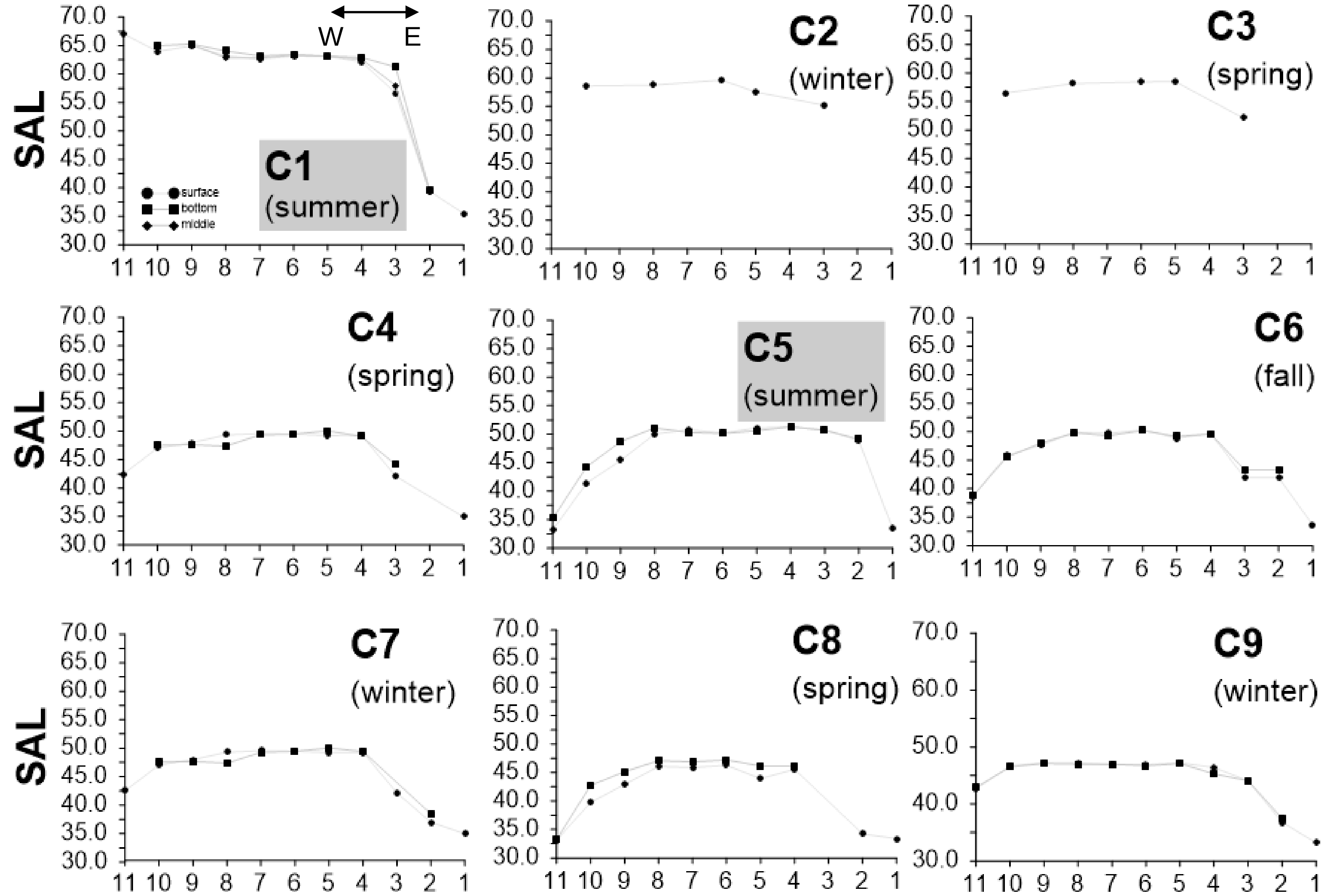

Source: Elaborated by the author, 2023.

LEGEND: Salinity decreased from C1 to C9. Three distinct sectors in AL were observed according to a salinity gradient – marine (stations 1–3; 32–35); hypersaline (stations 4–8; 45–70) and intermediate (stations 9–11; 35–50).

Figure 13 – Temperature

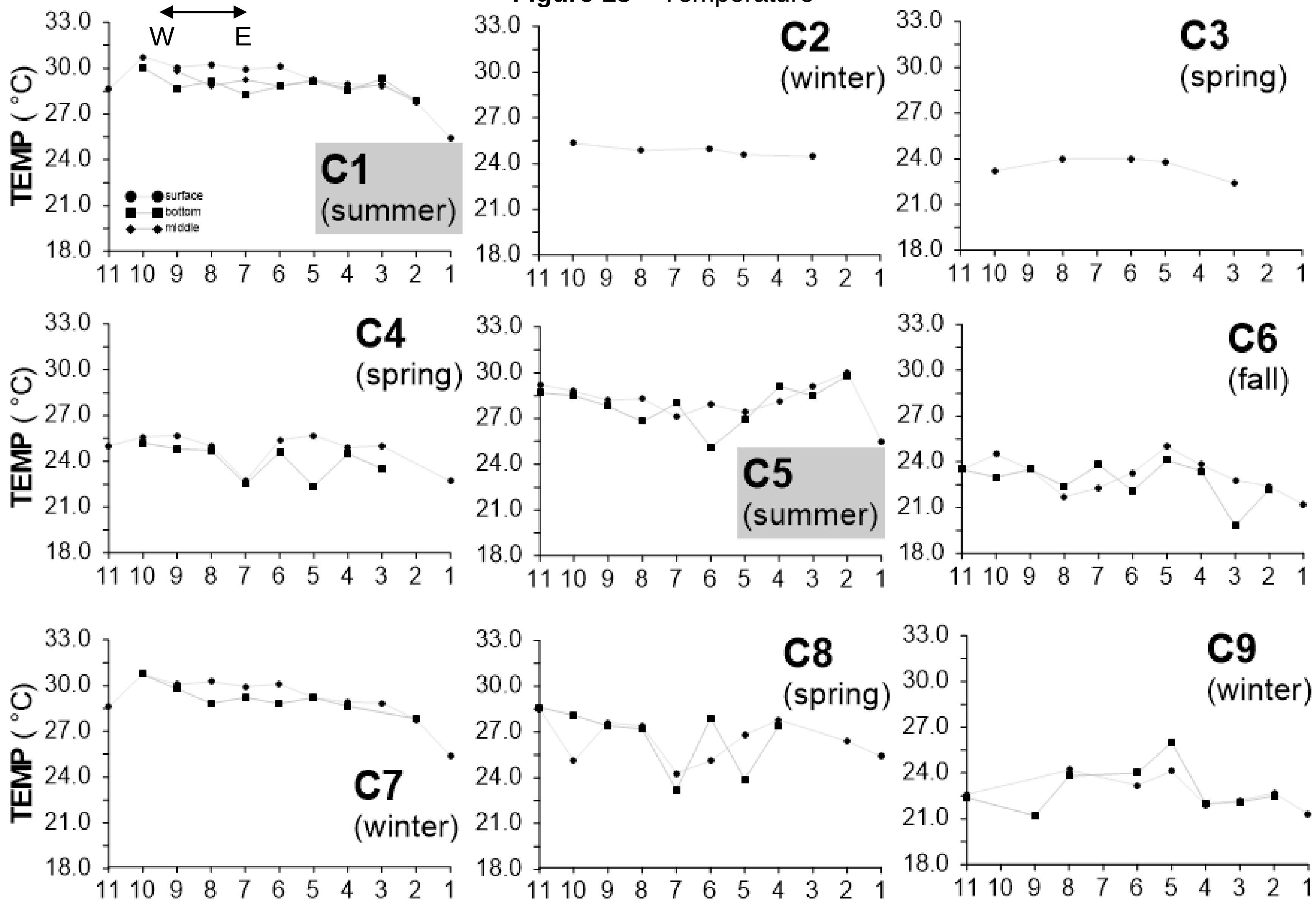

Source: Elaborated by the author, 2023.

LEGEND: Temperature varied seasonally, and turbid conditions (highlighted by gray boxes) presented higher temperatures (summer), however C7 (winter) showed an unexpected high temperature similar to the summer. Temperatures were smaller in the remaining campaigns.

Figure 14 – Turbidity

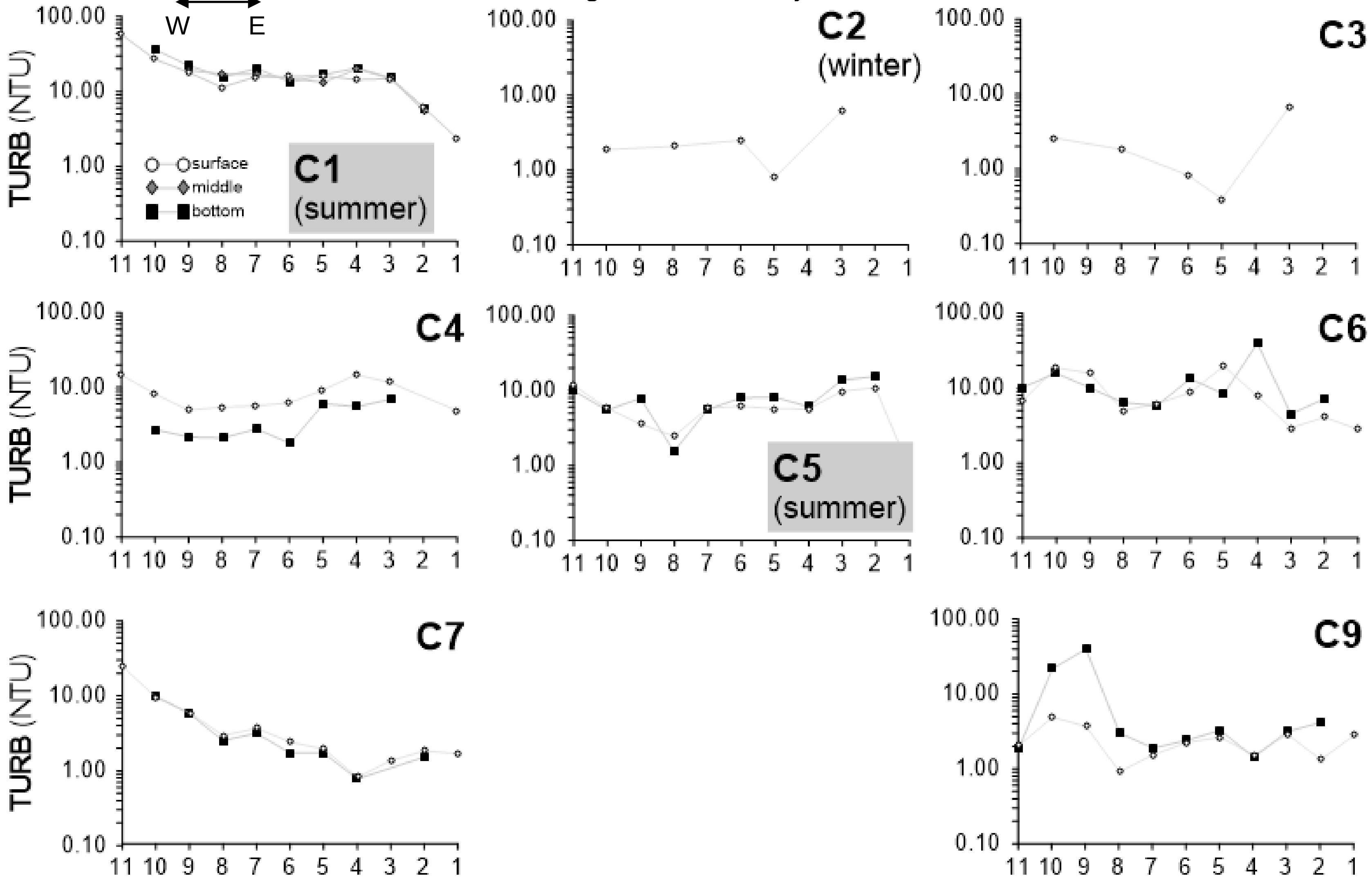

Source: Elaborated by the author, 2023.

LEGEND: Despite the variability, TURB tended to be greater in C1 and C5 (summer) and smaller in the other seasons. Values varied from 0.39 to 57.70 NTU.

TSS (Figure 15) presented high variability in depth, stations, and campaigns except for C2 which presented small values and variability which was related to the high transparency. No evident pattern was observed, and measurements were not in agreement with results from SEC and TURB.

4.3.4 Nutrients and primary production

Ammonium (Figure 16) varied spatially and temporally and higher values were generally distributed in the central area of the lagoon, but many stations presented values smaller than the detection limit.

The distribution of nitrite+nitrate, here after called N_{ox}, in AL (Figure 17) was higher values in turbid water and concentration diminished in non–turbid campaigns.

Variation of DIN in AL (Figure 18) shown higher values generally distributed in central portion of the lagoon and highest values were in C5 and C9. C1, C2, and C3 presented small variation among points, which did not happen in other campaigns.

Phosphate (Figure 19) was smaller than 3.0 µmol L^{-1} including values below of detection limit (0,08 µmol L^{-1}).

Despite the spatial–temporal variation of particulate nitrogen concentration among campaigns, (Figure 20), varied similarly between surface and bottom depths. The central sector exhibited the higher concentrations, while the smallest and the highest values were found in non–turbid waters. Values varied from 0.02 mg g^{-1} (station 3, C3) to 760 mg g^{-1} (station 4, C6).

Higher values of particulate phosphorus (Figure 21) were generally found in the central portion of the lagoon. The distribution of PP is coincident with PN, except in C2 and C3 (the first occurrences of non–turbid waters). The smallest value was 0.10 mg g^{-1} (C3, station 6) and the highest was 505 mg g^{-1} (station 5 C9), both in non–turbid water.

N:P ratios (Figure 22) varied widely spatially and temporally, and few points were below of 16:1 in C1, C4, C7 and C9, confirming the P–limitation in AL. The highest N:P ratio reached up to 560 in C9.

POC (Figure 23) presented high variation among campaigns and stations and there was a tendence of values diminish from turbid to non–turbid water, even with high variation. Non–turbid water presented the smallest values (0.37 mg g^{-1}), and the highest values (440 mg g^{-1}).

Figure 15 – TSS

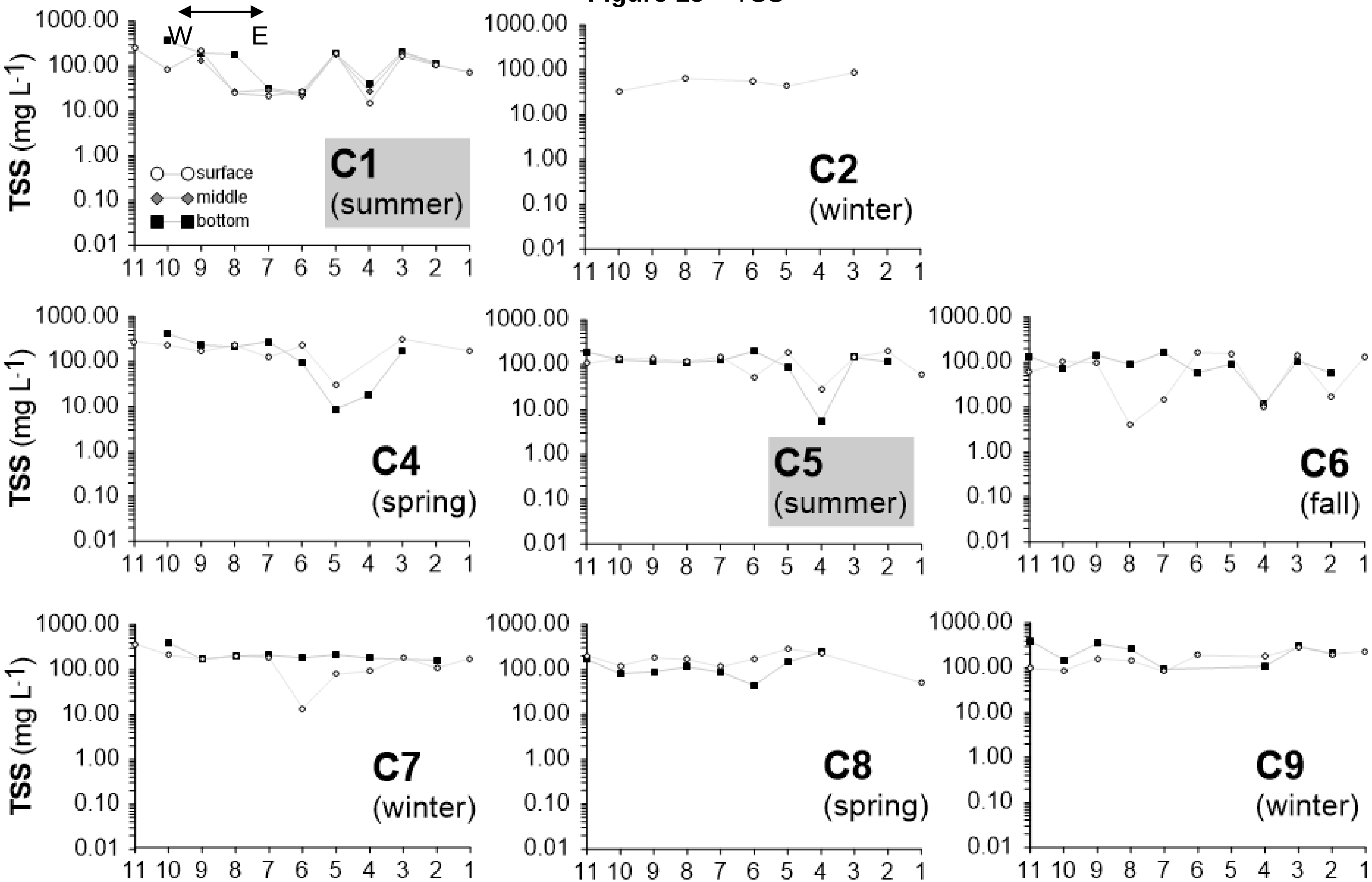

Source: Elaborated by the author, 2023.

LEGEND: TSS presented high spatial and temporal variation, and the highest value (station 10, C4) was circa 425 mg L^{-1}. TSS did not vary following TURB or CLH *a* behavior as it was expected.

Figure 16 – Ammonium

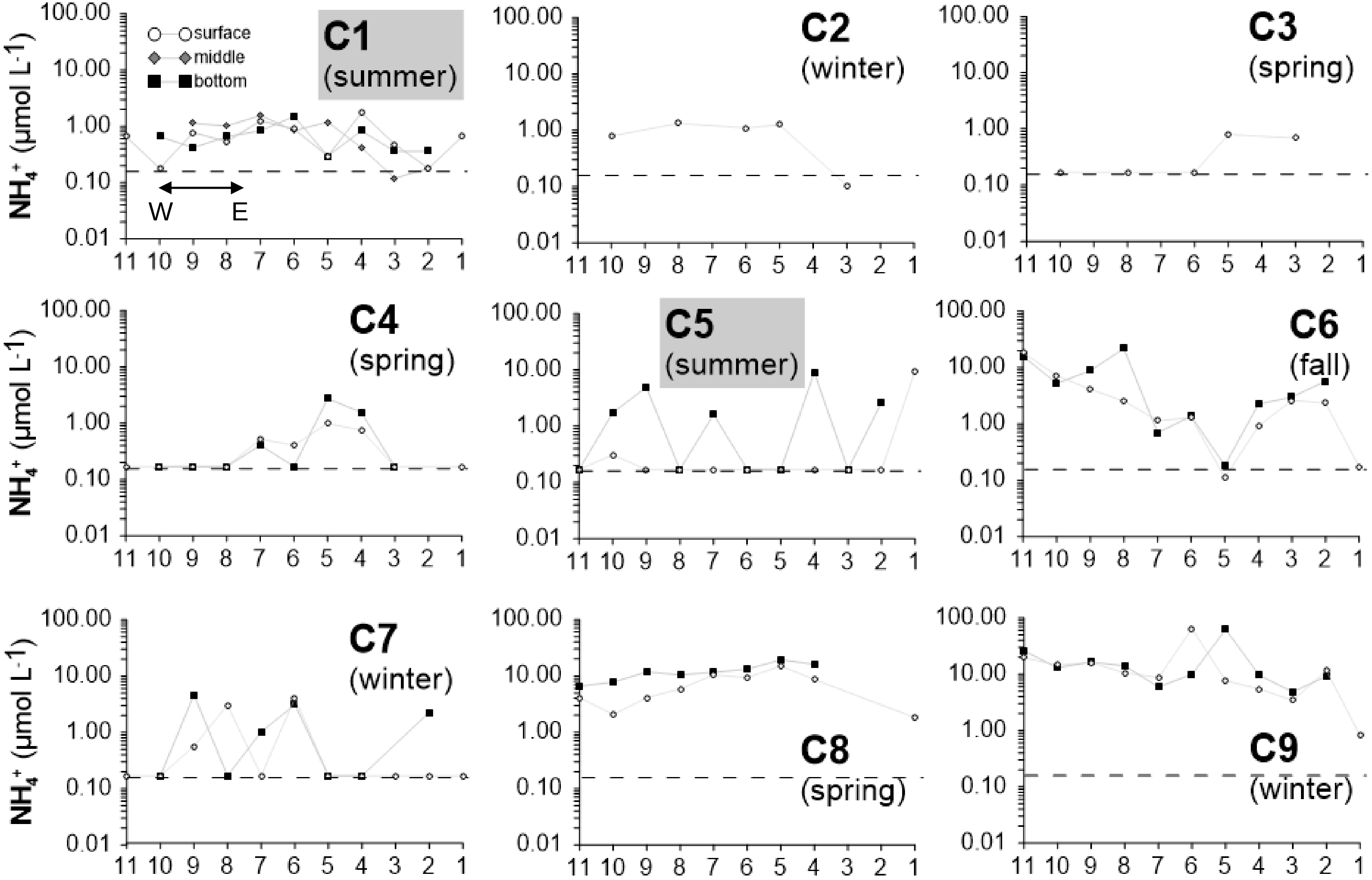

Source: Elaborated by the author, 2023.

LEGEND: Dashed lines indicate the detection limit of the method. Ammonium presented values smaller than 10 µmol L^{-1}, including values below the detection limit, and the highest values (stations 5 and 6, C9) reached about 65.0 µmol L^{-1}.

Figure 17 – N_{ox} (Nitrite + Nitrate)

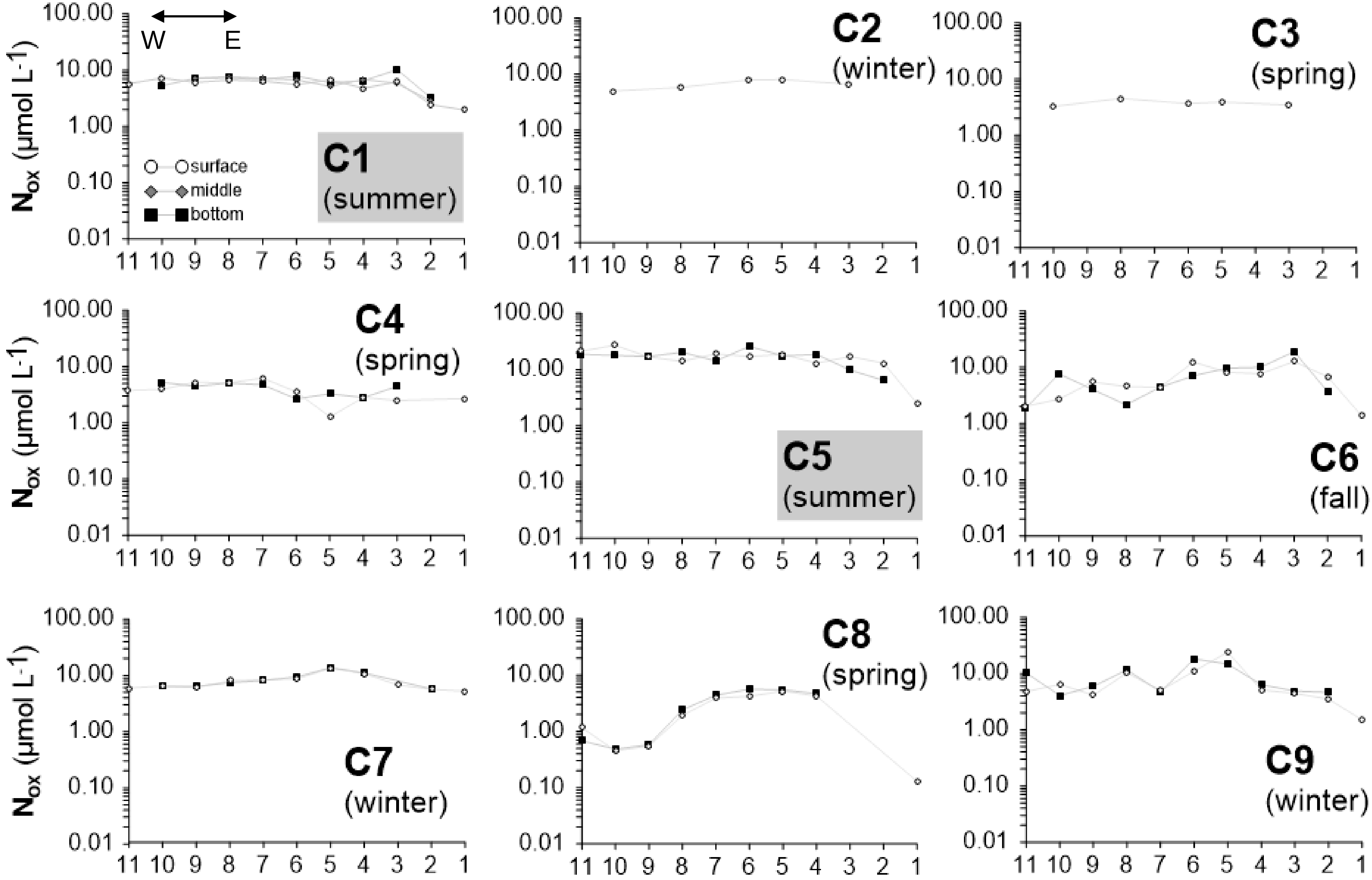

Source: Elaborated by the author, 2023.

LEGEND: Nox presented most values smaller than 20 µmol L⁻¹, and the highest value (station 10, C5) reached 27.5 µmol L⁻¹. In a general way, Nox was higher in turbid conditions.

Figure 18 – DIN

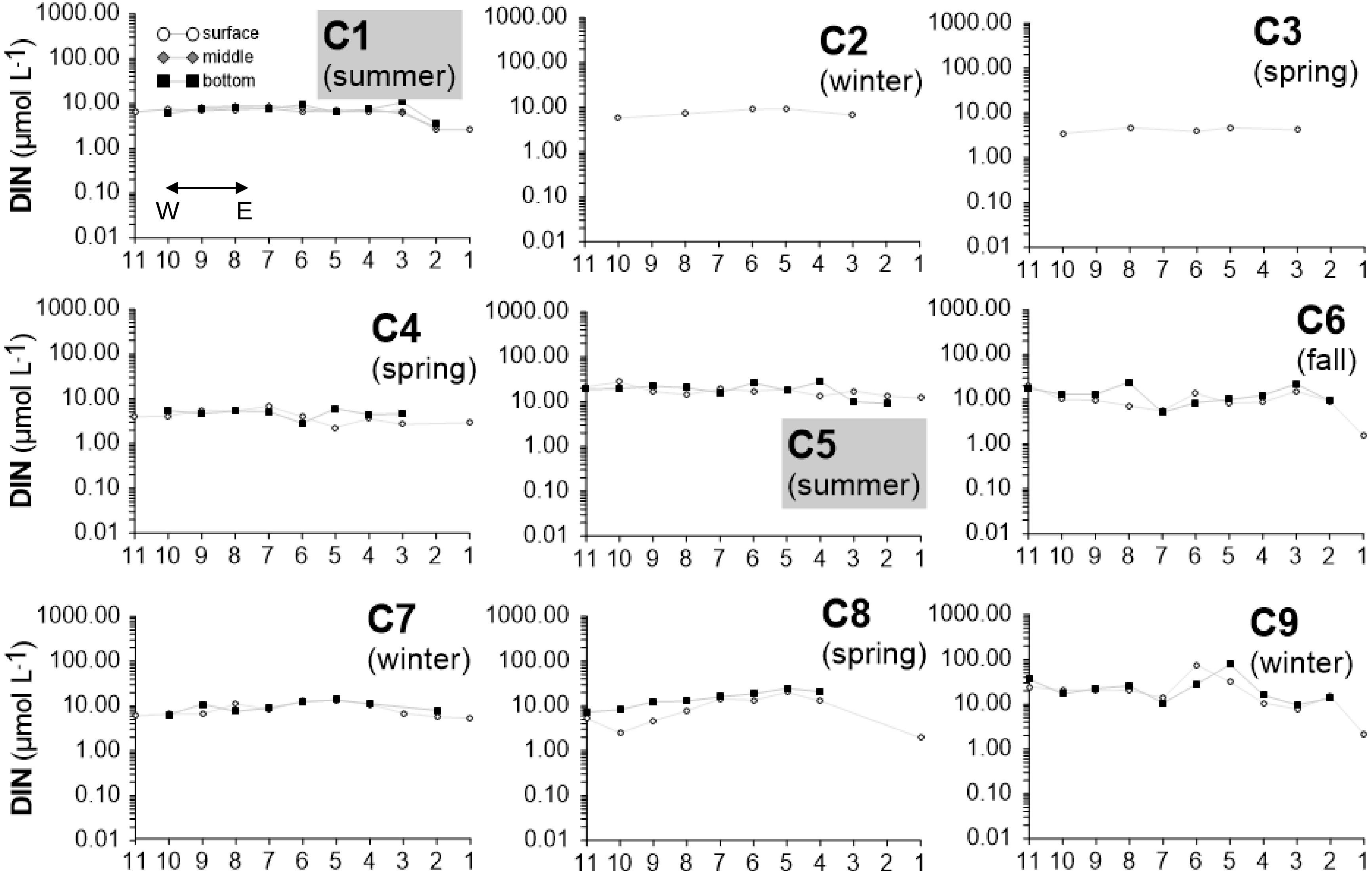

Source: Elaborated by the author, 2023.

LEGEND: DIN presented values smaller than 30 µmol L^{-1}, and the highest value (station 5, C9) was 80.0 µmol L^{-1}. Source: Elaborated by the author, 2023.

Figure 19 – Phosphate

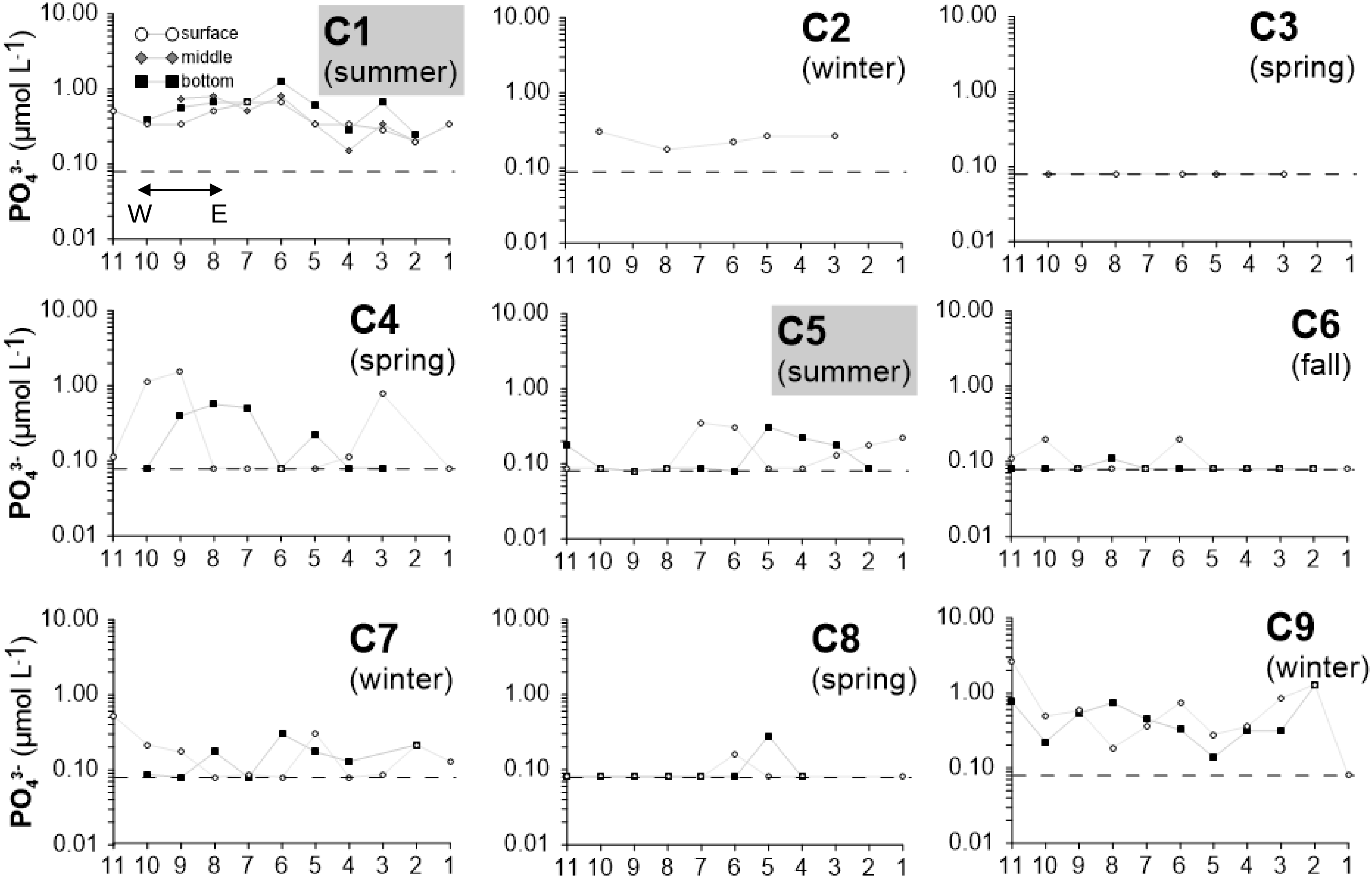

Source: Elaborated by the author, 2023.

LEGEND: Dashed lines indicate the detection limit of the method. Phosphate presented most values lower than 0.4 µmol L^{-1}, including stations below of the detection limit. The highest value (station 11, C9) reached 2.7 µmol L^{-1}.

Figure 20 – Particulate nitrogen

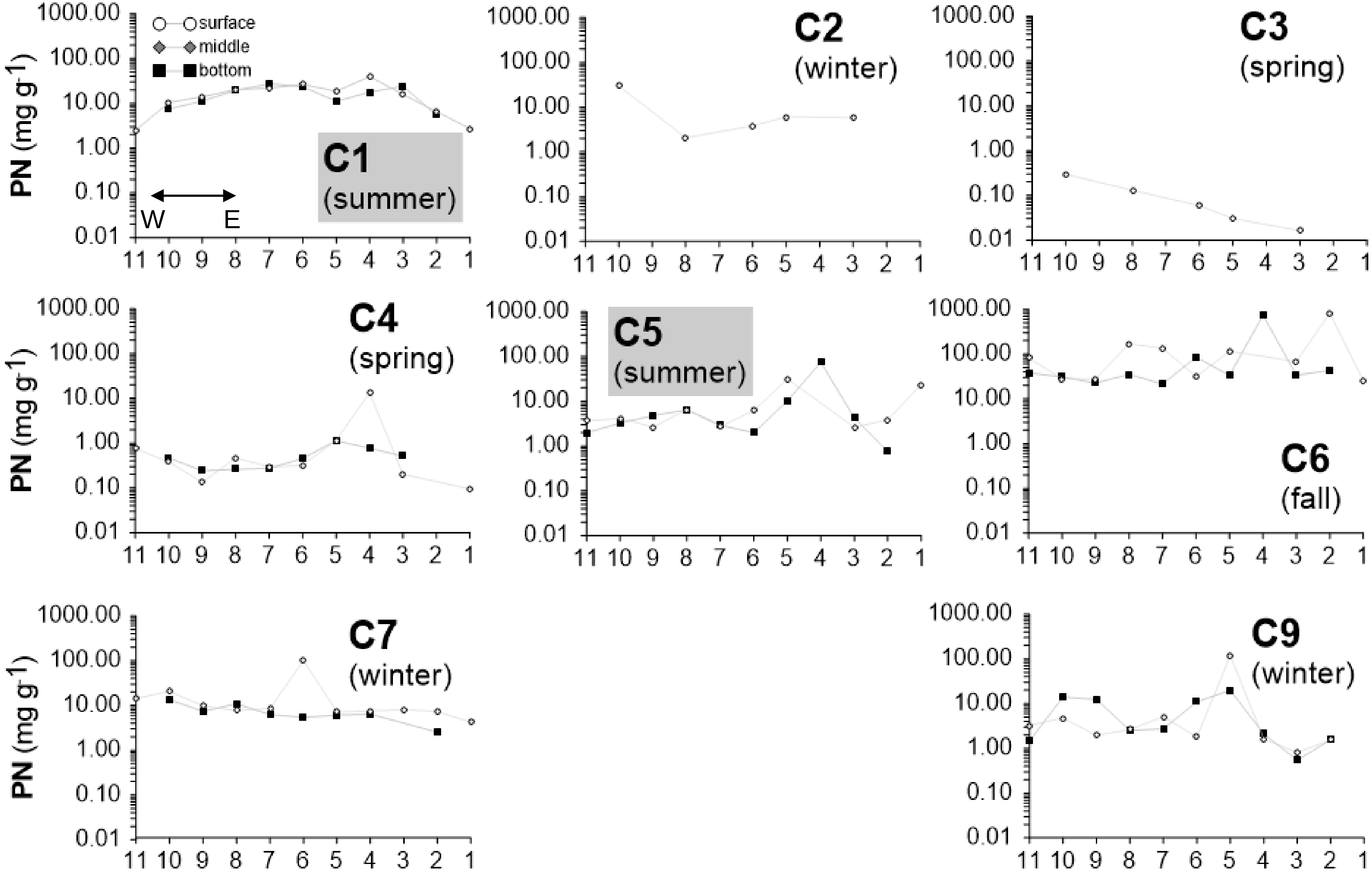

Source: Elaborated by the author, 2023.

LEGEND: PN presented high spatial and temporal variation and the highest value (station 4, C6) reached 700.0 mg g^{-1}. In a general way, there was a reduction of the PN concentration from C1 to C4, an increase from C5 and C6 and another reduction in C7 and C9.

Figure 21 – Particulate phosphorus

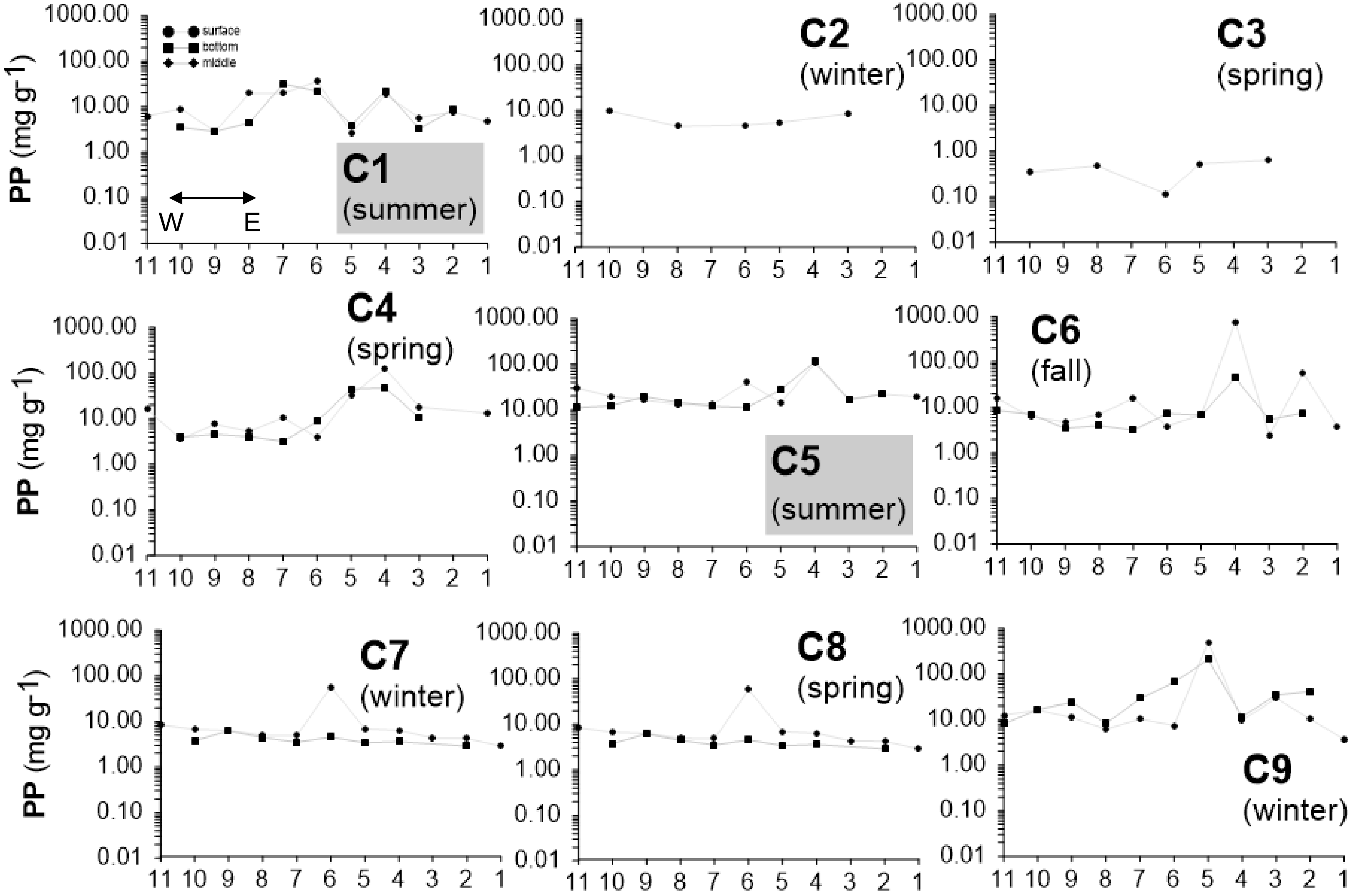

Source: Elaborated by the author, 2023.

LEGEND: PP distribution was similar to PN, despite PP was higher than PN; the highest value (station 4, C6) reached 700.0 mg g^{-1}. In a general way, there was a reduction of the PP concentration from C1 to C4, an increase from C5 and C6 and another reduction in C7 and C9.

Figure 22 – N:P ratio

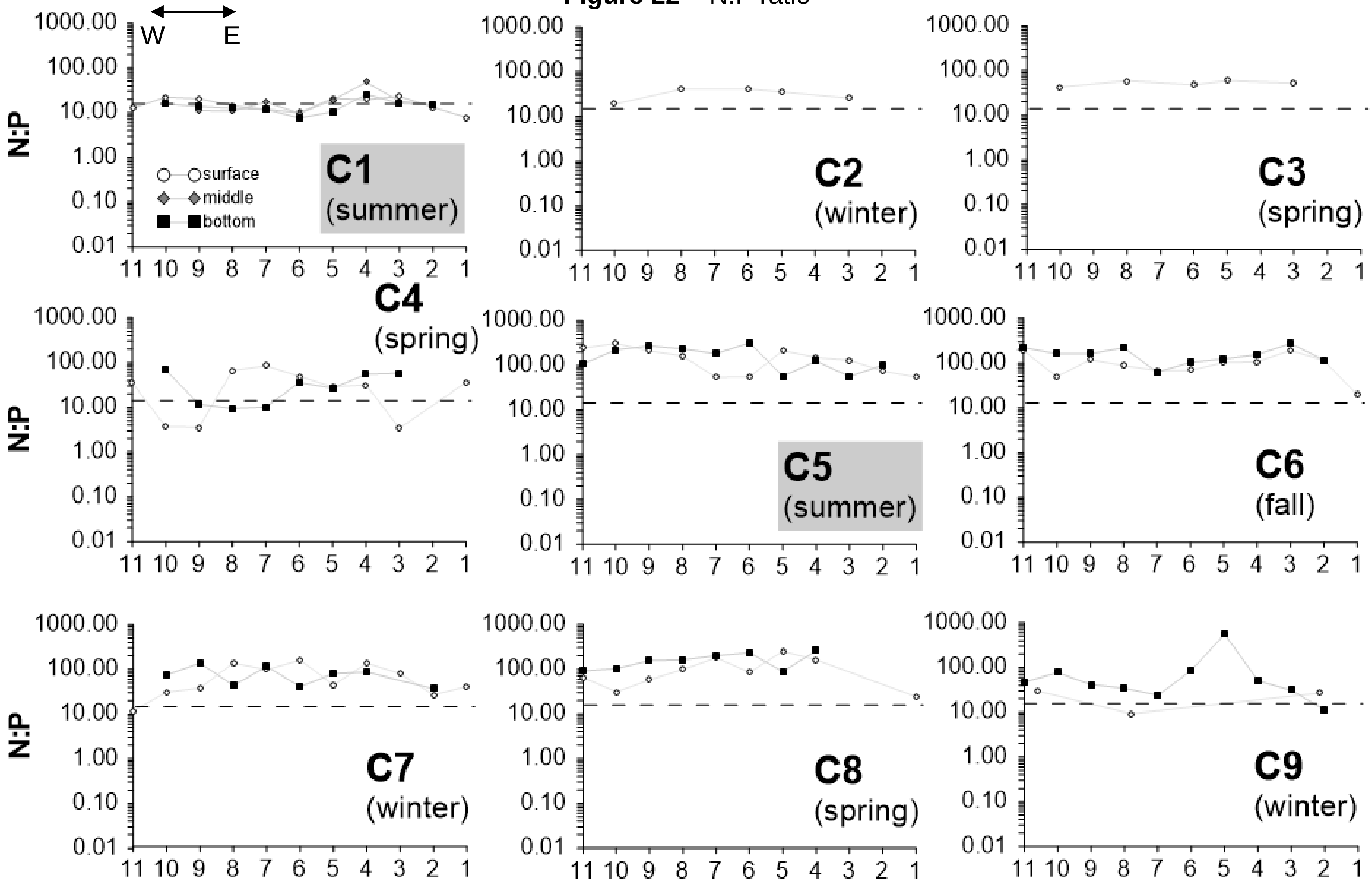

Source: Elaborated by the author, 2023.

LEGEND: Dashed lines indicate the Redfield ratio for N and P. N:P ratios varied spatially and temporally from 5 (N limitation, mainly in C1) to circa the maximum 560 (P limitation; station 5, C9). Except for C1, the other campaigns were generally higher than 16.

Figure 23 – Particulate organic carbon

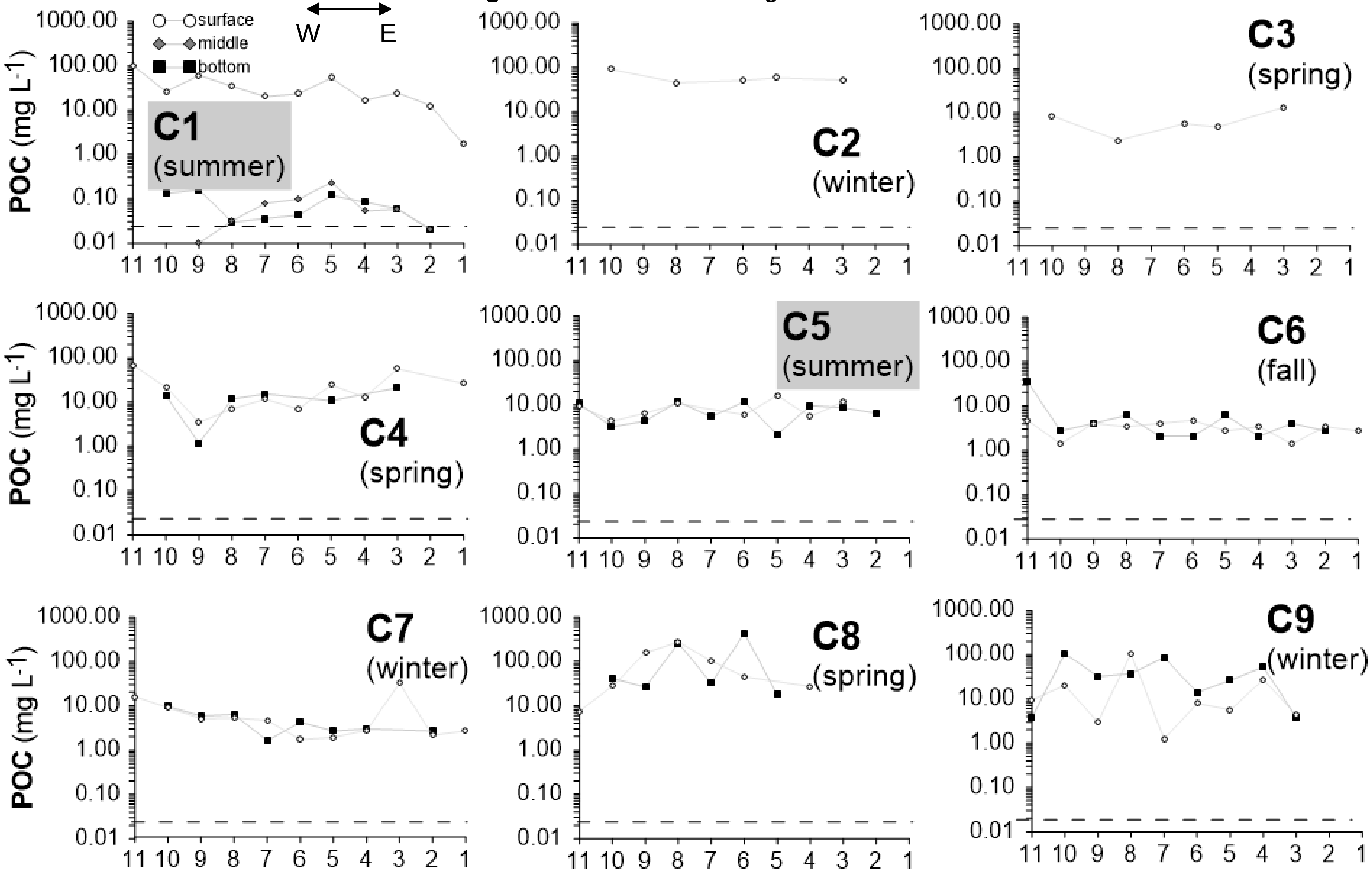

Source: Elaborated by the author, 2023.

LEGEND: POC exhibited high spatial and temporal variation, with a tendence of higher values in the western sector of AL. The highest values were in C8.

CHL*a* (Figure 24) presented values below of detection limit maybe related with higher SEC. C1 presented highest value of CHL*a* and a spatial variation among points. Despite C5 was considered turbid, most of points are below of the detection limit. Appendix B (Figure B2.6 and Figure B2.7) shows, respectively, chlorophyll wavelengths and an example of a result obtained by UV–VIS in C1.

PHAEO (Figure 25) were below of detection limit in most campaigns. Except in campaigns 4, 6, 8 and 9 where few stations were above the detection limit (0.04 mg L^{-1}) and are most distributed in central–western portion of the lagoon.

To identify the main parameters of trophic crises, a box-plot is shown in Figure 26. It is possible to note the great variation among parameters between turbid and non-turbid conditions.

Phytoplankton (Neves, 2019–2020) was collected few days later from our campaigns, but the cellular density was still coherent with SEC measurements. The cellular density (Figure 27) was higher in turbid water, which was possibly related to the higher temperatures and amount of nutrients in summer (C1 and C5).

4.4 Discussion

Comparing values from other studies (Table 8), results from Souza *et al.* (2003) also identified a great variation among the cells in AL. The concentration of dissolved nitrogen was higher, while phosphate was smaller in the current investigation. Also, N:P ratios were higher to West in the present work and lower in the former work. This alteration could be related to the change from the microbenthic to phytoplanktonic production occurred in 2005. Mello (2007) highlighted the potential occurrence of trophic crises due to the high residence time and nutrient loads in AL. Author also identified variation in N:P ratios varying from <16:1 to circa 35. In Vicente *et al*. (2021), results were smaller from this work possibly due to the abnormal high pluviosity occurred in 2010–2011.

Figure 24 – Chlorophyll *a*

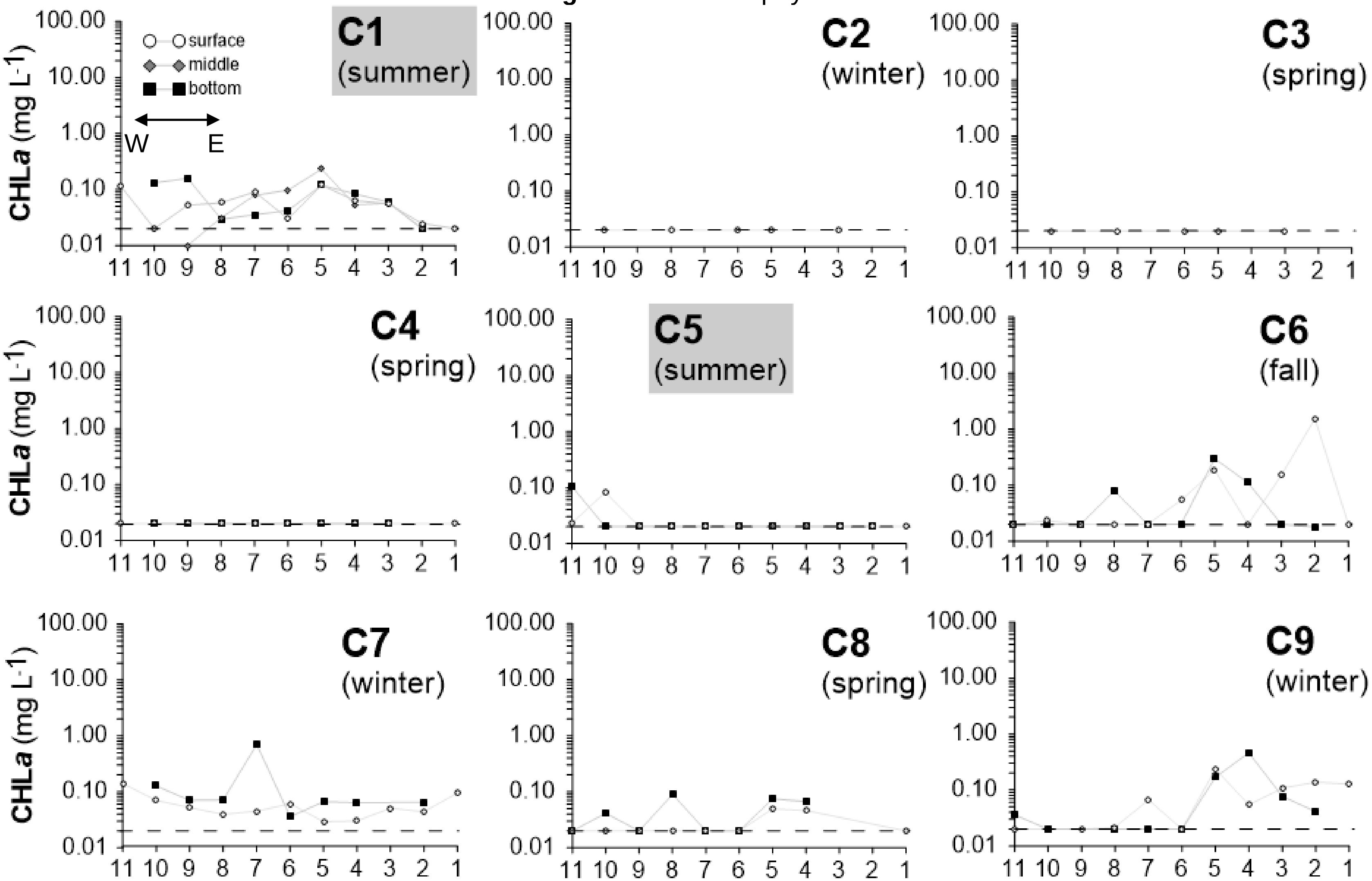

Source: Elaborated by the author, 2023.

LEGEND: CHL*a* was below the detection limit in most stations points, except in C1 and some points in C5, C6, C7 C8 and C9.

Figure 25 – Phaeopigments

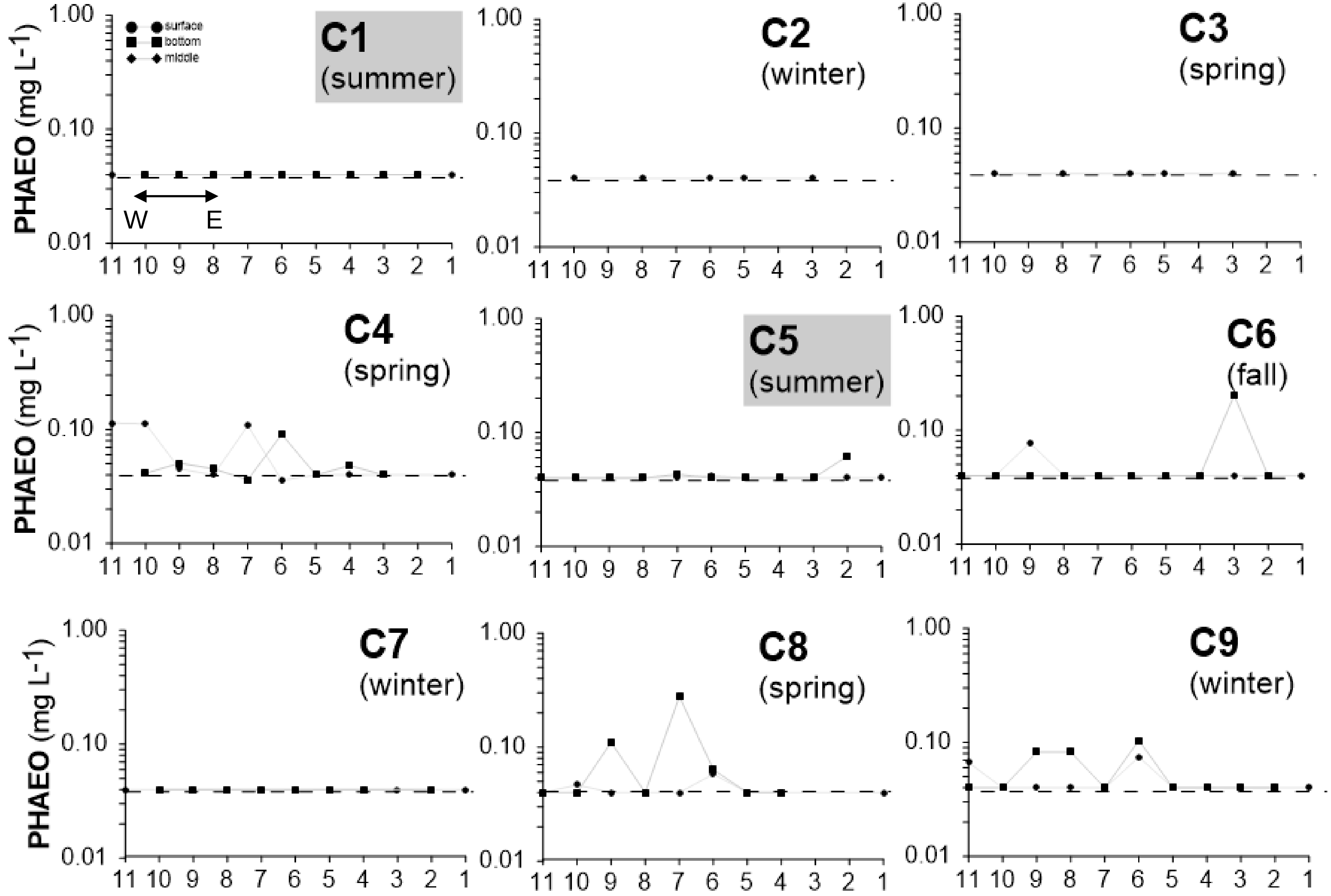

. Source: Elaborated by the author, 2023.

LEGEND: Most of PHAEO values were below the detection limit, and some points in C4, C5, C6, C8 and C9 varied from 0.05 to 0.30 mg L^{-1}

Figure 26 – Box-plot with distribution of the main parameters for trophic crises

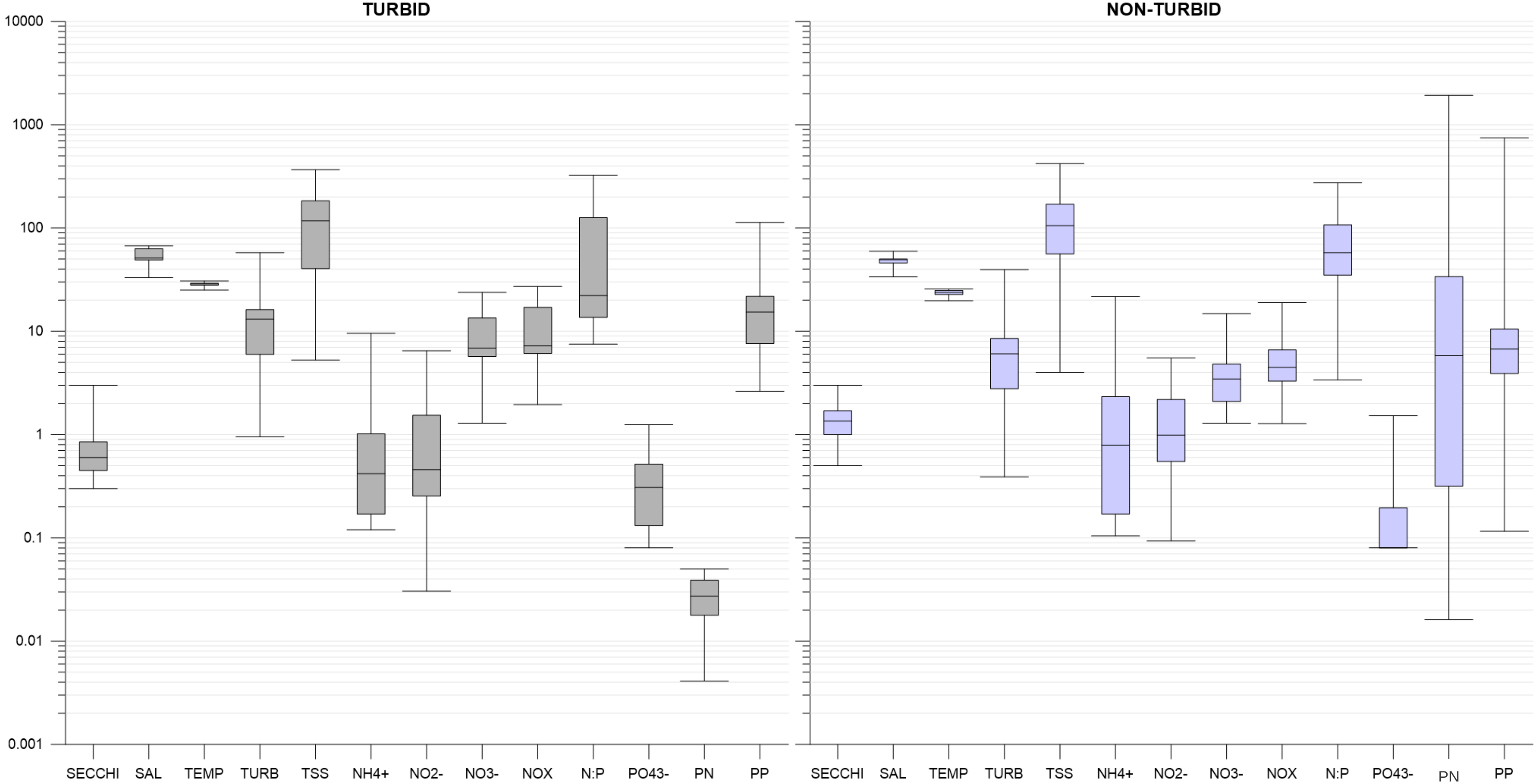

Source: Elaborated by the author, 2023.

LEGEND: Gray and blue box-plots show the variation of parameters in turbid and non-turbid conditions, the internal horizontal line are the mean values and whiskers represent the minimum and maximum values. Despite the behavior of parameters were similar, some differences were noted. Higher mean values of SEC, NH_4^+, NO_2^-, N:P, and PN were recorded in non-turbid conditions. TURB, TSS, NO_3^-, N_{OX}, PO_4^{3-} and PP were higher in turbid waters. Salinity varied little between the two water conditions, while temperature was slightly lower in non-turbid conditions. There was a great variation between minimum and maximum values, but N:P and PP presented the highest variation. PCA is in Appendix B (Figure B2.8).

Figure 27 – Phytoplankton distribution during 2019–2020

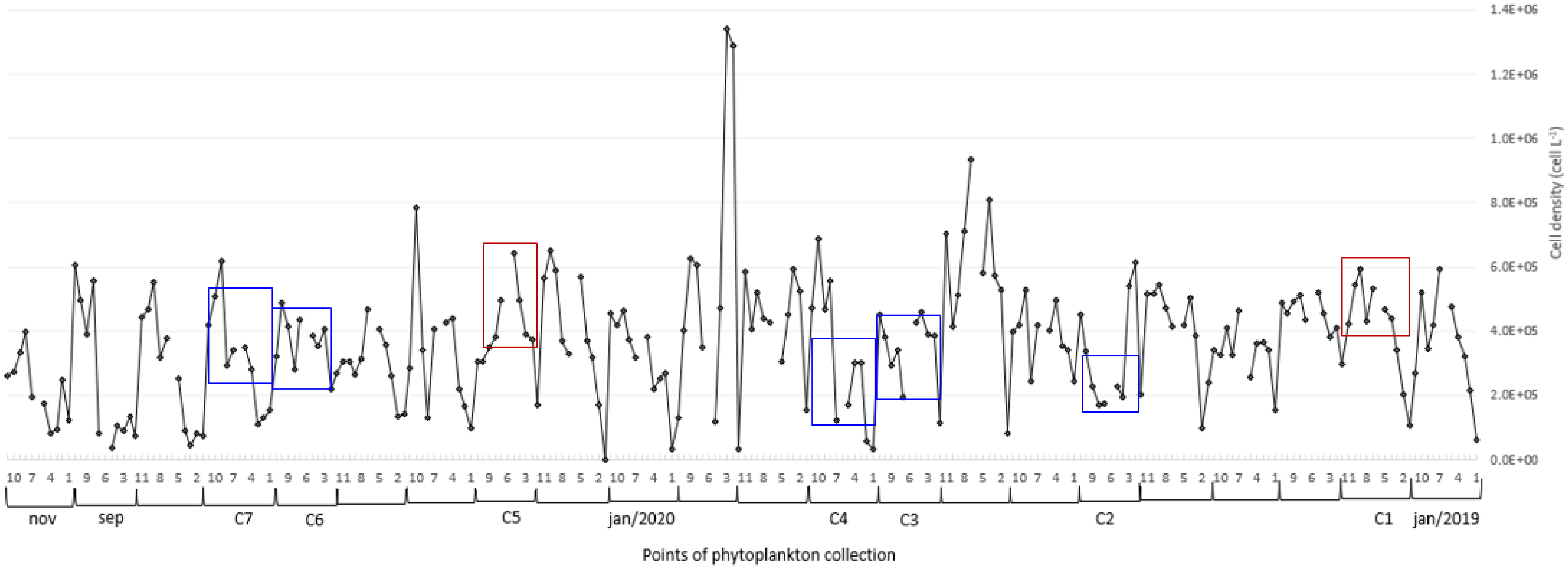

Source: Elaborated by the author, 2023, using the data collection from monitoring reports (Neves, 2019-2020).

LEGEND: □ non–turbid condition; □ turbid condition. Source: Data based on Neves (2019–2020), unpublished data from monitoring reports. The temporal order of the campaigns is shown from C1 (right side) to C7 (left side) to maintain the spatial distribution of the stations.

Table 8 – Nutrient variation over the years in AL and other coastal lagoons

NUTRIENT	NH_4^+ µmol L^{-1}	NO_2^- µmol L^{-1}	NO_3^- µmol L^{-1}	PO_4^{3-} µmol L^{-1}	SAL
Araruama Lagoon[1]	0.3–39.0	0.2–6.0	0.3–18.0	0.01–6.0	22–56
Araruama Lagoon[2]	0.005–0.4	0.00–0.21	0.01–1.07	0.03–0.56	38–8
Araruama Lagoon[3 £]	<0.1–0.4	<0.1	<0.07–0.11	<0.01–0.1	
Araruama Lagoon[4]	0.1–64.2	0.01–16.4	1.29–23.8	0.08–2.68	33–67
Celestun Lagoon (Mexico)[5]	1.75–6.12	0.32–2.15	2.8–60.8	0.62–1.22	3–33
Las Marites Lagoon (Venezuela)[6]	1.7–2.1	0.05–0.06	1.2–1.6	0.4–0.6	36–41
Coorong Lagoon (Australia) [7£]	50–100	0.005–0.01		0.005–0.015	20–90

Source: [1]Souza *et al.* (2003); [2]Mello (2007); [3]Vicente *et al*. (2021); [4]this study (2019–2022); [5]Herrera–Silveira (1996); [6]Lopez–Monroy (2017); [7] Mosley (2023).
LEGEND: [£]mg L^{-1}.

In Celestun and Chelem lagoons (Mexico), nutrient inputs stimulated productivity, organic decomposition, and sediment resuspension, causing changes in water quality. The exhibited seasonally pattern was the result of the mixed temperature conditions, rainfall, and winds (González, Herrera-Silveira, Aguirre-Macedo, 2008). Particularly, in Celestum Lagoon, the seasonality also influenced nutrient fluxes, which varied one or two orders of magnitude greater during the cycle rainy season than in the dry and the cold seasons . Phosphate was higher from November to February, and the lagoon was a source of phosphorus for the inner zone (Herrera–Silveira, 1996).

In Las Marites (Venezuela), due to the small depth (< 4m) the action of temperature is more accentuate and in the drought season there was an increase of nutrients and N:P in the water column (Lopez–Monroy, 2017). In AL, generally, ammonium was lower in wet season (coincident with turbid conditions) while the oxidized forms of nitrogen and phosphate were higher. Coorong Lagoon (Morey, 2023) presented an increase of salinity gradient due to the higher distance of the river mouth, and similarly to AL, the system was P-limited. AL presented higher concentration of Nox and phosphate and smaller ammonium if compared to the Coorong Lagoon.

Particularly, ORP, TSS, POC, and N:P showed higher variations among campaigns if compared to the other parameters, as demonstrated by the box plots (Figure 26). Although, data variation in water column was generally small between surface and bottom because of strong wind that mix the water column (Kjerfve *et* *al*.,1996; Trevisan *et al*., 2022). The spatial and temporal variability was also probably caused by the individual behavior of the elliptical cells (Vicente *et al.*, 2021; Souza, 2003). The fish mortality in 2019 could be related to the conditions in C1 that favored a toxic algal bloom (Rath; Mitbavkar; Anil, 2021). This assumption was based on the presence of toxic species in AL and the strong winds that do not allow DO depletion (anoxia).

Regarding the different measurements used to determine water transparency in AL, only TURB (Figure 14) identified changes in the water column, being inversely correlated with SEC (Figure 11). TSS and TURB derived from riverine flows were expected to be low in AL due to its small drainage basin and low amounts of terrigenous material (Souza *et al.*, 2003). Moreover, even the currents (20 cm s^{-1}) caused by the strong winds (Kjerfve *et al*., 1996) are not enough to resuspend the sediments. The resuspension can occur only near the shoreline of AL, where depth is very low, and winds affect sediments. Then TURB (Figure 14) and TSS (Figure 15) measured in the lagoon were mainly from the autochthone biogenic material. Trevisan *et al.* (2022) measured very low values for SEC depth due to the very high primary production in summer 2019.

CHLa (Figure 24) and TSS (Figure 15) were not enough to be associated with the cellular density of phytoplankton (Figure 27), during non–turbid waters in AL. The effect of CHL*a* over TSS was identified in prolonged algal blooms conditions (Baldizar; Rybicki, 2007). As pointed by Lee, Jones–Lee and Rast (1995), CHL*a* varies according to species, age of cells and can impact SEC measurements. Since different pigments allow primary production in low light environments/conditions (Blain; Shears, 2019), studies to identify such potential pigments should be done in AL. Phytoplankton is distributed in water column as a response for vertical heterogeneity of light and nutrient availability (Litchman, 2007). Padedda *et al.* (2019) observed that cell density was not linked with CHL*a* but with phosphate and TP in some mediterranean lagoons.

Seasonal patterns like rainfall regimes (Carmouze, Knoppers; Vasconcelos, 1991; Baumann *et al*. 2015), or interannual variations (Barrera–Alba; Abreu; Tenenbaum, 2019) are responsible for the variability of primary production. The pluviosity in AL (Appendix B, Figure B2.7) did not exhibit any relevant effect on phytoplankton productivity, even in C8 when higher pluviosity preceded the field work. Primary production presented higher cellular densities in summer and lower in winter (Neves, 2019–2020), except in C7 (winter). In this specific campaign, temperatures were as high as summer, the cellular density remained low, so other factors possibly influenced the primary productivity.

Beyond the climatic factors, peaks of primary production can occur in different seasons due to the consumer strategy adaptation (Cloern, 2018), or the competition among species for the same nutrient (Zhou *et al*., 2017). It could be occurring in AL because some local phytoplankton assemblage described in monitoring reports (Neves, 2019–2020) have preference for ammonium (Ketchum, 1954). Cyanobacteria are the prevalent phytoplankton species in AL, and it is possible that the nitrogen is being used in high quantities than phosphate in terms of nutritional requirements.

A mass balance (Souza, 2005) revealed a decrease in net autotrophy and net N fixation rates during that period. The observed increase in phosphate, though not of ammonium, resulted in a low DIN:DIP molar ratio. The authors considered that the low ammonium concentration was the result of a rapid ammonium uptake by the phytoplankton, or the transformation of this element into more oxidized forms such as nitrite and nitrate. Silva *et al*. (2013) showed that these trends continued in surveys carried out during a transition from the dry to the rainy period in 2003–2004. Low DIN:DIP and ammoniacal nitrogen in the lower estuary indicated phytoplankton limitation by N, while eutrophication in the inner estuary increased.

Particulate organic carbon varied largely, and it was not possible to associate to the trophic crises. However, refractory dissolved organic carbon (Carpenter; Pace, 1997; Hessen; Tranvik, 1998) or bacterioplankton (virus) (Stramski, 1991) could reduce SEC by altering color and light scattering. Also, variations in phytoplankton concentration control seasonal changes in UV and photosynthetically active radiation but do not influence Secchi (Rose *et al*., 2009). Also, higher temperature was an important factor for phytoplankton production, and SEC was negatively related with CHL*a* in Tai Lake (Guo *et al.*, 2017). SEC was negatively associated to DBO_5, which could be associated to sewage inputs previously identified by Vicente *et al.* (2021) and Trevisan *et al.* (2022).

Factors responsible for variations in SEC may not be linearly correlated with SEC measurements and can vary according to temporal scales. In a study from Sun *et al*. (2023), sea surface temperature and salinity were positively related to SEC in an interannual scale. While wind direction was responsible for effects at longer scales due to the alteration in ocean dynamic processes. Salinity affected negatively the turbidity at Negombo lagoon (Chandrasekara *et al.*, 2014), and Kjerfve *et al*. (1996), Moreira–Turcq (2000) have pointed the negative influence of desalinization in AL. In AL, the salinity and temperature were negatively correlated with SEC, which could be linked to a higher primary production in summer as demonstrated by the monitoring reports from Neves (2019–202). Phosphate increased in water column at higher salinity in Celestum Lagoon (Herrera–Silveira, 1996).

Ward (1984) described an increase of bacterial oxidation of ammonium at increasing depth and distance from shore. In shallow areas, the author observed that ammonium turnover was dominated by phytoplankton assimilation. While depth and salinity were positively associated with ammonium and nitrite oxidation rates, negative relations were described for dissolved oxygen and light (Heiss, 2016). In AL, it was possible to occur in some deeper stations, where ammonium concentrations were higher in bottom than in surface (Figure 16). Heiss (2016) emphasized that ammonium and nitrite oxidation were influenced by different environmental conditions and maybe not be always coupled.

4.4.1 Model of descriptors of trophic crises

A model was proposed (Figure 28) to summarize the descriptors in water column associated to trophic crises in AL. First, a spatial compartmentation was suggested for the lagoon, based on the salinity gradients and maximum depths (see Appendix B for bathymetry). The three sectors were named: i) marine sector (32–35) comprised stations 1 to 3; ii) central sector (50–70) included stations 4 to 8; and iii) interior sector (35–50) comprised stations 9 to 11. Shallower areas were found in the interior and marine sectors, while the depths at the central sector were greater.

Among all the parameters analyzed, few elements were identified as relevant for the shifts in water column. The indirect descriptors were temperature, salinity, and turbidity, while direct indicators were Secchi's disk, phosphate, ammonium, Nox and N:P ratios. Non–turbid water occurred at higher temperatures and smaller turbidity, while salinity decreased from C1 to C9 and may have favored species more adapted to those changes. Ammonium and phosphate concentrations were smaller in turbid waters, while Nox was smaller in non–turbid conditions.

Figure 28 – Model of the descriptors of trophic crises

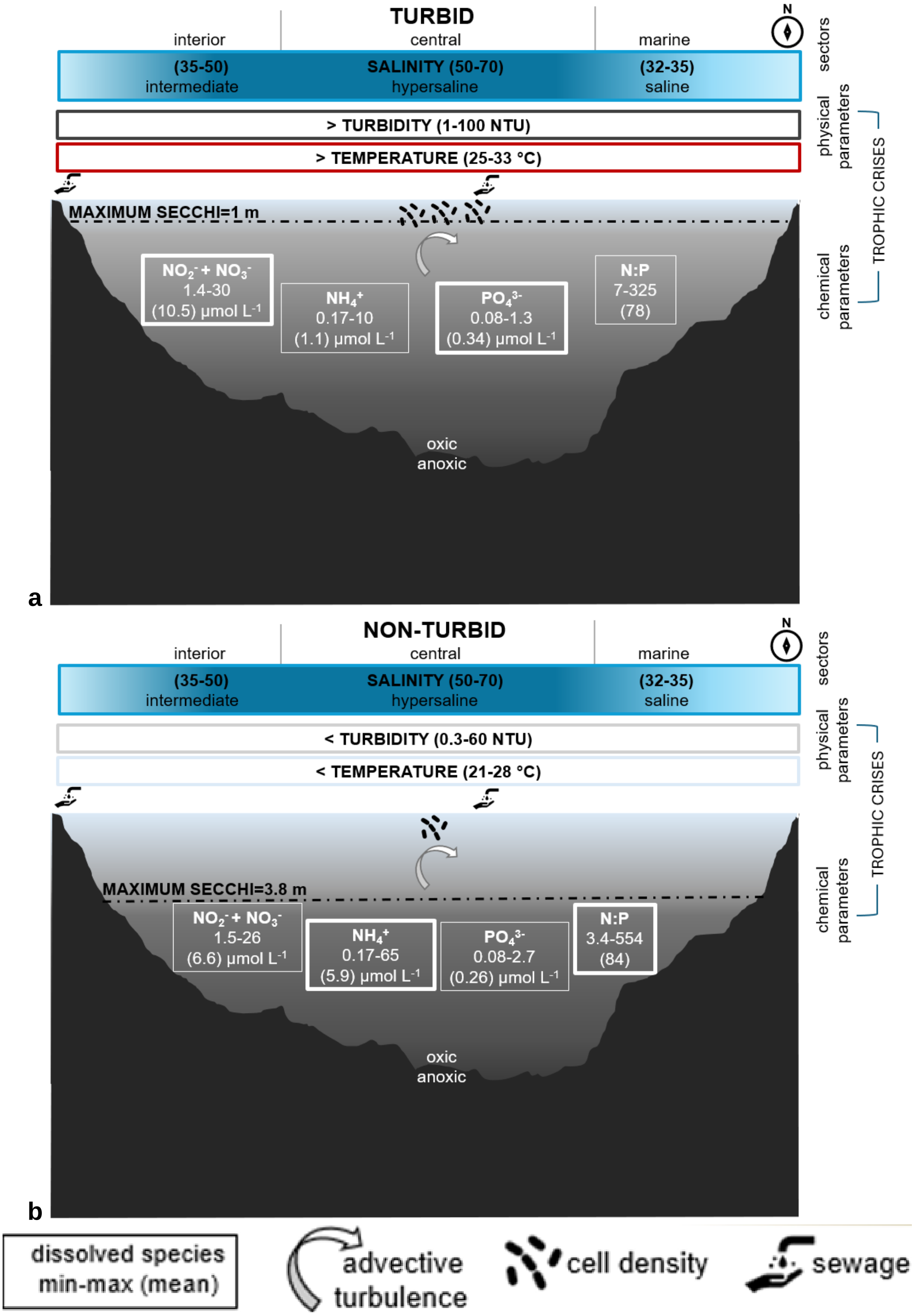

Source: Elaborated by the author, 2023.

LEGEND: Physical and chemical descriptors of trophic crises – a) turbid water; b) non–turbid water. Bolded boxes indicate higher concentrations between the two conditions. The main indicators were temperature, turbidity, salinity, NH_4^+, Nox, PO_4^{3+}, and N:P ratios. Despite the greater spatial-temporal variability of parameters, there was a pattern in turbid and non-turbid conditions. Higher turbidity, temperature, salinity, Nox, and phosphate, and smaller ammonium and N:P ratios marked turbid water in relation to non–turbid conditions. The variation of phytoplankton (cellular density) corroborated the results. The advective turbulence mixes the water column and promotes the uniform distribution of physical-chemical parameters.

As described in the earlier sections, two water conditions were identified in Araruama Lagoon and presented the behavior: the alternance between turbid and non–turbid condition. Few descriptors of such trophic crises were associated to them, in opposition to a first inference that many factors would lead to changes in water transparency.

Temperature, turbidity, and salinity were indirect descriptors for trophic crises, while ammonium, Nox, phosphate, and N:P were direct markers. Higher turbidity, temperature, salinity, Nox, and N:P ratios and smaller ammonium and phosphate determined turbid water, whereas non–turbid waters presented the opposite behavior. The variation of phytoplankton (cellular density) corroborated the results. There was a variation between N and P limitation in the lagoon, but it was not related with trophic crises. In the case of phosphate, even small variation in its concentration can favor algal production.

In this study, there was a lack of correlation among SEC, TSS and/or CHL*a*, possibly related to the reduction of light action. This could be a potential topic to study the role of primary producers' strategies to live in more turbid water. Other suggestion is the investigation of the nutritional needs of heterotrophic organisms to increase data about the interactions at the trophic chain.

5 DIFFUSIVE FLUXES OF NUTRIENTS AND THE TROPHIC CRISES

Coastal lagoons are among the most productive areas in the world (Rodrigues–Filho *et al.*, 2023), usually presenting small depths, and predominance of benthic over planktonic production (Kennish; de Jonge, 2011). However anthropic pressures due to agriculture/aquaculture, wastewater/untreated sewage (Lund, 1967; Malone; Newton, 2020; Valenzuela–Siu *et al.,* 2007) result in eutrophication – the nutrient enrichment in aquatic systems (Nixon, 1995). Shallow coastal areas, especially those with small tides, long residence time, and near to densely populated regions present elevated concentrations of nutrients. As previously considered, geochemical conditions of sediment influence nutrient fluxes (Bonometto *et al.*, 2019) affecting the biotic communities (Gallagher *et al.*, 2012; Nielsen *et al.*, 2003), nutrient cycling (Valenzuela–Siu *et al.*, 2007) and aquatic ecological status (Barbanti *et al.*, 1995; Cornwell; Glibert; Owens, 2014).

Zooming at the sediments, two key processes control nutrient fluxes at sediment–water interface (SWI): sedimentation of solid particles and entrapment of water in sediment pores. In this zone, chemical species with different concentrations moves between both media by diffusive fluxes according to Fick's Law (Poirier; Geiger, 2016). In this process, the exchanges between pore water to water (Håkanson, 2012) are affected by salinity, pH, water oxygenation, temperature and grain size (Schulz, 2006). All these interferences caused by nutrients increase biologic productivity and subsequently lead to trophic crises (Carlson, 1991). As defined by Lenzi and Cianchi (2022), dystrophy results in dissipation of accumulated organic matter and the starting of a new growth cycle.

Granulometry is an important factor for diffusive fluxes (Chapman; Wang, 2001). Coarse grains are more susceptible to suboxic chemical diagenesis, and the solute fluxes from sediment to water column are greater than from fine–grained sediments (Wolanski; Mclusky, 2011). Valiela (1984) described reversible episodes of dystrophy in aquatic environments related to diffusion of sulfides from sediments in anoxic conditions, and this could impact N and P fluxes in AL.

Looking at hypersaline environments, despite their importance, studies of nutrient fluxes are still scarce and the conditions of recent dystrophic episodes in Araruama Lagoon are unclear. Fluxes of nutrients can boost the concentration of nutrients in water column and favor the primary production. The objective of this chapter is to quantify nutrient fluxes and determine if they are connected to trophic crises.

5.1 Study area

Araruama Lagoon (AL, Figure 3) is highly productive and provides many ecosystem services (Esteves *et al.*, 2008), however is under pressure of anthropic activities (Amaral *et al.*, 2018; Lloret; Marín; Marín–Guirao, 2008). This hypersaline environment experienced reduction of the water quality and modifications in trophic state due to changes in the land use, such as salt extraction and irregular urbanization (Costa; Seabra, 2021; Bertucci *et al.*, 2016; Carmouze; Barroso, 1989; Carvalho; Costa; Rosa, 2014; Costa *et al.*, 2022). Water is well mixed by winds (Trevisan *et al.*, 2022) and the hydric deficit increases salinity inside the lagoon (Kjerfve; Oliveira, 2004). However decreasing in salinity impacted the ecological equilibrium of AL (Amaral *et al.*, 2018; Moreira–Turcq, 2000).

Shallow coastal lagoons often present benthic primary production over phytoplanktonic, however eutrophication influences biogeochemical processes at bottom sediments and overlying water altering this plant structure to phytoplanktonic (Kennish; de Jonge, 2011). Knoppers and Kjerfve (1999) determined a unimodal pattern of biologic production in the AL, measured as chlorophyll *a* content, with maximum concentrations in late summer and early fall fed by the autotrophic production. When primary producers were microphytobenthic mats, sustained by ammonia and orthophosphate from the sediment, the lagoon water column presented an oligotrophic state.

Regarding the increase of pollution in AL, studies identified changes through the years. Souza *et al.* (2003), in a study from 1991–1992, reported the variation of trophic status from oligotrophic to mesotrophic in the lagoon, and large amounts of nutrients in sediments. The occurrence of some species of benthic diatoms were observed between 1997–1998, and indicated polluted water at the northern and western portions of the lagoon (Sylvestre *et al*., 2001). Mello (2007) confirmed a shift from phytobenthic to phytoplanktonic communities in AL during 2005–2006. This change occurred because of water quality deterioration due to the enhancement of nutrient cycling in sediments and hypertrophic conditions.

Trevisan *et al.* (2022) confirmed the good oxygenation of the lagoon and the homogeneity of water column due to the intense winds. Authors also identified a decreasing water quality gradient westwards, where higher POC and POP were quantified. Laut *et al.* (2020) characterized distinct trophic conditions at eastern part of AL which were related to high hydrodynamic (good conditions at Itajuru canal), hypersalinity (moderate conditions, associated with the station 4 here), salt extraction (poor conditions between stations 2 and 3 of this thesis) and anthropic origin of organic matter (very poor conditions at the middle point of Itajuru canal).

Silva, Guimarães, and Wasserman (2019) quantified high concentrations of total nitrogen and total phosphorus in sediments that were associated with sewage loads. *In vitro* studies of nutrient fluxes determine a release of nitrogen and phosphorus from low–carbonate sediments in AL that could enhance primary production (Guimarães *et al.*, 2021). Vicente *et al.* (2021), using data from 2010 and 2011, verified that the water quality of AL was highly impacted by an unusual summer precipitation. In the study, authors observed that western portion of the lagoon were more affected than other sections, probably because the low hydrodynamic conditions. Lower salinity was cited as an important parameter for the release of nutrients to the water column in the lagoon (Guimarães *et al.*, 2021; Silva, 2019). Kjerfve *et al.* (1996), Due to the low water exchange, the residence time is high (about 85 days) which contributes to the increment of nutrient supplies (Wassmann, 2005).

Despite of its primary production, AL is P limited (Lourenço *et al.*, 2005; Mello, 2007; Moreira–Turcq, 2000; Souza, 1997; Souza *et al.*, 2003, Wasserman; Silva–Filho, 1995). However, Wasserman (2017) observed that N–limitation episodes are mainly due to phosphorus availability probably released from the sediments. Other conclusion was that ammonium reaches the lagoon mostly by wastewater loads due to the high population surrounding the lagoon. Guimarães *et al.* (2021) in a mesocosm experiment identified positive fluxes of nutrients when salinity decreases. Such negative impacts affected the water quality in the lagoon were observed by Moreira–Turcq (2000).

5.2 Materials and methods

Due to the purposes of this chapter and the concepts involved in it, the water collected at bottom depth is referred as "overlaying water". However, the graphics will present a "B" to identify the depth of the sample.

- Determination of nutrient fluxes

Results of dissolved species (ammonium, nitrite, nitrate and phosphate) from overlaying and pore waters were used to calculate nutrient fluxes according to Fick's law (Equation 1, Schulz, 2006). However, the particular condition of diffusion in sediment is lower than in a free solution environment due to sediment porosity. Thus, additional equations included: i) sediment diffusion in function of porosity depending on grain properties (Equation 2); ii) tortuosity expressing the path deviation to calculate the diffusion coefficient in sediments (Equation 3); iii) porosity calculated in function of pore water content (Equation 4); and iv) water content related to the difference between dry and wet weights (Equation 5).

$$J_{sed} = -\phi . D_{sed} . \frac{\partial C}{\partial x} \quad \text{(Equation 1)}$$

Where:

J_{sed}= molar diffusion flux of dissolved compound (mol m^{-2} d^{-1})
ϕ= sediment porosity
D_{sed}= diffusion coefficient, or diffusivity, of a specific ion in porewater (m^{-2} s^{-1}; temperature and porosity dependent)
C= molar concentration of a dissolved species (µmol L^{-1})
x= depth of the extracted sediment (cm)

The negative sign denotes a diffusive flux in opposition to the gradient's direction, i.e., from high to low concentration.

$$D_{sed} = \frac{D^{sw}}{\theta^2} \quad \text{(Equation 2)}$$

Where:
Dsed= diffusion coefficient, or diffusivity, of a specific ion in porewater (m^{-2} s^{-1}; temperature and porosity dependent)
Dsw= diffusion coefficient of a specific ion in free solution of seawater (m^{-2} s^{-1})
θ= tortuosity

The diffusion coefficient for free solution of seawater was calculated based on temperature variation and the dissolved chemical species (Appendix C, Table C3.1) gives the temperature variation and the values of Dsw for the studied compounds.

$$\theta^2 = 1 - ln(\phi^2) \quad \text{(Equation 3) (BOUDREAU, 1997)}$$

Where:
θ= tortuosity
ϕ= porosity

$$\phi = \frac{fw}{fw+(1-fw)pw/ps} \quad \text{(Equation 4)}$$

Where:
ϕ = porosity
fw= water weight percentage
pw= density of sediment particles
ps= density of pore water

$$fw = 1 - \frac{dry\ wt}{wet\ wt} \quad \text{(Equation 5)}$$

Where:
fw= water weight percentage
dry wt= sample dry weight
wet wt= sample wet weight

Each cell was delimited, and its area calculated using Google Earth®, Figure 29 and Table 9. To calculate the total flux in the lagoon, each punctual flux was multiplied by its respective area.

- Statistical analyses

After calculation of fluxes, nonparametric correlation coefficients (Spearman, $p<0.01$) were applied to identify patterns in nutrient fluxes among C5, C6, C7 and C9.

5.3 Results

Section 5.3.1 brings the results of dissolved nutrients from C5, C6, C7 and C9, while section 5.3.2 exhibits the related fluxes. C8 was not included in this discussion because there was no data of granulometry. Data of bottom water were used, and in this chapter, they were named “overlaying water” due to the connection with sediment-water interface. Also, because of the number of data, the figures and the tables cited but not displayed in this section are plotted in Appendix B.

Figure 29 – Boundaries of each cell for flux calculations

Source: Elaborated by the author, 2023.

Table 9 – Area of each cell

	A2	A3	A4	A5	A6	A7	A8	A9	A10	A11
Area (m^2)	963,949	16,337,529	41,696,424	15,961,274	26,063,840	51,973,909	29,153,362	19,596,279	10,391,995	7,943,538

Source: Elaborated by the author, 2023.

5.3.1 Overlaying and pore waters

Concentration of nutrients in water column at bottom depth (BW) is referred here as overlaying water due to the context of sediment–water interface. Data used in this calculation are listed in Appendix A (Tables A1.1 to A1.4) and Appendix C (Table C3.2). Concentration and distribution of nutrients (Figures 30 to 32) exhibited high variability, and pore water presented concentration many times higher than in overlaying water.

Phosphate in overlaying water (Figure 30) was below of detection limit (0.08 µmol L^{-1}) in most of the stations in C5 and C6. However, the highest value was 1.3 µmol L^{-1} in C9 (station 2). Concentration in pore water varied from 0.7 µmol L^{-1} (C5, station 2) up to 88 µmol L^{-1} in non–turbid water (C6, station 8). The variation of phosphate between pore and overlaying water reached up to 450 times higher in turbid water (C5, station 9).

Figure 30 – Concentration of PO_4^{3-} in pore and overlaying waters

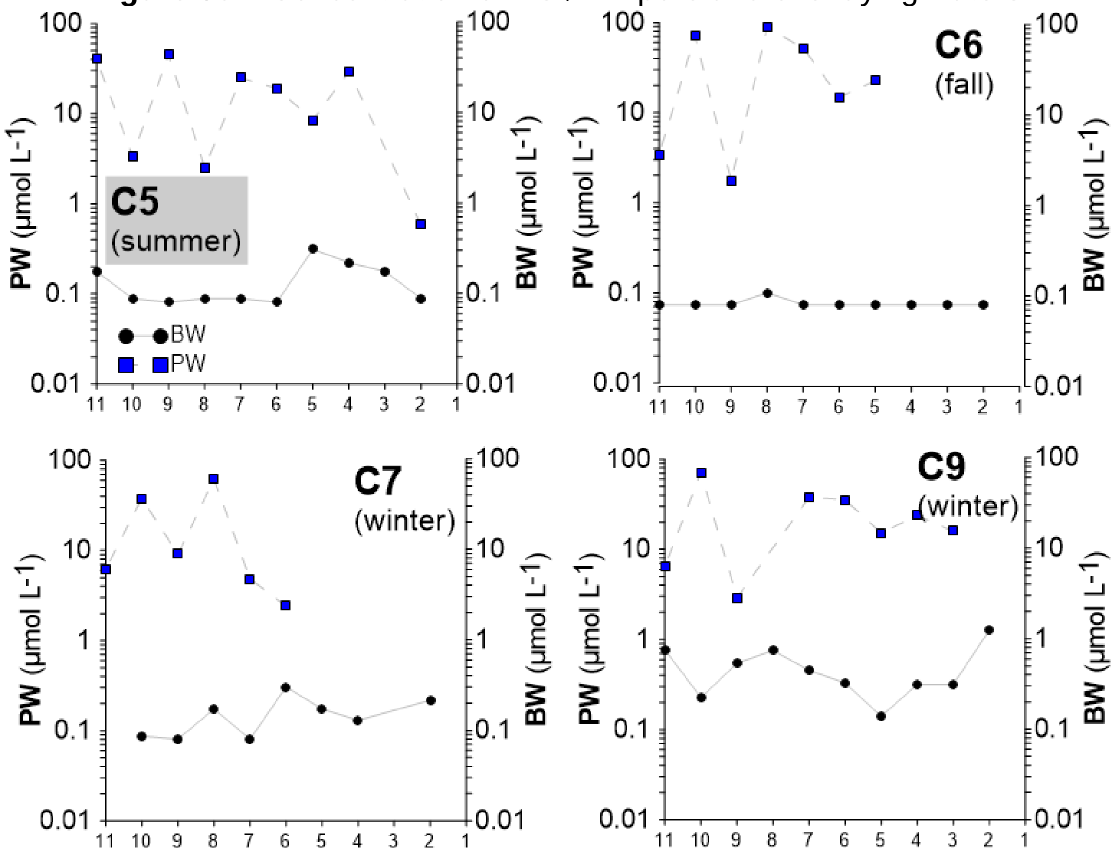

Source: Elaborated by the author, 2023.

LEGEND: BW= overlaying water; PW= pore water. Values bellow of detection limit of phosphate (0.08 µmol L^{-1}) in overlaying water prevailed in most of stations in C5 and C6 and increased in C7 and C9. Pore water (about 1 to 100 µmol L^{-1}) there was a prevalence of higher concentrations in central sector of the lagoon.

Ammonium concentration (Figure 31) in both overlaying and pore water presented a high spatial and temporal variability in the lagoon. The overlaying water varied from below of detection limit (0.17 µmol L^{-1}) to circa 65 µmol L^{-1} in non–turbid water (C9, station 5). Concentration of pore water varied from 2.8 µmol L^{-1} in C9 (station 3) to 663.35 µmol L^{-1} in turbid water (C5, station 10). Ammonium was the nitrogen–form that presented the highest values in sediment, possibly due to the association with nitrogen loads and reducing conditions in lagoon. Despite variations, phosphate tended to increase from east to west.

Nox (Figure 32) p1resented high variation but with a tendence of higher values in central sector of AL during turbid conditions. The smallest value for Nox in overlaying water was 1.84 µmol L^{-1} in non–turbid water (C6, station 11) and the highest was 25.85 µmol L^{-1}in turbid water (C5, station 6). Pore water presented the smallest value in non-turbid water 0.2 µmol L^{-1} (C7, station6) and highest in 199. 4 µmol L^{-1} (C5, station 4).

Figure 31 – Variation of NH_4^+ in pore and overlaying waters

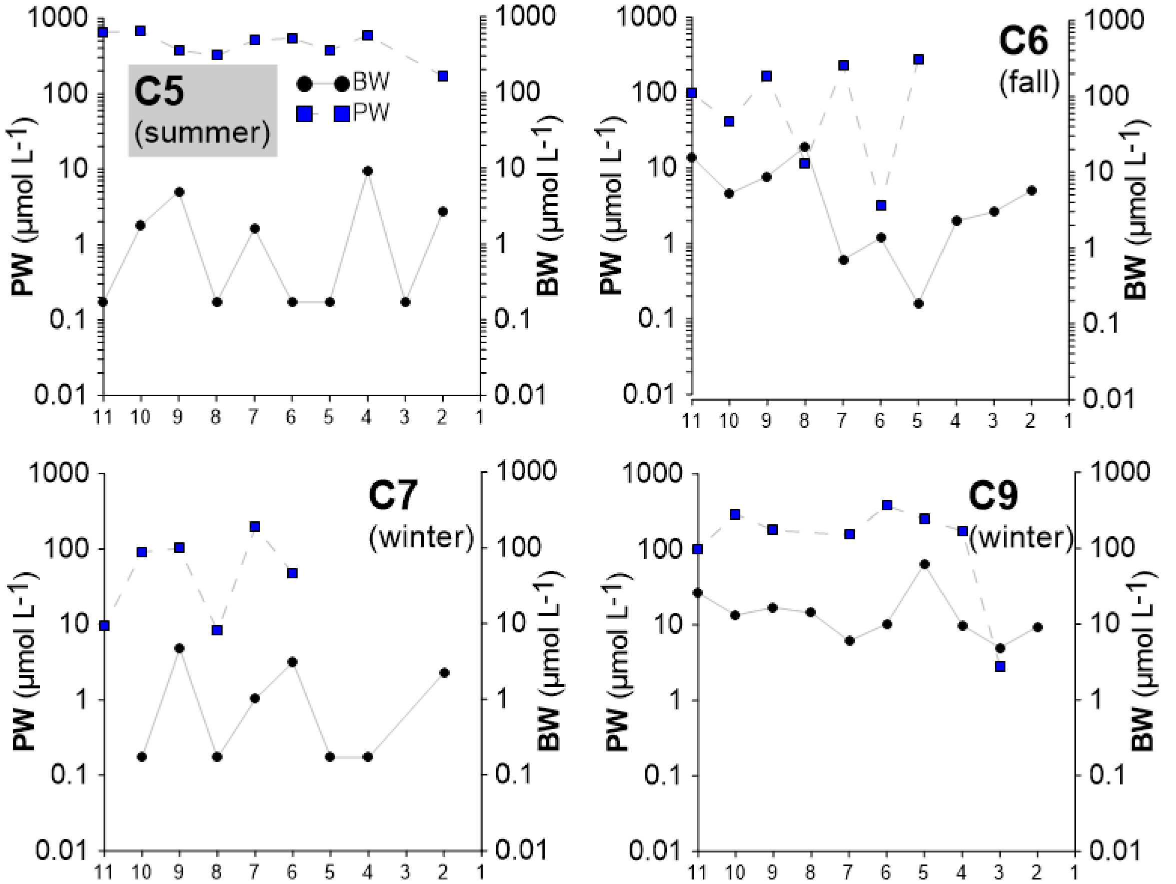

Source: Elaborated by the author, 2023.
LEGEND: BW= overlaying water; PW= pore water. Ammonium presented high spatial-temporal variation and pore water is almost 4 orders greater than overlaying water.

Figure 32 – Variation of Nox (NO_2^-+NO_3^-) in pore and overlaying waters

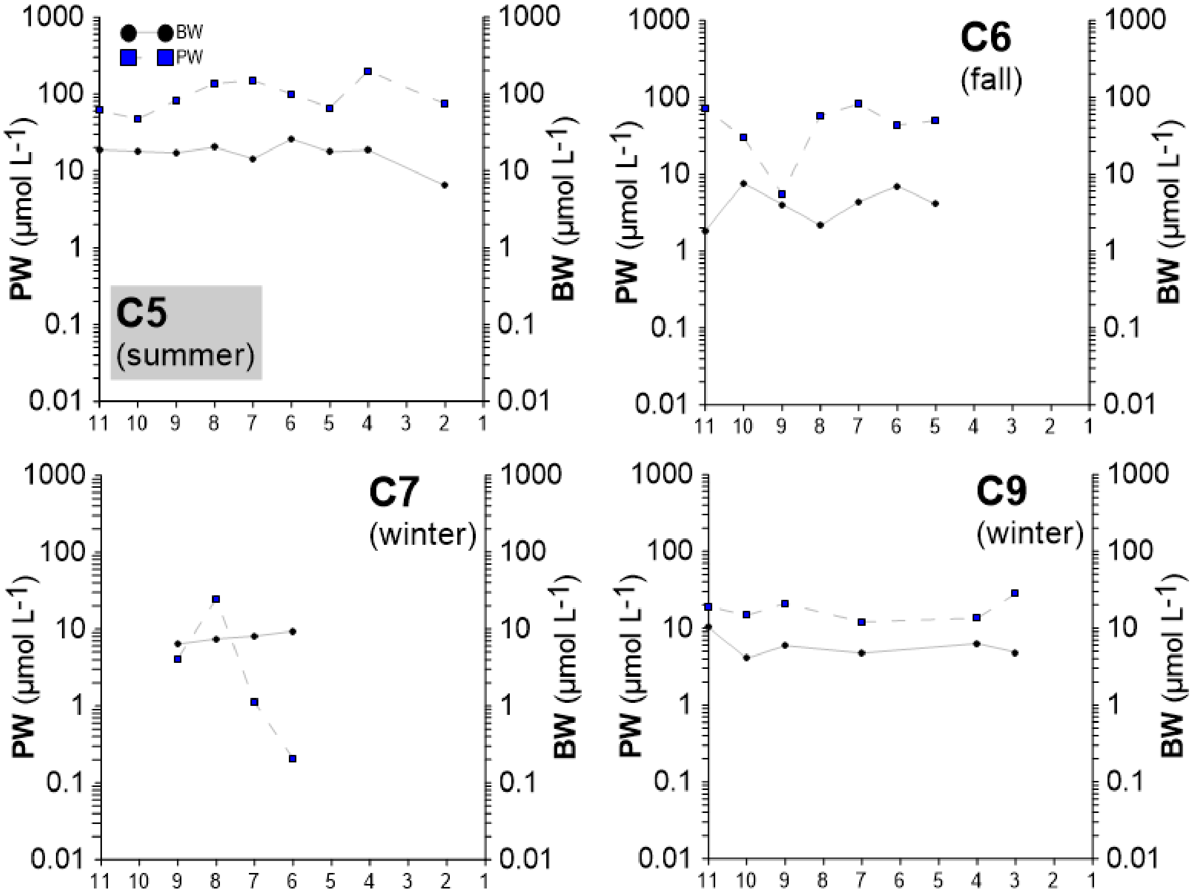

Source: Elaborated by the author, 2023.
LEGEND: BW= overlaying water; PW= pore water. Nox varied from C5 to C7 and was almost constant in C9. Pore water was almost 3 orders greater than overlaying water.

5.3.2 Nutrient fluxes

Sediments (Figure 33 and Appendix C – Table C3.3, Figure C3.4) were classified as sand > slightly gravelly sand > gravelly sand based on Wentworth scale (Wentworth, 1922). Carbonate content was higher than 30%, (Figure 34, Appendix C and Table C3.2), which characterized them as carbonate sediments and the carbonate shelves presented great variability in size (up to 10 mm–radius). Moreover, the granulometry and size of shelves were distributed in AL following the suggested compartmentation (Chapter 4). Except for carbonates in C5 (turbid), C6 and C7 (non-turbid) were slightly similar but in C9 (non-turbid) values were relatively higher. Also, Figure 34 also shows the variation of OM which were higher in C5 (turbid condition), while C6, C7 and C9 presented lower concentrations. Stations 4 (C5), 7 (C7) and 8 (C8) recorded the highest values of OM. The distribution of carbonates seems to fit the three suggested sectors of the lagoon. Due to the lack of data, this behavior was not well observed in OM, and only C5 barely followed it.

Figure 33 – Distribution of granulometry in Araruama Lagoon

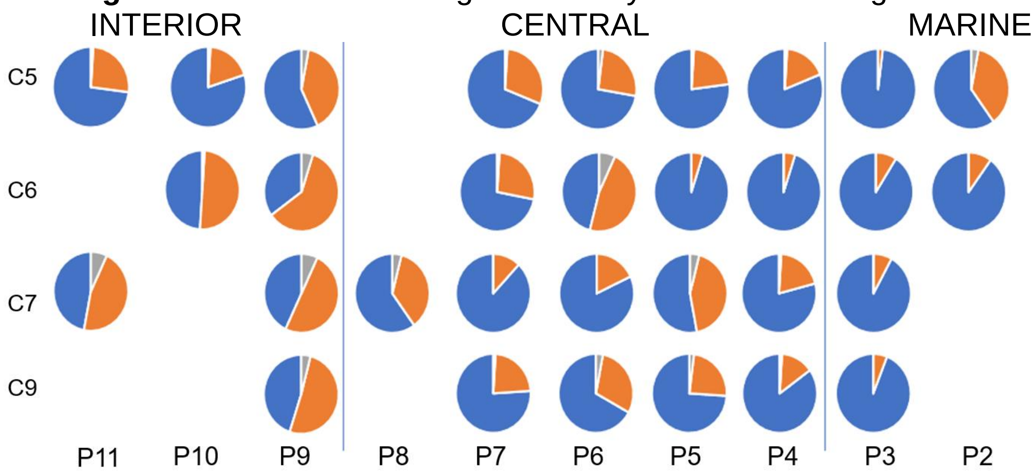

Source: Elaborated by the author, 2023.
LEGEND: Distribution of the granulometry along the sectors of AL. Grain size – silt/clay fine sand coarse/medium sand.

Figure 34 – Carbonate and organic matter in sediments

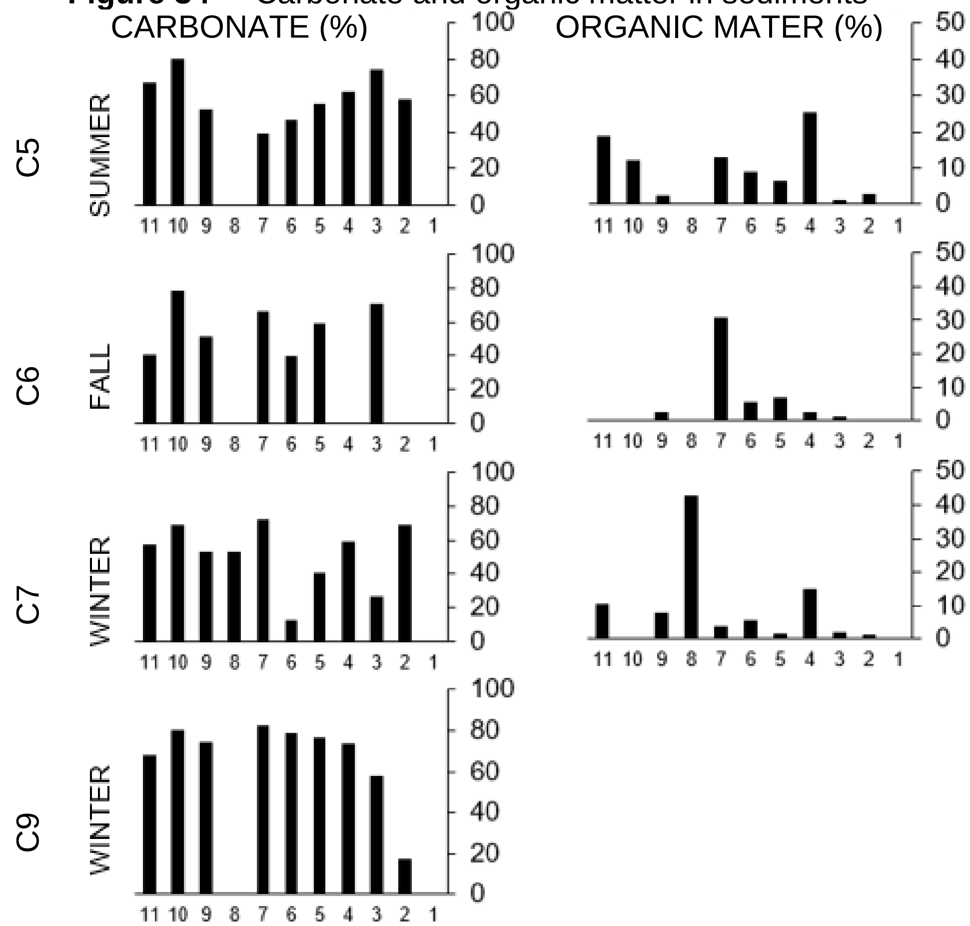

Source: Elaborated by the author, 2023.
LEGEND: Carbonate content (left side) and organic matter (right side) varied spatially and temporally in all campaigns, but C5 (turbid condition) was higher for both parameters.

Important to note that advective fluxes were not considered in this work, and Fick's law did not consider bioturbation, so this estimative comprised the minimum fluxes quantified in AL. Also, the massive presence of shelves could affect the fluxes in AL, depending on their distribution in sediments.

5.4 Discussion

Diffusive fluxes of nutrients varied spatially and temporally in AL (Figure 35 and Appendix B - Table B3.5) and turbid water presented higher fluxes than non–turbid. Phosphate fluxes tended to increase from east to west despite the variability among campaigns. It reduced the water quality and implied in worst sediment quality which led to higher fluxes of nutrients. Positive phosphate fluxes corroborated the results found in mesocosms experiments for AL from Guimarães *et al*. (2021). DIP coupled with carbonate dissolution/precipitation and carbonate sands were relevant for benthic DIP fluxes (Delgado–González *et al.*, 2021; Ning *et al.*, 2020). Like Silva (2019), the present investigation corroborated the link between phosphate in pore water to granulometry and carbonate.

The importance of anaerobic conditions over concentration gradients for P fluxes was identified by Moore, Reddy and Fisher (1998) in which anaerobic conditions favor P fluxes. In AL, the importance of sediment–water interface for P release was observed in anaerobic conditions and results agreed with Kraal *et al.* (2013). The cited authors observed positive phosphate fluxes even in oxidizing conditions due to high local eutrophication level. This means that, in eutrophic zones, the capacity of sediment supplies P surpasses the capacity of water oxygenation to retain P in sediments.

Phosphate can be rapidly mobilized in pore waters due to sulfate reduction in saline environments under anoxic conditions. This reduction would promote precipitation of Fe–sulfides and P–releasing to bottom waters (Williams; Lauer; Hackney, 2014). Phosphorus fractionation in sediments from AL did not identified high P–Fe fractions (Silva, 2019) possibly explained by the small availability of Fe in the local sediments. Studies from De Montigny and Prairie, (1993) reported an independent pattern for P and Fe in which most of dissolved iron would be combined with humic acids not phosphorus.

Figure 35 – Diffusive fluxes of nutrients in Araruama Lagoon

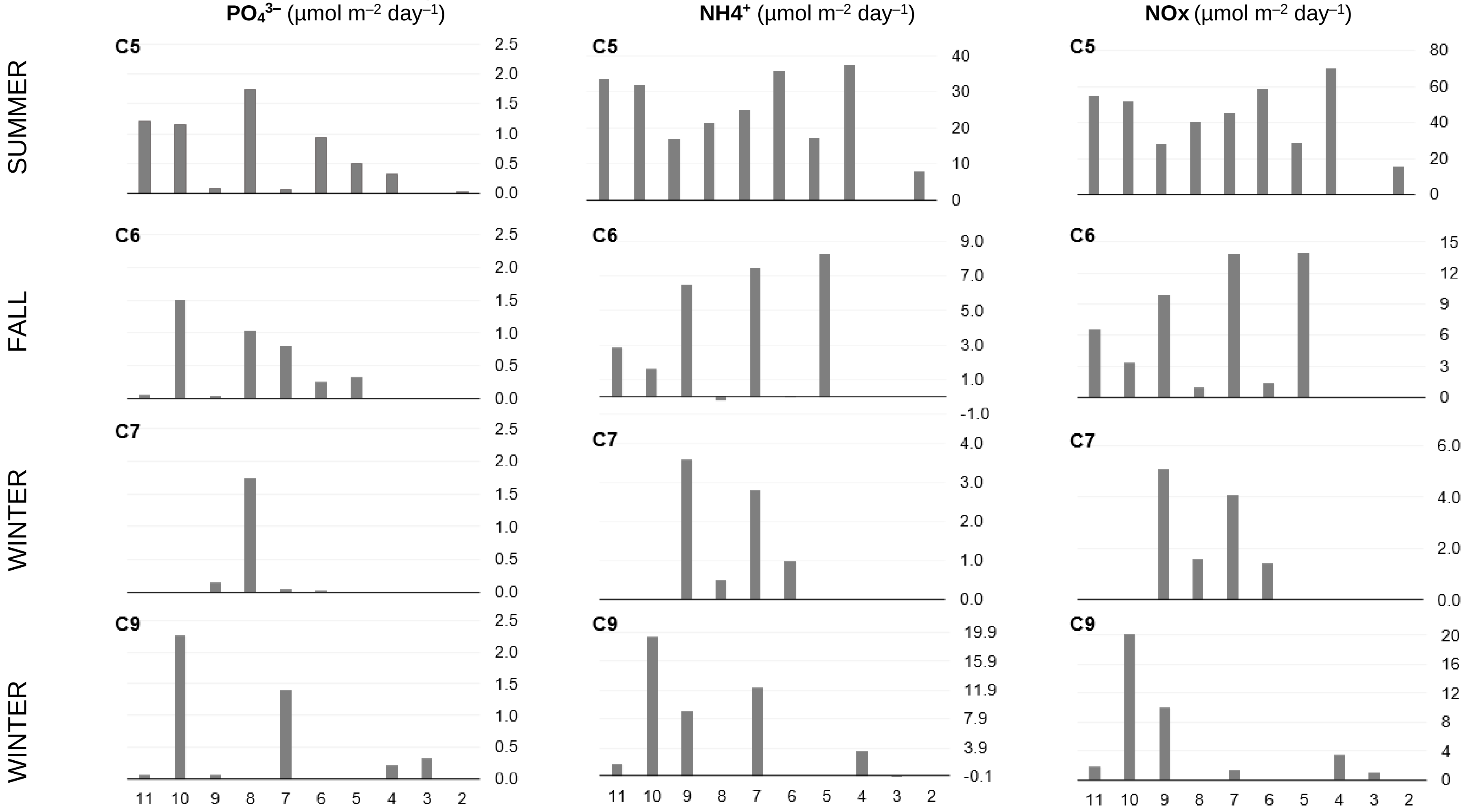

Source: Elaborated by the author, 2023.

LEGEND: Fluxes were higher in turbid (C5) than in non–turbid water (C6, C7, and C9) despite the spatial variation. Nitrogen fluxes were higher than phosphorus and varied similarly during the campaigns. Phosphorus and nitrogen fluxes presented a tendence to increase westwards.

Low DIP concentrations in bottom waters were measured in all campaigns of this study and were also observed by Guimarães *et al.* (2021) and in Coorong Lagoon by Huang *et al.* (2023). Silva (2019) observed that labile–P (authigenic and organic) were associated with a higher concentrations of DIP, possibly related to OM decomposition. AL presented a small content for phosphorus in water column, however the sediments contained substantial amounts of phosphate. The correlation between phosphate and OM is possible to occur due to the fast kinetics of phosphate on tropical Ca–carbonate sediments (about 30 min). This reactions could favor the continuous P efflux (Millero *et al*., 2001). In Chesapeake Bay, like in AL, ammonium and phosphate fluxes were higher in the warm seasons. But NOX was predominantly negative in Chesapeake Bay while in AL values were positive (Boyton; Kemp; Osborne, 1980).

Reactions such as adsorption of phosphate to carbonates is reduced by the formation of (Mg, Ca) sulfates or sulfate coating on carbonate particles (Millero *et al*., 2001). Moreover, Van Cappellen and Berner (1988) identified fine–grained carbonates responsible for nucleation of P–apatite and the P liberation could occur up to 1 hour, depending on oxireduction conditions. These two conditions may be happening in AL and affecting the phosphorus fluxes, due to the high concentration of carbonates. However, there was no studies about this kinetics in the lagoon.

N–processes, can be controlled by grain size because coarse grains present a tendency to higher potential for nitrification while fine sediments for denitrification (Li *et al.*, 2020). Ammonium fluxes presented a reduction between C5 and C6, turbid to non–turbid condition, respectively. Nox fluxes were similar to the ammonium but presented higher values and a sharp reduction between turbid to non–turbid water. This pattern was described in Salt Creek and Swan Island and Coorong Lagoon indicating a preferable ammonium concentration in anoxic conditions and higher fluxes to water column (Huang *et al.*, 2023). Those authors also correlated the anoxic sediments with a nitrification control and inhibition of nitrate production due to the sulfidic conditions in sediments. Other possibility was denitrification associated with the amount of nitrate (Nielsen *et al.*, 2003), i.e., in reducing sediment zones, nitrite–to–ammonium conversion would enhance ammonium fluxes to water column.

Disparities among nitrogen behavior could be due to its chemical forms present in the sediment (exchangeable, residual, or hydrolysable). Despite the great difference between AL and the Tibetan plateau, results from Wang (2018) described these three N–forms in sediments and the effects over N–fluxes. Such processes could occur in AL, but it would be necessary further studies to confirm such hypothesis. Anoxic conditions in sediments from AL and the constant positive DIN efflux could reflect the nitrifying and denitrifying organisms acting in sediment–water interface to maintain this condition (Li *et al.*, 2020). In AL, Nox was higher than ammonium, possibly by the good oxygenation of the lagoon, but the spatial and temporal behavior was similar to both.

Ammonium and nitrite fluxes were sensitive to temperature, and it was coincident with the study conducted by Velinsky *et al.* (2017). The authors associated such higher fluxes with the higher presence of denitrifying bacteria. Koomklang *et al*. (2018) also verified higher positive fluxes in summer and results did not show relation with organic matter in sediments. Higher positive fluxes of ammonium in Chesapeake Bay were observed in the spring/summer, while NOX was predominantly negative (Boyton; Kemp; Osborne, 1980). The present research and both cited studies related denitrification processes with temperature. Results of DIN agreed with Camacho–Ibar, Carriquiry and Smith (2003) that identified association among DIN fluxes and salinity gradients and an upwelling in San Quentin Lagoon. N fluxes were higher in the central sector of the AL where the salinity was higher In San Quentin Lagoon there is a biweekly upwelling cycle which supplies N and promotes high primary production.

The quantification of the diffusive fluxes in AL, in different seasons and covering all ellipsoids, identified positive fluxes of phosphorus and nitrogen and it could be attributed to: i) a massive retention of nutrients in sediments, indicated by the very high concentrations in pore water; ii) part of these nutrients may be used by benthic organisms, especially those related to N transformations; and iii) positive phosphate fluxes in oxidizing bottom conditions highlights the impact of eutrophication in benthic phosphorus fluxes.

5.4.1 Coupling nutrient fluxes to trophic crises

The focus on coupling diffusive fluxes to trophic crises was to determine the role of nutrient diffusion on trophic crises events, which resulted in turbid/non–turbid water. Adding the results of this chapter to those from Chapter 4, it was possible to identify close relations between both topics. The suggested model (Figure 36) shows the descriptors of trophic crises and diffusive fluxes in each water condition.

Figure 36 – Coupled model of descriptors and nutrient fluxes in trophic crises

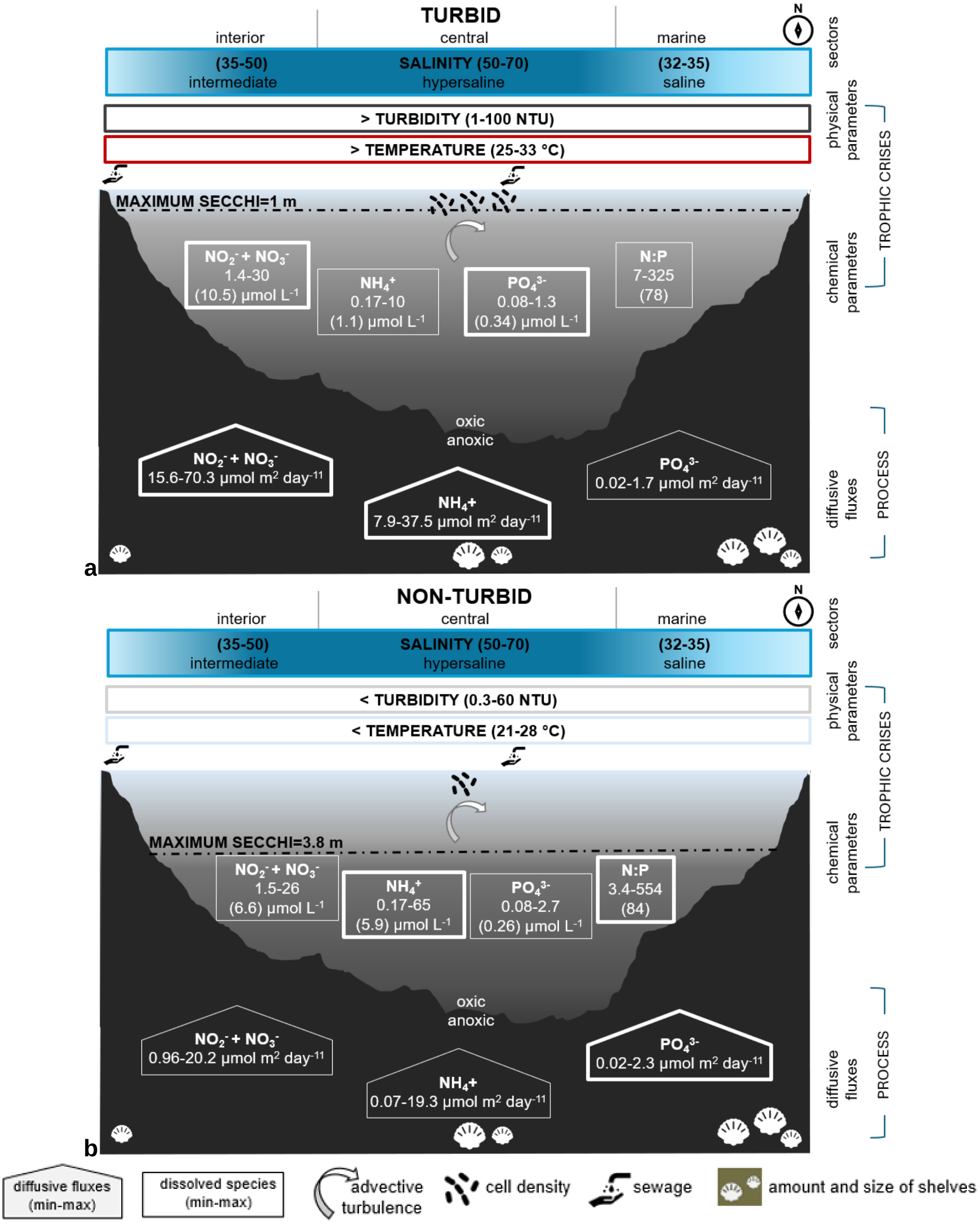

Source: Elaborated by the author, 2023.

LEGEND: Diffusive fluxes in trophic crises – a) turbid water; b) non–turbid water. Nutrient fluxes were included to the previously descriptors for trophic crises (see Chapter 4, Figure 28), and it is possible to note the link between trophic crises and diffusive fluxes of nutrients. The shifts in water conditions were driven by nutrient fluxes, particularly by nitrogen. In turbid conditions, fluxes of Nox and ammonium were higher than in non–turbid waters. Phosphate was slightly higher in turbid conditions, corroborating the role of P in the primary production in the lagoon. The variation in granulometry and shelf content could potentially affect the fluxes in the different sectors of the lagoon.

Results revealed interesting points: i) nitrogen and phosphorus, instead of only phosphorus, were responsible for the trophic crises; ii) phosphate presented lower fluxes if compared to N–forms; iii) N:P ratios, despite the great variations were higher in turbid conditions.

In Burano lagoon (Italy), there was a shift in water column conditions for 6 months, and a sequence of blooms of distinct species occurred. Phosphate ranged from 0.43 to 1.9 µM, ammonium from 0.07 to 143 µM, nitrite from 0.1 to 2 µM and nitrate from 30 to 557 µM. Both nitrogen and phosphorus were abundant, despite there was an imbalance favoring nitrogen, as it was also verified in AL. Fernández–Alías *et al.* (2022) described trophic crises in a Mediterranean coastal lagoon and identified a top–down to bottom–up control and it was the triggering dystrophic processes. In the study, authors found N:P ratios circa 5 in “break” conditions, and nitrate was responsible for the crisis. Basset *et al*. (2013) quantified TN for Lesina lagoon (Italy) and values varied from 0.73 to 21.98 µg L^{-1} for TP and 3.05 to 9.66 for TN which were higher than those found in AL.

Silva (2019) determined P–fractions in AL and the major presence was authigenic apatite and loosely–sorbed P which could favor the releasing of phosphorus. Moreover, faster decomposition of phosphorus than nitrogen (Redfield, 1958) associated with the long residence time and mixing in AL could favor P recycling over N. The low pelagic P and high benthic N content explain the low P and high N fluxes, causing imbalances in nutrient cycling. The results found in this work were similar to those from Knoppers *et al.* (1996) that measured benthic fluxes of phosphate in Araruama Lagoon. For the authors, sediment–water interface was the main source of ammonium to the water column. Whereas fluxes of phosphate were irrelevant, indicating a primary production limited by phosphorus. Moreover, processes such as authigenic apatite, inclusion on organic coats of carbonates and direct precipitation of amorphous calcium phosphate would be responsible for P–retention.

N–fluxes might be related with primary production seasonality, because from C5 to C6 (summer to fall) there was a very strong reduction in ammonium fluxes to water column. The cause of this shift in nitrogen fluxes could be due to the efflux of ammonium rapidly converted in nitrate in water column. In anoxic sediments, diffusion of sulfides could control NH_4^+ diffusion, due to the high contents of sulfides Compete With Nh_4^+ For O_2 Which Reduces Nitrification (Blackburn; Blackburn, 1993). Since sediments in AL present very reducing conditions, it could probably happen because it was measured ammonium flux higher than nitrate.

Advances in molecular stoichiometry shows an interplay between N and P starvation and uptake, each one regulating the other (Helliwell, 2023). The author identified strategies that could be used in P limiting conditions and enhance nitrogen uptake. Bourceau *et al.* (2023) identified sulfate reducing organisms that change their typical respiratory arrangements and use dissimilatory nitrate reduction to ammonium (DNRA). This shift occurs in alternate redox conditions and leads to reduction in denitrification rates and increase ammonium content, however in AL there is no study about the topic.

In this chapter, diffusive fluxes of nutrients were introduced to explain the variations in water column turbidity. The results identified the importance of sediment in nutrient fluxes and so to water column quality especially in central sector of AL.

Nutrient diffusive fluxes in AL presented high variation among seasons and stations. The predominant nutrient flux was nitrogen (as both ammonium and Nox), and nitrogen also presented the highest concentrations in water column and sediments. Higher fluxes of N-forms were determined in turbid conditions, while in non-turbid waters there was a great reduction in such fluxes, but in both situations, Nox fluxes were higher than ammonium. Phosphate did not present significant diffusive fluxes despite the concentration in pore water was higher than in overlaying water. However, these fluxes contributed to maintain primary production in AL. Phosphate fluxes exhibited a slightly tendency to increase values to west, which was possibly related to restrict hydrodynamic conditions.

This study corroborated the previous works about the association between low water quality and nutrient loads in AL. The western cells present smaller size and depths and are under lower wind stress, if compared to other cells. Despite the relevance of fluxes on water conditions, some points about the drivers of diffusive fluxes need to be done. Previous studies have demonstrated the importance of upper layers (up to 3 cm) for nutrient reactions in sediments, so more detailed sediment samplings would need to be analyzed.

Studies with isotopes that include autotrophic and heterotrophic production in both water column and sediment should be developed to have a complete view of nutrient cycling. Due to the variation of ORP at the sediment-water interface, nitrite may be considered a key factor in nitrogen fluxes and conversion between nitrite to ammonium or nitrate could be decisive to promote higher phytoplankton production.

6 MASS BALANCE OF NUTRIENTS FOR PRIMARY PRODUCTION

Phytoplankton is the base of the aquatic trophic chain, and is widespread in ocean, lakes, and rivers. Variation among the physical–chemical parameters, including nutrients in water drives the maintenance and abundance of different species at spatial and temporal scales (Harris, 1986). In confined coastal waters, large waste discharges may cause eutrophication problems if a critical capacity is and water renewal is not favorable (Economopoulos, 1993). Different autotrophic populations in aquatic systems can be classified as phytoplankton based, benthic microalgal and macrophyte systems, and algal mats. These primary populations will succeed in response of geomorphological features, sea water connection, flushing rates, nutrient limitation and salinity (Knoppers, 1994).

Availability (number) of elements – species, habitats, etc. – in an ecosystem is also linked to geological and pedological characteristics determining productivity of phytoplankton (Rizhinashvili, 2022). High primary production is caused or intensified by eutrophication resulting in environmental problems such as turbidity, bad smell, and harmful algal blooms (Anderson, 2009; Gowen *et al.*, 2012; Webster; Harris, 2004; WHO, 2021). However, species necessities vary depending on certain characteristics. The selective absorption describes a sense of “choice” by the phytoplankton: if two nutrients are present in a system, one in excess while other is limiting, species assimilate high proportion of the limiting nutrient, but would not absorb the one in excess if it was not necessary (Ketchum, 1954).

The most common factors which lead to the increasing of phytoplankton are light incidence and nutrient loading (Gowen *et al*., 2012), and temperature (Bestion *et al*., 2020). Primary production is also affected by dissolved oxygen, depth, water transparency, wind, rainfall, El Niño/La Niña, residence time of water (Barrera–Alba; Abreu; Tenenbaum, 2019; Kubryakov; Zatsepin; Stanichny, 2019; Winder; Cloern, 2010) and heavy metals (Cordero *et al.*, 2005; Okamura; Aoyama, 1994; Shahi *et al*., 2015). Whereas turbulence in water column enhances nutrient vertical distribution and controls phytoplankton assemblages (Dell’Aquila *et al.*, 2017; Durham *et al.*, 2013; Macintyre, 1998).

The current understanding is that nutrient requirements for living species in an ecosystem affect both growth potential and food web behavior (Glibert, 2017). Phosphorus and nitrogen are currently the limiting nutrients in water bodies and their variation plays an important role for phytoplankton growth (Davidson *et al*., 2014; Gowen *et al*., 2012). Elser *et al.* (2007) concluded that N and P limitation depends on the species but also the local ecological factors such as habitat, size of organisms, and species association. Also, the alteration of a specific nutrient could lead to quantitative changes in ecosystem production and qualitative shifts in nature of nutrient limitation (grazing or stoichiometry). And eutrophication in coastal zones poses concern about environmental quality.

Factors that influence P requirements are life stage and P–species present in water. Life stage was also relevant for P content in cells, being the older cells carrying more content of P than the younger. The form of phosphate also interferes on organism uptake, i.e., pyro–phosphate is used less effectively than ortho–phosphate for some organisms, while others can use alternative P–forms to grow (Ketchum, 1954).

According to Ketchum (1954), four concepts are necessary to understand the different approaches of nutritional requirements: i) the absolute requirement – algal growing, reproduction and photosynthesis cannot occur if the nutrient is lacking in environment and no other can replace it; ii) normal requirement – based on the statement of an ideal or normal cell composition, i.e., the quantity of a nutrient contained in each cell during growth if there is no nutrient limitation; iii) minimum requirement – it is the quantity of nutrient limiting the growth of a population, even if other nutrients are present in excess; such deficient cells would contain greater amount if it was available; iv) optimum concentration – is the range of concentration that allow the maximum growth rate, reproduction and photosynthesis of an algal population; it varies from the minimum required but not as high to be toxic.

At this point, it is necessary to introduce the size classification of phytoplankton, because they present high variation depending on the species. Despite many classifications of phytoplankton, this thesis is based on Dussart (1965), who considers: i) macrophytoplankton (>2000 µm); ii) mesophytoplankton (200–2,000 µm); iii) microphytoplankton (20–200 µm); iv) nanophytoplankton (2–20 µm); v) ultraphytoplankton (<2 µm; also called picophytoplankton). As pointed by Marañon (2015) both cell size and temperature control metabolic rates, as follows: the higher the cell size, which is smaller the metabolic rate. The light absorption by chlorophyll *a* is also a matter of size and it is lower in larger cells due to the self–shading effect.

Regarding nutrient requirements, small species have advantage in nutrient–deficient conditions due to high surface–to–volume ratio (known as specific surface). The large cells need higher concentrations, due to a deficient capacity to remove nutrients from the water column (Chisholm, 1992; Erdoğan *et al.*, 2021). According to Marcarelli; Fulweiler and Scott (2022), environmental stoichiometry is a link between organism and nutrition requirements and a way to understand the spatial–temporal dynamic of communities. Cell size and environmental stoichiometry are indicators for environmental alterations caused by climate changes, while climate changes lead to modification in phytoplankton community structure (Finkel *et al.*, 2009; Litchman; Klausmeier; Yoshiyama, 2009). Nutrient rich or in environments that present large pulses favor uptakes by larger cells, while small cell prefer environments with no disturbance or lower pulses (Harris, 1986).

The amount of nutrients required for cells is small for larger cells, which means that the higher the cell the lower nutrient concentration per unit of cell volume. Small cells are considered as having a lower uptake ability because the internal space available for biochemical reactions is reduced (Marañón, 2019). Different cell sizes also can contain different number of chloroplasts (Hasle, 1997), which influences on OM production. In AL, the sinking rates are low, due to the predominance of small phytoplankton over larger (Neves, monitoring reports, 2019–20). However larger cells present higher sinking rates, because they are heavier, and more advection is necessary to maintain these cells floating. Besides, nutrient can be chemically retained in sediments taking years to be released after their depletion (Coelho *et al.*, 2004). High ammonium concentrations are favorable for cyanobacteria; chlorophytes and dinoflagellate Burkholder (2003), while increase in nitrate benefits diatoms (Glibert, 2017).

In an attempt to identify environmental behaviors, a variety of models permit quantify compartments and evaluate changes, responses and stocks of nutrients and pollutants (Béthoux *et al.*, 1998; Kjerfve *et al.*, 1996; Lobo *et al.*, 2023; Tasnim *et al.,* 2021; Trevisan *et al.*, 2020; Vicente *et al.*, 2022). Nutrient modeling uses data from different compartments and are able to identify seasonality or influences of specific parameters on nutrient cycling (Biswas *et al.*, 2017; Cunha; Wasserman, 2003) as well as trophic chains demands (Almeida–Silva *et al.*, 2015; Cruz; Santos; Santos, 2018; da Silva *et al.*, 2005). In AL, it remains unclear if whether accumulation and remineralization in sediments are more important as source of nutrients than direct sewage discharges.

This chapter evaluated the capacity of sediment and sewage to support the phytoplankton production in AL. The objective was to quantify the nutrient requirements of local phytoplankton and identify the main sources capable to nourish the primary production in the lagoon. Local phytoplanktonic assemblages include diatoms species wide distributed in the lagoon and indicate anthropic impacts by freshwater and organic sewages discharges (Sylvestre *et al*., 2001).

6.1 Study area

Araruama Lagoon (Figure 3), like other hypersaline environments, presents specific characteristics regarding the biotic community and a complex food web (Almeida–Silva *et al.*, 2015; Leao *et al.,* 2018; Ramos *et al.,* 2017). It is essentially a touristic region, with a restricted drainage basin, where agricultural, livestock, and industrial activities are insignificant (Barroso; Bernardes, 1995). The main source of contamination in water is domestic sewage because local geology does not present any relevant anomaly of nutrients in soils and rocks (Penha, 1999). Seasonal shifts from autotrophs to heterotrophs assemblages is an important control in chocked tropical and sub–tropical lagoons. They usually present unimodal or bimodal pattern of primary production with highest rates in late summer (Knoppers, 1994). Monitoring reports (Neves, 2019–2020) indicated the presence of three main groups of phytoplankton by number of cells: cyanobacteria > dinoflagellates > diatoms. The main species presented sizes varying from 2 to 20 µm (nanophytoplankton).

However, it remains unclear if accumulation and remineralization in sediments are more important as source of nutrients than direct sewage discharges. To answer this question, a balance of primary production was developed, after the concept shown in Cunha and Wasserman (2003). The model allowed to identify if the nutrient supply from sewage is sufficient to support phytoplanktonic production in lagoon. This was a first study to quantify nitrogen and phosphorus requirements for different sizes of phytoplankton and is important for environmental management of coastal lagoons.

6.2 Materials and methods

- Phytoplankton collection and analyses

Water surface samples were collected in Sep 17, 18 and 19, 2022, using a van Dorn bottle and filtration was made *in situ* with a multifiltration system specially designed for this work (Figure 37). The equipment allowed to get simultaneously different phytoplankton sizes using membranes with varied apertures (S_P): i) S_P<25 µm; ii) 25 µm≤S_P<100 µm; iii) 100 µm≤S_P<150 µm; iv) 150 µm ≤S_P<200 µm; v) S_P≥ 200 µm. Membranes were kept in coolers and then analyzed in laboratory. The water sample that passed through the smaller membrane (25 µm) was filtered in the laboratory with a Manifold kit with glass fiber filters of circa 0.70 µm. After filtration, the particulate fraction of each size was analyzed for PN and PP as described in Section 3.2.

Figure 37 – Multifiltration system

Source: Elaborated by the author, 2023.

LEGEND: This system was used to sort the phytoplankton by size and to determine their nutritional requirements in AL. The equipment is composed by four sections, each one for a different aperture size of a membrane (from 25 to 200 µm). They are connected in a single multifiltration system, which the topside is the compartment from where water passes through to the below level. The white box indicates the smallest aperture (0.7 µm), and it is not part of the equipment. It corresponds to the fraction of the remaining water which will pass through a fiber-glass filter. Due to the species presented in AL, the fraction used to quantify N and P was that of the fiber glass filters (0.7 µm). Important to note that the system can be used at the field or in laboratory and it is adjustable if necessary. The number of compartments can vary, and the membranes can be replaced by other sizes, depending on the case to case.

- Mass balance model

Nutrient mass balance model for phytoplankton is composed by 4 groups of data according to a flux of information, Figure 37: i) data from sewage production, related to demographic data and water production by water treatment plants (WTP); ii) data of sediment reservoir was accessed via nutrient fluxes from Chapter 4; iii) water column reservoir; iv) phytoplankton requirements, data from different sizes collected and analyzed for N and P. In each reservoir, the mean concentration of nutrients and the stock during the residence time were calculated. Nitrogen and phosphorus were calculated for four reservoirs (sewage, sediment, water and phytoplankton) and compared to each other, allowing to evaluate the contribution of each one to phytoplankton production.

Figure 38 – General overview of the nutrient paths for phytoplankton nutrition model

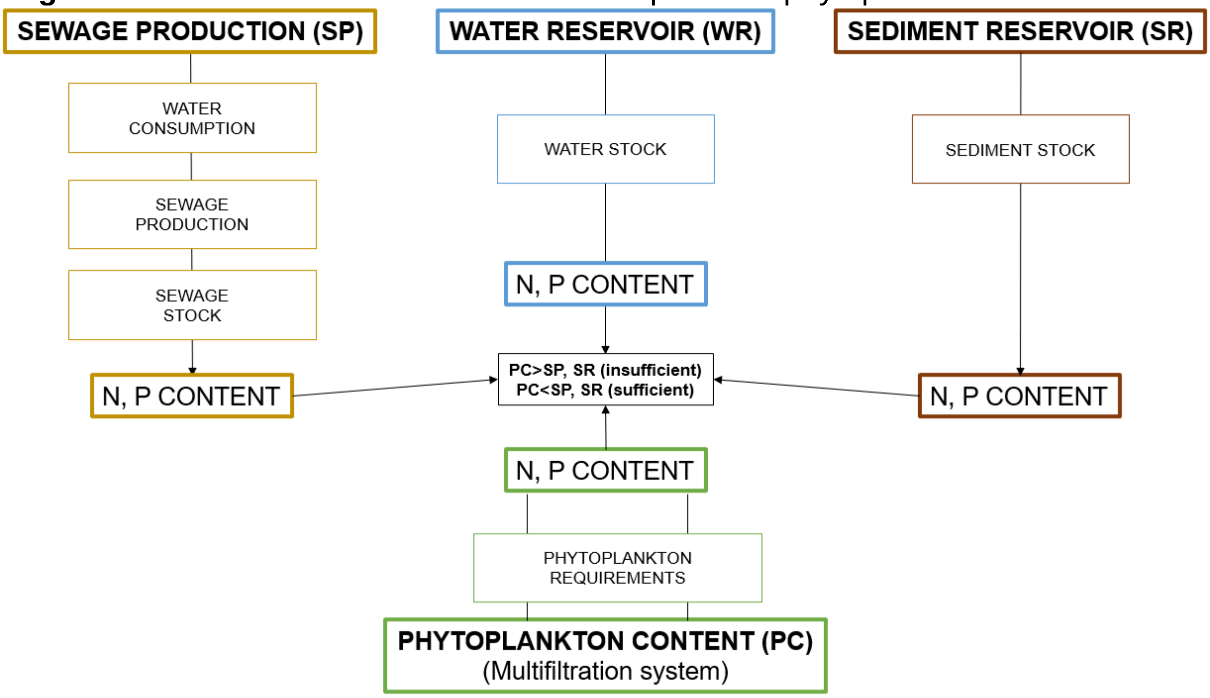

Source: Elaborated by the author, 2023.
LEGEND: Colored boxes indicate the nutrient reservoirs in AL and arrows indicate the pathways for the phytoplankton nutrition.

The sequence for calculate the stocks is shown in Figures 38 to 41. Depending on the compartment, a sequence of equations was developed. The water compartment used data from water column (Chapter 4), nutrient fluxes (Chapter 5) and phytoplankton requirements (next section).

Figure 39 – Sequence for calculation of N and P concentration in sewage

STEP 1

pop (hab)

STEP 2

WC = water consumption per capta (L day^{-1} hab^{-1})
T_{WC}= total water consumption (m^3 day^{-1})
$\mathbf{T_{WC} = pop \times WC}$

STEP 3

$[N]_{sew}$ = N in sewage (mg L^{-1})
$[P]_{sew}$ = P in sewage (mg L^{-1})
T_e^{-1}= residence time (day)
M_{Nsew} = mass of N due to WC (kg day^{-1})
M_{Psew} = mass of P due to WC (kg day^{-1})
$\mathbf{M_{Nsew} = [N]_{sew} \times T_{WC}}$
$\mathbf{M_{Psew} = [P]_{sew} \times T_{WC}}$
N_{sew} = total N in sewage (kg)
P_{sew} = total P in sewage (kg)
$\mathbf{N_{sew}} = M_{Nsew} \times \mathbf{T_e^{-1}}$
$\mathbf{P_{sew}} = M_{Psew} \times \mathbf{T_e^{-1}}$

STEP 4

V_{Te}^{-1} = volume in a residence time (m^3)
V = volume of the waterbody (m^3)
$\mathbf{V_{Te}^{-1} = V \times 63\%}$
TN_{sew}= total N concentration in sewage (mg L^{-1})
TP_{sew}= total P concentration in sewage (mg L^{-1})
$\mathbf{TN_{sew} = N_{sew} / V_{Te}^{-1}}$
$\mathbf{TP_{sew} = P_{sew} / V_{Te}^{-1}}$

Source: Elaborated by the author, 2023.

LEGEND: the contribution of nutrients from water treatment plants (TNsew and TPsew) is based on demographic data, reducing 35% of the total, in average for liquid wastes, due to efficiency of treatments (ECONOMOPOULOS, 1993).

Figure 40 – Sequence for calculation of N and P in water column

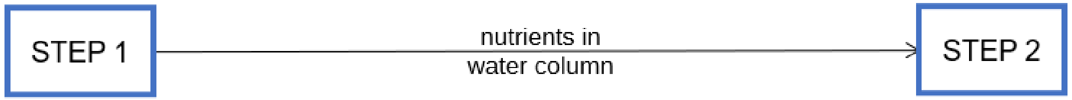

STEP 1

$\mathbf{[N]_{wc}}$ (mol L^{-1})=mean DIN concentration in water column
$\mathbf{[PN]_{wc}}$ (mol L^{-1})=mean particulate N in water column
$\mathbf{TN_{wc}}$ (mol L^{-1})=N amount in water column=$\mathbf{[N]_{wc}+[PN]_{wc}}$
$\mathbf{[P]_{wc}}$ (mol L^{-1})=mean DIP concentration in water column
$\mathbf{[PP]_{wc}}$ (mol L^{-1})=mean particulate P in water column
$\mathbf{TP_{wc}}$ (mol L^{-1})=P amount in water column=$\mathbf{[P]_{wc}+[PP]_{wc}}$

STEP 2

V (L)=volume of the water body
$\mathbf{V_{Te}^{-1}}$ (m^3)=volume in a residence time= **V.63%**
$\mathbf{N_{wc}}$ (mol)=N in water column=$\mathbf{[N]_{wc}.V_{Te}^{-1}}$
$\mathbf{P_{wc}}$ (mol)=P in water column=$\mathbf{[P]_{wc}.V_{Te}^{-1}}$

Source: Elaborated by the author, 2023.

LEGEND: Calculation of water column reservoir was based on data of the Chapter 4 of this thesis.

Figure 41 – Sequence for calculation of N and P in sediment

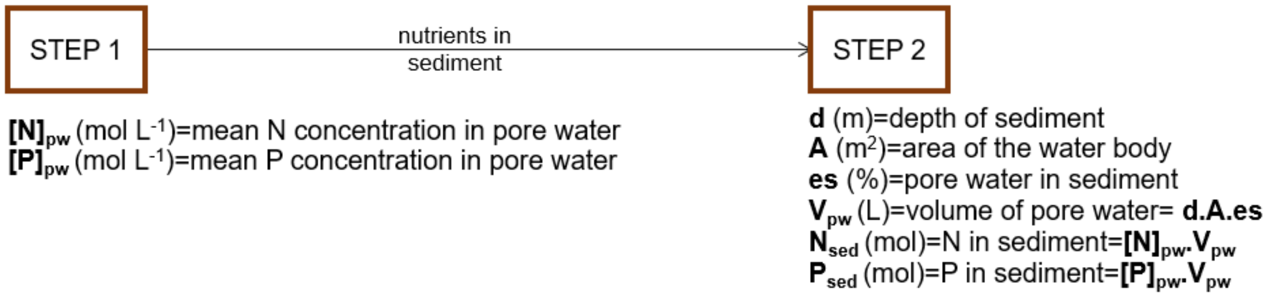

Source: Elaborated by the author, 2023.

LEGEND: Calculation of water column reservoir was based on data of the Chapter 4 of this thesis.

Figure 42 – Sequence for calculation of N and P required for phytoplankton

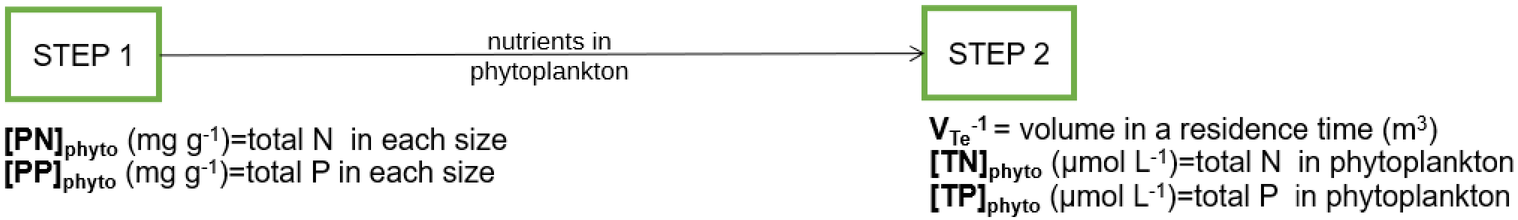

LEGEND: Source: Elaborated by the author, 2023.

Calculation of phytoplankton reservoir was based on material collected using the multifiltration system (this chapter, Figure 32).

6.3 Results

- Sewage discharges

Data from sewage production were obtained from water treatment plants, and calculated based on regular inhabitants surrounding AL, not considering floating population during holidays. Population includes municipalities of Araruama, Cabo Frio, Iguaba Grande, Arraial do Cabo, and São Pedro da Aldeia. Despite Saquarema belongs to the AL surroundings, it occupies a small portion of lagoon and population is irrelevant. Population of Búzios and part of the Cabo Frio (corresponding to Tamoios district) were not included because their sewage is not discharged in the lagoon. Initially, the nitrogen and phosphorus loads released into the AL via domestic sewage were calculated solely based on Figure 33 and the regular population (not considering fluctuations due to seasonality).

According to Economopoulos (1993), community, social and personal services produce atmosphere emissions, effluents and solid wastes as usual pollutants. The typical properties of municipal wastes in Brazil present 47.8% of putrescible components (comprise sludges from wastewater treatment plants among others, which do not present high content of toxic substances). Tables 10 to 13 are the results of the sequence shown in Figure 39.

Table 10 – Population of AL vicinities

CITY	INSIDE THE WS	INHABITANTS
Araruama	77,000	77,000
Cabo Frio	139,500	186,000
Iguaba Grande	23,000	23,000
Arraial do Cabo	29,000	29,000
São Pedro	100,000	100,000
Saquarema		NR
Total (hab)		368,500

Source: IBGE (2010).
LEGEND: WS= watershed area; NR not relevant.

Table 11 – Water consumption corresponding to the sewage generation*

PARAMETER (UNITY)	VALUE
Water consumption[1] (WC; L day^{-1} per capta)	225
Total consumption surrounding the lagoon (T_{WC}; m^3 day^{-1})	82,912.50
Total consumption surrounding the lagoon (T_{WC}; m^3 s^{-1})	0.96
Water distribution in Região dos Lagos[2] (m^3 s^{-1})	1.90

*It was not considered the treatment made by the water companies due to the uncertainties on nutrient removal. Source: [1]CEDAE, Rio de Janeiro. [2]Data from local water companies (Águas de Juturnaíba/PROLAGOS).

Table 12 – Nutrients due to sewage loadings

PARAMETER (UNITY)	VALUE
Residence time[1] (T_e^{-1}; days)	45
Nitrogen in sewage[2] ($[N]_{sew}$; mg L^{-1})	22.3
Mass of nitrogen (M_{Nsew}; kg day^{-1})	1848.9
Total N in sewage (N_{sew}; kg; per residence time)	83,202.7
Phosphorus in sewage[2] ($[P]_{sew}$; mg L^{-1})	3.0
Mass of phosphorus (M_{Psew}; kg day^{-1})	248.7
Total P in sewage (P_{sew}; kg; per residence time))	11,193.2

Sources: [1]Residence time (T_e^{-1}) – time to exchange 63% of the volume of a water mass in a system (Monsen *et al.*, 2002). [2]Economopoulos (1993).

Table 13 – Nutrient concentration due to sewage loadings

PARAMETER (UNITY)	VALUE
Area of AL* (m^2)	220,086,099
Mean depth[1] (m)	2.5
Volume of AL of exchanged water in a residence time[2] (V_{Te}^{-1}; 63%; m^3)	346,634,031
Total N concentration in sewage (TN sew mg L^{-1})	0.240
Total N concentration in sewage after treatment[3] (TN sew mg L^{-1})	0.156
Total P concentration in sewage (TP sew; mg L^{-1})	0.032
Total P concentration in sewage after treatment[3] (TP sew; mg L^{-1})	0.021
Mass of N in sewage after treatment in a residence time (ton)	54.1
Mass of P in sewage after treatment in a residence time (ton)	7.3

Source:*Google Earth® (this work); [1]Wasserman *et al.* (2006); [2]Residence time (T_e^{-1}) – time of exchange for 67% of volume of a waterbody (Monsen *et al.*, 2002). **[3]**Economopoulos (1993). Considering a secondary treatment for the sewage by the WTP, and an efficiency performance of about 35% in wastewater treatment processes for activated sludge.

TN_{sew} and TP_{sew}, 0.240 and 0.032 mg L^{-1} respectively, are values expected in water column due to sewage loadings from demographic data without treatment. Values after treatment (0.156 mg L^{-1} and 0.021 mg L^{-1} for TN_{sew} and TP_{sew} respectively) were calculated based on secondary treatment and an efficiency of 35% (Economopoulos, 1993). This concentration considers a complete mix during the residence time, when 63% of water volume is exchanged (Monsen *et al.*, 2002). It is assumed that the remaining 37% is not affected by nutrient loadings nor exchanged. Furthermore, the hydrodynamic conditions of the lagoon were not considered and seasonal patterns that could affect the sewage were simplified.

- Water reservoir

This section quantifies the water content of nutrients to compare with those from nutrient requirements for phytoplankton. Table 14 presents the results of the concept developed in Figure 40.

Table 14 – Water concentration (average C1–C9)

PARAMETER (UNIT)	NH_4^+	NO_2^-	NO_3^-	PO_4^{3-}
Concentration (mg L^{-1})	0.08	0.09	0.38	0.03
N:P	43.76			
V_{Te}^{-1} (L)	346,634,031			
Dissolved concentration in a RT (ton)	27.63	31.46	130.70	9.39
	189.79			8.96
Particulate concentration (mg L^{-1})	0.025			0.055
Particulate concentration in a RT (ton)	8.78			19.23
Total mass (ton)	189.47			28.63

Source: Elaborated by the author, 2023.

- Sediment reservoir

In sediments, as demonstrated in Chapter 5, pore water presented remarkably high concentration of nutrients, and favored positive fluxes to the water column. Following Figure 41, Table 15 shows the results of nutrient reservoir in sediments from AL.

Table 15 – Results of nutrient reservoir in sediments from AL

SEDIMENT RESERVOIR					
PARAMETER (UNIT)		NH_4^+	NO_2^-	NO_3^-	PO_4^{3-}
Concentration	µg L^{-1}	4,536.26	210.37	3,121.45	2.315,33
	mol L^{-1}	252.01	4.57	50.35	24.37
Area (m^2)		220,085,099			
Depth of sediment (m)		0.05			
Volume of sediment (L)		11,004,254,950			
Volume occupied by porewater* (51.9%; L)		5,711,208,319			
Total content in pore water (ton)		25.91	1.20	17.83	13.2
		44.9			13.2

Source: Elaborated by the author, 2023.
LEGEND: *based on the mean values of porosity from C5 to C9.

- Phytoplankton requirements

Table 16 shows the frequency of main species found in AL. The distribution of species follows a seasonal pattern (Neves, 2014–2020, monitoring reports), despite the variations in frequency of species during the period of 40 months (Table 19). Among the most frequent phytoplankton, the presence of toxic species in half of the monitoring reports is matter of concern. The nutrient estimations per cell were calculated using the summation of average density of the species of phytoplankton during the 40 months of data. The average density of species was 3,631,854 cells

L^{-1} (Neves, 2014–2020, monitoring reports), and the mean values of nutrients were 32.8 µg N g^{-1} and 26.7 µg P g^{-1}. The results are 6.9 pg N $cell^{-1}$ and 4.7 pg P $cell^{-1}$. Evidently, results from Table 16 showed the general value of nutrient requirements, and culture assays would determine more accurate values for each species.

Table 16 – List of most common species in AL

SPECIES	FREQUENCY
Pleurosigma sp.	39
Scripsiella Trocoidea sp.	38
Prorocentrum compressum	
Oscillatoria sp.	
Thalassiora sp.	33
Prorocentrum micans	30
Prorocentrum lima	28
Chaetocerus	
Cylindroteca closterium	27
Ceratium furca	26
Ceratium candelabrum	
Manguinea rigida	24
Proboscia alata	23
Synecochoccus sp.	
Protoperidinium stenii	
Diplopalis sp.	22
Navicula sp.	21
Rhizolenia robusta	
Ceratium fusus	20
Dynophysis acuminata	
Gyminodyminium sp.	
Enteroccocus faecalis	30

Source: Neves (2015–2020).

LEGEND: Frequency of species (data of 40 months; frequency≥20). Bolded species are toxic.

The main groups of phytoplankton found in AL varied between 2–20 µm (NEVES, 2019–2020) and cellular density was cyanobacteria > dinoflagellates > diatoms. Despite the collection had been made to quantify nutrients in different sizes, the only fraction of interest was small than 25 µm and larger than 0.70 µm. Hence, the fraction retained by the 0.70 µm filter was used to quantify the nutrient necessities of the phytoplankton. Tables 17 and 18 show the concentration and requirement of nutrients of phytoplankton in AL based on Figure 42. The multifiltration equipment developed in this study to group phytoplankton by sizes allowed to determine the local nutrient requirements with a good estimation.

Table 17 – Nutrient concentration in phytoplankton retained in 0.7 µm–filter

STATION (surface)	N (µmol L^{-1})	P (µmol L^{-1})
3	1.45	0.62
4	0.07	0.19
5	1.56	0.60
7	1.52	0.34
10	1.99	0.60
Mean (sd)	1.32 (0.72)	0.47 (0.19)

Source: Elaborated by the author, 2023.
LEGEND: sd= standart deviation.

Table 18 – Nutrient requirements of phytoplankton in AL

PHYTOPLANKTON REQUIREMENTS				
PARAMETERS (UNIT)	N		P	
Mean concentration (<25 µm)	µmol L^{-1}	µmol g^{-1}	µmol L^{-1}	µmol g^{-1}
	1.32	2.34	0.47	0.86
	mg L^{-1}	mg g^{-1}	mg L^{-1}	mg g^{-1}
	0.02	0.032	0.02	0.027
V_{Te}^{-1} (L)[1]	346,634,031			
Nutrient in a volume during a residence time	617 (kmol)		191 (kmol)	
	8.6 (ton)		5.9 (ton)	

Source: Elaborated by the author, 2023.
LEGEND: [1]Volume in a residence time (VT_e^{-1}) – time to exchange 63% volume of a waterbody (Monsen *et al.*, 2002).

Table 19 shows the stocks and concentration in sewage, water column, sediment, and phytoplankton in AL.

Table 19 – Nutrient comparison among compartments in AL

NUTRIENT EVALUATION						
COMPARTMENT (SOURCE)	STOCK (T_e^{-1}) (ton)		AVERAGE CONCENTRATION (µmol L^{-1})			
	N	P	N			P
Sewage[1]	54.1	7.3	0.16*			0.02*
Sediment[2]	44.9	13.2	252.01			24.37
Water[3]	198.57	28.63	NH_4^+ 4.43	NO_2^- 1.97	NO_3^- 6.08	PO_4^{3-} 0.29
Phytoplankton 0.7 µm	6.40	5.53	1.32			0.47

Source: Elaborated by the author, 2023.
LEGEND: *the original data from wastewater treatment plants are in mg L^{-1}. [1]after treatment; [2]based on concentration of the pore water (this work); [3]summation of dissolved and particulate fractions (stock; this work).

6.4 Discussion

The mass balance (Figure 43) summarizes the results of the content and concentration of reservoirs in AL obtained by the model (Table 19). Despite water and sewage were great reservoirs of nutrients, sediment presented the highest P, while sewage the highest N. These reservoirs favor the fluxes to water column (Chapter 4). Souza *et al*. (2003) quantified dissolved nutrients and, at the time, the average concentration (μmol L^{-1}) was 6.6 (ammonium), 1.4 (nitrite), 3.3 (nitrate) and 0.5 (phosphate). The authors also observed a P-limitation, N:P=38:1 and suggested such a limitation would be the result of the preferential ammonium releasing by benthic communities. However, the present work N:P the average was circa 50:1, and the nutrient fluxes might be one of the factors for this increasing.

In AL, nutrients in particulate fractions were 0.018 and 0.015 mg L^{-1} for N and P respectively, and N:P ratio in phytoplankton was 2.6. Klausmeier *et al*. (2004) modeled the N:P stoichiometry and values varied from 8.2 to 45 and N–fixing organisms often presented higher N:P stoichiometry than non–fixing species. For the authors, the association of biology and stoichiometry of ribosomes and proteins and the mixture of exponential growth and equilibrium phases were the main elements of the optimal values. These behavior could be present in the phytoplankton assemblage and influence the nutritional requirements in AL.

Figure 43 – Concentration and reservoirs of N and P in sewage, water column, sediment, and phytoplankton

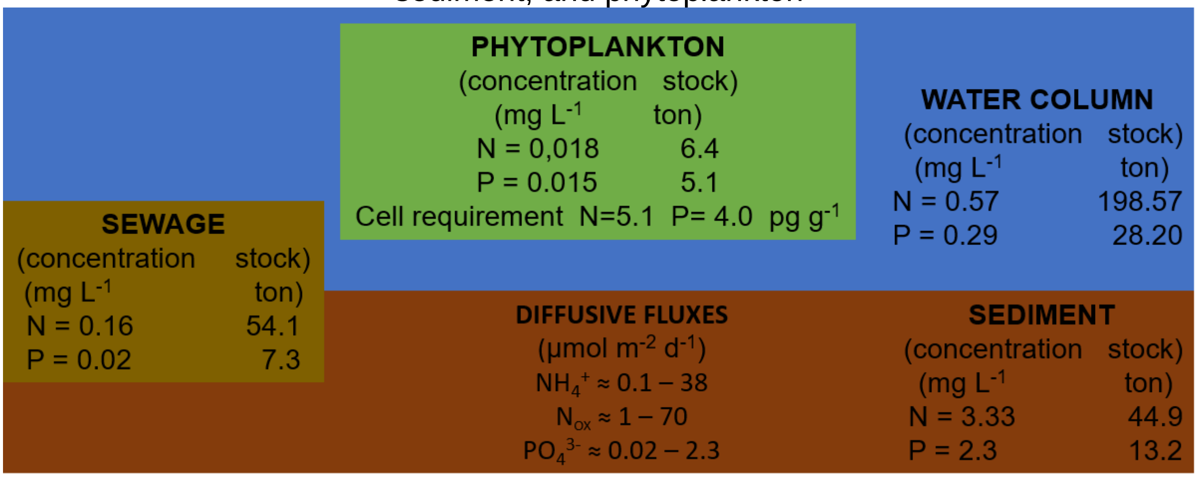

Source: Elaborated by the author, 2023.
LEGEND: The stock is referent to the residence time, except for sediment which is based on the pore water concentration. Diffusive fluxes of nutrients, from the minimum to the maximum, including all campaigns. Total mass of nitrogen and phosphorus in the compartments of AL was given in ton to better interpretation of the stocks.

Increase in ammonium concentrations favor cyanobacteria, chlorophytes and dinoflagellates (Burkholder, 2003), while nitrate benefits diatoms (Glibert, 2017). Seasonal variations were verified in phytoplanktonic productivity and assemblages in AL, with higher biodiversity and lower production in winter and the opposite in summer (Figure 24, Neves, 2019–2020). Data showed a reduction in cellular density from C1 to C2, particularly in the central stations, where the depths were higher. In campaigns considered non-turbid water, the distribution of phytoplankton was not regular in AL, and some points presented concentrations like those for turbid water. Cellular density presented a gradient from the external sections to the central portion, which could be related to the salinity gradient in AL. These differences may influence both nutritional requirements and uptake, and be influenced by nutrient fluxes, since higher efflux in turbid conditions are coincident with higher cellular density.

Seasonal changes in phytoplankton were noted by reducing diversity (Neves, 2019-2020), when opportunistic species grows fast (sharp fluctuations) until a limit expressed by unfavorable conditions (Harris, 1986). Other factor that could affect primary production is the predator–prey interactions that are tied to size and growth rates and would improve the access of nutrient cycling through time (Behrenfeld; Boss; Halsey, 2021). Zooplankton, for example, exhibits different contents of C, N, and P if compared to phytoplankton assemblages (Kütter *et al.*, 2014). Pulses of bacteria usually happens during the senescent phase of a phytoplankton bloom in consequence of the increase of phytodetritus and releasing of dissolved compounds (Kennish; de Jonge, 2011; Lalli; Parsons, 1997).

Bacterioplankton and phytoplankton present an important role in DIP removal even at low DIP and light conditions. Moreover, P pulses from sediment could favor planktonic production and small cells compete with larger phytoplankton nutrients at low supply or pulse of nutrients (Berthold; Schumann, 2020). The authors also concluded that the uptake rates were more associated with storage strategies than for growing necessarily. In that case, the dominant small cyanobacteria were identified as more able to live in environments with high N:P ratios. In AL, most phytoplankton are from 2 to 20 µm long (Neves, 2019-2020), mainly composed by cyanobacteria. So, P and N variation could be associate with the internal requirements of phytoplankton.

This chapter emphasized phytoplankton requirements and the supply of primary production in AL. The quantification of N and P determined the nutritional requirements of local phytoplankton (cyanobacteria, dinoflagellates, and diatoms) at 32.76 µg N g^{-1} and 26.66 µg P g^{-1}. Values indicated the importance of sediment in P–stocks even at small fluxes in water column, while sewage content was also an important source of nitrogen. The N and P present in the sediment and wastewater reservoirs and the high residence time in the lagoon allowed the pulses of nutrients to the water column. These pulses favored primary production in AL and promoted the shifts of water conditions (turbid to non-turbid and vice-versa).

P-limiting conditions (N:P>16) were observed mostly of time in the lagoon, corroborating the earlier works, however some N:P<16 could indicate a co-limitation by nitrogen. Focused on the of local phytoplankton determined the nutritional requirements of used by cyanobacteria, dinoflagellates, and diatoms at 5.1 pg N g^{-1} and 4.0 pg P g^{-1}. This could be related to the nitrogen requirements of the phytoplankton present in AL. Other possible explanation would be the different absorption rates of nitrogen and phosphorus by organisms which could lead to divergences in stocks. Also, trophic relations such as species succession and grazing could also contribute to nutrient supply and phytoplankton needs. The multifiltration system, developed to filtrate water sample at different aperture sizes, was valuable to group the local phytoplankton and allowed to have a good quantification of their nutritional requirements.

Sewage and sediments require attention due to the potential risk for algal blooms, including toxic species which could pose serious health problems. In Araruama Lagoon, a condition of high nutrients in water column, especially N-concentration as it was observed in turbid conditions, could favor such species. Particularly, sediment can be considered an environmental liability and address the importance of this characterization for stakeholders and environmental regulatory agencies.

Suggestions for further investigations include studies of *in vitro* cultures to quantify the nutritional requirements of each specie present in AL for both turbid and non-turbid waters. And despite the predominant size of phytoplankton is 2-20 µm in AL, other fractions may also present different N and P values and their relations must be investigated.

7 CONCLUSION

The trophic crises in Araruama Lagoon were defined by a concurrent association of few elements connecting physical, chemical, and biological systems. First, it was observed a spatial compartmentalization of the lagoon particularly associated to a W-E salinity gradient and different depths. The three sectors were identified as: i) marine sector (32–35) comprised stations 1 to 3; ii) central sector (50–70) included stations 4 to 8; and iii) interior sector (35–50) comprised stations 9 to 11. Shallower areas were found in the interior and marine sectors, while depths were greater in the central sector. The shifts in water conditions were more intense in the central sector of the lagoon, while marine and interior sectors did not undergo such a variation.

The descriptors of trophic crises were turbidity, salinity, temperature, NH_4^+, Nox, PO_4^{3+}, and N:P. Higher turbidity, temperature, salinity, Nox, and N:P ratios and smaller ammonium and phosphate determined turbid water, whereas non–turbid waters presented the opposite behavior. Turbidity was better to determine differences in primary productivity because chlorophyll *a* values were most of times bellow the detection limit of the method. It highlighted the importance of fluorimetric measurements to improve the quality of the data. Salinity and temperature were linked to climatic descriptors; salinity was linked to phytoplankton distribution, while higher temperature favored higher primary production. These parameters reflected the changes in local conditions, but also emphasized the global climatic crisis as an important factor for distribution of phytoplankton species.

Diffusive fluxes were credited as the main cause of the trophic crises, remarkably nitrogen, despite the primary production in AL is P-limited. The dissolved forms of nitrogen presented a relevant role in water turbidity in AL. Nitrogen fluxes (ammonium and Nox) were significantly higher than phosphate and impacted the water condition. In turbid conditions, N-fluxes from sediment to water column were higher than in non-turbid conditions and were important to maintain primary production in AL. Phosphorus was the limiting factor in the lagoon and despite its low fluxes, it was also important to phytoplankton production in less P-limiting conditions. The poor water quality in the western sector of the AL confirmed the urban pressures on this ecosystem.

Sediments were a large reservoir of phosphorus, while wastewater presented higher content of nitrogen, allowing the permanent phytoplankton production in Araruama Lagoon. Sediment reservoir could be considered as an environmental liability because of the high amounts of nutrients. So, dredging activities, often proposed as a solution for lagoon problems, are not indicated due to the nutrient releasing caused by changes in ORP. Some proposals for the environmental management to reduce the damages caused by wastewater and diffusive fluxes are suggested: i) nutrient cleanse in sediment using algae (environmental remediation); and ii) reduction of diffuse input (sewage) by improving the local infrastructure.

Phytoplankton requirements were determined using a filtration system specially developed for this work which provided a better quantification of the local nutritional needs. It was identified nitrogen concentrations higher than phosphorus which was in accordance with the main local species requirements.

Because high amounts of nutrients are still reaching AL, it poses risks to environmental quality in Araruama Lagoon. Environmental management plans, including improve the local infrastructure and the use of phycoremediation, need to be done to reduce nutrient in sediments and the risks of algal blooms. Otherwise, the high phytoplanktonic production will possibly be maintained or enhanced during the next years because of the releasing of nutrients from the sediment stock.

Despite the contributions of the thesis, some points remain unclear and are subject of future studies: i) identification of colored dissolved compounds, that reduced transparency in water column and the light efficiency - they could help to elucidate why SEC and TSS did not vary in the expected pattern; ii) the role of bioturbation on nutrient fluxes in AL, since the present study did not cover this subject and it can intensely modify the ORP and the behavior of N and P; ii) nitrite behavior and its importance to differentiation between ammonium and nitrate due to the variation in ORP at sediment-water interface.

REFERENCES

ABIDI, M.; AMOR, R. B.; GUEDDARI, M. Assessment of the Trophic Status of the South Lagoon of Tunis (Tunisia, Mediterranean Sea): geochemical and statistical approaches. **Journal of Chemistry**, v. 2018, p. 1–17, 2018.

ADIKARAM, M.; PITAWALA, A.; ISHIGA, H.; JAYAWARDANA, D. Geochemistry and grain size distribution of surface sediments of a large semi–enclosed lagoon connected to the western Bay of Bengal. **Estuarine, Coastal and Shelf Science**, v. 216, p. 4–13, 2019.

AL–AZRI, A. R. *et al*. Abundance of harmful algal blooms in the coastal waters of Oman: 2006–2011. **Aquatic Ecosystem Health &Amp. Management**, v. 18, n. 3, p. 269–281, mar. 2015.

ALBERT, S. *et al*. Influence of settling organic matter quantity and quality on benthic nitrogen cycling. **Limnology and Oceanography**, v. 66, n. 5, p. 1882-1895, may 2021.

ALEKSEENKO, E.; ROUX, B. Contribution to remediation of brackish lagoon: 3D simulation of salinity, bottom currents and resuspension of bottom sediments by strong winds. **Estuarine, Coastal and Shelf Science**, v. 216, p. 27–37, 2019.

ALMEIDA–SILVA, P. H. *et al.* Trophic ecology and food consumption of fishes in a hypersaline tropical lagoon. **J. Fish. Biol**., v. 86, n. 6, p. 1781–1795, Jun. 2015.

ALVAREZ–BORREGO, S. Chapter 10 Secondary Productivity in Coastal Lagoons. *In*: KJERFVE, B. (ed.). **Coastal lagoon processes.** Columbia, S.C.: Elsevier, 1994. p. 287–309 (Elsevier Oceanography Series, v. 60).

ALVES, A. R. **Modelagem numérica aplicada ao estudo da origem e evolução morfológica dos esporões da Lagoa de Araruama, RJ**. 2006. 135 f. Tese (Doutorado em Geologia e Geofísica Marinha) – Departamento de Geologia, Universidade Federal Fluminense, Niterói, 2006.

AMARAL, H. B. F.; REIS, R. P.; FIGUEIREDO, M. A. d. O.; PEDRINI, A. d. G. Decadal shifts in macroalgae assemblages in impacted urban lagoons in Brazil. **Ecological Indicators**, v. 85, p. 869–877, 2018.

ANDERSON, D. M. Approaches to monitoring, control and management of harmful algal blooms (HABs). **Ocean Coast Manag.**, v. 52, n. 7, p. 342, Jul. 2009.

ANTHONY, A. *et al*. Coastal lagoons and climate change: ecological and social ramifications in U.S. Atlantic and Gulf coast ecosystems. **Ecology and Society,** v. 14, n. 1, p. 8, 2009.

ARFI, R.; GUIRAL, D.; BOUVY, M. Sedimentation modified by wind induced resuspension in a shallow tropical lagoon (Cote d'Ivoire). **Netherland Journal of Aquatic Ecology**, v. 28, n. 3, p. 427–431, 1994.

ARTIOLI, Y. Adsorption. *In*: JØRGENSEN, S. E.; FATH, B. D. (ed.). **Encyclopedia of ecology**. Oxford: Academic Press, 2008. p. 60–65.

ASSMY, P.; SMETACEK, V. Algal Blooms. *In*: SCHAECHTER, Moselio (ed.). **Encyclopedia of microbiology.** Oxford: Elsevier, 2009. p. 27–41.

AUBERT, M. Mediators of microbiological origin and eutrophication phenomena. **Marine Pollution Bulletin**, v. 21, n. 1, p. 24–29, 1990.

BAIRD, D.; ULANOWICZ, R. The Seasonal dynamics of the Chesapeake Bay Ecosystem. **Ecological Monographs**, v. 59, p. 329–364, 1989.

BALDIZAR, J. M.; RYBICKI, N. B. Primary factors affecting water clarity at shallow water sites throughout the Chesapeake and Maryland coastal bays. *In*: FEDERAL INTERAGENCY SEDIMENTATION CONFERENCE, 8., 2007, Reno, N. V. **Proceedings...** Reno, N.V.: USGS, 2007.

BARBANTI, A. *et al*. Diagenetic processes and nutrient fluxes at the sediment–water interface, Northern Adriatic Sea, Italy. **Marine and Freshwater Research**, v. 46, n. 1, p. 55–67, 1995.

BARBIÉRE, E. B. Ritmo climático e extração do sal em Cabo Frio. **Rev. Bras. Geografia,** v. 37, n. 4, p. 23-109, 1975 .

BARNES, R. S. K. Lagoons. *In*: STEELE, J. H. (ed.). **Encyclopedia of Ocean Sciences**. Oxford: Academic Press, 2001. p. 1427–1438.

BARRERA–ALBA, J. J.; ABREU, P. C.; TENENBAUM, D. R. Seasonal and inter–annual variability i phytoplankton over a 22–year period in a tropical coastal region in the southwestern Atlantic Ocean. **Continental Shelf Research**, v. 176, p. 51–63, 2019.

BARROSO, L. V.; BERNARDES, M. C. Um patrimônio natural ameaçado: poluição, invasões e turismo sem contrôle ameaçam lagoas fluminenses. **Ciência Hoje,** v. 19, p. 70–74, 1995.

BASSET, A. *et al.* Resistance and resilience of ecosystem descriptors and properties to dystrophic events: A study case in a Mediterranean lagoon. **Transitional Waters Bulletin**, v. 7, p. 1–22, 2013.

BAUMANN, H.; WALLACE, R. B.; TAGLIAFERRI, T.; GOBLER, C. J. Large natural pH, CO2 and O2 fluctuations in a temperate Tidal Salt Marsh on Diel, Seasonal, and Interannual Time Scales. **Estuaries and Coasts**, v. 38, n. 1, p. 220–231, 2015.

BEGON, M.; TOWNSEND, C. R.; HARPER, J. L. **Ecology:** from Individuals to Ecosystems. 4th ed. New York: Blackwell Publishing, 2006.

BEHRENFELD, M. J.; BOSS, E. S.; HALSEY, K. H. Phytoplankton community structuring and succession in a competition–neutral resource landscape. **ISME Communications**, v. 1, n. 1, p. 12, 2021.

BENDSCHNEIDER, K.; ROBINSON, R. J. **A new spectrophotometric method for the determination of nitrite in sea water**. Washington: University of Washington, 1952.

BERNHARD, A. The Nitrogen cycle: processes, players and human impact. **Nature Education Knowledge**, v. 10, n. 3, p. 25, 2010.

BERTHOLD, M.; SCHUMANN, R. Phosphorus dynamics in a Eutrophic Lagoon: uptake and utilization of nutrient pulses by Phytoplankton. **Frontiers in Marine Science**, v. 7, n. 281, 2020–May–13 2020. Original Research.

BERTUCCI, T. C. P.; SILVA, E. P.; MARQUES JR., A. N.; MONTEIRO NETO, C. Tourism and urbanization: environmental problems of the Araruama Lagoon, State of Rio de Janeiro, Brazil. **Ambiente & Sociedade**, v. 19, p. 59–80, 2016.

BESTION, E. *et al.* Abrupt declines in marine phytoplankton production driven by warming and biodiversity loss in a microcosm experiment. **Ecol. Lett.**, v. 23, n. 3, p. 457–466, Mar 2020. Available in: https://doi.org/10.1111/ele.13444. Access in: 10 mar. 2023.

BÉTHOUX, J. P. *et al.* Nutrients in the Mediterranean Sea, mass balance and statistical analysis of concentrations with respect to environmental change. **Marine Chemistry**, v. 63, n. 1, p. 155–169, 1998.

BILOTTA, G. S.; BRAZIER, R. E. Understanding the influence of suspended solids on water quality and aquatic biota. **Water Research**, v. 42, n. 12, p. 2849–2861, 2008.

BIRD, E. C. F. Chapter 2 Physical setting and geomorphology of Coastal Lagoons. *In*: KJERFVE, B. (ed.). **Coastal lagoon processes.** [*S. l.*]: Elsevier, 1994. v. 60, p. 9–39. (Elsevier Oceanography Series)

BISWAS, J. K. *et al.* Nutrient modeling of an urban lake using best subset method. **International Journal of Environmental Science and Technology**, v. 15, n. 9, p. 1867–1878, 2017.

BLACKBURN, T. H.; BLACKBURN, N. D. Coupling of cycles and global significance of sediment diagenesis. **Marine Geology**, v. 113, n. 1, p. 101–110, 1993.

BLAIN, C. O.; SHEARS, N. T. Seasonal and spatial variation in photosynthetic response of the kelp Ecklonia radiata across a turbidity gradient. **Photosynth Res.**, v. 140, n. 1, p. 21–38, Apr 2019.

BLEAM, W. F. Chapter 8 – Redox Chemistry. *In*: BLEAM, W. F. (ed.). **Soil and Environmental chemistry**. Boston: Academic Press, 2012. p. 321–370.

BONOMETTO, A. *et al.* Factors controlling sediment and nutrient fluxes in a small microtidal salt marsh within the Venice Lagoon. **Science of The Total Environment**, v. 650, p. 1832–1845, 2019.

BOUDREAU, B. P. **Diagenetic models and their implementation: modelling transport and reactions in aquatic sediments**. Berlin; Heidelberg; New York; Barcelona; Budapest; Hong Kong; London; Milan; Paris; Santa Clara; Singapore; Tokyo: Springer, 1997.

BOURCEAU, O. M.; FERDELMAN, T.; LAVIK, G.; MUSSMANN, M. *et al.* Simultaneous sulfate and nitrate reduction in coastal sediments. **ISME Communications**, v. 3, n. 1, p. 17, 2023.

BRAGA, C. Z. F.; VIANNA, M. L.; KJERFVE, B. Environmental characterization of a hypersaline coastal lagoon from Landsat–5 Thematic Mapper data. **International Journal of Remote Sensing**, v. 24, n. 16, p. 3219–3234, Aug. 2003.

BRANCO, A. B.; KREMER, J. N. The Relative importance of Chlorophyll and colored dissolved organic matter (CDOM) to the prediction of the diffuse atenuation coefficient in Shallow Estuaries. **Estuaries**, v. 28, n. 5, p. 643–652, 2005.

BURKHOLDER, J. M. Eutrophication and Oligotrophication. *In*: LEVIN, S. A. (ed.). **Encyclopedia of biodiversity**. New York: Elsevier, 2003. p. 649–670.

BURTON, G. A. Sediment quality criteria in use around the world. **Limnology**, v. 3, p. 65–76, 2002.

CANUEL, E. A.; HARDISON, A. K. Carbon cycle. *In*: WHITE, W. M. (ed.). **Encyclopedia of geochemistry:** a comprehensive reference source on the chemistry of the Earth. Cham: Springer International Publishing, 2018. p. 191–194.

CARLSON, R. Expanding the trophic state concept to identify non–nutrient limited lakes and reservoirs. **Enhancing States' Lake Management Programs**, 1991.

CARMOUZE, J. P.; BARROSO, L. V. Recent environmental modifications of the lagoon of Saquarema and its watershed, Rio de Janeiro, Brazil. *In*: INTERNATIONAL SYMPOSIUM ON GLOBAL CHANGES IN SOUTH AMERICA DURING QUATERNARY: PAST – PRESENT – FUTURE, 1989, São Paulo, Brazil. **Abstracts […]** São Paulo: ABEQUA/INQUA, 1989. p. 65–69.

CARMOUZE, J. P.; KNOPPERS, B.; VASCONCELOS, P. Metabolism of a subtropical Brazilian lagoon. **Biogeochemistry**, v. 14, n. 2, p. 129–148, 1991.

CARPENTER, S. R. Submersed vegetation: an internal factor in lake ecosystem succession. **The American Naturalist**, v. 118, n. 3, p. 372–383, 1981.

CARPENTER, S. R. *et al.* Nonpoint pollution of surface waters with phosphorus and nitrogen. **Ecological Applications**, v. 8, n. 3, p. 559–568, 1998.

CARPENTER, S. R.; PACE, M. L. Dystrophy and eutrophy in lake ecosystems: implications of fluctuating inputs. **Oikos**, v. 78, n. 1, p. 3–14, 1997.

CARTIGNY, P. Nitrogen. *In*: WHITE, W. M. (ed.). **Encyclopedia of geochemistry:** a comprehensive reference source on the chemistry of the Earth. Cham: Springer International Publishing, 2018. p. 985–986.

CARVALHO, A. P.; COSTA, R.; ROSA, J. Campos dos Goytacazes, RJ. *In*: CARVALHO, A. P.; COSTA, R.; ROSA, J. **Eutrophication and introduction of exotic species in hypersaline estuary:** Araruama Lagoon, Rio de Janeiro, Brazil. [*S. l.*]: UPEA/IFF. 13, 2014.

CEBRIÁN, J. Grazing on benthic primary producers. *In*: NIELSEN, S. L.; BANTA, G. T. (ed.). **Estuarine nutrient cycling:** The Influence of Primary Producers: The Fate of Nutrients and Biomass. Dordrecht: Springer Netherlands, 2004. p. 153–185.

CHANDRASEKARA, C. M. K. N. K.; WEERASINGHE, K. D. N.; PIYADASA, R. U. K.; PATHIRANA, S. Salinity, pH and Turbidity changes of water in the Negambo lagoon. **Journal of Social Sciences and Humanities**, 2014.

CHAPMAN, P. M.; WANG, F. Assessing sediment contamination in estuaries. **Environmental Toxicology and Chemistry**, v. 20, n. 1, p. 3–22, 2001. Available in: https://doi.org/10.1002/etc.5620200102. Access in: 12 oct. 2022.

CHEN, Q. *et al.* The role of nutrients, wind speed, and rainfall in determining the composition of the algal community of shallow lakes in the Taoge water system, upstream from Lake Taihu, China. **Environmental Science and Pollution Research**, v. 30, n. 6, p. 16195–16209, 2023.

CHESAPEAKE BAY PROGRAM. **Habitats**. 2012. Available in: http://www.chesapeakebay.net/discover/bayecosystem. Access in: 22 feb. 2023.

CHISHOLM, S. W. Phytoplankton size. *In*: FALKOWSKI, P. G.; WOODHEAD, A. D. (ed.). **Primary productivity and biogeochemical cycles in the Sea**. Boston, MA: Springer US, 1992. p. 213–237.

CLADAS, Y.; PAPANTONIOU, G.; BEKIARI, V.; FRAGKOPOULU, N. Dystrophic crisis event in Papas Lagoon, Araxos Cape, Western Greece in the summer 2012. **Mediterranean Marine Science**, v. 17, n. 1, p. 32–38, 2015.

COELHO, J. P. *et al.* Phosphorus speciation and availability in intertidal sediments of a temperate estuary: relation to eutrophication and annual P–fluxes. **Estuarine Coastal and Shelf Science**, v. 61, n. 4, p. 583–590, Dec. 2004.

COOLEY, S. *et al.* **Climate Change 2022:** impacts, adaptation and vulnerability. *In*: Contribution of Working Group II to the Sixth Assessment Report of the Intergovernmental Panel on Climate Change. Cambridge, UK; New York, NY, USA, 2022. p. 379–550.

CORDERO, J.; GUEVARA, M.; MORALES, E.; LODEIROS, C. [Effect of heavy metals on the growth of tropical microalga Tetrasermis chuii (Prasinophyceae)]. **Revista de biología tropical**, v. 53, p. 325–330, 2005.

COREY, A. T.; AUVERMANN, B. W. Transport by advection and diffusion revisited. **Vadose Zone Journal**, v. 2, n. 4, p. 655–663, 2003.

CORNWELL, J. C.; GLIBERT, P. M.; OWENS, M. S. Nutrient fluxes from sediments in the San Francisco Bay Delta. **Estuaries and Coasts**, v. 37, n. 5, p. 1120–1133, 2014.

COSTA, E.; SANTOS, M.; SILVA, J.; SEABRA, V. Mapeamento multitemporal e cadastral das salinas da Lagoa de Araruama – RJ. **GEOgraphia**, v. 24, 2022.

COSTA, E.; SEABRA, V. Dinâmicas naturais e atividades socioeconômicas na planície costeira da Lagoa de Araruama –RJ. **Formação (Online)**, v. 27, p. 353, 2021.

COTNER, J. B.; SUPLEE, M. W.; CHEN, N. W.; SHORMANN, D. E. Nutrient, sulfur and carbon dynamics in a hypersaline lagoon. **Estuarine, Coastal and Shelf Science**, v. 59, n. 4, p. 639–652, 2004.

COVICH, A. P. Energy flow and ecosystems. *In*: **Encyclopedia of biodiversity**. San Diego, CA: Academic Press, 2001. p. 509–523.

CRUZ, L. R.; SANTOS, L. N.; SANTOS, A. F. G. N. Changes of fish trophic guilds in Araruama Lagoon, Brazil: What can be inferred about functioning and structure of hypersaline lagoons? **Estuarine, Coastal and Shelf Science**, v. 211, p. 90–99, 2018.

CUNHA, L. C. D.; WASSERMAN, J. C. Relationships between nutrients and macroalgal biomass in a brazilian coastal lagoon: the impact of a lock construction. **Chemistry and Ecology**, v. 19, n. 4, p. 283–298, 2003.

CUTRIM, M. V. J. *et al.* Trophic state of an urban coastal lagoon (northern Brazil), seasonal variation of the phytoplankton community and environmental variables. **Estuarine, Coastal and Shelf Science**, v. 216, p. 98–109, 2019.

DA SILVA, E.; SOARES–GOMES, A.; FERNANDES, F.; DE ABREU, C. M. Sandy beach macrobenthos assemblages at an hypersaline coastal Lagoon, Lagoa de Araruama, RJ, Brazil. **Journal of Coastal Research**, p. 265–270, SPR 2005.

DANILOV, R. A.; EKELUND, N. G. A. Effects of solar radiation, humic substances and nutrients on phytoplankton biomass and distribution in Lake Solumsjö, Sweden. **Hydrobiologia**, v. 444, n. 1, p. 203–212, 2001.

DANOVARO, R.; PUSCEDDU, A. Biodiversity and ecosystem functioning in coastal lagoons: Does microbial diversity play any role? **Estuarine, Coastal and Shelf Science**, v. 75, n. 1, p. 4–12, 2007.

DAVIDSON, K.; GOWEN, R. J.; HARRISON, P. J.; FLEMING, L. E. *et al.* Anthropogenic nutrients and harmful algae in coastal waters. **J. Environ. Manage.**, v. 146, p. 206–216, Dec. 2014.

DE MONTIGNY, C.; PRAIRIE, Y. T. The relative importance of biological and chemical processes in the release of phosphorus from a highly organic sediment. **Hydrobiologia**, v. 253, n. 1, p. 141–150, 1993.

DE OLIVEIRA, A. R. G. *et al.* How does the phytoplankton community respond to the effects of La Niña and post–drought events in a tide–dominated Amazon estuary? **Aquatic Sciences**, v. 85, n. 1, p. 9, 2022.

DEFFOREY, D.; PAYTAN, A. Phosphorus cycling in marine sediments: advances and challenges. **Chemical Geology**, v. 477, p. 1–11, 2018.

DELGADO–GONZÁLEZ, L. *et al.* Phosphorus retention by granulated apatite: assessing maximum retention capacity, kinetics and retention processes. **Water Sci. Technol.**, v. 83, n. 4, p. 792–802, Feb. 2021.

DELL'ANNO, A.; MEI, M. L.; PUSCEDDU, A.; DANOVARO, R. Assessing the trophic state and eutrophication of coastal marine systems: a new approach based on the biochemical composition of sediment organic matter. **Mar. Pollut. Bull.**, v. 44, n. 7, p. 611–622, Jul. 2002.

DELL'AQUILA, G. *et al.* Nutrient consumption and chain tuning in diatoms exposed to storm–like turbulence. **Scientific Reports**, v. 7, n. 1, p. 1828, 2017.

DENNIS, D. T. Oxidation–reduction reactions. *In*: DENNIS, D. T. (ed.). **The biochemistry of energy utilization in plants**. Dordrecht: Springer Netherlands, 1987. p. 9–18.

DIAMANTOPOULOU, E. *et al.* Seasonal fluctuations of nutrients in a hypersaline Mediterranean lagoon. **Desalination**, v. 224, n. 1–3, p. 271–279, 2008.

DODDS, W. K.; WHILES, M. R. **Freshwater ecology:** concepts and environmental applications of limnology. 2nd ed. [*S. l.*]: Academic Press, 2010. (Aquatic Ecology Series).

DORGHAM, M. M. Effects of eutrophication. *In*: ANSARI, A. A.; GILL, S. S. (ed.). **Eutrophication:** causes, consequences and control: volume 2. Dordrecht: Springer Netherlands, 2014. p. 29–44.

DRAREDJA, M. *et al.* Seasonal variations of phytoplankton community in relation to environmental factors in a protected meso–oligotrophic southern Mediterranean marine ecosystem (Mellah lagoon, Algeria) with an emphasis of HAB species. **Environmental Monitoring and Assessment**, v. 191, n. 603, 2019.

DUNN, J.; GRIDER, M. H. **Physiology, Adenosine Triphosphate**. StatPearls [Internet], Treasure Island (FL), Updated 2023 Feb 13 2023 Available in: https://www.ncbi.nlm.nih.gov/books/NBK553175/. Access in: 20 feb. 2023.

DURHAM, W. M. *et al.* Turbulence drives microscale patches of motile phytoplankton. **Nature Communications**, v. 4, n. 1, p. 2148, 2013.

DUSSART, B. H. Les différentes catégories de plancton. **Hydrobiologia**, v. 26, n. 1, p. 72–74, 1965.

ECONOMOPOULOS, A. P. **Assessment of sources of air, water, and land pollution:** a guide to rapid source inventory techniques and their use in Equationting environmental control strategies. Geneva: World Health Organization, 1993.

ELSER, J. J. *et al.* Global analysis of nitrogen and phosphorus limitation of primary producers in freshwater, marine and terrestrial ecosystems. **Ecol. Lett.**, v. 10, n. 12, p. 1135–1142, Dec. 2007. Available in: https://doi.org/10.1111/j.1461–0248.2007.01113.x. Access in: 4 apr. 2022.

ENRICH-PRAST, A*. et al.* Sediment denitrification in two contrasting tropical shallow Lagoons. **Estuaries and Coasts,** v. 39, n. 3, p. 657-663, May 2016.

ERDOĞAN, Ş. *et al.* Determinants of phytoplankton size structure in warm, shallow lakes. **Journal of Plankton Research**, v. 43, n. 3, p. 353–366, 2021.

ESTEBAN, G. F.; FINLAY, B. J. Cryptic freshwater ciliates in a hypersaline lagoon. **Protist**, v. 154, n. 3–4, p. 411–418, Oct. 2003.

ESTEVES, F. A. *et al.* Neotropical coastal lagoons: an appraisal of their biodiversity, functioning, threats and conservation management. **Brazilian Journal of Biology**, v. 68, 2008.

FAKHRAEE, M.; PLANAVSKY, N. J.; REINHARD, C. T. The role of environmental factors in the long–term evolution of the marine biological pump. **Nature Geoscience**, v. 13, n. 12, p. 812–816, 2020.

FALKOWSKI, P. G.; WOODHEAD, A. D.; VIVIRITO, K. e. **Primary productivity and biogeochemical cycles in the Sea**. New York, NY: Springer, 1992. 550 p. (Environmental Science Research, v. 43).

FENCHEL, T.; KING, G. M.; BLACKBURN, T. H. Aquatic sediments. *In*: FENCHEL, T.; KING, G. M.; BLACKBURN, T. H. **Bacterial biogeochemistry**: the ecophysiology of mineral cycling. 3. ed. [*S. l.*]: Academic Press, 2012. p. 121–142.

FERNÁNDEZ–ALÍAS, A. *et al.* Nutrient overload promotes the transition from top–down to bottom–up control and triggers dystrophic crises in a Mediterranean coastal lagoon. **Science of The Total Environment**, v. 846, p. 157388, 2022.

FINKEL, Z. V. *et al.* Phytoplankton in a changing world: cell size and elemental stoichiometry. **Journal of Plankton Research**, v. 32, n. 1, p. 119–137, 2009.

FOSTER, S. Q.; FULWEILER, R. W. Spatial and historic variability of benthic nitrogen cycling in an anthropogenically impacted estuary. **Frontiers in Marine Science**, v. 1, Nov. 2014. Original Research.

FRANCO, A. C. S. *et al.* From meso to hyperhaline: the importance of Neotropical coastal lagoons in supporting the functional fish diversity at regional scale. **Hydrobiologia**, v. 849, n. 17, p. 4101–4118, 2022.

FROELICH, P. N. *et al.* Early oxidation of organic matter in pelagic sediments of the eastern equatorial Atlantic: suboxic diagenesis. **Geochimica et Cosmochimica Acta**, v. 43, p. 1075–1090, 1979.

GALLAGHER, K. L. *et al.* Inside the alkalinity engine: the role of electron donors in the organomineralization potential of sulfate–reducing bacteria. **Geobiology**, v. 10, n. 6, p. 518–530, 2012.

GALLARDO–RODRÍGUEZ, J. J. *et al.* A critical review on control methods for harmful algal blooms. **Reviews in Aquaculture**, v. 11, n. 3, p. 661–684, 2019. Available in: https://doi.org/10.1111/
raq.12251. Access in: 15 jan. 2023.

GANGULY, D. *et al.* Influence of nutrient input on the trophic state of a tropical brackish water lagoon. **J. Earth Syst. Sci.**, 2015.

GLIBERT, P. M. Eutrophication, harmful algae and biodiversity — Challenging paradigms in a world of complex nutrient changes. **Marine Pollution Bulletin**, v. 124, n. 2, p. 591–606, 2017.

GOWEN, R. *et al.* Iron bioavailability in the Southern Ocean. **Oceanography and Marine Biology: An Annual Review**, v. 50, p. 10–73, 2012.

GRASSHOFF, K.; EHRHARDT, M.; KREMLING, K. **Methods of seawater analysis**. 2nd ed. Weinheim: Verlag–Chemie, 1983. 419 p.

GREGORY, R.; EDZWALD, J. Sedimentation & flotation. *In*: **Water Quality & Treatment**. 6th ed. [*S. l.*]: AWWA & McGrawHill, 2010. Chapt. 9.

GRENZ, C. *et al.* Benthic ecology of tropical coastal lagoons: Environmental changes over the last decades in the Términos Lagoon, Mexico. **Comptes Rendus Geoscience**, v. 349, n. 6–7, p. 319–329, 2017.

GROTZINGER, J. P.; JORDAN, T. H. **Understanding Earth**. 7th ed. New York, N.Y: W.H. Freeman and Company, 2014.

GUIMARÃES, T. C. S. M.; MONTENEGRO, K. S.; WASSERMAN, M. A. V.; WASSERMAN, J. C. Innovative microcosm experiments for the evaluation of the regeneration rates of nutrients in sediments of a hypersaline lagoon. **Marine Pollution Bulletin**, v. 166, p. 112252, 2021.

HÅKANSON, L. Sedimentation processes in lakes. *In*: BENGTSSON, L.; HERSCHY, R. W. (ed.). **Encyclopedia of Lakes and Reservoirs**. Dordrecht: Springer Netherlands, 2012. p. 701–710.

HAMDOUN, H. *et al.* Characterization of harbor sediments from the English Channel: assessment of heavy metal enrichment, biological effect and mobility. **Marine Pollution Bulletin**, v. 90, n. 1, p. 273–280, 2015.

HAN, C. *et al.* Dynamics of phosphorus–iron–sulfur at the sediment–water interface influenced by algae blooms decomposition. **J Hazard Mater**, v. 300, p. 329–337, Dec. 2015.

HARRIS, G. Lagoons. *In*: JØRGENSEN, S. E.; FATH, B. D. (ed.). **Encyclopedia of ecology**. Oxford: Academic Press, 2008. p. 2061–2068.

HARRIS, G. P. **Phytoplankton ecology:** structure, function and fluctuation. London; New York: Chapman and Hall, 1986.

HASSI, M.; MOHAMED, A.; FAARAS, M.; STAITI, M. Qualitative and quantitative study of the spring phytoplankton community in the Naïla lagoon (Moroccan Atlantic coast). **Journal of Materials and Environmental Science**, v. 11, p. 977–987, 2020.

HEISS, E. M.; FULWEILER, R. W. Coastal water column ammonium and nitrite oxidation are decoupled in summer. **Estuarine, Coastal and Shelf Science**, v. 178, p. 110–119, 2016.

HELLIWELL, K. E. Emerging trends in nitrogen and phosphorus signalling in photosynthetic eukaryotes. **Trends in Plant Science**, v. 28, n. 3, p. 344–358, 2023.

HESSEN, D. O.; TRANVIK, L. J. Humic substances as ecosystem modifiers — introduction. *In*: HESSEN, D. O.; TRANVIK, L. J. (ed.). **Aquatic humic substances:** ecology and biogeochemistry. Berlin, Heidelberg: Springer Berlin Heidelberg, 1998. p. 1–6.

HOWARTH, R.; MARINO, R. Nitrogen as the limiting nutrient for eutrophication in coastal marine ecosystems: evolving views over Three Decades. **Limnology and Oceanography**, v. 51, p. 364–376, 2006.

HUANG, J. *et al.* **Coorong nutrient cycling and fluxes**. [*S. l.*]: Goyder Institute, 2023.

HUETTEL, M.; ZIEBIS, W.; FORSTER, S.; LUTHER, G. W. Advective transport affecting metal and nutrient distributions and interfacial fluxes in permeable sediments. **Geochimica et Cosmochimica Acta**, v. 62, n. 4, p. 613–631, 1998.

HWANG, S. J. Eutrophication and the Ecological Health Risk. **Int. J. Environ. Res. Public Health**, v. 17, n. 17, Aug. 2020.

IBANEZ, J. *et al.* **Environmental chemistry:** fundamentals. New York: Springer, 2007.

ISAJI, Y. *et al.* Efficient recycling of nutrients in modern and past hypersaline environments. **Scientific Reports**, v. 9, n. 1, p. 3718, 2019.

KAREIVA, P.; MARVIER, M. Ecology, concept and theories in. **Encyclopedia of biodiversity,** v. 2, p. 1–8, 2001.

KASTEN, S. Pore waters. *In*: REITNER, J.; THIEL, V. (ed.). **Encyclopedia of geobiology**. Dordrecht: Springer Netherlands, 2011. p. 742–746.

KENNISH, M. J.; DE JONGE, V. N. 8.05 – Chemical introductions to the systems: diffuse and nonpoint source pollution from chemicals (Nutrients: Eutrophication). *In*: WOLANSKI, E.; MCLUSKY, D. (ed.). **Treatise on estuarine and coastal science**. Waltham: Academic Press, 2011. p. 113–148.

KENNISH, M. J. K.; PAERL, H. W. e. **Coastal lagoons:** critical habitats of environmental change**.** Florida, USA: CRC Press. Taylor & Francis Group, 2010. 555 p. (CRC Marine science series).

KJERFVE, B. Comparative oceanography of Coastal Lagoons. *In*: WOLFE, D. A. (ed.). **Eastuarine variability**. New York: Academic Press, 1986. p. 63–81.

KJERFVE, B. Coastal lagoon processes. *In*: KJERFVE, B. (ed.). **Coastal lagoon processes**: Q Elsevier Science Publishers B.V., 1994. v. 60, Chapter 1, p. 1–8. (Elsevier Oceanography Series).

KJERFVE, B.; OLIVEIRA, A. Modelling of Circulation and Water Exchange in a Hypersaline Coastal Lagoon: Lagoa de Araruama, Brazil. *In*: LACERDA, L. D. de *et al*. **Environmental geochemistry in tropical and subtropical environments.** Berlin: Springer, 2004. p. 235-251.

KJERFVE, B. *et al.* Hydrology and salt balance in a large, hypersaline Coastal Lagoon: Lagoa de Araruama, Brazil. **Estuarine, Coastal and Shelf Science**, v. 42, n. 6, p. 701–725, 1996.

KNOPPERS, B. Chapter 9 Aquatic primary production in Coastal Lagoons. *In*: KJERFVE, B. (ed.). **Elsevier Oceanography Series**, v. 60, p. 243–286, 1994.

KNOPPERS, B.; KJERFVE, B. Coastal Lagoons of Southeastern Brazil: physical and biogeochemical characteristics. *In*: PERILLO, G. M. E.; PICCOLO, M. C. (ed.). **Estuaries of South America:** their geomorphology and dynamics. Berlin, Heidelberg: Springer Berlin Heidelberg, 1999. p. 35–66.

KNOPPERS, B.; KJERFVE, B.; CARMOUZE, J.–P. Trophic state and water turn–over time in six choked coastal lagoons in Brazil. **Biogeochemistry**, v. 14, n. 2, p. 149–166, 1991.

KNOPPERS, B. *et al.* In situ measurements of benthic primary production, respiration and nutrient fluxes in a hypersaline coastal lagoon of SE Brazil. **Revista Brasileira de Oceanografia**, v. 44, 1996.

KOSKI–VAHALA, J.; HARTIKAINEN, H. Assessment of the risk of phosphorus loading due to resuspended sediment. **J. Environ. Qual.**, v. 30, n. 3, p. 960–966, May–Jun 2001. Available in: https://doi.org/10.2134/jeq2001.303960x. Access in: 3 Nov. 2022.

KRAAL, P. *et al.* Decoupling between water column oxygenation and benthic phosphate dynamics in a Shallow Eutrophic Estuary. **Environmental science & technology**, v. 47, 2013.

KRAUSKOPF, K. B. **Introduction to geochemistry**. 3rd ed. New York: McGraw–Hill, 1995.

KRUMBEIN, W. C.; SLOSS, L. L. **Stratigraphy and sedimentatio**. 2nd. ed. San Francisco: W.H. Freeman and Company, 1963.

KU, T. C. W. *et al.* Coupling between sulfur recycling and syndepositional carbonate dissolution: evidence from oxygen and sulfur isotope composition of pore water sulfate, South Florida Platform, U.S.A. **Geochimica et Cosmochimica Acta**, v. 63, n. 17, p. 2529–2546, 1999.

KUBRYAKOV, A. A.; ZATSEPIN, A. G.; STANICHNY, S. V. Anomalous summer–autumn phytoplankton bloom in 2015 in the Black Sea caused by several strong wind events. **Journal of Marine Systems**, v. 194, p. 11–24, 2019.

KULSHRESHTHA, A.; SHANMUGAM, P. Estimation of secchi transparency in turbid Coastal Waters. **Aquatic Procedia,** v. 4, p. 1114–1118, 2015.

KÜTTER, V. T. *et al.* Carbon, nitrogen, and phosphorus stoichiometry of plankton and the nutrient regime in Cabo Frio Bay, SE Brazil. **Environmental Monitoring and Assessment**, v. 186, n. 1, p. 559–573, 2014.

LALLI, C. M.; PARSONS, T. R. **Biological oceanography:** an introduction. 2nd ed. [*S. l.*]: Elsevier Butterworth–Heinemann, 1997.

LAUT, L. *et al.* Assessment of the trophic state of a hypersaline–carbonatic environment: Vermelha Lagoon (Brazil). **PLoS One**, v. 12, n. 9, p. e0184819, 2017.

LEAO, P. *et al.* Association of magnetotactic multicellular prokaryotes with Pseudoalteromonas species in a natural lagoon environment. **Antonie Van Leeuwenhoek**, v. 111, n. 11, p. 2213–2223, Nov. 2018.

LEE, G. F.; JONES–LEE, A.; RAST, W. **Secchi depth as a water quality Parameter**. El Macero, CA. 1995.

LEI, P. *et al.* Distribution of Nitrogen and Phosphorus in pore water profiles and estimation of their diffusive fluxes and annual loads in guanting reservoir (GTR), Northern China. **Bulletin of Environmental Contamination and Toxicology**, v. 106, n. 1, p. 10–17, 2021.

LEMLEY, D. A.; ADAMS, J. B. Eutrophication. *In*: FATH, B. (ed.). **Encyclopedia of ecology.** 2nd ed. Oxford: Elsevier, 2019. p. 86–90.

LENZI, M.; CIANCHI, F. Summer dystrophic criticalities of Non–Tidal Lagoons: the case study of a Mediterranean Lagoon. **Diversity**, v. 14, n. 9, p. 771, 2022.

LI, Y. *et al.* Total phytoplankton abundance is determined by phosphorus input: evidence from an 18–month fertilization experiment in four subtropical ponds. **Canadian Journal of Fisheries and Aquatic Sciences**, v. 74, n. 9, p. 1454–1461, 2017.

LI, Y. *et al.* Grain size tunes microbial community assembly and nitrogen transformation activity under frequent hyporheic exchange: a column experiment. **Water Research**, v. 182, p. 116040, 2020.

LI, Z.; SHENG, Y.; YANG, J.; BURTON, E. D. Phosphorus release from coastal sediments: Impacts of the oxidation–reduction potential and sulfide. **Marine Pollution Bulletin**, v. 113, n. 1, p. 176–181, 2016.

LIANG, Y. Diffusion. **Encyclopedia of Geochemistry,** p. 363–375, 2018. Doi: 10.1007/978-3-319-39312-4_336.

LIANG, Y.; BLAKE, R. Oxygen isotope fractionation between apatite and aqueous–phase phosphate: 20–45 °C. **Chemical Geology**, v. 238, p. 121–133, 2007.

LITCHMAN, E. Resource competition and the ecological success of Phytoplankton. *In*: FALKOWSKI, P. G.; KNOLL, A. H. (ed.). **Evolution of primary producers in the sea**. Burlington: Academic Press, 2007. Chapter 16, p. 351–375.

LITCHMAN, E.; KLAUSMEIER, C. A.; YOSHIYAMA, K. Contrasting size evolution in marine and freshwater diatoms. **Proceedings of the National Academy of Sciences**, v. 106, n. 8, p. 2665–2670, 2009.

LLORET, J.; MARÍN, A.; MARÍN–GUIRAO, L. Is coastal lagoon eutrophication likely to be aggravated by global climate change? **Estuarine, Coastal and Shelf Science**, v. 78, n. 2, p. 403–412, 2008.

LOBO, M. *et al.* Phosphorus spatial distribution and mass balance in the Itaipu lagoon (Rio de Janeiro, Brazil). **Ocean and Coastal Research**, v. 71, 2023.

LOPEZ–ABBATE, M. C. *et al.* Long–term changes on estuarine ciliates linked with modifications on wind patterns and water turbidity. **Mar. Environ. Res.**, v. 144, p. 46–55, Feb. 2019.

LOPEZ–MONROY, F. M.; TROCCOLI–GHINAGLIA, L. E.; POBLETE, E.; VALERIO–GONZALEZ, L. R. Nutrients dynamics in a Tropical Hypersaline Coastal Lagoon (Las Marites, Margarita Island, Venezuela). **Revista Bio Ciencias**, v. 4, n. 6, p. 1–16, 2017.

LOURENCO, S. O.; BARBARINO, E.; NASCIMENTO, A.; PARANHOS, R. Seasonal variations in tissue nitrogen and phosphorus of eight macroalgae from a tropical hypersaline coastal environment. **Cryptogamie Algologie**, v. 26, n. 4, p. 355–371, Nov. 2005.

LUND, J. W. Eutrophication. **Nature**, v. 214, n. 5088, p. 557–558, 1967.

LÜRLING, M. *et al.* Response of natural Cyanobacteria and Algae Assemblages to a nutrient pulse and elevated temperature. **Frontiers in Microbiology**, v. 9, p. 1851, 2018.

MACINTYRE, S. Turbulent mixing and resource supply to Phytoplankton. *In*: IMBERGER, J. (ed.). **Physical processes in lakes and oceans.** [*S. l.*]: American Geophysical Union, 1998. p. 561–590. (Coastal and Estuarine Studies).

MACKEY, K. R. M.; PAYTAN, A. Phosphorus Cycle. *In*: SCHAECHTER, M. (ed.). **Encyclopedia of microbiology.** 3rd ed. Oxford: Academic Press, 2009. p. 322–334.

MAHIQUES, M. M. de *et al.* The Southern Brazilian shelf: general characteristics, quaternary evolution and sediment distribution. **Brazilian Journal of Oceanography**, v. 58, p. 25–34, 2010.

MALONE, T. C.; NEWTON, A. The globalization of cultural eutrophication in the Coastal Ocean: causes and consequences. **Frontiers in Marine Science**, v. 7, 2020. Review.

MANCINELLI, R. L. The role of nitrogen in the evolution of life. **Origins of life and evolution of the biosphere**, v. 19, n. 3, p. 387–388, 1989.

MARAÑÓN, E. Phytoplankton size structure☆. *In*: COCHRAN, J. K.; BOKUNIEWICZ, H. J. (ed.). **Encyclopedia of ocean sciences.** 3rd ed. Oxford: Academic Press, 2019. p. 599–605.

MARCARELLI, A. M.; FULWEILER, R. W.; SCOTT, J. T. Nitrogen fixation: a poorly understood process along the freshwater–marine continuum. **Limnology and Oceanography Letters**, v. 7, n. 1, p. 1–10, 2022.

MARGALEF, R. Diversity, stability and maturity in natural ecosystems. *In*: VAN DOBBEN, W. H.; LOWE–MCCONNELL, R. H. (ed.). **Unifying concepts in ecology:** report of the plenary sessions of the First international congress of ecology, The Hague, the Netherlands, September 8–14, 1974. Dordrecht: Springer Netherlands, 1975. p. 151–160.

MARIANI, R.; LESSA, G. C.; MARTA–ALMEIDA, M. Long–term variability of the salinity field in a Large Tropical, Well–Mixed Estuary: the influence of climatic trends. **Estuaries and Coasts**, v. 45, n. 3, p. 721–736, 2022.

MARTIN, L.; LANDIM DOMINGUEZ, J. M. Geological history of Coastal Lagoons. *In*: KJERFVE, B. (ed.). **Coastal lagoon processes.** Columbia: Elsevier, 1994. Chapter 3, p. 41–68. (Elsevier oceanography series, v. 60)

MARTIN, L. *et al.* Quaternary sea–level history and variation in dynamics along the Central Brazilian Coast: consequences on coastal plain construction. **An. Acad. Bras. Cienc.**, v. 68, 1996.

MARTIN, L.; SUGUIO, K.; FLEXOR, J. M. As flutuações de nível do mar durante o Quaternário Superior e a evolução geológica de "deltas" brasileiros. **Boletim IG–USP**, (publicação especial), v. 15, p. 1–186, 1993.

MATOS, C. R. *et al.* Nutrient regeneration susceptibility under contrasting sedimentary conditions from the Rio de Janeiro coast, Brazil. **Mar. Pollut. Bull.**, v. 108, n. 1–2, p. 297–302, Jul. 2016.

MELLO, T. B. M. **Caracterização biogeoquímica da Lagoa de Araruama, RJ**. 2007. 82 f. Dissertação (Mestrado em Geociências - Geoquímica Ambiental) – Programa de Pós-Graduação em Geociências (Geoquímica), Universidade Federal Fluminense, Niterói, 2007.

MESNAGE, V.; PICOT, B. The distribution of phosphate in sediments and its relation with eutrophication of a Mediterranean Coastal Lagoon. **Hydrobiologia**, v. 297, n. 1, p. 29–41, Feb. 1995.

MIDDELBURG, J. Reviews and syntheses: to the bottom of carbon processing at the seafloor. **Biogeosciences**, v. 15, p. 413–427, 2018.

MILLERO, F. *et al.* Adsorption and desorption of Phosphate on Calcite and Aragonite in Seawater. **Aquatic Geochemistry**, v. 7, n. 1, p. 33–56, 2001.

MILLERO, F. J. Physico–chemical controls on Seawater. *In*: HOLLAND, H. D.; TUREKIAN, K. K. (ed.). **Treatise on geochemistry.** 2nd ed. Oxford: Elsevier, 2014. p. 1–18.

MIRANDA, L. B. d.; CASTRO FILHO, B. M. d.; KJERFVE, B. **Princípios de oceanografia física de estuários**. São Paulo: Edusp, 2002.

MONSEN, N. E.; CLOERN, J. E.; LUCAS, L. V.; MONISMITH, S. G. A comment on the use of flushing time, residence time, and age as transport time scales. **Limnology and Oceanography**, v. 47, n. 5, p. 1545–1553, 2002. Available in: https://doi.org/10.4319/lo.2002.47.5.1545. Access in: 18 jun. 2022.

MONTAÑEZ, I. P.; CROSSEY, L. J. Diagenesis. *In*: WHITE, W. M. (ed.). **Encyclopedia of geochemistry:** a comprehensive reference source on the chemistry of the Earth. Cham: Springer International Publishing, 2018. p. 353–362.

MOORE–MALEY, B.; ALLEN, S. E. Wind–driven upwelling and surface nutrient delivery in a semi–enclosed coastal sea. **Ocean Sci.**, v. 18, n. 1, p. 143–167, 2022.

MOORE, P. A.; REDDY, K. R.; FISHER, M. M. Phosphorus flux between sediment and overlying water in Lake Okeechobee, Florida: Spatial and temporal variations. **Journal of Environmental Quality**, v. 27, n. 6, p. 1428–1439, Nov.–Dec. 1998.

MOREIRA–TURCQ, P. F. Impact of a low salinity year on the metabolism of a hypersaline coastal lagoon (Brazil). **Hydrobiologia**, v. 429, n. 1/3, p. 133–140, 2000.

MOSES, C. O. Acid–base reactions. *In*: WHITE, W. M. (ed.). **Encyclopedia of geochemistry:** a comprehensive reference source on the chemistry of the Earth. Cham: Springer International Publishing, 2016. p. 1–5.

MOSLEY, L. *et al.* Extreme eutrophication and salinisation in the Coorong estuarine–lagoon ecosystem of Australia's largest river basin (Murray–Darling). **Marine Pollution Bulletin**, v. 188, p. 114648, 2023.

MUEHE, D. **Gênese da morfologia do fundo da lagoa de Araruama e cordões litorâneos associados**. [*S. l.: s. n.*], 2006.

NEVES, M. H. B. **Monthly monitoring reports of water quality in Araruama Lagoon**. Comitê de Bacias Lagos–São João, 2019–2020.

NICHOLLS, R. J. *et al.* **Coastal systems and low–lying areas**. Cambridge, UK, p. 315–356. 2007.

NIELSEN, D. L.; BROCK, M. A.; REES, G. N.; BALDWIN, D. S. Effects of increasing salinity on freshwater ecosystems in Australia. **Australian Journal of Botany**, v. 51, n. 6, p. 655–665, 2003.

NING, Z. *et al.* Influences of phosphorus concentration and porewater advection on phosphorus dynamics in carbonate sands around the Weizhou Island, northern South China Sea. **Mar. Pollut. Bull.**, v. 160, p. 111668, Nov. 2020.

NIXON, S. W. Coastal marine eutrophication: a definition, social causes, and future concerns. **Ophelia**, v. 41, n. 1, p. 199–219, 1995.

NORICI, A.; HELL, R.; GIORDANO, M. Sulfur and primary production in aquatic environments: an ecological perspective. **Photosynthesis Research**, v. 86, n. 3, p. 409–417, 2005.

ODUM, E. P. **Fundamentos de ecologia**. 6. ed. Lisboa: Fundação Calouste Gulbenkian, 2001. 820 p.

OKAMURA, H.; AOYAMA, I. Interactive toxic effect and distribution of heavy metals in phytoplankton. **Environmental Toxicology and Water Quality**, v. 9, n. 1, p. 7–15, 1994. Available in: https://doi.org/10.1002/tox.2530090103. Access in: 27 may. 2022.

OLIVEIRA, M. M. *et al.* Presença de microcistina durante eventos de florações de microalgas na Lagoa de Araruama. **Boletim do Observatório Ambiental Alberto Ribeiro Lamego**, v. 5, n. 1, p. 35–45, jan./jun. 2011.

OLIVEIRA, M. M. *et al.* Mugil liza (Valenciennes, 1836) biomarker responses in a hypersaline lagoon in southeastern Brazil before and after a microalgal bloom. **International Aquatic Research**, v. 12, n. 4, p. 231–241, Dec. 2020.

PADEDDA, B. *et al.* Eutrophication and Nutrient Fluxes in Mediterranean Coastal Lagoons. *In:* MAURICE, P. (ed.). **Encyclopedia of Water:** science, technology, and society. [*S. l.*]: Wiley, 2019. p. 1–16.
PALMA, P.; LEDO, L.; ALVARENGA, P. Assessment of trace element pollution and its environmental risk to freshwater sediments influenced by anthropogenic contributions: the case study of Alqueva reservoir (Guadiana Basin). **Catena**, v. 128, p. 174–184, 2015.

PALTA, M. M.; HARTNETT, H. E. Nitrogen cycle. *In*: WHITE, W. M. (ed.). **Encyclopedia of geochemistry:** a comprehensive reference source on the chemistry of the Earth. Cham: Springer International Publishing, 2018. p. 987–991.

PENHA, H. M. A synthesis of the geology of the east Fluminense Coast, State od Rio de Janeiro, Brazil. *In*: KNOPPERS, B. A. B., E. D. *et al.* (ed.). **Environmental geochemistry of Coastal Lagoon systems of Rio de Janeiro, Brazil**. Niterói: UFF/FINEP, 1999. Cap. 1, v. 6, p.3–10.

PÉREZ–RUZAFA, A. *et al.* Long–term dynamic in nutrients, chlorophyll a, and water quality parameters in a Coastal Lagoon during a process of Eutrophication for Decades, a sudden break and a relatively rapid recovery. **Frontiers in Marine Science**, v. 6, 2019.

PERRIN, P. Physiography and surface formations of the East Fluminense Coast, State of Rio de Janeiro, Brazil. *In*: KNOPPERS, B. A. *et al* (ed.). **Environmental geochemistry of Coastal Lagoon systems of Rio de Janeiro, Brazil**. Niterói: UFF/FINEP, 1999. v. 6, p. 11–23. (Série Geoquímica Ambiental).

POIRIER, D. R.; GEIGER, G. H. Fick's law and diffusivity of materials. *In*: POIRIER, D. R.; GEIGER, G. H. (ed.). **Transport phenomena in materials processing**. Cham: Springer International Publishing, 2016. p. 419–461.

PREFERENTIAL phosphorus retention in lakes alters the balance of global nutrient cycles. **Nature Geoscience**, v. 15, n. 6, p. 434–435, 2022.

PRIESTLEY, S. *et al.* N and C Isotope variations along an extreme eutrophication and salinity gradient in the Coorong Lagoon, South Australia. **Frontiers in Earth Science**, v. 9, 2022.

RABOUILLE, C. *et al.* Biogeochemical and contaminant cycling in sediments from a human–impacted coastal lagoon – introduction and summary. **Estuarine, Coastal and Shelf Science**, v. 72, n. 3, p. 387–392, 2007.

RAMOS, V. M. C. *et al.* Cyanobacterial diversity in microbial mats from the hypersaline Lagoon System of Araruama, Brazil: an in–depth Polyphasic study. **Front Microbiol.**, v. 8, n. 1233, p. 1233, 2017.

REDFIELD, A. C. The biological control of chemical factors in the environment. **American Scientist**, v. 46, n. 3, p. 230A–221, 1958.

REEDER, B. C. Primary productivity limitations in relatively low alkalinity, high phosphorus, oligotrophic Kentucky reservoirs. **Ecological Engineering**, v. 108, p. 477–481, 2017.

REYNOLDS, C. S. Plants in motion: physical – biological interaction in the Plankton. *In*: IMBERGER, J. (ed.). **Physical processes in lakes and oceans.** [*S. l.*]: American Geophysical Union, 1998. p. 535–560. (Coastal and Estuarine Studies).

RICH, V. I.; MAIER, R. M. Aquatic environments. *In*: PEPPER, I. L. *et al* (ed.). **Environmental microbiology.** 3rd ed. San Diego: Academic Press, 2015. Chapter 6, p. 111–138.

RIZHINASHVILI, A. L. An Outline of the theory of the functioning of aquatic ecosystems: nutrient limitation. **Biology Bulletin Reviews**, v. 12, n. 6, p. 596–608, 2022.

RODELLAS, V. *et al*. Temporal variations in porewater fluxes to a coastal lagoon driven by wind waves and changes in lagoon water depths. **Journal of Hydrology**, v. 581, Feb. 2020.

RODRIGUES–FILHO, J. L. *et al.* From ecological functions to ecosystem services: linking coastal lagoons biodiversity with human well–being. **Hydrobiologia**, p. 1–43, 2023.

ROSA, J.; BATISTA, L. Spatial and temporal variability of the zooplankton community at Araruama Lagoon. **Biotemas**, v. 33, p. 1–10, 2020.

ROSE, K. C. *et al.* Patterns of spatial and temporal variability of UV transparency in Lake Tahoe, California–Nevada. **Journal of Geophysical Research: Biogeosciences**, v. 114, n. G2, 2009.

ROWE, G. T.; CLIFFORD, C. H.; SMITH, K. L.; HAMILTON, P. L. Benthic nutrient regeneration and its coupling to primary productivity in coastal waters. **Nature**, v. 255, n. 5505, p. 215–217, 1975.

RUTTENBERG, K. The global Phosphorus cycle. **Treatise on Geochemistry**, v. 8, p. 585–643, 2003.

SCHEINER, S.; WILLIG, M. A general theory of ecology. Theor Ecol 1:21–28. **Theoretical Ecology**, v. 1, p. 21–28, 2008.

SCHULZ, H. D.; ZABEL, M. **Marine Geochemistry**. Berlin Heidelberg: Springer–Verlag, January 2006.

SEELIGER, U. The Patos Lagoon Estuary, Brazil. *In*: SEELIGER, U.; KJERFVE, B. **Coastal Marine Ecosystems of Latin America.** [*S. l.*]: Springer, 2001. p. 167–183.

SEGURO, I. *et al.* Seasonal changes of the microplankton community along a tropical estuary. **Regional Studies in Marine Science**, v. 2, p. 189–202, 2015.

SELLNER, K.; DOUCETTE, G.; KIRKPATRICK, G. Harmful algal blooms: Causes, impacts and detection. **Journal of industrial microbiology & biotechnology**, v. 30, p. 383–406, 2003.

SETHURAMAN, S. Structure of turbulence over water during High Winds. **Journal of Applied Meteorology (1962–1982)**, v. 18, n. 3, p. 324–328, 1979.

SHAHI, N. *et al.* The relationship between variation of phytoplankton species composition and physico–chemical parameters in northern coastal waters of Mumbai, India. **Indian Journal of Geo-Marine Science**, v. 44, n. 5, p. 673–684, 2015.

SHEN, Y. *et al.* The nitrogen reduction in eutrophic water column driven by Microcystis blooms. **Journal of Hazardous Materials**, v. 385, p. 121578, 2020.

SHINN, M. B. Colorimetric method for determination of nitrate. **Industrial & Engineering Chemistry Analytical Edition**, v. 13, n. 1, p. 33–35, 1941.

SILVA, K. M.; GUIMARÃES, T. C.; WASSERMAN, J. C. Distribuição espacial da concentração de nutrientes em sedimentos na laguna hipersalina de Araruama – RJ, Brasil. **Geochimica Brasiliensis**, v. 33, n. 1, p. 16–27, 2019.

SILVA, K. M. d. **Estudo da geoquímica do Fósforo em sedimentos da Laguna de Araruama – RJ, para avaliação do processo de eutrofização**. 2019. 104 f. Dissertação (Mestrado) – Departamento de Saneamento e Saúde Ambiental, Escola Nacional de Saúde Pública Sérgio Arouca, Rio de Janeiro, 2019.

SILVA, L. C. d. **Geologia do Estado do Rio de Janeiro: texto explicativo do mapa geológico do Estado do Rio de Janeiro. Programa Levantamentos Geológicos Básicos do Brasil**. Brasília: CPRM, 2001.

SMIL, V. Phosphorus in the environment: natural flows and human interferences. **Annual Review of Energy and the Environment**, v. 25, n. 1, p. 53–88, 2000.

SOUZA, F. P. d.; AZEVEDO, J. P. S. Panorama das lagoas urbanas no Rio de Janeiro: aspectos relevantes na gestão das Lagoas Rodrigo de Freitas, Araruama e Complexo Lagunar de Jacarepaguá. **Engenharia Sanitaria e Ambiental**, v. 25, p. 197–204, 2020.

SOUZA, M. F. L. *et al.* Nutrient budgets and trophic state in a hypersaline coastal lagoon: Lagoa de Araruama, Brazil. **Estuarine, Coastal and Shelf Science**, v. 57, n. 5–6, p. 843–858, 2003.

SOUZA, P. C. M. d.; SCHMITT, R. d. S.; STANTON, N. Meso–Cenozoic tectonic evolution of the SE Brazilian continental margin: Petrographic, kinematic and dynamic analysis of the onshore Araruama Lagoon Fault System. **Journal of Structural Geology**, v. 102, p. 37–57, 2017.

STRICKLAND, J. D. H. *et al.* A practical handbook of seawater analysis. **Journal of the Fisheries Research Board of Canada**, v. 167, 1972.

STRUYF, E. *et al.* The global biogeochemical silicon cycle. **Silicon**, v. 1, n. 4, p. 207–213, 2009.

STUMM, W.; MORGAN, J. J. **Aquatic chemistry:** an introduction emphasizing chemical equilibria in natural waters. 2nd ed. New York: John Wiley & Sons Ltd., 1981.

STUMM, W.; MORGAN, J. J. **Aquatic chemistry, chemical equilibria and rates in natural waters**. 3rd ed. New York: John Wiley & Sons, Inc., 1996. (Environmental Science and Technology: A Wiley–Interscience Series of Textsand Monographs).

SYLVESTRE, F.; BECK–EICHLER, B.; DULEBA, W.; DEBENAY, J.–P. Modern benthic diatom distribution in a hypersaline coastal lagoon: the Lagoa de Araruama (R.J.), Brazil. **Hydrobiologia**, v. 443, n. 1, p. 213–231, 2001.

TAPIA GONZÁLEZ, F. U.; HERRERA–SILVEIRA, J. A.; AGUIRRE–MACEDO, M. L. Water quality variability and eutrophic trends in karstic tropical coastal lagoons of the Yucatán Peninsula. **Estuarine, Coastal and Shelf Science**, v. 76, n. 2, p. 418–430, 2008.

TASNIM, B.; FANG, X.; HAYWORTH, J. S.; TIAN, D. Simulating nutrients and Phytoplankton dynamics in Lakes: model development and applications. **Water**, v. 13, n. 15, DOI: 10.3390/w13152088.

THEY, N. H.; MARINS, L. F.; MÖLLER, O. O.; ABREU, P. C. High bacterial activity in nutrient rich saltwater: evidence from the uncoupling between salinity and nutrients in the Patos Lagoon estuary. **Estuarine, Coastal and Shelf Science**, v. 216, p. 148–156, 2019.

TREVISAN, C. *et al.* Short term assessment of nutrients and physicochemical parameters considering different depths in a hypersaline lagoon – Araruama Lagoon –RJ. **Geochimica Brasiliensis**, v. 36, p. e–22001, 2022.

TREVISAN, C. L.; VICENTE, M. C.; ROCHA, B. C. S.; WASSERMAN, J. C. Development of a dredging sensitivity index, applied to an industrialized coastal environment in Brazil. **Sci. Total Environ.**, v. 748, p. 141294, Dec. 2020.

TUGRUL, S.; OZHAN, K.; AKCAY, I. Assessment of trophic status of the northeastern Mediterranean coastal waters: eutrophication classification tools revisited. **Environ. Sci. Pollut. Res. Int.**, v. 26, n. 15, p. 14742–14754, May 2019.

TURCQ, B. *et al.* Origin and evolution of the Quaternary Coastal Plain between Guaratiba and Cabo Frio, State of Rio de Janeiro, Brazil. **Environmental Geochemistry of Coastal Lagoon Systems**, v. 6, p. 25–46, 1999.

TURNER, A.; MILLWARD, G. E. Suspended particles: their role in estuarine biogeochemical cycles. **Estuarine, Coastal and Shelf Science**, v. 55, n. 6, p. 857–883, 2002.

TURNER, J. S.; FALL, K. A.; FRIEDRICHS, C. T. Clarifying water clarity: a call to use metrics best suited to corresponding research and management goals in aquatic ecosystems. **Limnology and Oceanography Letters**, v. 8, n. 3, p. 388–397, 2023.

UNITED STATES. Environmental Protection Agency. **Method 180.1:** determination of Turbidity by Nephelometry. Cincinnati, Ohio: USEPA, 1993.

VALENZUELA–SIU, M.; ARREOLA–LIZARRAGA, J. A.; SANCHEZ–CARRILLO, S.; PADILLA–ARREDONDO, G . Nutrient fluxes and net metabolism in Lobos coastal lagoon, México. **Hidrobiológica [online]**, v. 17, n. 3, p. 193–202, 2007.

VALIELA, I. **Marine ecological processes**. [*S. l.*]: Springer–Verlag, 1984.

VAN CAPPELLEN, P.; BERNER, R. A. A mathematical model for the early diagenesis of phosphorus and fluorine in marine sediments; apatite precipitation. **American Journal of Science**, v. 288, p. 289–333, 1988.

VAN DER PLOEG, S. W. F. Basic concepts of ecology. *In*: HUTZINGER, O. (ed.). **The natural environment and the biogeochemical cycles**. Berlin, Heidelberg: Springer, 1982. v. 1, p. 1–45. (The Handbook of Environmental Chemistry).

VEIGA, F. A. **Processos morfodinâmicos e sedimentológicos na plataforma continental rasa paranaense**. 2005. 193 f. (Doctorate (Ph.D.)) – Setor de Ciẹncias da Terra, Programa de Pós–Graduação em Geologia, Universidade Federal do Paraná, Curitiba, 2005.

VIAROLI, P. *et al.* Evolution of the Trophic Conditions and Dystrophic Outbreaks in the Sacca di Goro Lagoon (Northern Adriatic Sea). *In*: FARANDA, F. M.; GUGLIELMO, L. (ed.). **Mediterranean ecosystems:** structures and processes. Milano: Springer Milan, 2001. p. 467–475.

VICENTE, M. C. *et al.* Spatial–temporal distribution of dissolved inorganic nutrients in the hypersaline Araruama Lagoon, Rio de Janeiro, Brazil. **Regional Studies in Marine Science**, p. 101787, 2021.

VICENTE, M. C. *et al.* A method to reproduce pH and Eh environmental changes due to sediment resuspension. **MethodsX**, p. 101751, 2022.

VIEIRA–CAMPOS, A. A.; COSTA, B. V. M.; YOGUI, G. T. **Determinação gravimétrica do teor de carbonato de cálcio em amostras de solo e sedimento.** Procedimento Operacional Padrão OrganoMAR–2017–01. Laboratório de Compostos Orgânicos em Ecossistemas Costeiros e Marinhos, Departamento de Oceanografia. Recife: Universidade Federal de Pernambuco, 2017. 11 p.

VILARIÑO, N.; LOUZAO, M. C. Human poisoning from marine toxins: unknowns for optimal consumer protection. **Toxins**, v. 10, n. 8, Aug 9 2018.

VINCENT, S. G. T.; JENNERJAHN, T.; RAMASAMY, K. Source and composition of organic matter and its role in designing sediment microbial communities. *In*:

VINCENT, S. G. T.; JENNERJAHN, T. C.; RAMASAMY, K. **Microbial communities in coastal sediments:** structure and functions. [*S. l.*]: Elsevier, 2021. p. 1–45.
VOLLENWEIDER, R. A. Coastal marine eutrophication: principles and control. *In*: VOLLENWEIDER, R. A.; MARCHETTI, R. (ed.). **Marine coastal eutrophication**. Amsterdam: Elsevier, 1992. p. 1–20.

WANG, B.; XIN, M.; WEI, Q.; XIE, L. A historical overview of coastal eutrophication in the China Seas. **Mar. Pollut. Bull.**, v. 136, p. 394–400, Nov. 2018.

WARD, B. B.; TALBOT, M. C.; PERRY, M. J. Contributions of phytoplankton and nitrifying bacteria to ammonium and nitrite dynamics in coastal waters. **Continental Shelf Research**, v. 3, n. 4, p. 383–398, 1984.

WASSERMAN, J. C. **Os programas de monitoramento da Laguna de Araruama:** avaliação integrada de mais de 10 anos de dados. Niterói: Rede UFF de Meio Ambiente e Desenvolvimento Sustentável – REMADSUFF, 2017.

WASSERMAN, J. C. *et al.* **A qualidade da água e as mortandades de peixes na laguna de Araruama**. Niterói: Rede UFF de Meio Ambiente e Desenvolvimento Sustentável – REMADSUFF, 2017.

WASSERMAN, J. C. *et al.* **Relatório de pesquisa:** avaliação ambiental da Laguna de Araruama, para subsídiar um programa de recuperação e gestão. Niterói: Rede de Meio Ambiente e Desenvolvimento Sustentável – REMADS, 2006.

WASSERMAN, J. C.; SILVA–FILHO, E. V. **Relatório resumido do monitoramento do Projeto Perynas (Araruama) para instalação de um condomínio de casas com marina e hotel. AGS, Empreendimentos Turísticos e Hoteleiros SA**. Rio de Janeiro: *s. n*., 1995. 6 p.

WASSMANN, P. Cultural eutrophication: perspectives and prospects. **Drainage Basin Inputs and Eutrophication: An Integrated Approach.** Norway: University Tromso, 2005.

WEATHERS, K. C.; STRAYER, D. L.; LIKENS, G. E. **Fundamentals of ecosystem science**. 2nd ed. [*S. l.*]: Academic Press, 2021.

WEBSTER, I. T.; HARRIS, G. P. Anthropogenic impacts on the ecosystems of coastal lagoons: modelling fundamental biogeochemical processes and management implications. **Marine and Freshwater Research**, v. 55, n. 1, p. 67, 2004.

WENTWORTH, C. K. A scale of grade and class terms for clastic sediments. **The Journal of Geology**, v. 30, p. 377–392, 1922.

WESTHEIMER, F. H. Why Nature Chose Phosphates. **Science**, v. 235, n. 4793, p. 1173–1178, 1987.

WETZEL, R. G. **Limnology**. 2nd ed. Philadelphia: Saunders College Publishing, 1983.

WETZEL, R. G. **Limnology:** lake and river ecosystems. 3rd ed. San Diego: Academic Press, 2001.

WHEELER, J. D.; SECCHI, E.; RUSCONI, R.; STOCKER, R. Not Just Going with the Flow: the effects of fluid flow on bacteria and plankton. **Annual Review of Cell and Developmental Biology**, v. 35, n. 1, p. 213–237, 2019.

WORLD HEALTH ORGANIZATION. **Guidelines on recreational water quality**. Geneva: WHO, 2021.

WILLIAMS, A. A.; LAUER, N.; HACKNEY, C. Soil Phosphorus Dynamics and Saltwater Intrusion in a Florida Estuary. **Wetlands**, v. 34, p. 535–544, 2014.

WINDER, M.; CLOERN, J. E. The annual cycles of phytoplankton biomass. **Philos Trans. R. Soc. Lond. B Biol. Sci.**, v. 365, n. 1555, p. 3215–3226, oct 2010.

WOLANSKI, E.; MCLUSKY, D. **Treatise on estuarine and coastal science**. [*S. l.*]: Academic Press, 2012 2011. 4590 p.

WU, T. *et al.* Spatial distribution of sediment nitrogen and phosphorus in Lake Taihu from a hydrodynamics–induced transport perspective. **Sci. Total Environ.**, v. 650, n. Pt 1, p. 1554–1565, feb. 2019.

ZHANG, J.–Z.; FISCHER, C. J. A simplified resorcinol method for direct spectrophotometric determination of nitrate in seawater. **Marine Chemistry**, v. 99, n. 1–4, p. 220–226, 2006.

ZHANG, S. *et al.* Dynamic sulfur–iron cycle promoted phosphorus mobilization in sediments driven by the algae decomposition. **Ecotoxicology**, v. 30, n. 8, p. 1662–1671, 2021.

ZHOU, Y. *et al.* Nutrients structure changes impact the competition and succession between diatom and dinoflagellate in the East China Sea. **Sci. Total Environ.**, v. 574, p. 499–508, jan. 2017.

APPENDIXS

APPENDIX A

Table A1.1 – Physical–chemical parameters in water column

POINT	DEPTH m	SECCHI m	pH	SAL	TEMP °C	ORP mV
C1_1S	3.00	3.00	8.4	35.5	25.4	61.4
C1_2S	3.43	0.85	8.3	39.4	27.8	56.1
C1_2M	3.43	0.85	8.2	39.4	27.8	56.1
C1_2B	3.43	0.85	8.2	39.5	27.9	56.2
C1_3S	3.45	0.50	8.4	56.6	28.9	43.2
C1_3M	3.45	0.50	8.4	57.9	28.9	44.2
C1_3B	3.45	0.50	8.4	61.2	29.3	43.4
C1_4S	12.79	0.50	8.4	62.1	28.9	65.5
C1_4M	12.79	0.50	8.4	62.6	28.6	67.7
C1_4B	12.79	0.50	8.4	62.9	28.5	52.0
C1_5S	4.17	0.50	8.4	63.1	29.2	59.9
C1_5M	4.17	0.50	8.5	63.1	29.2	59.2
C1_5B	4.17	0.50	8.5	63.1	29.2	56.7
C1_6S	8.00	0.45	8.4	63.2	30.1	165.4
C1_6M	8.00	0.45	8.4	63.4	28.8	171.9
C1_6B	8.00	0.45	8.4	63.4	28.8	176.6
C1_7S	5.76	0.43	8.4	62.6	29.9	165.1
C1_7M	5.76	0.43	8.5	62.8	29.2	165.8
C1_7B	5.76	0.43	8.5	63.2	28.3	110.0
C1_8S	8.00	0.45	8.5	63.2	30.3	128.3
C1_8M	8.00	0.45	8.5	62.9	28.8	127.7
C1_8B	8.00	0.45	8.5	64.1	29.1	127.6
C1_9S	4.50	0.40	8.5	64.9	30.1	95.4
C1_9M	4.50	0.40	8.5	65.2	29.8	94.5
C1_9B	4.50	0.40	8.5	65.3	28.7	93.4
C1_10S	2.50	0.35	8.6	64.0	30.8	81.3
C1_10B	2.50	0.35	8.6	65.0	30.1	80.4
C1_11S	0.30	0.30	8.7	67.0	28.6	–51.0
C2_3S	1.90	0.70	8.6	55.2	24.5	30.2
C2_5S	4.80	2.30	8.3	57.5	24.6	–37.7
C2_6S	12.30	2.00	8.3	59.6	25.0	–10.5
C2_8S	8.20	1.80	8.3	58.7	24.9	42.8
C2_10S	3.40	1.70	8.3	58.6	25.3	33.2
C3_3S	1.80	0.60	8.2	52.1	22.4	112.9
C3_5S	3.50	1.80	8.1	58.5	23.8	60.5
C3_6S	4.10	2.30	8.1	58.4	24.0	45.5
C3_8S	8.30	2.40	8.3	58.1	24.0	134.0
C3_10S	3.30	0.84	8.2	56.5	23.2	–58.3
C4_1S	3.00	3.00	7.9	35.0	22.7	35.1
C4_3S	3.30	0.52	8.1	42.1	25.0	71.6
C4_3B	3.30	0.52	8.1	44.1	23.5	112.4

Table A1.1 – Physical–chemical parameters in water column (continuation)

POINT	DEPTH m	SECCHI m	pH	SAL	TEMP °C	ORP mV
C4_4S	10.50	1.40	8.1	49.3	24.9	37.0
C4_4B	10.50	1.40	8.1	49.1	24.5	57.0
C4_5S	2.30	1.38	8.1	49.2	25.7	55.0
C4_5B	2.30	1.38	7.4	50.1	22.3	200.0
C4_6S	9.20	1.75	8.1	49.5	25.4	99.0
C4_6B	9.20	1.75	8.1	49.5	24.6	113.0
C4_7S	5.50	1.45	8.1	49.6	22.7	42.8
C4_7B	5.50	1.45	8.1	49.3	22.5	88.0
C4_8S	7.90	1.35	8.2	49.3	25.0	45.0
C4_8B	7.90	1.35	8.1	47.4	24.7	105.3
C4_9S	4.90	1.10	8.4	48.0	25.7	34.8
C4_9B	4.90	1.10	8.3	47.6	24.8	19.5
C4_10S	3.20	0.70	8.2	47.1	25.6	22.2
C4_10B	3.20	0.70	8.1	47.5	25.2	33.2
C4_11S	1.90	0.50	8.2	42.5	25.0	43.9
C5_1S	3.00	3.00	8.0	33.4	25.5	62.1
C5_2S	2.50	0.60	8.3	48.9	30.0	2.5
C5_2B	2.50	0.60	8.4	49.1	29.8	0.7
C5_3S	1.80	0.70	8.2	50.7	29.1	31.1
C5_3B	1.80	0.70	7.9	50.7	28.5	29.5
C5_4S	14.20	0.85	8.3	51.3	28.1	25.0
C5_4B	14.20	0.85	8.0	51.3	29.1	–30.0
C5_5S	4.70	0.70	8.2	51.1	27.4	39.2
C5_5B	4.70	0.70	8.1	50.6	26.9	38.8
C5_6S	9.80	0.90	8.3	50.2	27.9	29.0
C5_6B	9.80	0.90	8.3	50.1	25.1	
C5_7S	5.80	1.00	8.3	50.8	27.1	0.2
C5_7B	5.80	1.00	8.2	50.3	28.0	–15.7
C5_8S	8.10	0.91	8.1	50.0	28.3	33.6
C5_8B	8.10	0.91	8.0	51.1	26.8	40.0
C5_9S	5.00	1.00	8.3	45.4	28.2	–24.9
C5_9B	5.00	1.00	8.0	48.7	27.8	
C5_10S	3.40	0.75	8.4	41.4	28.8	–5.0
C5_10B	3.40	0.75	8.3	44.3	28.5	–19.5
C5_11S	1.80	0.60	8.5	33.2	29.2	–7.1
C5_11B	1.80	0.60		35.2	28.7	–18.0
C6_1S	3.00	3.00	8.2	33.6	21.2	227.8
C6_2S	1.80	1.60	8.0	41.9	22.4	122.7
C6_2B	1.80	1.60	7.8	43.3	22.2	134.3
C6_3S	1.70	1.70	7.6	41.9	22.8	47.5
C6_3B	1.70	1.70	7.7	43.3	19.8	15.6
C6_4S	3.60	1.35	7.9	49.7	23.8	28.0
C6_4B	3.60	1.35	7.9	49.6	23.4	59.4
C6_5S	4.80	1.35	8.0	48.9	25.0	55.1
C6_5B	4.80	1.35	7.9	49.2	24.1	–4.5

Table A1.1 – Physical–chemical parameters in water column (continuation)

POINT	DEPTH m	SECCHI m	pH	SAL	TEMP °C	ORP mV
C6_6S	10.00	1.50	8.0	50.3	23.3	92.3
C6_6B	10.00	1.50	8.0	50.2	22.1	128.1
C6_7S	5.90	1.30	7.8	49.7	22.3	–14.5
C6_7B	5.90	1.30	7.8	49.3	23.8	–5.7
C6_8S	8.00	1.35	7.9	49.9	21.7	88.7
C6_8B	8.00	1.35	8.0	49.8	22.4	96.8
C6_9S	5.00	1.00	8.0	47.7	23.5	85.2
C6_9B	5.00	1.00	8.1	48.0	23.5	83.4
C6_10S	3.30	1.00	8.0	45.8	24.5	64.3
C6_10B	3.30	1.00	7.9	45.5	23.0	44.2
C6_11S	1.60	0.80	8.1	38.6	23.5	242.1
C6_11B	1.60	0.80	7.8	38.7	23.5	102.3
C7_1S	1.80	1.80	8.2	35.0	25.4	80.5
C7_2S	3.10	2.80	7.9	37.0	27.8	70.0
C7_2B	3.10	2.80	8.1	38.4	27.8	68.9
C7_3S	1.30	1.30	7.9	42.1	28.9	134.9
C7_4S	13.50	2.00	7.2	49.3	28.9	64.9
C7_4B	13.50	2.00	7.8	49.4	28.6	77.0
C7_5S	4.10	3.60	7.4	49.2	29.2	42.9
C7_5B	4.10	3.60	7.5	50.1	29.2	54.9
C7_6S	10.00	1.70	8.0	49.5	30.1	30.0
C7_6B	10.00	1.70	8.0	49.5	28.8	5.7
C7_7S	5.80	1.40	8.0	49.6	29.9	47.6
C7_7B	5.80	1.40	8.0	49.3	29.2	43.1
C7_8S	8.00	1.35	8.0	49.3	30.3	39.7
C7_8B	8.00	1.35	8.0	47.4	28.8	40.0
C7_9S	5.40	0.80	8.1	48.0	30.1	22.5
C7_9B	5.40	0.80	8.1	47.6	29.8	–7.1
C7_10S	3.40	0.65	8.1	47.1	30.8	24.7
C7_10B	3.40	0.65	8.6	47.5	30.7	2.6
C7_11S	1.60	0.40	8.2	42.5	28.6	13.8
C8_1S	1.50	1.00	8.3	33.4	25.4	–0.8
C8_2S	0.30	0.30	8.4	34.2	26.4	–15.0
C8_4S	12.00	3.80	7.8	45.6	27.8	72.7
C8_4B	12.00	3.80	7.7	46.2	27.4	67.4
C8_5S	4.60	2.20	7.6	43.9	26.8	14.3
C8_5B	4.60	2.20	7.6	46.2	23.9	23.4
C8_6S	10.20	2.40	7.8	46.2	25.1	5.1
C8_6B	10.20	2.40	7.6	47.2	27..9	–6.1
C8_7S	6.00	2.20	8.5	45.9	24.3	–64.0
C8_7B	6.00	2.20	8.4	46.9	23.2	–44.3
C8_8S	8.20	1.30	8.1	46.1	27.4	–40.0
C8_8B	8.20	1.30	8.0	47.1	27.2	–30.8
C8_9S	5.00	1.10	8.1	42.9	27.6	–90.2
C8_9B	5.00	1.10	7.8	45.1	27.4	–70.8

Table A1.1 – Physical–chemical parameters in water column (continuation)

POINT	DEPTH m	SECCHI m	pH	SAL	TEMP °C	ORP mV
C8_10S	3.50	0.90	8.2	39.8	25.1	–49.5
C8_10B	3.50	0.90	8.3	42.7	28.1	–27.8
C8_11S	1.70	0.75	8.2	33.1	28.5	38.0
C8_11B	1.70	0.75	8.2	33.2	28.6	–32.3
C9_1S	0.50	0.50		33.2	21.3	57.3
C9_2S	2.30	2.15	8.1	36.8	22.7	33.8
C9_2B	2.30	2.15	8.1	37.5	22.5	33.5
C9_3S	1.40	1.40	8.1	44.1	22.2	106.0
C9_3B	1.40	1.40	8.1	44.1	22.1	175.0
C9_4S	11.70	2.50	8.1	46.4	21.9	185.0
C9_4B	11.70	2.50	8.0	45.3	22.0	222.0
C9_5S	4.80	2.00	7.6	47.2	24.1	7.6
C9_5B	4.80	2.00	8.4	47.1	26.0	–19.8
C9_6S	10.20	2.40		46.9	23.2	77.0
C9_6B	10.20	2.40		46.7	24.0	85.2
C9_7S	5.60	2.15	8.0	46.9		55.0
C9_7B	5.60	2.15	8.0	47.0		90.0
C9_8S	8.00	3.00		47.2	24.2	51.2
C9_8B	8.00	3.00		47.0	23.8	76.0
C9_9S	5.00	1.82	7.9	47.2		79.7
C9_9B	5.00	1.82	7.9	47.1	21.2	79.2
C9_10S	3.30	1.20	9.9	46.7		113.0
C9_10B	3.30	1.20	8.0	46.5		117.4
C9_11S	1.50	1.50	7.8	42.6	22.6	155.0
C9_11B	1.50	1.50	7.9	42.9	22.4	176.6

Source: the author, 2023.

Table A1.2 – Physical–chemical parameters in water column

POINT	TURB	TSS	DO	BOD_5	CHL–a	PHAEO	POC
	NTU	mg L^{-1}					
C1_1S	2.39	72.60	8.56	1.96	0.02	0.04	1.67
C1_2S	6.22	104.82	7.55	2.35	0.02	0.04	12.50
C1_2M	5.31	111.05	7.72	3.82	0.02	0.04	11.67
C1_2B	5.99	116.98	7.67	3.17	0.02	0.04	11.67
C1_3S	14.70	167.02	8.96	3.20	0.06	0.04	24.58
C1_3M	14.70	195.30	8.57	5.57	0.06	0.04	20.42
C1_3B	15.10	206.40	7.85	3.65	0.06	0.04	22.92
C1_4S	14.20	15.13	9.12	2.90	0.06	0.04	16.33
C1_4M	19.40	27.87	7.94	3.24	0.05	0.04	22.22
C1_4B	20.60	40.44	10.00	5.90	0.08	0.04	18.89
C1_5S	16.20	192.11	9.70	4.40	0.12	0.04	53.33
C1_5M	13.10	183.38	9.18	5.38	0.23	0.04	56.67
C1_5B	16.80	187.42	8.81	5.61	0.12	0.04	51.67
C1_6S	15.70	27.33	9.44	3.10	0.03	0.04	23.33
C1_6M	14.60	21.37	8.88	5.68	0.10	0.04	15.56
C1_6B	13.20	24.72	7.62	3.12	0.04	0.04	14.81
C1_7S	15.50	21.33	10.57	4.30	0.09	0.04	20.00
C1_7M	16.80	29.72	11.15	7.25	0.08	0.04	26.67
C1_7B	20.20	32.00	11.71	2.71	0.04	0.04	20.00
C1_8S	11.30	24.24	11.30	2.96	0.06	0.04	34.17
C1_8M	16.80	26.06	16.80	12.60	0.03	0.04	19.17
C1_8B	15.60	180.76	15.60	3.40	0.03	0.04	46.67
C1_9S	18.00	217.19	9.89	2.12	0.05	0.04	60.83
C1_9M	18.70	136.61	9.15	5.75	0.01	0.04	56.67
C1_9B	21.80	193.73	5.83	3.23	0.16	0.04	45.00
C1_10S	26.90	82.27	11.65	3.51	0.02	0.04	26.19
C1_10B	35.70	367.56	9.75	3.22	0.13	0.04	54.17
C1_11S	57.70	249.11	8.91	2.07	0.11	0.04	100.00
C2_3S	6.29	86.66			0.02	0.04	51.75
C2_5S	0.81	43.01			0.02	0.04	57.75
C2_6S	2.55	56.13			0.02	0.04	50.25
C2_8S	2.12	63.38			0.02	0.04	45.00
C2_10S	1.91	33.61			0.02	0.04	90.00
C3_3S	6.52		10.53	2.24	0.02	0.04	13.13
C3_5S	0.39		8.99	1.90	0.02	0.04	4.69
C3_6S	0.81		8.41	1.12	0.02	0.04	5.63
C3_8S	1.80		9.38	2.00	0.02	0.04	2.34
C3_10S	2.56		8.34	2.46	0.02	0.04	8.44
C4_1S	4.85	172.69	8.82	1.34	0.02	0.04	26.54
C4_3S	11.50	319.98	11.59	2.70	0.02	0.04	55.38
C4_3B	7.11	170.32	7.82	1.29	0.02	0.04	20.77
C4_4S	14.50		7.63	0.99	0.02	0.04	12.69
C4_4B	5.63	18.38	6.37	1.10	0.02	0.05	
C4_5S	8.95	30.60	7.50	1.32	0.02	0.04	24.18
C4_5B	6.21	8.56	7.44	1.11	0.02	0.04	10.55

Table A1.2 – Physical–chemical parameters in water column (continuation)

POINT	TURB	TSS	DO	BOD_5	CHL–a	PHAEO	POC
	NTU	mg L^{-1}					
C4_6S	6.06	228.34	8.05	0.92	0.02	0.04	6.92
C4_6B	1.83	95.85	7.70	0.95	0.02	0.09	
C4_7S	5.55	123.47	8.11	1.74	0.02	0.11	11.54
C4_7B	2.85	281.60	7.78	0.36	0.02	0.04	15.00
C4_8S	5.34	232.42	9.31	2.61	0.02	0.04	6.92
C4_8B	2.16	214.05	7.68	0.18	0.02	0.05	11.54
C4_9S	4.86	168.25	9.16	2.59	0.02	0.05	3.46
C4_9B	2.22	233.75	7.43	0.32	0.02	0.05	1.15
C4_10S	8.14	235.71	9.48	3.30	0.02	0.11	21.92
C4_10B	2.78	419.28	6.98	1.11	0.02	0.04	13.85
C4_11S	14.50	279.25	9.82	5.46	0.02	0.11	66.92
C5_1S	0.95	59.22	8.61	0.42	0.02	0.04	
C5_2S	11.10	194.83	9.97	3.37	0.02	0.04	
C5_2B	15.50	116.21	10.10	2.76	0.02	0.06	6.43
C5_3S	9.89	147.83	10.13	3.18	0.02	0.04	11.79
C5_3B	13.90	145.67	9.42	1.44	0.02	0.04	8.57
C5_4S	5.70	28.83	10.16	2.65	0.02	0.04	5.36
C5_4B	6.15	5.28	8.02	1.19	0.02	0.04	9.64
C5_5S	5.82	183.33	9.61	2.16	0.02	0.04	16.07
C5_5B	8.20	89.17	9.67	1.87	0.02	0.04	2.14
C5_6S	6.22	53.67	9.46	1.97	0.02	0.04	5.89
C5_6B	8.09	197.31	8.43	0.73	0.02	0.04	11.79
C5_7S	5.92	148.63	9.49	2.10	0.02	0.04	0.00
C5_7B	5.62	124.17	6.48	1.30	0.02	0.04	5.36
C5_8S	2.50	118.50	8.87	1.23	0.02	0.04	10.71
C5_8B	1.55	112.02	6.70	1.20	0.02	0.04	11.79
C5_9S	3.61	136.17	8.37	1.78	0.02	0.04	6.43
C5_9B	7.93	117.07	7.90	2.62	0.02	0.04	4.29
C5_10S	5.91	137.67	9.02	3.83	0.08	0.04	4.29
C5_10B	5.50	128.47	8.11	1.95	0.02	0.04	3.21
C5_11S	11.90	106.33	9.24	4.35	0.02	0.04	9.64
C5_11B	10.10	191.50	8.03	3.76	0.11	0.04	10.71
C6_1S	2.76	134.36	9.34	2.03	0.02	0.04	2.73
C6_2S	3.99	17.50	8.95	1.38	1.55	0.04	3.41
C6_2B	7.14	57.53	8.95	1.38	0.02	0.04	2.73
C6_3S	2.87	144.50	9.61	1.39	0.15	0.04	1.36
C6_3B	4.50	108.33	9.73	1.45	0.02	0.20	4.09
C6_4S	7.61	10.50	8.59	1.38	0.02	0.04	3.41
C6_4B	39.60	11.83	8.39	1.02	0.11	0.04	2.05
C6_5S	19.30	155.80	8.87	1.09	0.19	0.04	2.73
C6_5B	8.32	90.84	8.66	1.10	0.30	0.04	6.14
C6_6S	8.51	162.59	8.86	1.53	0.05	0.04	4.77
C6_6B	13.30	57.59	8.74	1.52	0.02	0.04	2.05
C6_7S	6.05	15.00	8.94	1.46	0.02	0.04	4.09
C6_7B	5.82	165.00	9.00	1.68	0.02	0.04	2.05

Table A1.2 – Physical–chemical parameters in water column (continuation)

POINT	TURB	TSS	DO	BOD_5	CHL–a	PHAEO	POC
	NTU	mg L^{-1}					
C6_8S	4.90	4.00	8.62	1.20	0.02	0.04	3.41
C6_8B	6.40	89.74	8.59	1.41	0.08	0.04	6.14
C6_9S	15.50	96.41	8.38	1.32	0.02	0.08	4.09
C6_9B	10.10	146.07	8.57	2.12	0.01	0.04	4.09
C6_10S	18.30	105.32	7.97	1.77	0.02	0.04	1.36
C6_10B	15.80	69.97	7.85	1.15	0.02	0.04	2.73
C6_11S	6.57	59.90	10.82	4.54	0.02	0.04	4.77
C6_11B	10.10	136.83	11.56	4.46	0.02	0.04	34.77
C7_1S	1.66	176.52	8.76	0.38	0.09	0.04	2.68
C7_2S	1.81	108.09	8.46	1.16	0.04	0.04	2.14
C7_2B	1.48	161.31	8.37	0.07	0.07	0.04	2.68
C7_3S	1.35	184.16	8.40	1.02	0.05	0.04	32.14
C7_4S	0.81	92.31	7.78	0.28	0.03	0.04	2.79
C7_4B	0.76	179.09	8.04	0.45	0.06	0.04	3.00
C7_5S	1.92	78.39	5.15	1.11	0.03	0.04	1.93
C7_5B	1.68	216.39	5.62	1.62	0.07	0.04	2.68
C7_6S	2.37	13.73	8.70	1.17	0.06	0.04	1.71
C7_6B	1.68	182.81	8.35	0.33	0.04	0.04	4.29
C7_7S	3.64	182.38	9.15	1.88	0.05	0.04	4.71
C7_7B	3.08	210.10	8.27	0.89	0.70	0.04	1.61
C7_8S	2.92	204.25	8.34	1.07	0.04	0.04	5.36
C7_8B	2.46	201.39	7.95	0.56	0.07	0.04	6.43
C7_9S	5.84	170.34	9.40	2.99	0.05	0.04	5.14
C7_9B	5.65	170.42	8.32	1.80	0.07	0.04	5.89
C7_10S	9.31	210.87	10.27	4.23	0.07	0.04	9.11
C7_10B	9.65	399.27	7.43	1.39	0.13	0.04	9.64
C7_11S	24.30	376.25	11.16	7.55	0.14	0.04	16.07
C8_1S		51.18	8.66	2.69	0.02	0.04	
C8_2S			3.29	3.29			
C8_4S		225.84	5.97	0.90	0.05	0.04	27.00
C8_4B		242.28	7.17	1.49	0.07	0.04	
C8_5S		289.56	11.05	4.48	0.05	0.04	
C8_5B		146.27	10.15	5.38	0.07	0.04	17.50
C8_6S		171.38	11.35	4.78	0.02	0.06	45.00
C8_6B		44.65	5.97	1.49	0.02	0.06	435.00
C8_7S		113.41	8.36	3.58	0.00	0.04	102.50
C8_7B		86.86	11.65	6.87	0.02	0.28	32.50
C8_8S		167.45	13.14	8.06	0.02	0.04	277.50
C8_8B		114.46	13.14	6.57	0.09	0.04	258.75
C8_9S		181.77	8.66	2.69	0.02	0.04	156.00
C8_9B		89.16	10.15	4.48	0.02	0.11	26.25
C8_10S		121.01	11.35	6.27	0.02	0.05	27.50
C8_10B		80.51	9.56	1.49	0.04	0.04	41.25
C8_11S		205.51	10.75	5.08	0.02	0.04	7.50
C8_11B		164.77	10.75	5.38	0.02	0.04	

Table A1.2 – Physical–chemical parameters in water column (continuation)

POINT	TURB	TSS	DO	BOD_5	CHL–a	PHAEO	POC
	NTU	mg L^{-1}					
C9_1S	2.80	235.37	8.96	1.02	0.13	0.04	
C9_2S	1.32						
C9_2B	4.14	207.11	8.78	1.94	0.04	0.04	
C9_3S	2.87	291.41	8.50	0.91	0.11	0.04	4.29
C9_3B	3.14	300.30	8.15	0.38	0.08	0.04	3.75
C9_4S	1.52	175.78	8.08	0.22	0.05	0.04	27.00
C9_4B	1.42	106.59	7.64	0.51	0.46	0.04	52.50
C9_5S	2.63		8.55	0.54	0.24	0.04	5.63
C9_5B	3.25		8.41	0.40	0.17	0.04	26.25
C9_6S	2.22	189.80	8.87	0.54	0.02	0.07	7.88
C9_6B	2.39		8.17	0.27	0.02	0.10	13.88
C9_7S	1.53	83.30	8.38	0.50	0.07	0.04	1.25
C9_7B	1.88	93.80	8.02	0.20	0.02	0.04	85.00
C9_8S	0.91	142.23	8.72	0.30	0.02	0.04	105.00
C9_8B	2.99	255.96	8.82	0.12	0.02	0.08	37.50
C9_9S	3.67	160.96	8.03	0.03	0.02	0.04	3.00
C9_9B	39.60	350.96	8.19	0.15	0.00	0.08	31.88
C9_10S	4.86	88.01	9.16	1.16	0.00	0.04	20.00
C9_10B	21.60	148.76	9.21	1.34	0.02	0.04	105.00
C9_11S	2.03	96.65	7.12	0.12	0.02	0.07	9.38
C9_11B	1.9	398.90	7.77	0.16	0.04	0.04	3.75

Source: the author, 2023.

Table A1.3 – Physical–chemical parameters in water column

POINT	PN	PP	NH_4^+	NO_2^-	NO_3^-	DIN	PO_4^{3-}	N:P
	µmol L^{-1}							
C1_1S	0.24	0.42	0.66	0.07	1.88	2.61	0.33	7.79
C1_2S	0.81	0.95	0.18	0.03	2.41	2.62	0.20	13.25
C1_2M	1.42	1.00	0.18	0.09	2.73	3.00	0.20	15.17
C1_2B	0.67	1.06	0.36	0.07	3.16	3.59	0.24	14.73
C1_3S	2.86	1.03	0.48	0.17	6.03	6.68	0.29	23.10
C1_3M	2.27	1.55	0.12	0.15	5.71	5.98	0.33	17.86
C1_3B	5.20	0.71	0.36	0.32	9.96	10.64	0.65	16.26
C1_4S	1.57	0.72	1.74	0.25	4.54	6.53	0.33	19.50
C1_4M	1.58	0.93	0.42	0.11	6.77	7.30	0.15	47.99
C1_4B	0.72	0.90	0.84	0.17	6.35	7.36	0.29	25.45
C1_5S	4.15	0.59	0.30	0.23	6.45	6.99	0.33	20.87
C1_5M	2.72	0.86	1.20	0.32	4.86	6.37	0.33	19.03
C1_5B	2.19	0.78	0.30	0.34	5.71	6.34	0.61	10.42
C1_6S	0.72	0.98	0.90	0.40	5.18	6.47	0.65	9.89
C1_6M	0.62	0.65	0.84	0.46	6.35	7.64	0.79	9.66
C1_6B	0.56	0.52	1.50	0.66	7.20	9.36	1.25	7.50
C1_7S	0.70	0.61	1.26	0.52	5.92	7.70	0.65	11.76
C1_7M	0.63	0.64	1.56	0.42	6.77	8.75	0.52	16.90
C1_7B	0.88	1.02	0.84	0.62	6.24	7.70	0.65	11.76
C1_8S	0.70	0.67	0.54	0.25	6.45	7.25	0.52	14.00
C1_8M	1.69	0.52	1.02	0.34	7.30	8.66	0.79	10.94
C1_8B	3.73	0.84	0.66	0.34	7.09	8.09	0.65	12.36
C1_9S	3.49	0.71	0.78	0.29	5.82	6.89	0.33	20.57
C1_9M	1.98	0.80	1.14	0.36	6.77	8.27	0.75	11.08
C1_9B	2.24	0.56	0.42	0.38	6.88	7.67	0.56	13.63
C1_10S	1.20	1.03	0.18	0.25	6.99	7.42	0.33	22.16
C1_10B	2.91	1.35	0.66	0.21	5.07	5.94	0.38	15.62
C1_11S	0.72	1.80	0.66	0.27	5.50	6.43	0.52	12.42
C2_3S	0.63	0.45	0.10	0.35	6.26	6.72	0.26	25.63
C2_5S	0.33	0.29	1.25	0.21	7.78	9.23	0.26	35.23
C2_6S	0.26	0.32	1.10	0.23	7.63	8.95	0.22	41.01
C2_8S	0.15	0.33	1.32	0.14	5.65	7.12	0.17	40.76
C2_10S	1.36	0.44	0.79	0.23	4.75	5.76	0.31	18.85
C3_3S	0.16	1.42	0.69	0.62	2.85	4.16	0.08	52.02
C3_5S	0.02	0.34	0.80	0.72	3.18	4.70	0.08	58.77
C3_6S	0.17	0.34	0.17	0.49	3.18	3.84	0.08	48.02
C3_8S	0.13	0.47	0.17	0.52	4.01	4.69	0.08	58.67
C3_10S	0.67	0.78	0.17	0.26	3.02	3.44	0.08	43.05
C4_1S	0.02	2.51	0.17	0.17	2.55	2.88	0.08	36.02
C4_3S	0.07	3.24	0.17	0.41	2.09	2.67	0.79	3.38
C4_3B	0.10	2.03	0.17	2.27	2.17	4.62	0.08	57.71
C4_4S	0.27	2.54	0.76	0.74	2.09	3.59	0.11	31.78
C4_4B	0.03	2.03	1.57	0.93	1.88	4.38	0.08	54.80
C4_5S	0.06	1.86	0.99	1.28		2.27	0.08	28.37
C4_5B	0.03	1.87	2.73	1.24	2.05	6.02	0.23	26.65

Table A1.3 – Physical–chemical parameters in water column (continuation)

POINT	PN	PP	NH_4^+	NO_2^-	NO_3^-	DIN	PO_4^{3-}	N:P
	µmol L^{-1}							
C4_6S	0.08	0.97	0.41	1.80	1.76	3.97	0.08	49.57
C4_6B	0.05	1.05	0.17	1.07	1.60	2.84	0.08	35.50
C4_7S	0.04	1.55	0.52	1.16	5.11	6.79	0.08	84.85
C4_7B	0.08	0.97	0.41	1.03	3.70	5.14	0.51	10.11
C4_8S	0.12	1.35	0.17	1.51	3.66	5.34	0.08	66.75
C4_8B	0.06	0.96	0.17	1.32	3.79	5.28	0.56	9.34
C4_9S	0.03	1.45	0.17	1.47	3.79	5.42	1.53	3.55
C4_9B	0.06	1.16	0.17	1.05	3.41	4.64	0.40	11.73
C4_10S	0.10	0.92	0.17	0.76	3.17	4.10	1.13	3.63
C4_10B	0.22	0.93	0.17	0.85	4.41	5.42	0.08	67.78
C4_11S	0.24	2.57	0.17	0.83	2.96	3.96	0.11	35.01
C5_1S	1.40	1.15	9.57	1.16	1.29	12.02	0.22	54.79
C5_2S	0.75	4.24	0.17	1.30	11.72	13.20	0.18	75.23
C5_2B	0.10	3.01	2.67	1.21	5.17	9.05	0.09	103.19
C5_3S	0.39	2.39	0.17	1.26	15.86	17.29	0.13	131.39
C5_3B	0.62	2.47	0.17	1.87	7.93	9.97	0.18	56.85
C5_4S	0.02	3.06	0.17	2.30	10.69	13.16	0.09	150.00
C5_4B	2.20	3.38	9.07	2.73	15.86	27.66	0.22	126.11
C5_5S	5.77	2.59	0.17	2.75	15.86	18.78	0.09	214.10
C5_5B	1.16	3.15	0.17	2.44	15.17	17.78	0.31	57.92
C5_6S	0.34	2.17	0.17	1.87	15.17	17.21	0.31	56.07
C5_6B	0.44	2.49	0.17	2.06	23.79	26.02	0.08	325.31
C5_7S	0.44	2.11	0.17	1.78	17.24	19.19	0.35	54.69
C5_7B	0.36	1.48	1.61	1.54	12.76	15.91	0.09	181.42
C5_8S	0.78	1.56	0.17	1.26	12.76	14.18	0.09	161.70
C5_8B	0.88	1.99	0.17	1.35	18.97	20.49	0.09	233.54
C5_9S	0.18	1.10	0.17	1.16	15.52	16.85	0.08	210.60
C5_9B	0.67	2.71	4.91	1.26	15.86	22.02	0.08	275.31
C5_10S	0.57	2.72	0.31	6.49	20.69	27.49	0.09	313.42
C5_10B	0.49	1.85	1.74	6.49	11.38	19.61	0.09	223.57
C5_11S	0.39	3.22	0.17	5.36	15.86	21.39	0.09	243.82
C5_11B	0.41	2.35	0.17	5.26	13.45	18.88	0.18	107.61
C6_1S	2.90	0.44	0.17	0.09	1.29	1.55	0.08	19.42
C6_2S	8.51	0.58	2.33	2.27	4.48	9.09	0.08	113.57
C6_2B	3.08	0.54	5.70	2.33	1.29	9.32	0.08	116.53
C6_3S	7.45	0.26	2.61	3.93	8.62	15.16	0.08	189.53
C6_3B	3.67	0.58	2.98	4.10	14.83	21.90	0.08	273.79
C6_4S	8.97	3.49	0.92	3.54	4.14	8.59	0.08	107.43
C6_4B	8.74	0.52	2.24	3.43	6.55	12.23	0.08	152.85
C6_5S	7.84	0.47	0.11	4.35	3.79	8.25	0.08	103.12
C6_5B	3.85	0.77	0.18	5.51	4.14	9.83	0.08	122.88
C6_6S	4.16	0.52	1.29	2.38	10.00	13.66	0.20	69.83
C6_6B	6.31	0.54	1.36	2.19	4.83	8.38	0.08	104.71
C6_7S	5.66	0.66	1.14	2.29	2.07	5.50	0.08	68.77

Table A1.3 – Physical–chemical parameters in water column (continuation)

POINT	PN	PP	NH_4^+	NO_2^-	NO_3^-	DIN	PO_4^{3-}	N:P
	μmol L^{-1}							
C6_8S	8.56	0.35	2.54	1.11	3.45	7.09	0.08	88.69
C6_8B	3.75	0.42	21.65	0.86	1.29	23.81	0.11	219.01
C6_9S	3.31	0.56	4.08	0.61	4.83	9.52	0.08	119.01
C6_9B	3.83	0.59	8.79	0.59	3.45	12.83	0.08	160.33
C6_10S	3.96	0.87	7.17	0.99	1.72	9.88	0.20	50.49
C6_10B	2.87	0.65	5.18	0.72	6.90	12.80	0.08	159.95
C6_11S	6.26	1.21	18.42	0.28	1.72	20.42	0.11	187.89
C6_11B	5.95	1.34	15.85	0.55	1.29	17.69	0.08	221.07
C7_1S	0.81	0.56	0.17	0.04	5.17	5.38	0.13	41.62
C7_2S	1.72	1.00	0.17	0.43	5.17	5.78	0.22	26.80
C7_2B	0.45	0.52	2.26	0.54	5.17	7.97	0.22	36.98
C7_3S	1.65	0.89	0.17	1.57	5.17	6.91	0.09	80.19
C7_4S	1.54	1.29	0.17	5.19	5.52	10.87	0.08	135.91
C7_4B	1.27	0.72	0.17	5.17	5.86	11.20	0.13	86.59
C7_5S	0.63	0.61	0.17	8.22	5.17	13.57	0.30	44.96
C7_5B	1.46	0.82	0.17	8.10	5.52	13.79	0.17	79.96
C7_6S	1.40	0.79	4.07	3.16	5.52	12.75	0.08	159.33
C7_6B	1.11	0.92	3.11	2.81	6.55	12.47	0.30	41.33
C7_7S	1.75	0.98	0.17	2.73	5.52	8.41	0.09	97.61
C7_7B	1.46	0.83	1.02	2.58	5.52	9.12	0.08	113.96
C7_8S	1.75	1.13	3.05	1.47	6.55	11.07	0.08	138.37
C7_8B	2.44	1.00	0.17	1.57	5.86	7.60	0.17	44.09
C7_9S	1.85	1.19	0.56	0.54	5.52	6.62	0.17	38.39
C7_9B	1.44	1.20	4.63	0.48	5.86	10.97	0.08	137.13
C7_10S	4.82	1.57	0.17	0.60	5.86	6.63	0.22	30.77
C7_10B	5.97	1.69	0.17	0.43	5.86	6.47	0.09	75.01
C7_11S	6.03	3.49	0.17	0.04	5.86	6.07	0.52	11.74
C8_1S	2.25	1.19	1.82	0.13		1.95	0.08	24.34
C8_2S								
C8_4S	0.97	1.52	8.64	4.26		12.89	0.08	161.18
C8_4B	1.12	1.35	16.14	4.68		20.81	0.08	260.17
C8_5S	0.89	3.84	15.00	5.19		20.19	0.08	252.42
C8_5B	1.29	1.49	19.32	5.48		24.80	0.28	87.87
C8_6S	1.10	3.94	9.32	4.19		13.51	0.16	83.77
C8_6B	1.30	4.06	13.18	5.61		18.79	0.08	234.93
C8_7S	1.12	1.95	10.45	3.90		14.36	0.08	179.47
C8_7B	1.81	2.85	11.59	4.39		15.98	0.08	199.73
C8_8S	2.09	4.06	5.91	1.94		7.84	0.08	98.06
C8_8B	1.84	2.37	10.45	2.42		12.87	0.08	160.92
C8_9S	1.30	2.46	4.09	0.55		4.64	0.08	57.99
C8_9B	1.99	3.87	11.82	0.58		12.40	0.08	154.99
C8_10S	3.21	3.53	2.05	0.45		2.50	0.08	31.21
C8_10B	4.71	4.04	7.73	0.48		8.21	0.08	102.64
C8_11S	4.45	3.61	4.09	1.16		5.25	0.08	65.65
C8_11B	6.67	2.40	6.59	0.68		7.27	0.08	90.85

Table A1.3 – Physical–chemical parameters in water column (continuation)

POINT	PN	PP	NH_4^+	NO_2^-	NO_3^-	DIN	PO_4^{3-}	N:P
	μmol L^{-1}							
C9_1S	0.02	0.96	0.81	0.03	1.29	2.13	0.08	26.66
C9_2S	0.37	2.46	11.59	2.08	1.42	15.08	1.29	11.65
C9_2B	0.38	10.19	9.19	2.54	2.05	13.78	1.25	11.02
C9_3S	0.32	11.65	3.41	2.62	1.78	7.81	0.85	9.21
C9_3B	0.19	12.02	4.84	3.44	1.42	9.69	0.31	31.00
C9_4S	0.39	2.34	5.49	3.60	1.51	10.60	0.36	29.67
C9_4B	0.33	1.82	9.58	4.31	1.96	15.86	0.31	50.74
C9_5S	0.53	2.27	7.64	6.67	17.33	31.64	0.28	113.91
C9_5B	0.13	1.38	62.29	6.77	8.00	77.06	0.14	554.81
C9_6S	0.43	1.78	64.22	6.35	4.67	75.25	0.74	101.58
C9_6B	0.30	1.83	9.96	6.71	11.33	28.00	0.32	86.41
C9_7S	0.68	1.37	8.73	3.50	1.46	13.69	0.36	38.34
C9_7B	0.39	4.15	5.94	3.21	1.51	10.65	0.45	23.87
C9_8S	0.51	1.18	10.58	4.96	5.33	20.88	0.19	112.75
C9_8B	0.42	1.37	14.07	5.06	6.67	25.80	0.74	34.83
C9_9S	0.52	2.89	16.01	2.72	1.37	20.10	0.58	34.64
C9_9B	5.63	10.83	16.53	3.90	2.01	22.43	0.54	41.87
C9_10S	0.66	2.22	14.51	3.92	2.47	20.90	0.49	42.55
C9_10B	2.78	3.32	13.02	2.45	1.60	17.07	0.22	76.47
C9_11S	0.46	1.79	19.58	2.60	2.15	24.32	2.68	9.08
C9_11B	0.66	3.58	25.88	7.93	2.28	36.09	0.76	47.56

Source: the author, 2023.

Figure B2.1 – pH

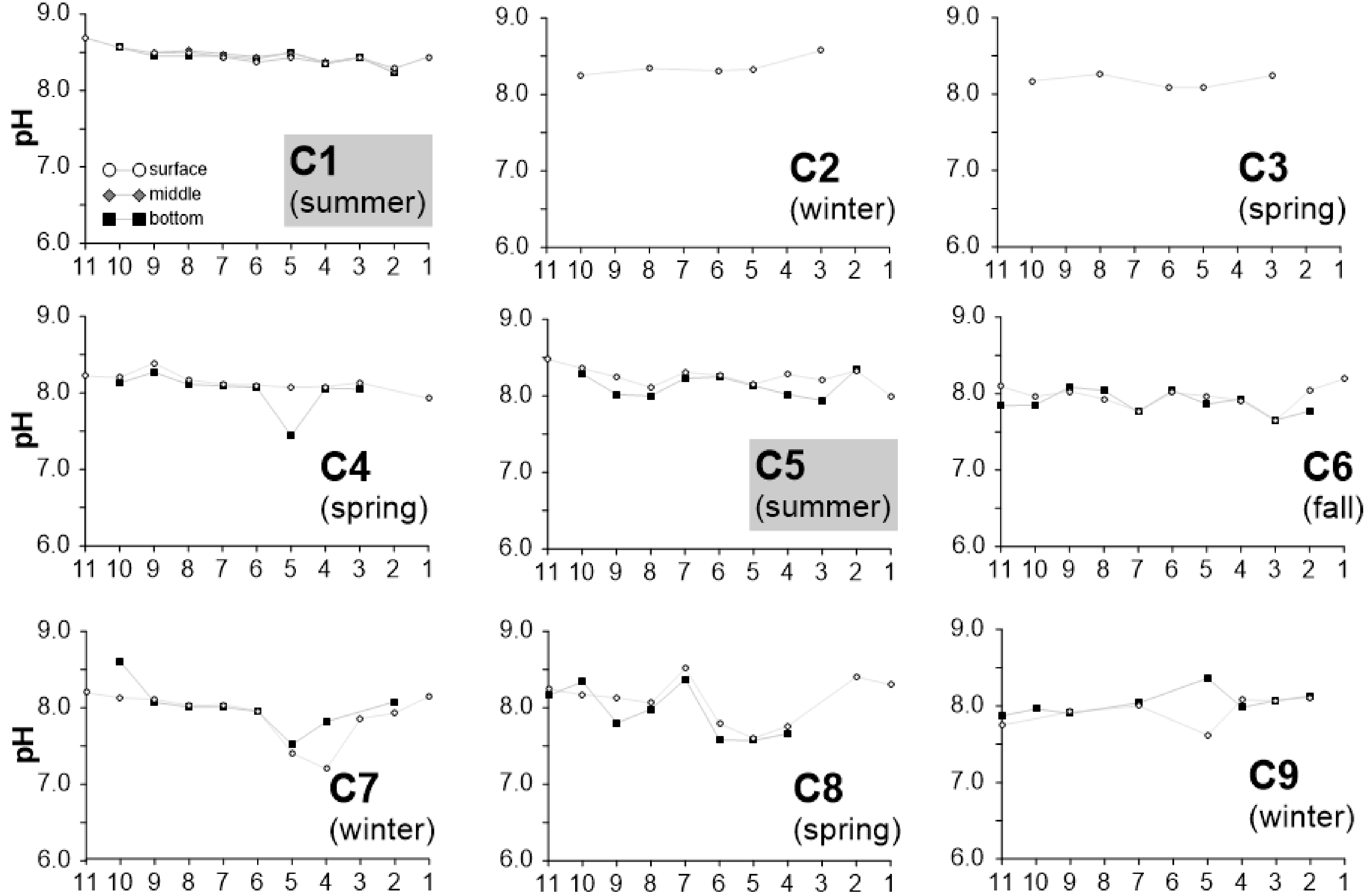

Source: Elaborated by the author, 2023.

LEGEND: pH exhibited low variation from C1 to C4 and a slightly higher variation from C5 to C9. C8 presented the higher spatial variation among campaigns.

Figure B2.2 – ORP

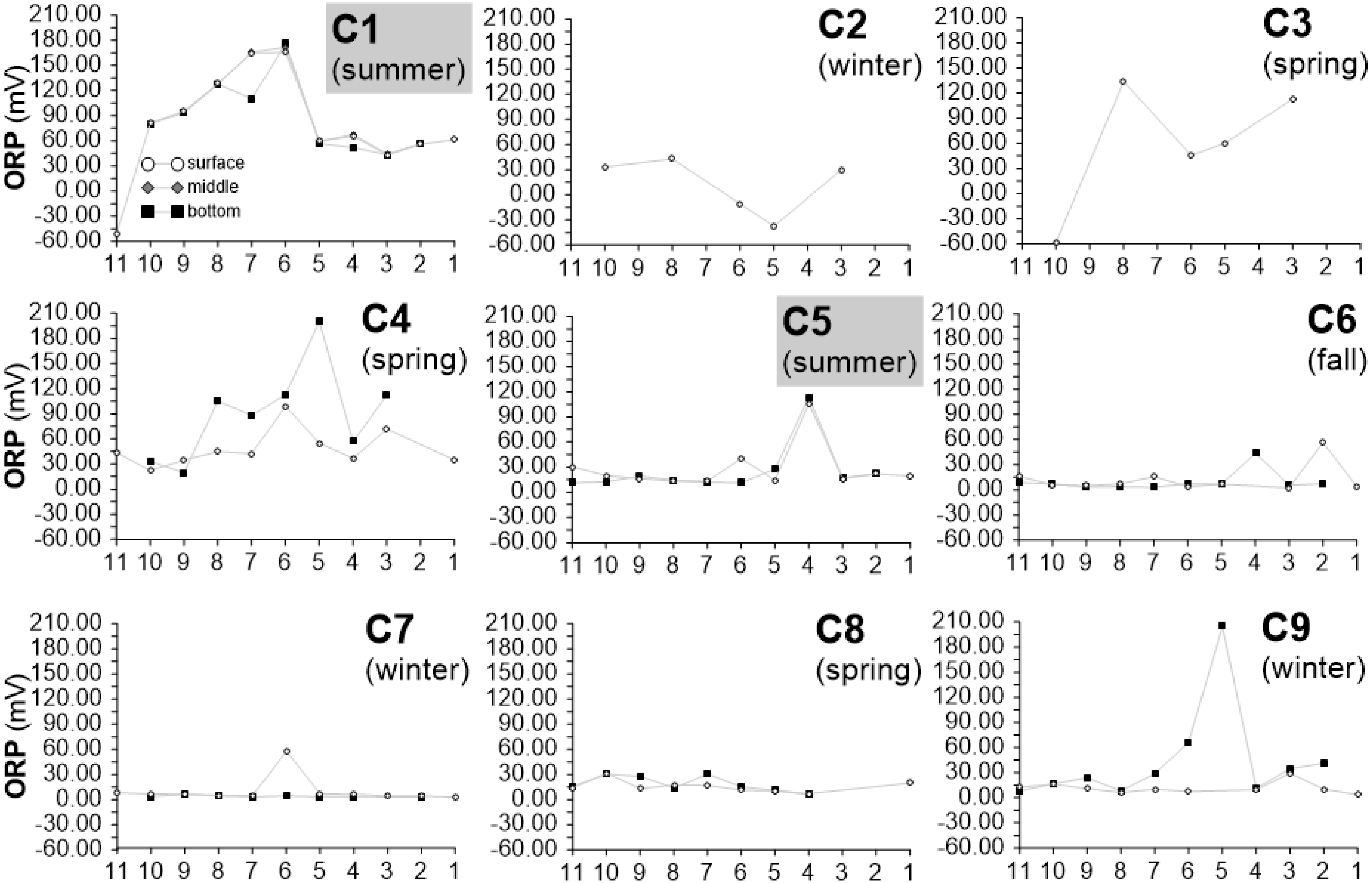

Source: Elaborated by the author, 2023.

LEGEND: ORP varied spatial and temporally from C1 to C4 and then was smaller and more constant from C5 to C9.

Figure B2.3 – Dissolved oxygen

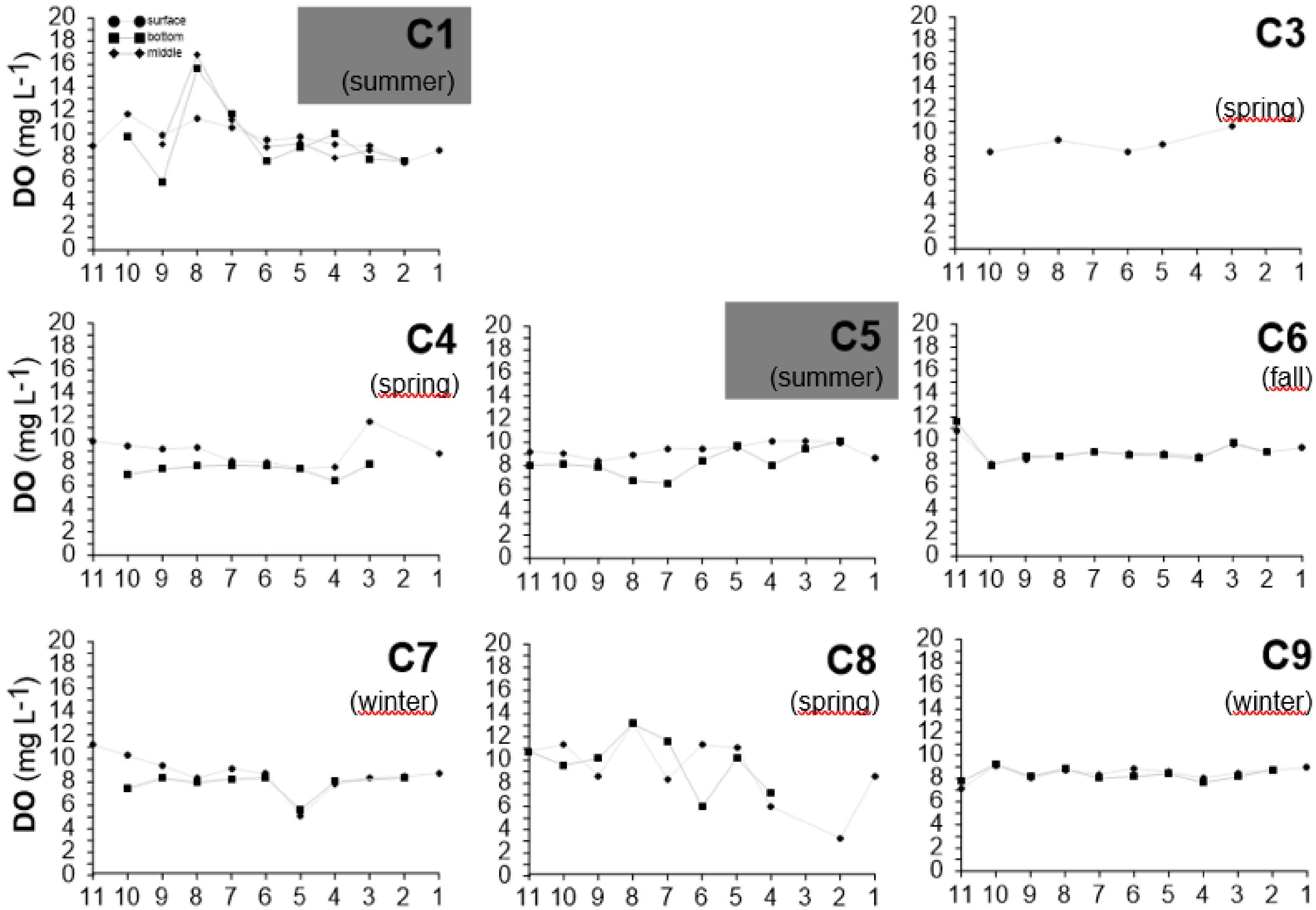

Source: Elaborated by the author, 2023.

LEGEND: DO varied little during campaigns and values were typical from well oxygenated waters, however C1 and C8 exhibited high spatial variation

Figure B2.4 – Biochemical oxygen demand

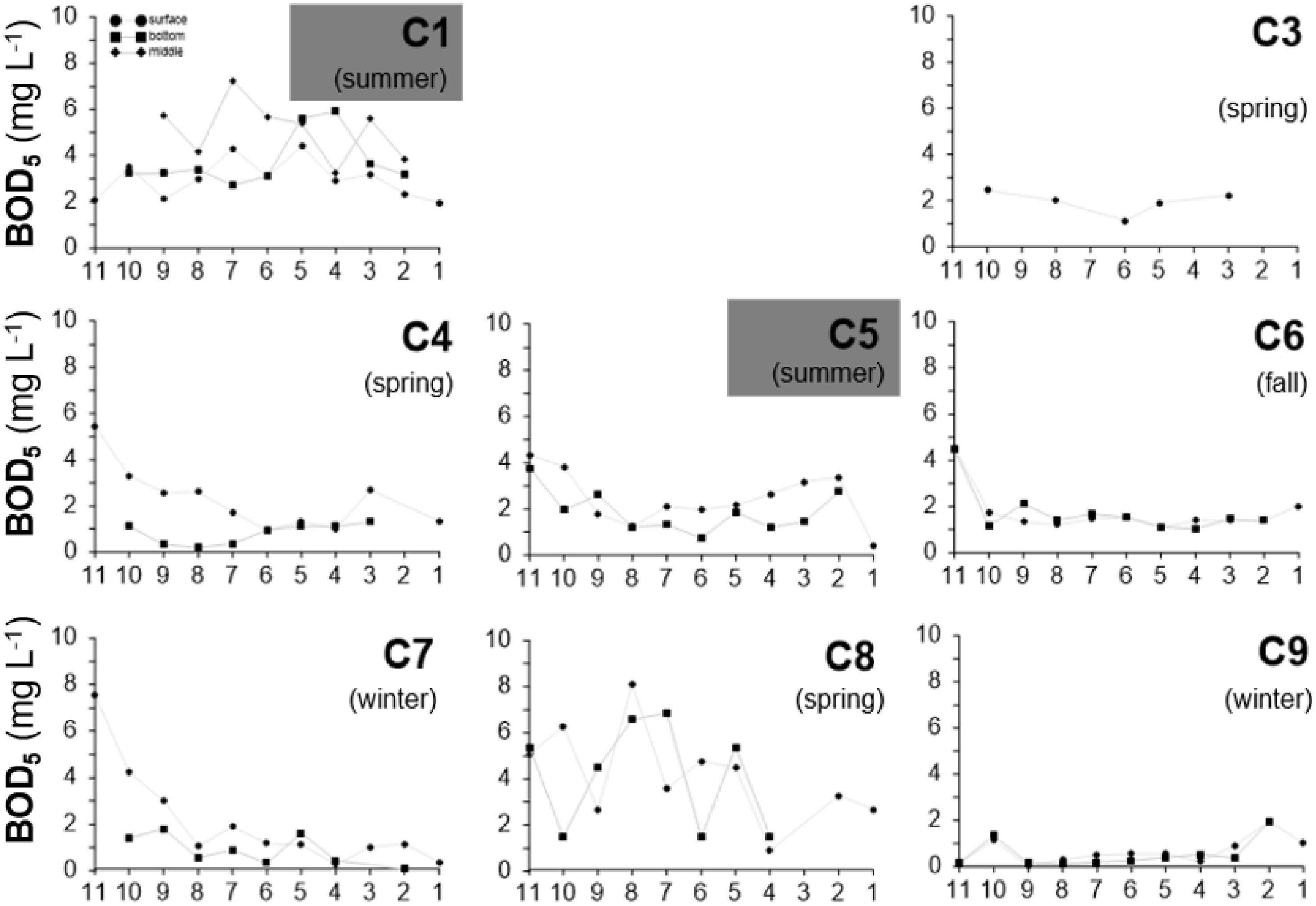

Source: Elaborated by the author, 2023.

LEGEND: BOD was higher in C1 and can be corroborated by the high cell density and turbid values. C8 was also higher, but turbidity was not as high as C1. And non-turbid campaigns presented smaller values of BOD.

Figure B2.5 – Wavelengths of chlorophyll pigment

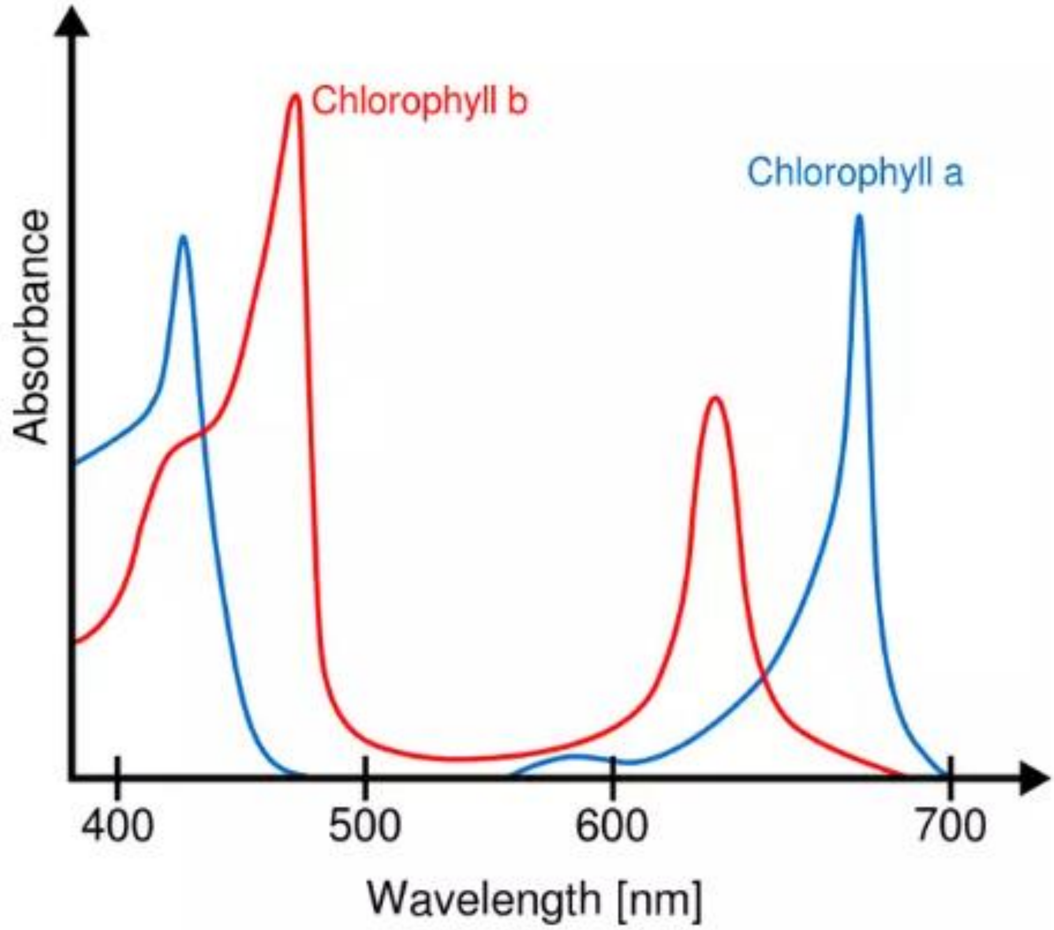

Source: Milne, *et al*. (2015). "Unraveling the Intrinsic Color of Chlorophyll," Angewandte Chemie International Edition 54 (7), 2170–2173. Authorized use.

Figure B2.6 – Example of UV–VIS results for chlorophyll (C1, Station 4, middle)

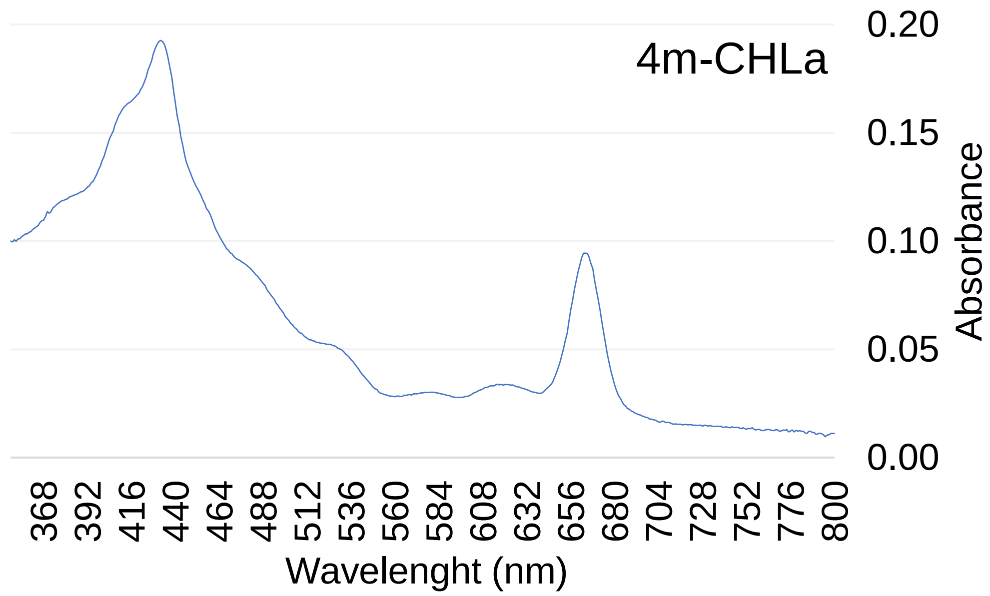

Source: the author, 2023

Figure B2.7 – Daily pluviosity (Jan 01,2019 – Sep 30, 2022)

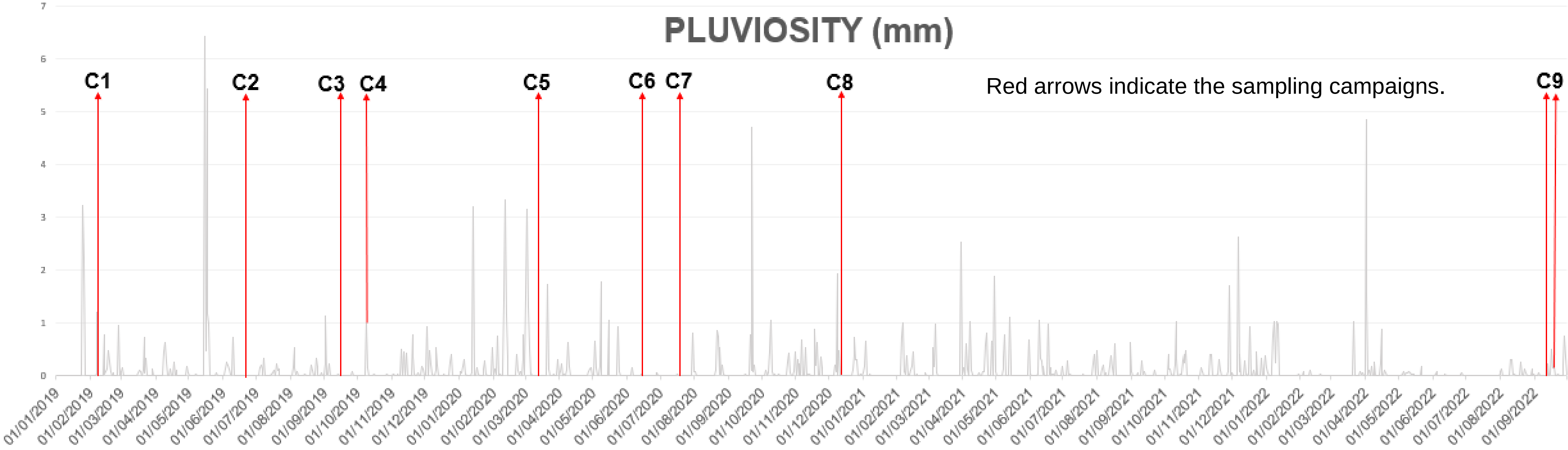

Source: the author, 2023.
LEGEND; Pluviosity was low during the period of the campaigns.

Figure B2.8 – PCA of turbid and non-turbid conditions

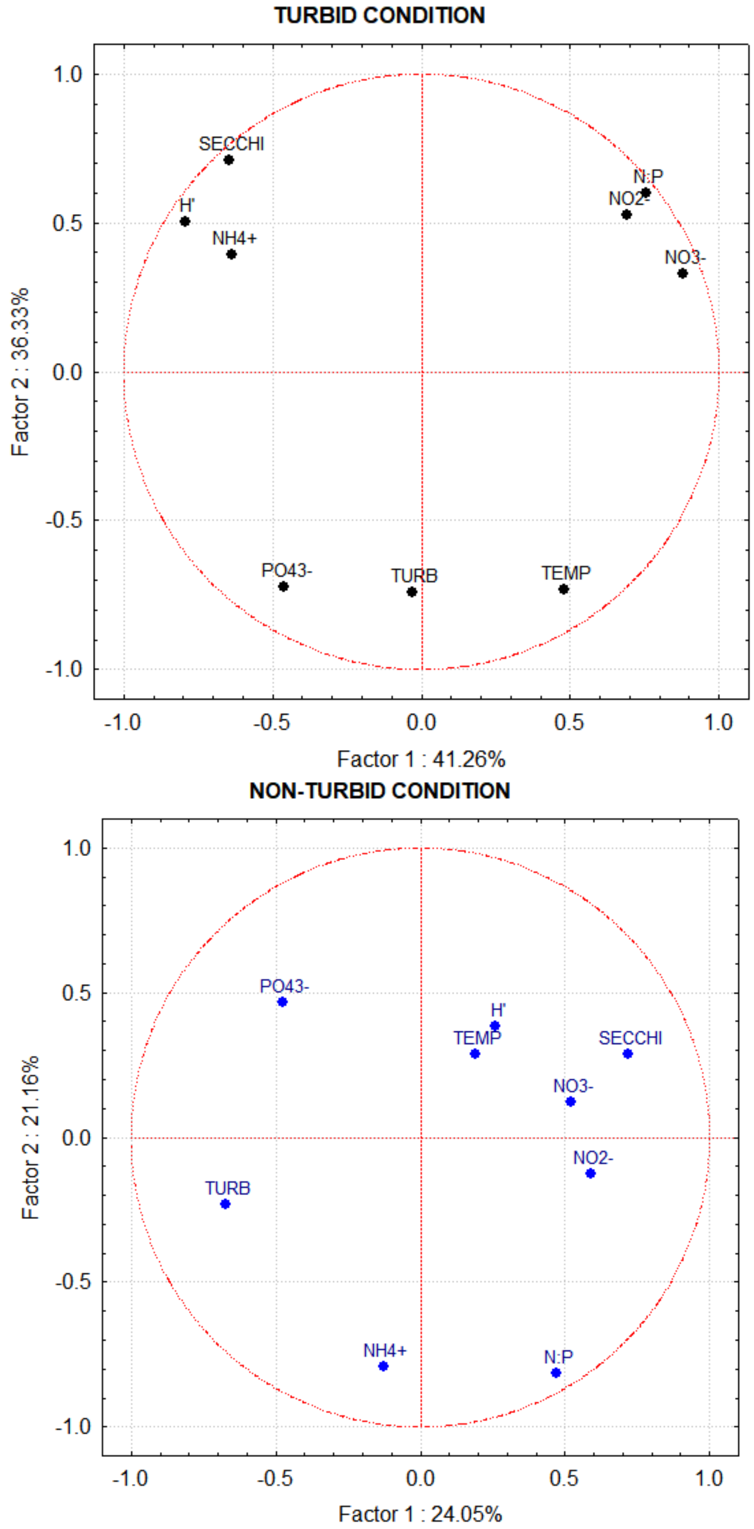

Source: the author, 2023.

LEGEND: The distribution of factors in turbid and non-turbid conditions. In turbid conditions, SEC was negatively correlated with TURB and TEMP, and PO_4^{3-}, while NH_4^+ and N:P ratios were more important in non-turbid water.

APPENDIX C

Table C3.1 – Diffusion coefficient of a specific ion for seawater free solution

CAMPAIGN		T SEAWATER °C	DIFFUSION COEFFICIENT ($m^{-2}\ s^{-1}$)			
			PO_4^{3-}	NH_4^+	NO_2^-	NO_3^-
C5	2	29.90	5.99E–10	1.20E–09	1.90E–09	1.20E–09
	3	29.50	5.95E–10	1.20E–09	1.89E–09	1.20E–09
	4	29.10	5.91E–10	1.19E–09	1.87E–09	1.19E–09
	5	26.90	5.69E–10	1.17E–09	1.81E–09	1.17E–09
	6	25.10	5.51E–10	1.15E–09	1.75E–09	1.15E–09
	7	28.00	5.80E–10	1.18E–09	1.84E–09	1.18E–09
	8	27.55	5.76E–10	1.18E–09	1.83E–09	1.18E–09
	9	28.00	5.80E–10	1.18E–09	1.84E–09	1.18E–09
	10	28.50	5.85E–10	1.19E–09	1.86E–09	1.19E–09
	11	28.70	5.87E–10	1.19E–09	1.86E–09	1.19E–09
C6	3	19.80	4.98E–10	1.10E–09	1.59E–09	1.10E–09
	4	23.40	5.34E–10	1.13E–09	1.70E–09	1.13E–09
	5	24.10	5.41E–10	1.14E–09	1.72E–09	1.14E–09
	6	22.10	5.21E–10	1.12E–09	1.66E–09	1.12E–09
	7	23.80	5.38E–10	1.14E–09	1.71E–09	1.14E–09
	8	22.40	5.24E–10	1.12E–09	1.67E–09	1.12E–09
	9	23.50	5.35E–10	1.14E–09	1.71E–09	1.14E–09
	10	23.00	5.30E–10	1.13E–09	1.69E–09	1.13E–09
	11	23.50	5.35E–10	1.14E–09	1.71E–09	1.14E–09
C7	2	21.20	5.12E–10	1.11E–09	1.64E–09	1.11E–09
	3	20.90	5.09E–10	1.11E–09	1.63E–09	1.11E–09
	5	21.70	5.17E–10	1.12E–09	1.65E–09	1.12E–09
	6	21.60	5.16E–10	1.12E–09	1.65E–09	1.12E–09
	7	21.60	5.16E–10	1.12E–09	1.65E–09	1.12E–09
	8	21.50	5.15E–10	1.12E–09	1.65E–09	1.12E–09
	9	21.40	5.14E–10	1.11E–09	1.64E–09	1.11E–09
C9	2	22.60	5.26E–10	1.13E–09	1.68E–09	1.13E–09
	3	22.15	5.22E–10	1.12E–09	1.66E–09	1.12E–09
	4	21.95	5.20E–10	1.12E–09	1.66E–09	1.12E–09
	5	25.05	5.51E–10	1.15E–09	1.75E–09	1.15E–09
	6	23.60	5.36E–10	1.14E–09	1.71E–09	1.14E–09
	7	23.40	5.34E–10	1.13E–09	1.70E–09	1.13E–09
	9	21.20	5.12E–10	1.11E–09	1.64E–09	1.11E–09
	10	22.30	5.23E–10	1.12E–09	1.67E–09	1.12E–09
	11	22.50	5.25E–10	1.13E–09	1.68E–09	1.13E–09

Source: the author 2023.

Table C3.2 – Geochemical parameters of sediment

STATION	PORE WATER							GRAINS						
	pH_S	ORP_S	$TEMP_S$	$NH_4^+{}_S$	$NO_2^-{}_S$	$NO_3^-{}_S$	$PO_4^{3-}{}_S$	TN_S	TP_S	TOC_S	CARB	COARSE	FINE SAND	MUDDY
		mV	°C	$\mu mol\ L^{-1}$				$mg\ g^{-1}$			%			
C5_2				169.2	1.8	71.8	0.7					60.2	36.6	3.2
C5_3	8.1	–300.7	27.5								74.4	98.0	2.0	0.0
C5_4	6.9	–207.7	27.0	589.3	7.9	191.6	35.3	27.2	2.0	94.1	61.6	81.2	18.2	0.6
C5_5	7.0	–377.6	26.6	371.2	1.9	64.4	10.2				55.8	76.6	22.3	1.1
C5_6	7.2	–388.9	25.0	541.6	2.8	97.1	22.8	4.1	2.1	56.1	46.4	72.7	25.8	1.5
C5_7	7.0	–396.8	27.0	507.3	8.7	141.4	29.8	6.8	0.8	28.8	39.4	68.7	30.0	1.3
C5_8	6.8	–387.2	26.8	320.0	3.1	59.8	3.0	24.6	4.5	28.6				
C5_9	7.0	–381.0	27.3	376.1	23.2	44.3	54.1	16.2	0.5	25.8	52.2	57.5	39.8	2.7
C5_10	7.1	–405.0	27.9	663.4	2.9	58.6	4.0	48.1	7.3		79.7	80.7	18.8	0.5
C5_11	7.3	–394.5	28.7	661.4	2.6	134.5	48.4	35.6	2.7	75.3	66.5	73.3	25.3	1.4
C6_3	7.8	–190.9	23.3					1.3	0.8		70.2	90.7	8.9	0.4
C6_4	7.8	–240.0	22.8									95.0	5.0	0.0
C6_5	7.2	–319.5	24.3	269.8	3.7	45.5	22.5	4.9	0.2		59.0	53.2	43.3	3.5
C6_6	7.0	–322.1	23.5	3.1	3.6	39.3	14.8	3.4	0.5		39.7	46.4	47.0	6.6
C6_7	7.3	–355.9	23.2	228.6	4.9	77.2	51.7				66.1	72.5	26.9	0.6
C6_8	7.0	–366.9	23.5	11.7	3.3	54.5	88.2	6.7	2.7			0.0	0.0	0.0
C6_9	7.0	–315.3	22.9	167.0	1.0	4.1	1.7				50.9	34.7	60.5	4.8
C6_10	7.3	–331.3	23.8	40.9	1.9	27.6	71.1	5.3	4.1		78.5	48.6	49.7	1.7
C6_11				99.0	6.1	64.8	3.4	2.9	0.2		40.3	0.0	0.0	0.0
C7_2											68.5	89.6	10.2	0.2
C7_4	7.8	–101.2	26.7	169.3	11.2	9.5	2.4					79.2	20.0	0.8
C7_6	7.1	–404.0	27.0	176.1	14.2	36.9	51.2					82.1	17.6	0.3
C7_7	7.2	–404.9	24.5	106.8	3.7	30.8	49.8					87.8	11.8	0.4

Table C3.2 – Geochemical parameters of sediment (continuation)

STATION	PORE WATER							GRAINS						
	pH_S	ORP_S	$TEMP_S$	$NH_4^+{}_S$	$NO_2^-{}_S$	$NO_3^-{}_S$	$PO_4^{3-}{}_S$	TN_S	TP_S	TOC_S	CARB	COARSE	FINE SAND	MUDDY
		mV	°C	µmol L^{-1}				mg g^{-1}			%			
C8_8	7.1	–390.3	22.0	122.7	8.9	33.0	43.3					60.5	35.8	3.7
C8_9	7.4	–382.5	25.1	208.0	3.0	23.5	3.4					43.2	49.6	7.2
C8_10	7.8	–393.7	22.5	1055.7	1.4	54.1	16.9					0.0	0.0	0.0
C8_11	7.9	–356.9	28.2	143.2	2.5	38.1	1.2					47.0	46.3	6.7
C9_2	8.1	40.0	22.6					0.1	0.8					
C9_3	8.1	–300.0	22.1	2.8	0.2	27.9	15.8	0.3	1.5			94.2	6.0	0.0
C9_4	8.0	–120.0	21.8	177.7	3.2	7.1	23.8	1.0	1.8			85.0	13.9	1.2
C9_5	8.4	–325.9	26.0	250.8	5.0	29.0	15.2	0.3	1.0			74.1	24.2	2.1
C9_6	8.0	–334.9	24.0	381.7	2.7	132.9	35.5	1.4	2.3			67.0	30.1	2.9
C9_7	8.0	–219.0	23.8	157.1	0.1	11.4	37.9	0.6	1.5			75.9	23.1	1.0
C9_9	7.9	–298.0	21.2	181.1	0.2	20.1	2.9	0.9	1.9			45.1	51.2	4.1
C9_10	8.0	–300.0		294.4	0.4	13.9	70.8	0.7	2.0					
C9_11	7.9	50.0	22.4	102.2	0.0	19.2	6.5	0.3	1.0					

Source: the author, 2023.

Figure C3.1 – Ternary diagram for granulometry in Araruama Lagoon

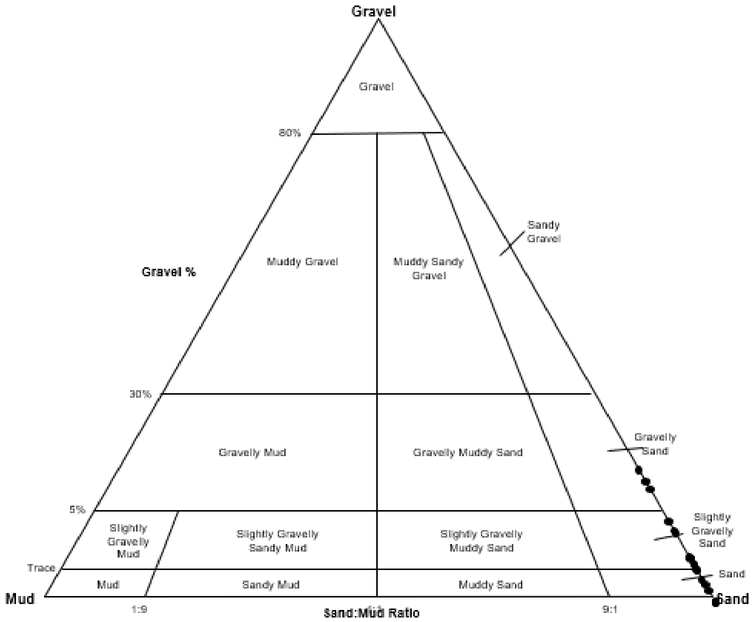

Source: Krumbein; Sloss, 1963; Wentworth, 1922. Graphic generated by Gradistat.
LEGEND; Sediment class sizes – i) sand (> 80% sand); ii) slightly gravelly sand (0.01% to < 5% gravel); and iii) gravelly sand (sand > gravel > 10%).

Table C3.3 – Nutrient fluxes in AL

NUTRIENT FLUXES				
CAMPAIGN	STATION	J PO_4^{3-}	J NH_4^+	JNO_2^-+NO_3^-
C5	2	0.02	7.87	15.60
	4	0.32	37.50	70.30
	5	0.50	17.10	28.70
	6	0.94	35.70	59.10
	7	0.07	24.90	45.20
	8	1.74	21.40	40.30
	9	0.09	16.80	28.10
	10	1.15	31.90	51.60
	11	1.21	33.70	55.20
C6	5	0.33	8.31	14.00
	6	0.26	0.07	1.40
	7	0.80	7.50	13.80
	8	1.03	–0.25	0.96
	9	0.03	6.50	9.80
	10	1.50	1.60	3.30
	11	0.05	2.90	6.50
C7	6	0.02	1.00	1.40
	7	0.03	2.80	4.10
	8	1.74	0.49	1.60
	9	0.15	3.60	5.10
C9	3	0.32	–0.09	1.10
	4	0.22	3.40	3.50
	7	1.40	12.20	1.30
	9	0.06	9.00	10.00
	10	2.26	19.30	20.20
	11	0.06	1.60	1.90

Source: the author, 2023.

ANNEXS

ANNEX A

Article published with the results of salinity and temperature profiles from CTD measurements from C1 (Tevisan *et al*., 2022). Please, follow the link https://doi.org/10.21715/GB2358-2812.202236001 to read the full version of the paper.

DOI:10.21715/GB2358-2812.202236001

Short term assessment of nutrients and physicochemical parameters considering different depths in a hypersaline lagoon – Araruama Lagoon –RJ

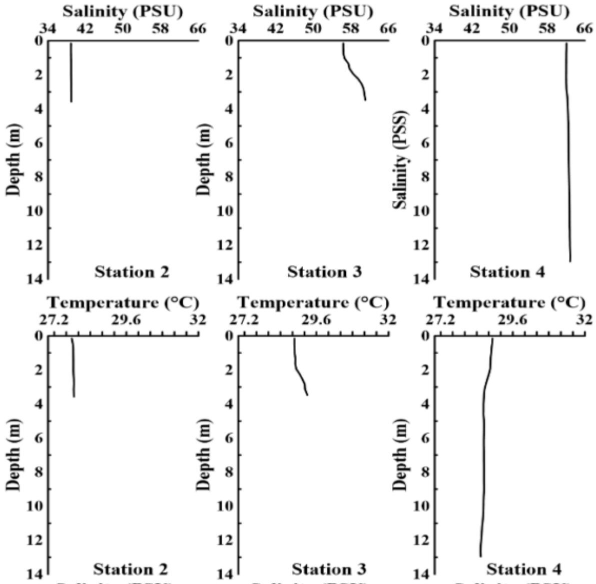

LEGEND: Water column profiles of temperature and salinity in C1. Data exhibited a regular profile for both parameters in most of the stations (except station 8). The strong winds promote a good mixing of the water column in Araruama Lagoon.

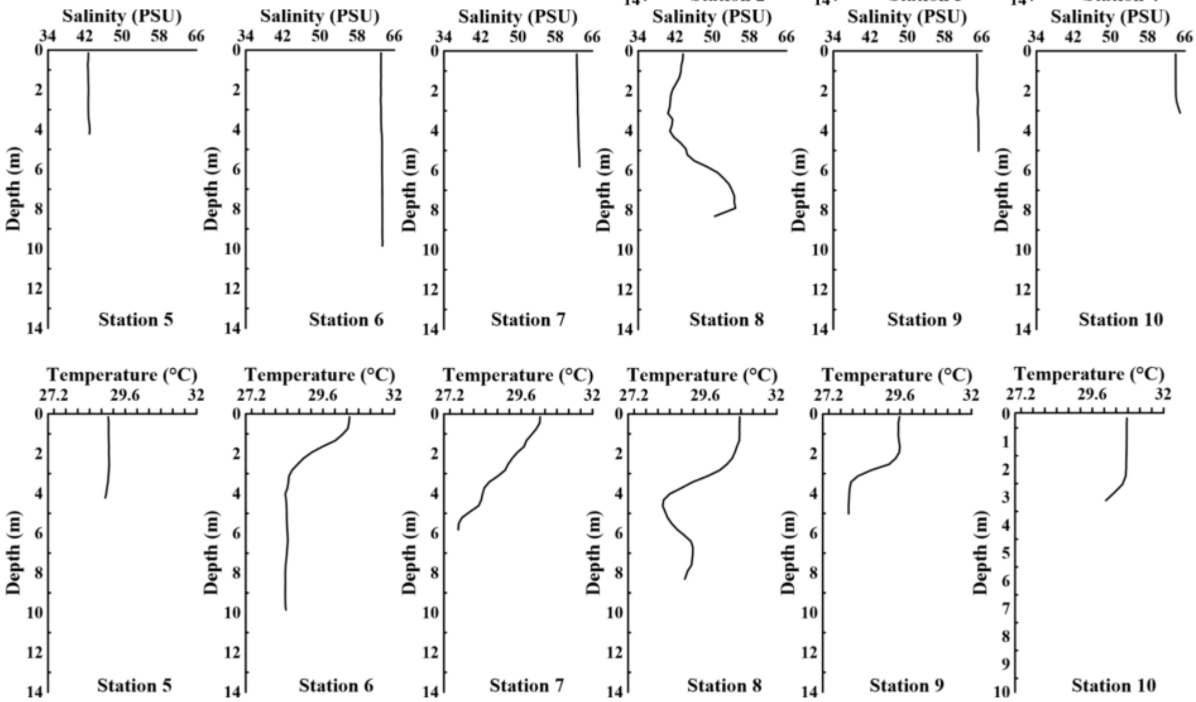

ANNEX B

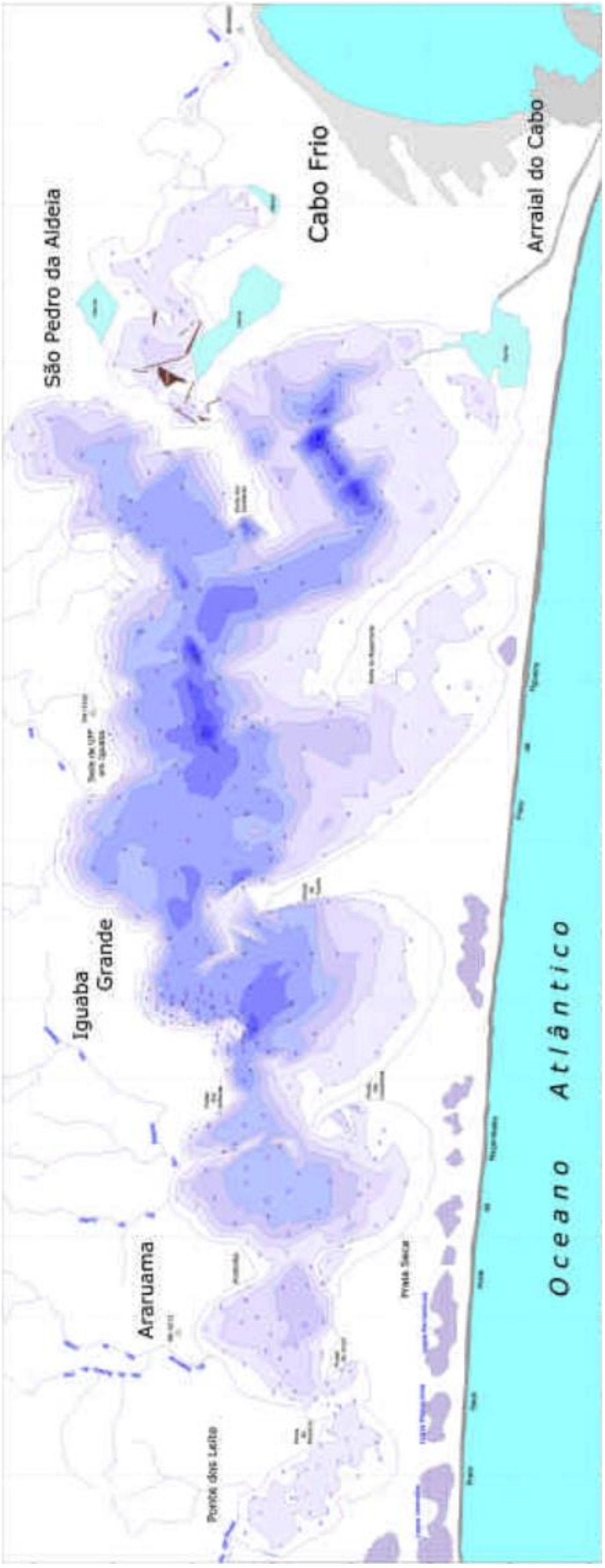

LEGEND: Bathymetry of Araruama Lagoon – 0 –3 m 3–7 m 7–12 m 12–15 m. Source: Wasserman et *al.* (2006).